ORJIP
Bird Collision
Avoidance Study

Final Report - April 2018
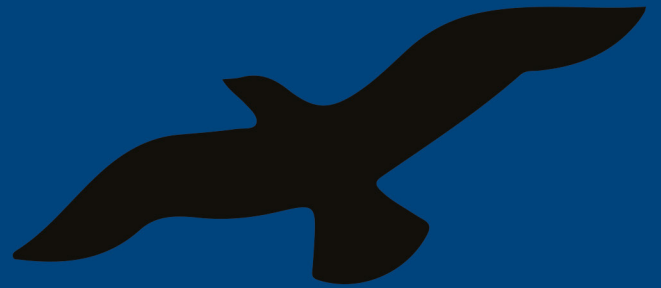
Authors – Henrik Skov[1], Stefan Heinänen[1], Tim Norman[2], Robin Ward[2], Sara Méndez-Roldán[2], Ian Ellis[2]

1 DHI, https://www.dhigroup.com

2 NIRAS Consulting Ltd, www.nirasconsulting.co.uk

Table of Contents

GLOSSARY

ATTRACTION	Potential for a wind farm to attract birds as a result of new habitat creation, which may encourage aggregation of fish, or lighting of wind turbines which may attract birds at night (Band 2012).
AVOIDANCE BEHAVIOUR	Any action taken by a bird, when close to an operational wind farm, which prevents collision (SNH 2010). Such action may be taken early enough to avoid entering into the wind farm (macro avoidance), or taken within the wind farm, avoiding the rotor-swept zone (RSZ) (meso avoidance) or individual blades (micro avoidance).
AVOIDANCE RATE (AR)	Correction factor applied in collision risk models in order to take account of the likely degree of successful avoidance of a wind farm by a bird.
BARRIER EFFECTS	Barrier effects occur where a wind farm acts as a 'barrier' for a bird getting from A to B and where the bird alters its flight trajectory in response to the wind farm presence. As a consequence, birds may use more circuitous routes to fly between, for example, breeding and foraging grounds, and thus use up more energy to acquire food (Band 2012).
BIRD FLUX RATE	Total number of birds crossing an imaginary surface within the airspace expressed as birds / sec or birds / s per m^2. The bird flux rate is directly related to bird density, but depends on the speed of the birds (if they were stationary, there would be no flux). Together with the probability of a bird colliding with a turbine (Pcoll), it can be used to estimate the predicted number of collisions in the absence of avoidance action (C_{pred}) (Cook et al. 2011). C_{pred} = (Flux rate * P_{coll}) + error.
COLLISION RISK	Risk of birds to result injured or killed by an encounter or collision with turbines or rotor blades at a wind farm (Band 2012).
COLLISION RISK MODELLING (CRM)	Tool used to quantify the risk of birds colliding with wind turbines (collision risk). The collision risk is expressed in terms of the likely number of birds per month or per year, which will collide with the wind farm, and the range of uncertainty surrounding that estimate.
CLUTTER	Clutter is a term used for unwanted echoes in electronic systems, particularly in reference to radars. Sea clutter refers to those echoes returned from sea, which can cause serious performance issues with radar systems.
DETECTION PROBABILITY	Probability for the sensor to pick up a bird or a flock of birds, which is dependent on distance, orientation, shape, size, clutter, etc. The maximum detection is the distance where the detection probability falls below 0.5 (equal chance of detecting a bird or not).
DETECTION PROBABILITY CURVE (DPC)	Probability curve for the sensor to detect a bird or a flock of birds over distance.

DETECTION RANGE Maximum distance at which any object can be detected by the sensor.

DISPLACEMENT A reduction in the number of birds using the area inside or adjacent to an offshore wind farm as a habitat for foraging, resting or roosting.

EMPIRICAL AVOIDANCE RATE (EAR) Empirical Avoidance rate derived from data collected by this study, considered to indicate the likely degree of successful avoidance to the wind farm. The overall empirical avoidance rate is composed of combining an empirical macro avoidance rate, an empirical meso avoidance rate, and an empirical micro avoidance rate.

MACRO AVOIDANCE Bird behavioural responses to the presence of the wind farm occurring beyond its perimeter, resulting in a redistribution of birds inside and outside the wind farm. In this study, empirical macro avoidance is quantified up to 3 km outside the wind farm.

MESO AVOIDANCE Bird behavioural response within the wind farm footprint to individual turbines (considering a 10 m buffer around the rotor-swept zone (RSZ)) and resulting in a redistribution of the birds within the wind farm footprint.

MICRO AVOIDANCE Bird behavioural response to single blade(s) within 10 m of the rotor-swept zone, considered as the bird's 'last-second action' taken to avoid collision.

OBSERVER Part of the two-person observer team with responsibility for operating the laser rangefinder (Vectronix 21 Aero). The observer also provides visual identification and associated parameters of the targets being tracked on radars at turbine G01 (SCANTER radar) and turbine G05 (LAWR radar) by the technician.

RADAR BLIND SECTOR Area set where no radar pulses will be transmitted due to either safety issues or structures obstructing the radar beam.

ROTOR Part of a wind farm that extract kinetic energy from the air and coverts this wind into rotational energy in the drive train. The current generation of horizontal axis turbines have rotors with three blades.

ROTOR-SWEPT ZONE (RSZ) Zone swept by the rotating turbine blades of a wind farm. For Thanet Offshore Wind Farm the rotor-swept zone has a diameter of 90 m. For the purposes of analysing empirical micro avoidance, the RSZ refers to the circle drawn by the rotor blades, while the rotor refers to the ellipse representing the blades at any given time.

SCANNING RANGE Sensor scanning range set for this study (radars). The scanning range of the radars has been set to allow seabird detection in the main area of interest, considering detection specific probability curves (DPC).

SENSOR The radars, laser rangefinders and cameras used in this study to detect flying seabirds and collect bird behavioural information at different scales (macro, meso, micro) as well as detailed data on flight heights.

NIRAS DHI CARBON TRUST

TECHNICIAN

Part of the two-person observer team with responsibility for operating the radar during survey deployment turbine G01 (SCANTER radar) and turbine G05 (LAWR radar), detecting, selecting and following on the radar screen potential bird tracks by using DHI's BirdTracker software.

TRACK

Recorded trajectory of one or several birds by study sensors. A track is made of different recorded positions or nodes.

TRACK ABUNDANCE METHOD

Estimation of empirical avoidance rates based on a ratio of the abundance of bird tracks detected in avoidance/non-avoidance areas.

TRACK DENSITY METHOD

Estimation of empirical avoidance rates based on a ratio of the density of bird tracks detected in avoidance/non-avoidance areas. This can be estimated using the number of tracks within a given area, or using the lengths of tracks within a given area.

NIRAS DHI CARBON TRUST

EXECUTIVE SUMMARY

The Offshore Renewables Joint Industry Programme (ORJIP) Bird Collision Avoidance (BCA) Study

The ORJIP BCA study, 2014 - 2017, has been designed to improve the evidence base for seabird avoidance behaviour and collisions around offshore wind farms, with the aim of informing impact assessment and supporting consenting applications for the offshore wind industry.

Driven by ambitious renewable energy targets and reduced costs, the offshore wind industry has experienced a significant growth over the last 20 years, particularly in Europe, where the majority of installed capacity can be found.

The consenting process of offshore wind projects requires the identification, prediction and evaluation of the environmental effects of those proposed projects. In this context, the risk of birds colliding with turbine blades during operation is potentially one of the most significant environmental impacts predicted. In order to quantify bird collision risk, collision risk models (CRM) are used and parametrised with technical specifications of the turbines, bird densities, morphology and flight behaviour of existing bird populations present on site. The CRM e.g. the Band model (Band 2012), provides an estimate of the potential number of bird collisions likely to occur at a proposed wind farm assuming that birds take no action to avoid colliding with the wind turbines. In order to obtain realistic risk estimates, the collision risk modelling is subsequently corrected to take account of behavioural responses of birds to the presence of wind farms (i.e. avoidance). However, there is considerable uncertainty over the scale of such impacts due to the relatively few offshore monitoring studies so far undertaken, that have gathered empirical evidence.

As the number of offshore wind farm projects increases, it is widely recognised that in order to minimise consenting risks for future project applications, further robust evidence on the avoidance behaviour of seabirds is required to inform CRM and environmental impact assessments.

This study has centred its work around four main phases:

I. **Development of a bird monitoring system,** that allows detecting and tracking bird movements at the species level in and around an operational offshore wind farm, including testing and validation of video monitoring coupled with radar technology under different weather and visibility conditions.

II. **Monitoring of bird behaviour at Thanet Offshore Wind Farm**, deploying a multiple sensor monitoring system partly operated by experienced seabird observers (laser rangefinders and radar equipment), and partly automated through the collection of video evidence, with a focus on five target species: Northern Gannet, Black-legged Kittiwake and three species of large gulls (Lesser Black-backed Gull, Herring Gull, Great Black-backed Gull).

III. Development of an appropriate methodology for data analysis to **quantify empirical avoidance behaviour** termed as empirical avoidance rates (EARs), based on existing research and equipment / data limitations.

IV. **Formulation of recommendations** on the use of empirical evidence gathered by this study in support of collision risk assessments in offshore wind planning applications.

This report presents the final publication of the study and presents findings associated with these four phases.

Development of a bird monitoring system

The study's monitoring system was designed to collect reliable data on bird avoidance behaviour at the three different spatial scales into which bird avoidance behaviour can be broken down:

- **macro avoidance,** defined in this study as bird avoidance responses to the presence of the wind farm occurring beyond the wind farm perimeter up to 3 km, considered to result in a redistribution of birds. Data used to inform macro avoidance have been collected by experienced seabird observers from two different turbines located at the corner and along the periphery of the wind farm. In addition to bird observers, radar equipment was used for bird detection and tracking (SCANTER and LAWR radars), and laser rangefinders for flight height measurements and tracking (with detectability up to 1.5 km). While the SCANTER radar has a high and uniform detection probability across the area of interest, LAWR radar's detection is variable and more sensitive to sea clutter, resulting in a lower sample size. Accordingly, although useful to guide target selection by observers using rangefinders, the LAWR radar data has eventually not been used to quantify macro avoidance.

- **meso avoidance**, defined in this study as bird avoidance responses within the wind farm footprint to individual turbines (considering a 10 m buffer around the rotor-swept zone), resulting in a redistribution of the birds within the wind farm footprint. Data used to inform meso avoidance have been collected from two different turbines located inside the wind farm, using 24/7 automated LAWR radars for bird detection (recording initial detection points or 'trigger points') connected to Thermal Animal Detection System (TADS) cameras that follow recorded bird movements by the radar. Only data collected within the high detection zones of the LAWR radar have been used to quantify meso avoidance. To ensure applicability in the Band CRM birds recorded flying either above or below the rotor-swept zone without vertical adjustments of flight behaviour were not included in the estimation of meso avoidance. The development of software for integration of radar and camera tracking has been a major component of this study, tested and validated at test sites before deployment at Thanet Offshore Wind Farm.

- **micro avoidance,** defined as bird behavioural responses to single blade(s) within the rotor-swept zone (including a 10 m buffer), it is considered as the bird's 'last-second' action taken to avoid collision. Unlike for meso avoidance, micro avoidance has been assessed using a dynamic ellipse (rather than a circle) represented by the rotor blades during each crossing of the RSZ by a seabird. Birds recorded in the rotor-swept zone when the rotor was not spinning (due to either low wind speed or service operations) were not included in the estimation of micro avoidance. As in the case of meso avoidance, data used to inform micro avoidance has relied on data collected by the automated LAWR radar and TADS camera systems, which have also been able to record collision events.

Equipment characteristics and limitations are further discussed in the report.

Monitoring of bird behaviour at Thanet Offshore Wind Farm

Located approximately 12 km off Margate, Kent (UK), Thanet Offshore Wind Farm is considered a representative example of UK Round 3 offshore wind developments, with 100 3 MW turbines distributed over an area of 35 km^2. The site was considered appropriate for the study of target species' behaviour, given the greater abundance of these target species during post-construction surveys and due to logistical suitability in contrast with other sites considered.

The monitoring system was installed at Thanet during the summer of 2014, with data collection commencing the 1 July 2014 by seabird observers using laser rangefinders from two different turbines, prior to installation of the SCANTER and LAWR radars in August 2014. Deployment of seabird observers, subject to weather and vessel availability, continued up to April 2016, with a total of 230 deployment days achieved.

Automated tracking by the TADS Camera system coupled with LAWR radars was delayed to late October 2014, and continued up to June 2016, when all equipment was decommissioned.

Observers operating the radars located at the corner and periphery of the wind farm collected a total of 1,555 tracks for the five target species, of which 1,205 were collected using the SCANTER radar (and included in the analyses). 1,390 tracks were collected using the laser rangefinders (and included in the analyses) from both observer platforms.

The TADS camera system coupled with the LAWR radar collected a total of 12,131 daylight videos showing bird movements within the wind farm. Due to the use of magnetron radars coupled with the camera system, highly sensitive to wave and rain clutter, data collection resulted in a large number of additional videos being

NIRAS DHI CARBON TRUST

recorded without bird presence (high false positive rate).

At the meso scale, video evidence and associated radar trigger points have been used to quantify meso avoidance at the species level, with the exception of Lesser Black-backed Gull. At the micro scale, due to the limited number of birds approaching the rotor, it has only been possible to quantify behaviour for all seabird species as a whole, and for large gulls as a group.

Although a total of 459,164 videos were collected during night time, only a sample of 48,000 night videos has been processed, finding that only 0.2% had recorded flying bird activity, and therefore limiting analysis of nocturnal seabird avoidance.

Development of an appropriate methodology for data analysis to quantify Empirical Avoidance Rates (EARs)

The Empirical Avoidance Rates (EARs) methodology was developed to be suitable for quantifying the avoidance rates based on the collected data in this specific study and the specific data challenges at each EAR scale. Therefore EARs derived by this study are considered to represent the likely degree of successful avoidance of an offshore wind farm by seabirds. The overall EAR is composed of combining EARs at the three different spatial scales mentioned above:

- **macro avoidance,** quantified by comparing the observed density of bird tracks density (measured as track length per unit area) inside the wind farm area with a hypothetical situation in the absence of the wind farm in which the same total track length would have been observed in the whole area (inside and outside the wind farm up to 3 km).

- **meso avoidance,** quantified by comparing the observed density of bird tracks (measured as track length per unit area) inside the rotor-swept zone (considering a 10 m buffer) within the wind farm, with an hypothetical situation in the absence of the wind farm in which the same total track length would have been observed in the whole area (inside and outside to rotor-swept zone and buffer).

- **micro avoidance,** quantified by calculating the proportion of birds adjusting to the presence of blades to all birds entering the rotor-swept zone, considering bird movement in relation to the rotor, represented as a dynamic ellipse, surrounded by a 10 m buffer that changes its orientation with the wind direction.

The methodology used for the calculation of EARs at macro and meso avoidance scales was developed through the course of the study, considering different options for the treatment and analysis of radar and rangefinder data. The original methodology based on the comparison of track counts in avoidance areas within 3 km distance, was revised to account for the size of areas compared, i.e. quantification of track densities. In order to avoid results being influenced by dissimilarity in the size (and geometry) of areas compared, these were analysed by dividing these areas into units of same size, and track density calculations were approached by measuring the length of bird tracks within each unit area

At the macro scale, the availability of full radar and rangefinder tracks has enabled the easy calculation of track lengths. However, at the meso scale, only radar trigger points were collected, requiring special treatment for the modelling of mean track lengths, thereafter classified in line with behaviour observed in video evidence, and corrected by the use of flight speed data collected by laser rangefinders to ensure these were as close to reality as possible.

Study results and behavioural interpretation

In relation to **macro avoidance analysis,** the majority of Northern Gannets were observed to avoid the wind farm (macro EAR = 0.797 ± 0.153 SD; the given standard deviation reflects the variability based on bootstrapping combined with other assumed uncertainty components). Of the total number of observed Northern Gannets, a large number were observed to be concentrated within 1.5 km distance outside the wind farm, which may be attributed to a redistribution of birds or "ponding" caused by the introduction of the wind farm. On average this species was recorded to fly in a southerly direction during all seasons and below the rotor tip (17 m,

median value), showing a bimodal flight distribution, with 27% of birds recorded with the rangefinder flying at rotor height, and at flight speeds that coincide with previous studies (mean of 13 m/s). Similarly, Black-legged Kittiwake data (macro EAR = 0.566 ± 0.169 SD) showed an aggregation of birds just outside the wind farm, on average flying at 33 m (median value), having 77% of birds flying at rotor height, and average flight speeds of 8.7 m/s.

Large gulls were observed to show variable flight patterns. The sample size for Lesser Black-backed Gull (macro EAR = 0.619 ± 0.198 SD) was the smallest of all target species, showing slight changes in behaviour between platforms, flying on average at the rotor height (median 31 m, 67% of birds flying at rotor height) and flight speed measured at 10.1 m/s. The sample size for Great Black-backed Gull (macro EAR = 0.464 ± 0.196 SD) was the largest among large gull species, showing signs of aggregation closer to the wind farm and lower avoidance. This species had the highest recorded median flight height in this study, 40 m, with 81% of birds recorded using the rangefinder flying at rotor height, and flight speeds in the order of 9.8 m/s. The pattern observed for Herring Gull (macro EAR = 0.422 ± 0.199 SD) also indicates a low degree of avoidance, and those birds recorded entering the wind farm did not seem to penetrate beyond the first two turbine rows inside the wind farm. The median height recorded for this species was 36 m, with 77% of birds (recorded using the rangefinder) flying at rotor height. The mean recorded flight speed was 9.7 m/s.

Interpretation of data collected by this study suggests that there is a degree of avoidance shown by large gulls, however, local factors, such as the presence of fishing vessels in the vicinity of the area situated outside the wind farm, may have played a role in the redistribution of birds observed.

Although it is recognised that there is a difficulty in disentangling the relative importance of different factors that may be influencing the results, it is considered that the range of 3 km used to analyse macro avoidance is an appropriate compromise between behaviour observed (in this study and others) and equipment limitations. It must be acknowledged that there is uncertainty on the extent to which avoidance may have occurred beyond 3 km, which has not been captured by the study's data.

A large sample on meso avoidance was achieved, and the **meso avoidance analysis** final results show that empirical meso avoidance is significantly stronger than macro avoidance in all target species, with rates estimated at 0.961 (±0.175 SD) for Herring Gull, 0.921 (± 0.174 SD) for Northern Gannet, 0.916 (±0.177 SD) for Black-legged Kittiwake, 0.894 (± 0.174 SD) for Lesser and Great Black-backed combined, and 0.842 (±0.177 SD) for Great Black-backed Gull.

The vast majority (96.8%) of recorded seabirds avoided the turbines by flying between the turbine rows, while 3.2%, displayed meso avoidance by adjusting flight height to fly below the rotor-swept zone.

Regarding **micro avoidance analysis,** an empirical micro avoidance rate of 0.950 (±0.114 SD) was calculated for all seabirds recorded as a whole, slightly higher if only large gulls are considered in this quantification (0.957 ±0.115 SD).

These high rates reflect bird behaviour observed in videos. Of the 299 videos with birds recorded within the rotor-swept zone (including a 10 m buffer), only 6 collisions were recorded, with most of birds observed crossing the rotor-swept zone with adjustments in their flight path, with birds often flying parallel to the rotor. However, since only 15 instances of seabirds crossing perpendicularly to the spinning rotor were observed, this indicates a high risk of collision by seabirds when crossing perpendicularly to the spinning rotor blades.

The small sample of night videos analysed indicates that seabird flight activity around offshore wind farms during night time is very limited when compared to daylight activity (nocturnal activity has been estimated at 3%), which suggest that risk of collision reduces significantly overnight.

Considering the different avoidance components described above, overall EARs have been estimated, in which the bootstrap standard deviation (describing variability) are combined with other assumed components of uncertainty (which cannot be quantified) to reflect the overall uncertainty around each EAR. These "unknown" uncertainties have been given values based on informed assumptions.

The uncertainty represents a combination of uncertainties associated with each scale. It is considered that it would be more appropriate to use EARs as a range of values, instead of just using the mean value. EAR estimates ± standard deviations (combining variability and uncertainty components) are:

- Northern Gannet: 0.999 ± 0.003

- Black-legged Kittiwake: 0.998 ± 0.006

- Herring Gull: 0.999 ± 0.005

- Great Black-backed Gull: 0.996 ± 0. 011

- Lesser Black-backed Gull: 0.998 ± 0.006

- All large gulls: 0.998 ± 0.007

A sensitivity test was also undertaken to better understand the contribution of each scale of avoidance to overall EAR calculations concluding that micro and meso scales are the most influential in comparison to macro.

Recommendations on use of empirical evidence gathered by this study

This study provides important and enhanced input for CRM, including species-specific data on flight speed and track speeds that can inform the estimation of more realistic flux of birds; nocturnal night activity, which seems to contribute to a negligible proportion of total flight activity of target species (< 5%); and detailed data on the frequency of flight heights.

This study indicates that bird avoidance behaviour is likely to lead to a greater reduction in estimated collision rates than current correction factors (Avoidance Rates) applied to CRM assume. The differences between Avoidance Rates (ARs) and EARs are mainly driven by the fact that the former have been developed from land-based studies using the Band CRM to fit the observed number of collisions from carcass surveys while assuming flight speeds through the wind farm as linear flight patterns. However, the empirical flight speeds obtained by this and other studies clearly indicate that seabirds typically perform non-linear movements within a wind farm. It is therefore recommended to apply empirical flight speed data like the ones from this study when using the EARs with the Band CRM.

The *study's EARs* are considered the best available empirical information to account for avoidance behaviour in seabirds which can be readily applied in CRM. However, there are inherent limitations, including the fact that they rely on data collected at one site only, largely during daylight and benign weather conditions at the macro scale, and therefore may not capture all the variability in relation to weather conditions or visibility and regional differences.

This study has generated the most extensive dataset of observations of seabird behaviour in and around an operational offshore wind farm that is currently available. It is recommended that Statutory Nature Conservation Bodies, and other technical advisers to planning decision-makers, consider their advice on appropriate Avoidance Rates for collision risk modelling to better reflect the unprecedented collection of empirical seabird avoidance behaviour and EARs derived in this study.

① INTRODUCTION

1.1. BACKGROUND TO THE STUDY

1.1.1. The development of renewable energy sources is becoming increasingly important in the decarbonisation of our global economy. Within the renewable energy mix, wind energy is becoming a key player, with a total wind capacity of 486 GW installed worldwide at the end of 2016, 14.4 GW of which is generated offshore (GWEC 2017). At the European scale, wind energy covers around 10.4% of the EU's electricity demand and it is overtaking coal as the second largest form of power generation capacity (WindEurope 2017). Europe also accounts for 87.5% of offshore wind energy produced worldwide, and it is considered on track to reach at least 24 GW of cumulative installed capacity by 2020 (GWEC 2017).

1.1.2. As in the case of other industries, there are a number of potential environmental impacts associated with the location, construction, operation and removal phases of offshore wind energy developments. In Europe, the Environmental Impact Assessment (EIA) Directive 85/337/EEC (as amended) provides a legal framework for the assessment of environmental effects of projects that are likely to have significant effects on the environment, which is often applicable to new offshore wind projects. An EIA is a systematic process that identifies, predicts and evaluates environmental effects of proposed projects, and identifies any required mitigation measures, informing the project's design.

1.1.3. Cornerstones to EU's biodiversity policy, the Habitats 92/43/EEC and Birds 2009/147/EC Directives include strict legal provisions relating to the assessment of planned developments that have the potential to affect nature conservation interests, including Special Areas for Conservation (SAC) and Special Protection Areas (SPA), belonging to the Natura 2000 network, the Ramsar Convention and national legislation, as well as specific protection afforded by various multilateral agreements.

1.1.4. The construction and operation of offshore wind farms can affect bird populations through reduced habitat utilisation, barrier to movements and collision mortality (Langston and Pullan 2003). Environmental assessments are often required to include a quantitative estimate of collision risk for all bird species present on the site for which the level of risk has the potential to be important (Band 2012). To quantify bird collision risk, collision risk models (CRM) (see Band (2000), Band et al. (2007), and Band (2012), promoted in guidance published by Scottish Natural Heritage (e.g. SNH 2000)) use technical specifications of the turbines and flight speed and behaviour of existing bird populations on site. Models are often finally corrected to take account of behavioural responses of birds to the presence of wind farms and the turbines within, by multiplying the model's outcome with a correction factor that takes into account, among other things, avoidance.

1.1.5. Correction factors currently used in CRM to account for avoidance behaviour are based on post-construction comparisons of the number of estimated/modelled collisions. They are often based on data from onshore wind farms (with specific turbine designs in a different landscape where birds potentially behave differently), and the number of collisions predicted pre-construction based on high bird speeds with linear flight patterns (Cook et al. 2014). Compliance with regulatory requirements increasingly demands clear evidence on how seabirds behave within and around offshore wind farms, and therefore further robust evidence on the level of avoidance behaviour offshore is required.

1.1.6. To fill-in this gap and improve understanding of bird behaviour around offshore wind farms, the use of radars has increasingly been applied for tracking movements of waterbirds and seabirds over open sea and obtain empirical evidence. As surveys only represent snapshots and telemetry is based on few individuals, radars have become an indispensable tool for obtaining long-term monitoring data on seabird behaviour at wind farms. In this context, the use of surveillance radars (e.g. LAWR 25 radar) with limited detection range (up to 3 – 4 km) and capacity to suppress sea clutter has been the predominant choice (Blew et al. 2008; Petersen et al. 2006; Krijgsveld et al. 2011; Skov et al. 2012; Plonczkier and Simms 2012). Video recording of bird activity within offshore wind farms has also been considered (Desholm 2003; 2005), although to date only small samples of bird behaviours around turbines offshore have been available.

NIRAS DHI CARBON TRUST

1.1.7. With the aim of reducing consenting risks for offshore wind and marine energy projects, the Offshore Renewables Joint Industry Programme (ORJIP) Bird Collision Avoidance study has been designed to use efficient technologies for the monitoring of seabird movements and avoidance behaviour at an operational offshore wind farm, considering different spatial scales.

1.1.8. The empirical evidence collected by this study is expected to better calibrate assumptions about the avoidance of seabirds when modelling collision risk.

1.2. STUDY OBJECTIVES

1.2.1. The ORJIP BCA study has been designed to improve the evidence base for bird avoidance behaviour and collisions around offshore wind farms through the monitoring of seabird behaviour, focusing on five target species; and to support consenting applications for offshore wind development.

1.2.2. The objectives of the study include:

Objective 1 – Select suitable equipment that can be deployed to measure micro, meso and macro avoidance behaviour and, if appropriate, collision impacts.

Objective 2 – Measure the level of bird behaviour at an offshore wind farm (i.e. Thanet Offshore Wind Farm, UK) and provide robust evidence on the rates of avoidance and collision for several target species identified as being at risk from collision with offshore wind turbines.

Objective 3 – Determine how data from this study can be applied to support consenting applications for other sites.

1.3. REPORT STRUCTURE

1.3.1. This report summarises main findings and recommendations related to Objectives 1 – 3 above:

Section 2
describes the scope of the study, including limitations and assumptions associated with concepts used to define and quantify bird avoidance behaviour in relation to the way avoidance is accounted for in CRM.

Section 3
presents the monitoring system implemented as part of the study, considering the initial design, testing and validation of the equipment, and its deployment offshore (installation, operation and decommissioning). An overview of data collected and sample size for each scale of avoidance is also provided.

Section 4
provides a brief overview of the development history of data analysis methods, and describes the final methodology applied to data collected as part of the study for the five target species at the three avoidance scales considered: macro, meso and micro. Analytical steps followed in the analysis of night videos, and rangefinder data in relation to flight speed and flight height are also presented.

Section 5
presents the study's results, including the quantification of bird avoidance behaviour, expressed as empirical avoidance rates (EARs); as well as flight speed and flight heights recorded using the rangefinders.

Section 6

provides a descriptive overview of bird behaviour observed and interpreted, comparing findings with relevant literature. This includes interpretation of nocturnal activity observed in video evidence collected by this study.

Section 7

introduces collision risk assessment and the role that avoidance plays in current CRM. The applicability of findings from this stu ssed.

Section 8

identifies existing gaps and study limitations, and provides recommendations for future work based on lessons learned from this study.

Section 9

concludes with a summary of main findings of the study and final recommendations.

1.3.2. In addition, this report includes the following appendices:

Appendix 1 – Detailed description of the Sensor Equipment characteristics, including tests undertaken before deployment of the equipment at Thanet Offshore Wind Farm, and the equipment application throughout the duration of the study

Appendix 2 – Exploration of data collected at the macro scale

Appendix 3 – Observer protocol for data collection

Appendix 4 – Fieldwork effort and recommendations on the design and deployment of monitoring systems

Appendix 5 – Weather conditions recorded during the monitoring period at Thanet Offshore Wind Farm

Appendix 6 – Monthly breakdown of radar / rangefinder track data used in analysis

Appendix 7 – Monthly breakdown of video data used in analysis

Appendix 8 – Options considered and/or tested in the analysis of radar and rangefinder track data

Appendix 9 – Sample size and precision

Appendix 10 – Influence of flight speed and pre-construction bird density on flux factor

1.3.3. Figure 1.1 illustrates the structure of the report identifying the content of sections and their supporting appendices.

Figure 1.1   Report structure.

INTRODUCTION
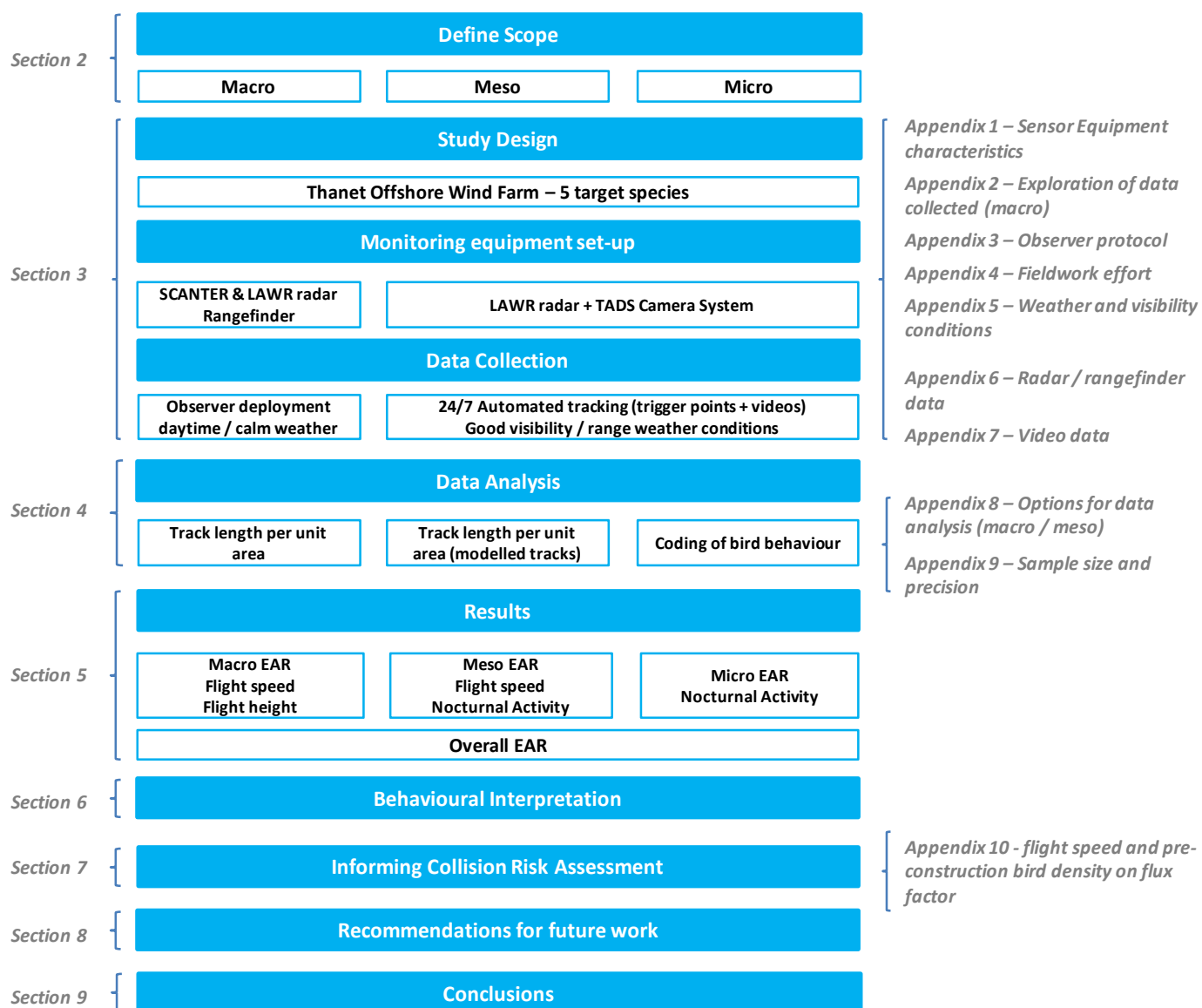
② SCOPE OF THE STUDY

2.1. STUDY AREA AND STUDY SPECIES

2.1.1. Thanet Offshore Wind Farm (hereafter referred to as Thanet) was selected as the host for the deployment of the study's monitoring system given its size, considered to represent most of proposed developments under Round 3; anticipated abundance of target species, and lack of logistical constraints, as opposed to some of the other sites that were originally considered, such as Walney or Burbo Bank offshore wind farms, where construction works were scheduled to coincide with the monitoring programme.

2.1.2. Thanet is located approximately 11 km off Foreness Point, Margate, at the most eastern part of Kent in the UK (Figure 2.1), and consists of 100 Vestas V90 3 MW wind turbines located in water depths of 15-25 m below chart datum, covering an area of 35 km².

Figure 2.1.   Thanet Offshore Wind Farm location. The figure is not to scale.
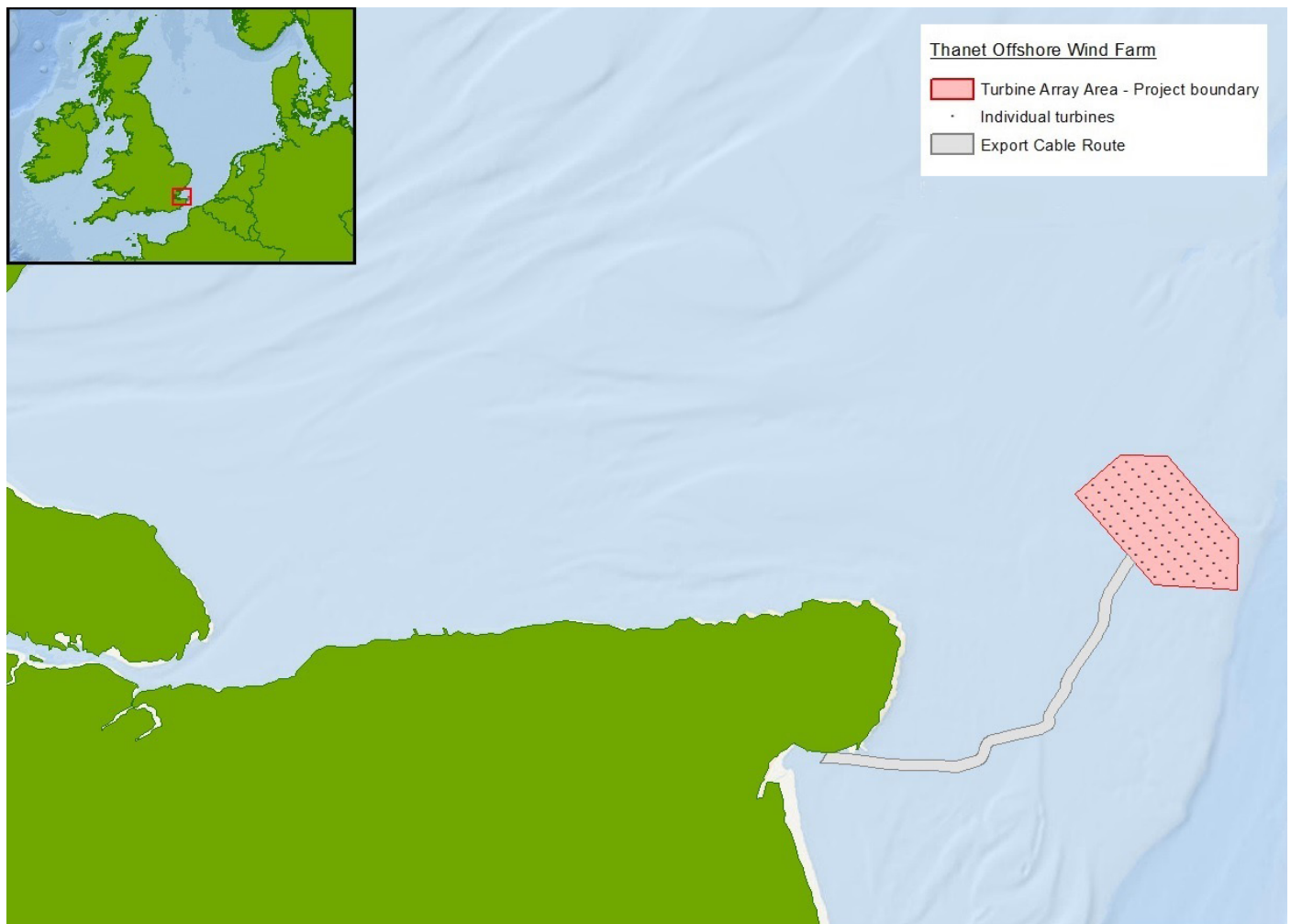
2.1.3. Table 2.1 provides an overview of key characteristics of Thanet's configuration.

Thanet Offshore Wind Farm facts and figures.

Source: https://corporate.vattenfall.co.uk/projects/operational-wind-farms/thanet/

Year of commissioning	**2010**
Wind farm site	**35 km²**
Number of wind turbines	**100**
Wind turbine type	**Vestas V90 3MW**
Maximum installed capacity	**300 MW**
Distance between wind turbines	**500m (along rows) & 800m (between rows)**
Rotor diameter	**90 m**
Hub height	**70 m**
Lower and upper tip of the rotor	**25 m/115 m above sea level**
Turbine platform height (placement of monitoring system)	**13 m above sea level**

2.1.4. Pre-construction boat-based surveys[1] undertaken at Thanet during winter 2009 recorded the five target species at mean densities across the survey area peaking between 0.2 – 1.3 birds/km² dependent upon species, with an even distribution across the area, except for small aggregations commonly found in association with trawlers. Most species were recorded flying below rotor height (22.5 m) (Royal Haskoning 2009).

---

[1] Survey methods included boat-based line transects of the study area. Pre-construction surveys consist of three surveys within the 2009 winter period, with one survey undertaken in Feb 2009 (including the wind farm site itself, a control area south of the site and two buffer zones (1 km and 4 km) surrounding the wind farm site) and two surveys undertaken in Mar 2009 (including the wind farm site itself, a control area south of the site and two buffer zones (1 km and 2 km) surrounding the wind farm site).

[2] The post-construction monitoring programme includes twelve surveys per annum undertaken between 2010 – 2013 during the wind farm operation, comprising bi-monthly surveys during the key overwintering season between October and March. The surveys cover the wind farm site itself, a control area south of the site and two buffer zones (1 km and 2 km) surrounding the wind farm site.

2.1.5. Post-construction boat-based surveys[2] undertaken between October 2010 and March 2011 at Thanet show similar abundance of target species, with increased activity for Great Black-backed Gull and Black-legged Kittiwake (Royal Haskoning 2011). Large gulls and Black-legged Kittiwake were widely distributed across the surveyed area, while Northern Gannet were more frequently recorded in the eastern part of the surveyed area. The proportion of birds flying at rotor height varied between species: Northern Gannet (7%), Black-legged Kittiwake (17%) and large gulls (30 – 42%).

2.1.6. Thanet is an area where the target species can be considered comparatively abundant, particularly during winter. During the rest of the year, it is considered that the abundance of large gulls remains high, while that of Northern Gannet and Black-legged Kittiwake is markedly lower during the breeding season.

2.1.7. The seasonal changes in bird distribution is also one of the reasons why the study has not attempted to distinguish between behaviour observed during different parts of the year, as sample sizes were anticipated to vary significantly, particularly in the case of Black-legged Kittiwake and Northern Gannet.

2.2. SCALES OF BIRD AVOIDANCE BEHAVIOUR

2.2.1. Collision risk assessment is undertaken using Collision Risk Modelling (CRM), e.g. the Band model (Band 2012), which provides an estimate of the potential number of bird collisions likely to occur at a proposed wind farm assuming that birds take no action to avoid colliding with the wind turbines. An avoidance rate factor is then applied to take account of the likely degree of successful avoidance. Species-specific generic avoidance rates currently used are mostly based on mortality rates observed at onshore wind farms with no consideration of actual avoidance behaviour (see Section 7).

2.2.2. Birds can avoid colliding with wind farm structures through avoidance behaviour, often comprising fleeing responses, activity shifts or changed habitat utilisation. Avoidance responses therefore result in a reduced number of birds entering and possibly avoiding wind turbines, influenced by external factors, such as wind and topography (May 2015).

2.2.3. To facilitate the understanding of seabird avoidance-related decisions, the concept of avoidance can be considered at three different spatial scales: birds may avoid the wind farm area (i.e. macro avoidance), turbine arrays or single wind turbines (i.e. meso avoidance) and last-second evasion of rotor blades (i.e. micro avoidance) (Cook et al. 2014).

2.2.4. The definitions of these scales originally provided by Cook et al. (2014) have been modified in this study in order to be as suitable as possible for the analysis of the study's collected data, and as much as aligned as possible to the assumptions made by the Band model (Band 2007) on bird behaviour.

2.2.5. Avoidance can be studied through the identification of underlying mechanisms for avoidance, but it can also be analysed and quantified through the distributional patterns assumed to result from such behaviour. While the former approach is used to analyse micro avoidance, the latter approach is mainly used to analyse macro and meso avoidance. However, there is some degree of uncertainty on whether observed redistribution patterns are fully a consequence of the wind farm's introduction, as local conditions may play a role.

2.2.6. This section describes the three scales considered by the study and identifies limitations associated with the data and methods and assumptions made that have been necessary to interpret the results.

a. Macro Avoidance

2.2.7. In this study, macro avoidance is defined as bird avoidance responses to the presence of the wind farm occurring beyond its perimeter (and the rotor-swept zone (RSZ) of the outermost turbines), resulting in a redistribution of birds. Macro avoidance results in a bird altering its flight trajectory in response to the wind farm presence, which can pose a barrier to movements (i.e. barrier effect), or affect the birds' underlying habitat (i.e. displacement).

NIRAS DHI CARBON TRUST

2.2.8. Given that flight height distribution outside the wind farm is a parameter separately used in CRM, in this study, macro avoidance is quantified based on the horizontal re-distribution assumed to result from the introduction of the offshore wind farm. At the same time, given that there is no pre-construction data suitable for comparison[3], the observed distribution of bird track density (measured as track length per unit area) inside the wind farm area is compared with a hypothetical situation in the absence of the wind farm, in which the same total track length would have been observed, but with the same bird density inside and outside the wind farm up to 3 km (see Section 4.2). Figure 2.2 illustrates the redistribution concept at the

Figure 2.2. Illustration of macro avoidance concept and approach to analysis considered in this Study. Blue birds represent bird track density calculated outside the wind farm (red line defines its perimeter) up to 3 km (red dotted line), while orange birds represent bird track density calculated inside the wind farm perimeter. Blue circles represent turbine positions and the green square represents the area used to illustrate meso avoidance (see Figure 2-2).
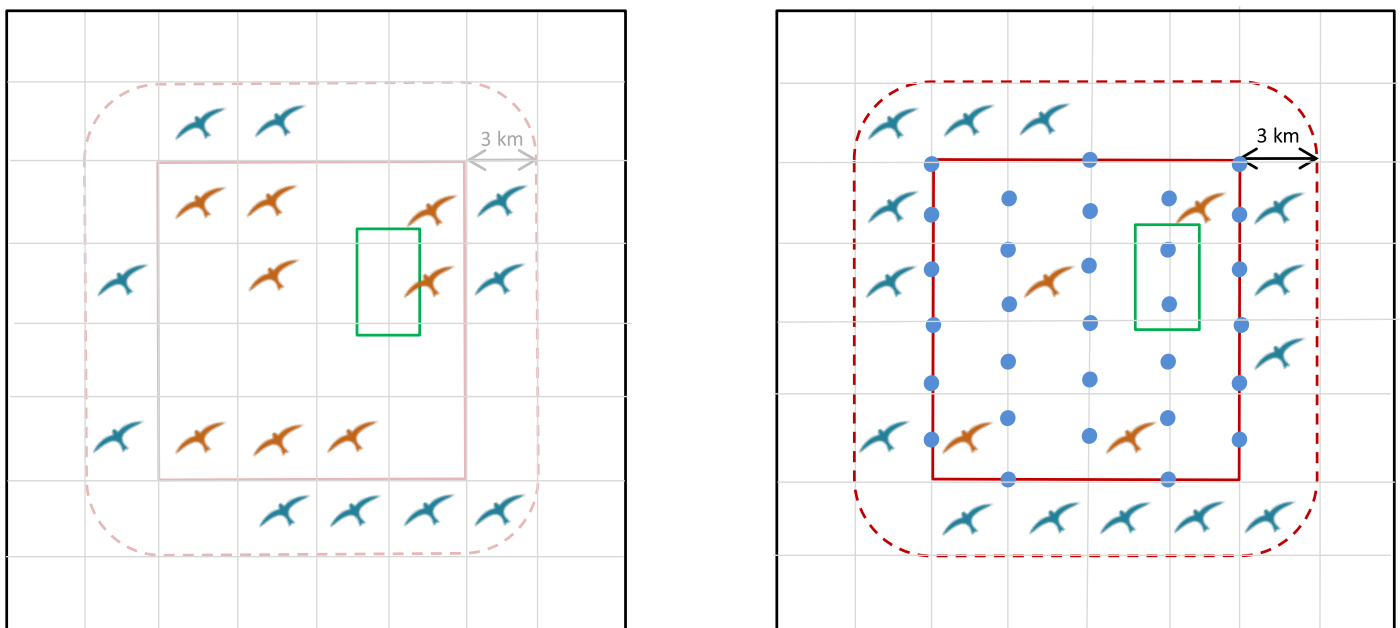
In the absence of the wind farm

assumes same bird density inside / outside the wind farm up to 3 km

Wind farm presence

observes redistribution inside / outside the wind farm up to 3 km

Outside area	10 birds /20 cells	0.5 birds / cell	Outside area	14 birds /20 cells	0.7 birds / cell
Inside area	8 birds / 16 cells	0.5 birds / cell	Inside area	4 birds / 16 cells	0.25 birds / cell
Total	18 birds / 36 cells	0.5 bird / cell	Total	18 birds / 36 cells	0.5 bird / cell

---

[3] Pre-construction data was collected through boat-based surveys of the wind farm plus a 2 km buffer, and provide a few snapshots only of seabird distribution. The age of the data (2009) makes population changes over the years very possible, and difficult to quantify with existing data.

macro scale using a simplified example with no more than one bird per cell representing track density.

2.2.9. In this study, macro avoidance is analysed using data collected from two different turbines (see Section 3.1) using radar equipment for bird detection and tracking (on a turbine located at a corner of the wind farm), and rangefinders for flight height measurements and tracking within 1.5 km outside the wind farm (on turbines located at the corner and along the periphery of the wind farm). Data collection relies on fieldwork effort and equipment performance (see Section 3.3 and 3.4), and therefore no absolute densities can be calculated. However, the tracking effort is similar inside and outside the wind farm, allowing for comparison between areas.

2.2.10. Only data collected within 3 km outside the wind farm is used in macro avoidance analysis, considered as the optimal range for the analyses given a trade-off between the optimal range of radar detection and observed bird distribution (see Appendix 2, Section 4). The analysis of detections of bird echoes from a selection of radar screen images recorded by the SCANTER radar corroborates the occurrence of aggregations of flying seabirds at distances shorter than 2 km from the wind farm periphery at Thanet (see Appendix 2, Section 1). Although there is uncertainty as to whether this redistribution is solely a consequence of the wind farm's installation, these findings do not seem to be specific to the Thanet site, but have also been reported by other post-construction studies at offshore wind farms:

2.2.11. Petersen et al. (2006) found that the response of waterbirds towards the Nysted Offshore Wind Farm was graded with a tendency for significant deflection to occur in two steps: a first and relatively slight deflection at distances between 1.0 and 3.0 km, and a more radical deflection at 0.5 km or closer.

2.2.12. Krijgsveld et al. (2011) found bird density within 5.5 km of Egmond aan Zee Offshore Wind Farm, to initially increase with distance from the wind farm to a peak at 750–1,500 m, and thereafter decrease or remain constant. It was also found that alteration in flight direction in response to the wind farm most commonly occurred within 1 km of the site.

2.2.13. Skov et al. (2012a) found when waterbirds and seabirds responded to Horns Rev 2 Wind Farm, most did so when within 2 km distance of the site.

2.2.14. The displacement distances reported by Welcker & Nehls (2016) for a number of seabird species or species groups indicated also that the displacement levelled off within 3 km.

Assumptions in macro avoidance analysis

2.2.15. Macro avoidance analysis assumes that the same total track length (track density) is observed post-construction within the wind farm + buffer, as would have been observed in that area in the absence of the wind farm, and therefore assumes no displacement caused by the wind farm beyond 3 km (see Section 4.2). This assumption is supported by the radar screen data collected over a larger geographical areas outside the wind farm (Appendix 2).

2.2.16. Macro avoidance analysis assumes that the track density (track length per unit area) in the absence of the wind farm would have been uniform across the wind farm + buffer, i.e. one would have observed the same track density within both wind farm site and buffer (in the absence of the wind farm).

2.2.17. Macro avoidance analysis assumes that the bird speed is the same within the wind farm as within the buffer.

2.2.18. The comparison of bird track density inside and outside the wind farm collected by the study's monitoring system assumes that equipment detection of seabirds is comparable in both areas (see Appendix 2, Section 1).

2.2.19. Data informing empirical macro avoidance has been collected from two locations, a turbine located at the corner (by use of a radar and rangefinder) and a turbine located at the periphery of the wind farm (by use of a rangefinder only). Given that data are combined, and more data were collected from the corner it is likely that estimates are more representative of the corner of the wind farm. However, avoidance at the

corner is slightly lower, and scaling up of data to the wind farm provides a conservative estimate that is assumed to be representative for the whole wind farm (see Section 2.3).

2.2.20. The radar data used to analyse macro avoidance have only been extracted within 3 km distance, representing the area of redistribution. However, the rangefinders data have only been extracted within 1.5 km distance (Section 3.1). Comparison of datasets collected by both types of sensors indicates that the density recorded within this range by the rangefinder is representative for the whole 3 km area, and accordingly that the different data sets can be combined.

Limitations in macro avoidance analysis

2.2.21. Data analysis quantifies distributional patterns, i.e. differential use of the wind farm area and surroundings (up to 3 km) in relation to the assumed situation in the absence of the wind farm, which is independent of the underlying mechanisms for avoidance. However, there is a degree of uncertainty on whether this redistribution is a sole consequence of the wind farm's introduction, or whether other factors, such as the presence of fishing vessels have influenced the distribution by causing attraction of gulls to specific fishing areas outside the wind farm. Data collected is interpreted separately (see Section 6).

2.2.22. Collected data does not allow assessing potential displacement / barrier effects occurring beyond 3 km, and therefore a level of uncertainty still exists regarding seabird's potential responses to wind farms beyond this distance. Consequently, overall macro avoidance may be underestimated.

2.2.23. Species identification by observers is limited beyond 1.5 – 2 km (see Appendix 1), and therefore birds that do not reach distances within 1.5 – 2 km, or that are lost, may not be identified at species level and therefore not included in the analysis (the average proportion of unidentified tracks collected is approximately 46% varying significantly with distance (see Appendix 2, Section 6)). Here, it should be noted that seabirds were often detected and tracked by radar over distances beyond 2 km before they were identified. Consequently, this might lead to a bias if the patterns are not the same inside as outside the wind farm.

2.2.24. Data used to inform macro avoidance have only been collected during daylight hours and relatively calm weather conditions (< sea state 4) (see Section 3.4 and Appendices 3 and 4). Consequently, a level of uncertainty still exists on whether observed behavioural responses are representative of any weather / visibility conditions. Adding to this, there is uncertainty related to the oceanographic and habitat variability in time and space which cannot be accounted for within the scope of the study.

2.2.25. Uncertainty exists regarding the use of macro EARs based on data from one wind farm only.

b. Meso Avoidance

2.2.26. Meso avoidance is defined as bird avoidance responses within the wind farm footprint to individual turbines (considering a 10 m buffer around the RSZ) resulting in a redistribution of the birds within the wind farm footprint.

2.2.27. Based on the study's observations, the use of a 10 m buffer around the RSZ proposed by Cook et al. (2014) is considered to provide a good indication of bird responses at this scale.

2.2.28. Meso avoidance analysis relies on the visual assessment of responses to individual turbines (RSZ + 10 m buffer) in video evidence. Avoidance responses include changing the flight path to fly above / below the RSZ + 10 m, or flying between turbines. All birds recorded flying within the RSZ + 10 m buffer are not considered to avoid the meso zone and are further analysed at the micro scale (see Section c below). Birds not changing flight path recorded flying below/above the RSZ have not been included in the estimation of meso avoidance, because flight height is already considered within the Band CRM model. However, the effect of excluding these observations on the estimated meso EARs has been assessed in order to inform the quantification of uncertainties surrounding the meso EARs.

2.2.29. Distance to the RSZ+ 10 m buffer is visually assessed, and should therefore be considered as an approximation. Similarly to macro avoidance analysis, and as illustrated in Figure 2.3, in this study, meso avoidance is then quantified by comparing the observed distribution of bird track density (measured as track length per unit area) inside the RSZ + 10 m buffer within the wind farm, with an hypothetical situation in the absence of the wind farm, in which the same bird track density would have been observed inside / outside the RSZ +10 m buffer within the wind farm.

Figure 2.3.   Illustration of meso avoidance concept and approach to analysis considered in this study. Within the wind farm perimeter, Blue birds represent bird track density calculated outside the RSZ (blue circle) + 10 m buffer (red dotted line), while orange birds represent bird track density calculated inside the RSZ + 10 m buffer.
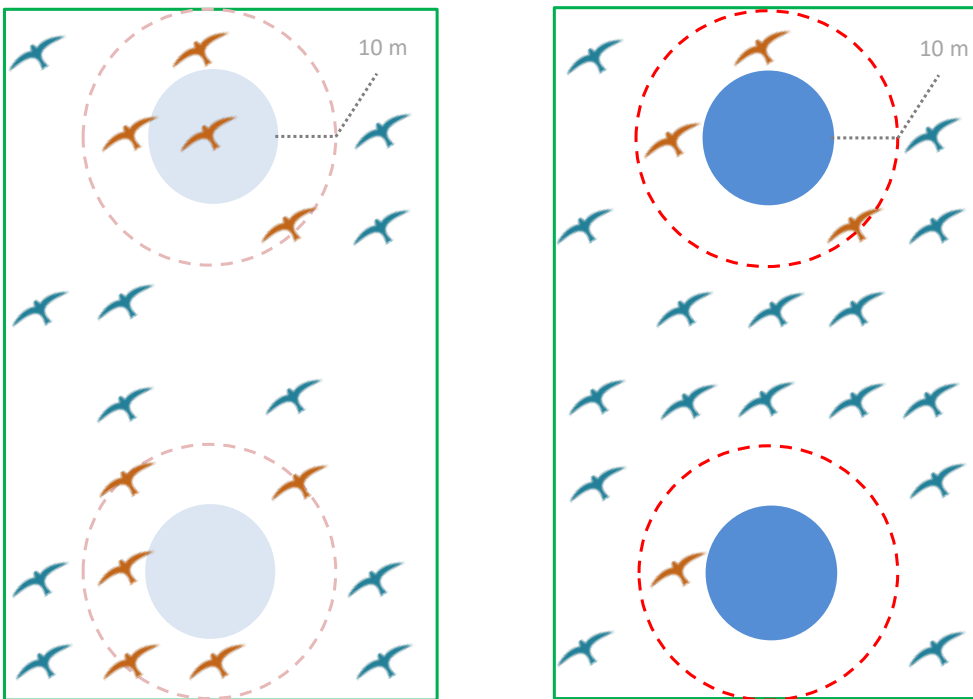
Pre-construction

assumes same track density and same total bird flights inside / outside the RSZ + 10 m buffer

Post-construction

observes redistribution inside / outside the RSZ + 10 m buffer

Outside area	11 birds / 22 cells	0.5 birds / cell	Outside area	16 birds /22 cells	0.73 birds / cell
Inside area	9 birds / 18 cells	0.5 birds / cell	Inside area	4 birds / 18 cells	0.22 birds / cell
Total	20 birds / 40 cells	0.5 bird / cell	Total	20 birds / 40 cells	0.5 bird / cell

2.2.30.   Meso avoidance is analysed using data collected from two different turbines located inside the wind farm (see Section 3.1) using radar equipment for bird detection connected to a camera system that tracks and records bird movement within the wind farm. The monitoring system can only track one target at a time and therefore does not collect data on accurate passage rates of birds through the wind farm. Tracking effort inside and outside individual turbines (RSZ + 10 m buffer) is considered similar, as only radar data from zone of high detection probability for seabirds have been included.

Assumptions in meso avoidance analysis

2.2.31.   Meso avoidance analysis assumes that the track density (track length per unit area) in the absence of the wind farm would have been uniform inside the wind farm, i.e. one would have observed the same track density both inside and outside the RSZ + 10 m buffer within the wind farm area (in the absence of the wind farm).

2.2.32.   Comparison of bird track density inside and outside the RSZ + 10 m collected by the study's monitoring system assumes that equipment detection of seabirds is comparable in both areas (see Appendix 2, Section 1).

2.2.33.   In the absence of seabird tracks for the analysis of meso avoidance inside the wind farm, the use of mean track lengths (corrected for flight speed) is considered to provide a good approximation for the calculation of track density (track length per unit area) both inside and outside the RSZ + 10 m within the wind farm, also supported by video evidence (see Section 4.3).

2.2.34.   Data collected are considered representative for the whole wind farm (see Section 2.3)

2.2.35.   Data collected are considered representative for all wind situations and sea states

Limitations in meso avoidance analysis

2.2.36.   Data analysis quantifies distributional patterns, i.e. differential use of the wind farm area in relation to the assumed pre-construction situation, which is independent of type of bird behaviour. For instance, although birds flying across the wind farm at heights below the RSZ +_10 m buffer have been removed from the analysis, there is a certain degree of uncertainty on the coding of behaviour and classification of tracks, as information is only provided by short videos (20 s). Seabird behaviour is separately interpreted (see Section 6).

2.2.37.   In the absence of seabird tracks for the analysis of meso avoidance inside the wind farm, video evidence associated with bird targets detected by the monitoring system is used to visually assess bird positions relative to the rotor from videos, which is subject to video quality and visibility conditions, and has some associated degree of uncertainty. A coding protocol was applied to ensure consistency in the analysis of video evidence.

2.2.38.   Species identification may not be possible for all targets detected by the system, as it depends on visibility conditions and proximity of targets. In addition, although a large range of weather conditions have been captured in data collected, the data used in the quantification of meso EAR is limited to day time, and therefore there is associated uncertainty on whether the data represents poor visibility and night conditions.

2.2.39.   Uncertainty exists regarding the use of meso EARs more widely based on data from one wind farm only.

c. Micro Avoidance

2.2.40.   Micro avoidance is defined as bird behavioural responses to single blade(s) within the RSZ + 10 m buffer, considered as the bird's 'last-second' action taken to avoid collision.

Figure 2.4.   Illustration of micro avoidance concept and approach to analysis considered in this study. Within the RSZ (blue circle) + 10 m buffer (red circle), arrows represent bird movement in relation to the rotor (dark blue ellipse + 10 m buffer (red ellipse). The light blue arrow represents wind direction. Birds have been observed to adjust their flight in order to avoid individual blades (dotted arrow), not to adjust but survive when crossing the rotor when operative (solid arrow) or in rare occasions collide (double arrow).
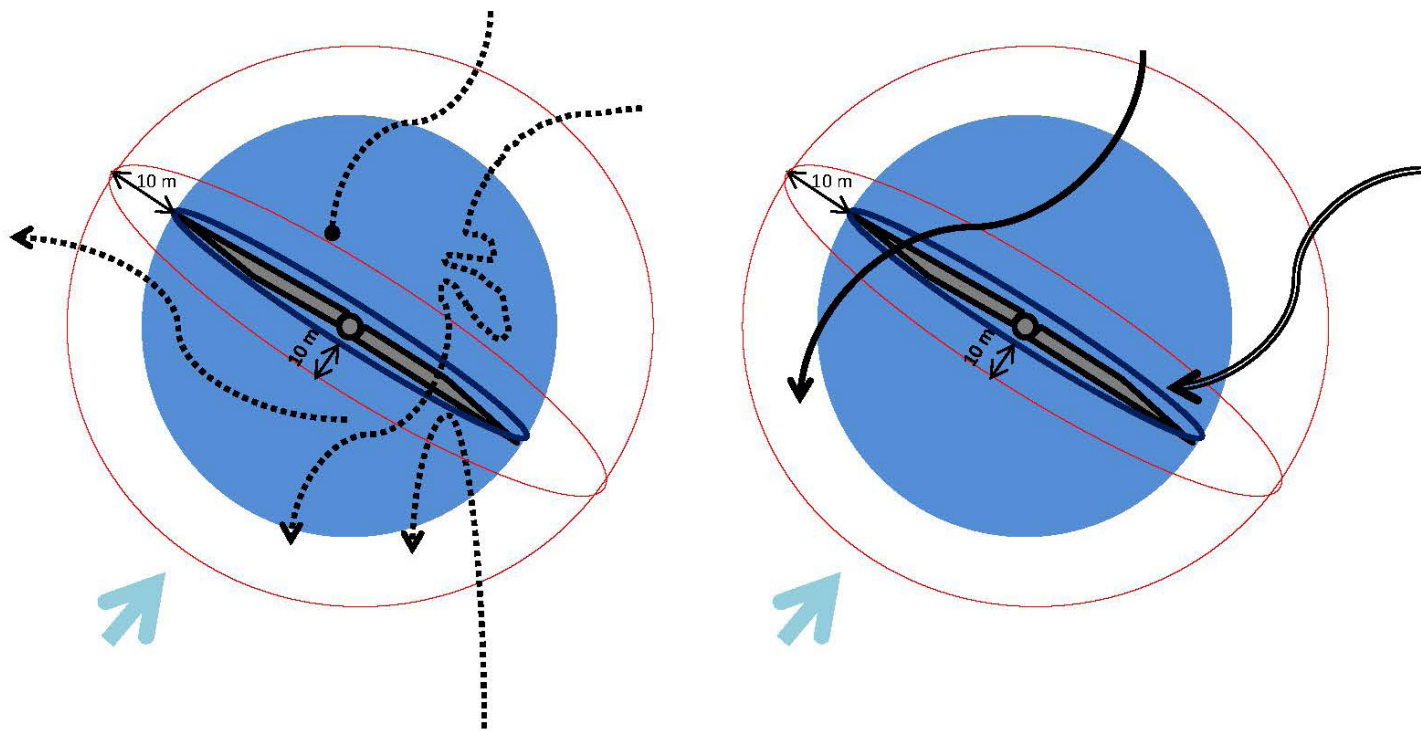
Example bird tracks where a bird adjusts its behaviour to the presence of the wind turbine

●┄┄┄┄ Adjusts - stops before

◄┄┄┄ Adjusts

Example bird tracks where a bird does not adjust its behaviour to the presence of the wind turbine

◄─── Does not adjust

◄─── Collides

2.2.41. As indicated above, it is considered that the 10 m buffer proposed by Cook et al. (2014) to analyse micro avoidance behaviour is appropriate based on observations made.

2.2.42. As illustrated in Figure 2.4. in this study and in contrast to other studies, micro avoidance is quantified by calculating the proportion of birds adjusting or not to the presence of blades, considering bird movement in relation to the rotor, represented as a dynamic ellipse, surrounded by a 10 m buffer. The dynamic ellipse changes its orientation with the wind direction (positioned perpendicularly to wind direction), which is considered to reflect the underlying mechanisms of avoidance behaviour at this scale. Adjustment refers to flight paths relative to the plane of the sweeping blades. Additional information on bird behaviour coding at this scale can be found in Section 4.4.

2.2.43. As in the case of meso avoidance, micro avoidance is analysed using data collected from two different turbines located inside the wind farm (see Section 3.1) using radar equipment for bird detection connected to a TADS camera system that tracks and records bird movement within the wind farm. The monitoring system can only track one target at a time and therefore does not collect data on accurate passage rates of birds through the RSZ. Accordingly, it does not provide absolute number of collisions.

Assumptions in micro avoidance analysis

2.2.44. All observations are considered representative for the whole wind farm (see Section 2.3)

2.2.45. Data collected are considered representative for all wind situations and sea states.
Limitations in micro avoidance analysis

2.2.46. Due to increasing levels of avoidance at macro and meso avoidance scales, the number of birds observed within the RSZ + 10 m is rather limited, providing a reduced sample size for analysis. Consequently, micro avoidance can only be quantified by species groups and needs to be applied across all species.

2.2.47. Micro avoidance analysis relies on the visual assessment of bird positions relative to the rotor blades from videos, and has some associated degree of uncertainty. A coding protocol was applied to ensure consistency in the analysis of video evidence.

2.2.48. Species identification may not be possible for all targets detected by the system, as it depends on visibility conditions and proximity of targets. In addition, although a large range of weather conditions have been captured in data collected, the data used in the quantification of micro EAR is limited to day time, and therefore there is associated uncertainty on whether the data represents poor visibility / night conditions.

2.2.49. Uncertainty exists regarding the use of micro EARs based on data from one wind farm only.

2.2.50. The limitations and sources of uncertainty listed above for all three scales have been considered carefully and have been quantified separately in order to ensure that mean EARs are accompanied by a realistic level of uncertainty around its calculation (see Section 5.5).

2.3. SCALING UP DATA COLLECTED TO THE WHOLE WIND FARM

2.3.1. As further explained in Appendix 2, data collected by the LAWR radar from turbine G05 (located along the periphery) was not used in the analysis of empirical macro avoidance due to a) the low confidence in data's representation given equipment detection limitations over distance and b) the small sample size obtained.

2.3.2. Accordingly, given the stronger weighting of data collected from turbine G01 (located at the corner) on the quantification of empirical macro avoidance, it is possible that data collected at macro scale is more representative of bird activity at offshore wind farm corners. At the same time, distribution of tracks and their analysis seem to suggest that avoidance is slightly lower at the corners than at the periphery, making the scaling up to the whole wind farm conservative.

2.3.3. Data collected from turbines F04 and D05 inside the wind farm are considered representative for the whole wind farm, i.e. the probability of a bird entered the RSZ+10 m is considered the same throughout the whole wind farm. However, it should be noted that higher numbers of gulls were observed at D05 located in proximity to the transformer station. As above, this is considered to have introduced a certain degree of precaution on estimates, as higher activity may have translated into lower avoidance.

2.3.4. In relation to collisions recorded, the design of sampling at the micro avoidance level aimed at providing statistics on the proportion of birds avoiding/not avoiding, as opposed to the estimation of total flux of birds through the RSZ, or to the total numbers of collisions on the eight monitored turbines. This study has sampled a part of the wind farm and there will be variability across the whole wind farm. In order to be able to extrapolate the number collisions to the represent the whole wind farm, the sampling design would have had to focus on recording bird movements at more locations to measure the variability across the wind farm site. Accordingly, extrapolation of collisions observed in this study to the whole wind farm will not be accurate and wind farm are not recommended.

③ MONITORING SYSTEM

3.1. DESIGN

3.1.1. The study's monitoring system was designed to collect representative data on bird avoidance behaviour at the three different spatial scales into which bird avoidance behaviour can be broken down: macro avoidance, meso avoidance and micro avoidance. Accordingly, a monitoring system composed of a variety of detectors was selected to be deployed from four different turbines at Thanet, with species either identified on site or through video.

3.1.2. The inspection of post-construction monitoring data available for Thanet (see Section 2.1), indicated that large numbers of seabirds had been recorded around the entire periphery of the wind farm, showing no particular preferences in distribution. Seabird movements around offshore wind farms have, however, been observed to lead to higher densities around wind farm's corners, with decreasing gradients along the periphery between corners (Christensen et al. 2006; Krijgsveld et al. 2011). Accordingly, the placement of equipment at Thanet (see Figure 3.1) was designed to cover the perceived gradient of the use of the wind farm area by seabirds, aiming to sample behavioural responses of seabirds around a corner and along one side of the wind farm (macro avoidance), as well as at two different locations within the wind farm (meso and micro avoidance).

3.1.3. The placement of equipment was also dictated by Vattenfall's operational requirements and the need for the equipment to be located on the laydown area of a turbine's work platform, of which all faced east. This positioning introduced constraints in the field of view, limiting data collection inside the wind farm in comparison to the outside area, as illustrated by Figure 3.2.

Figure 3.1.   Sketch of installed monitoring system at Thanet Offshore Wind Farm. Radars: Scanter (turbine G01), LAWR (turbines G05, F04, D05).
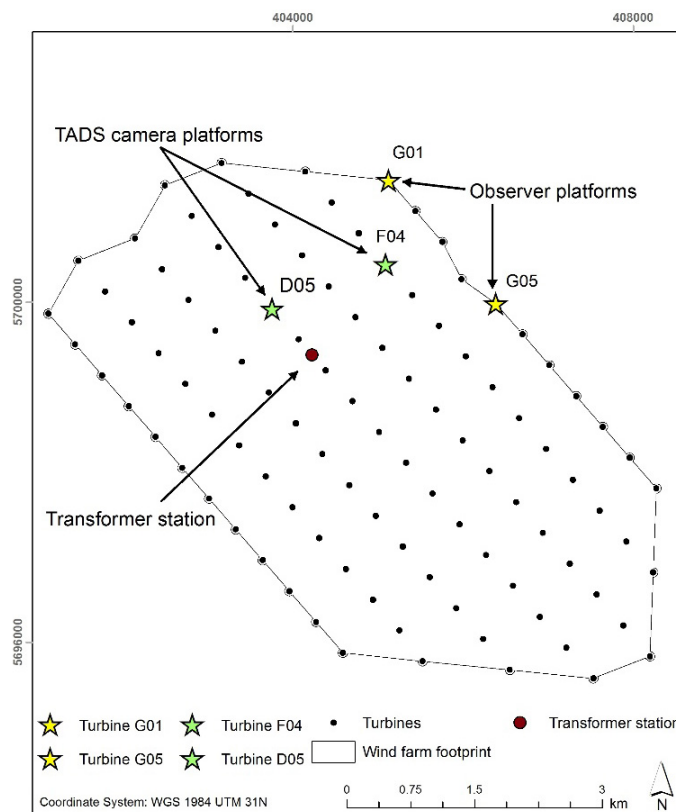
Figure 3.2. **Angle of the blind zone at turbine G01 (left) and turbine G05 (right) for both radars and rangefinder positioning. Green line defines the blind sector for the radar. Blue and red lines define the blind sector for the rangefinder, the blue showing fully obstructed view and between red and blue partially obstructed view by turbine metal structures.**
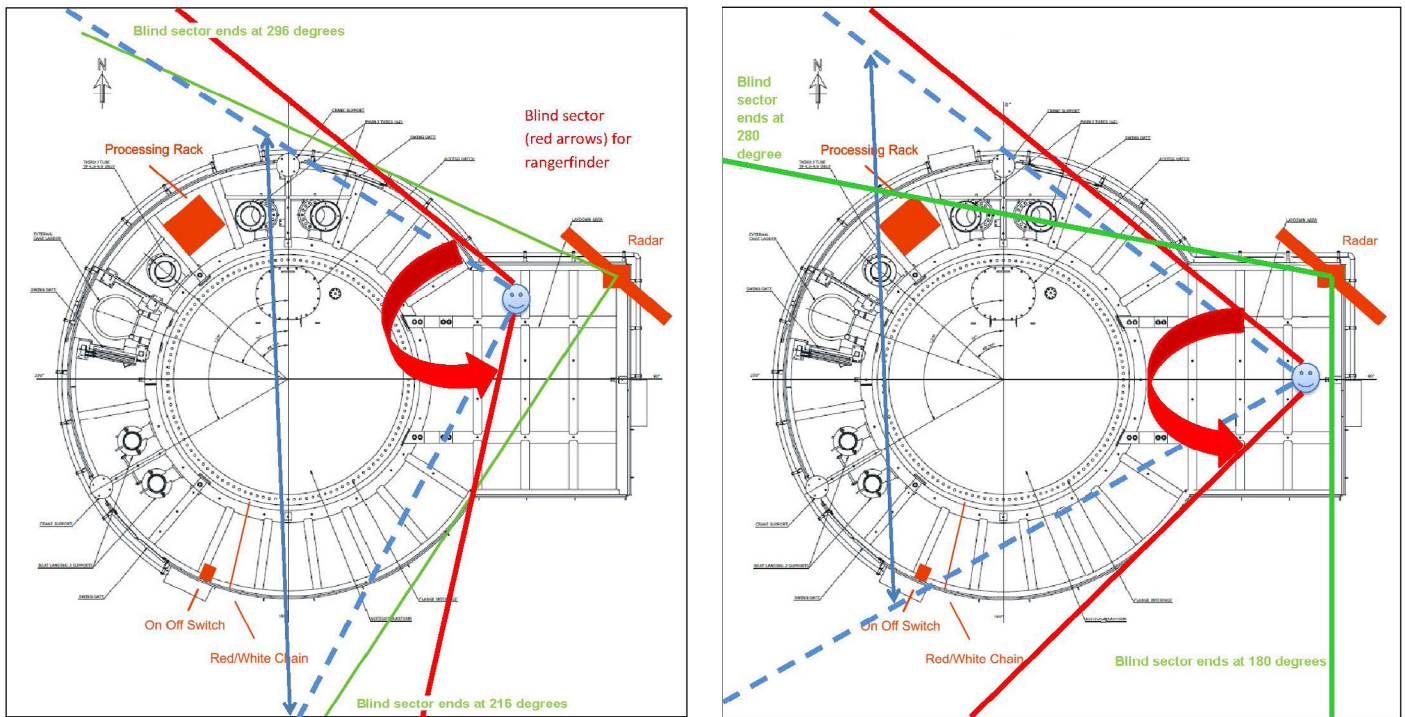
3.1.4. It is important to note that birds tracked by the monitoring system only constitute a proportion of the total number of birds moving through the area investigated. This is a result of the limitations in the number of bird tracks possible to track (see below), equipment performance (see Section 3.3) or sampling frequency (Section 3.4). At the same time, recording of a given bird more than twice although possible is considered to have been rare. Given that the study does not attempt to calculate total density of birds or flux of birds inside the wind farm, this is not considered to influence estimates of avoidance, which are based on proportions of recorded track densities inside/outside meso and macro avoidance zones.

3.1.5. This section provides an overview of the monitoring system components and characteristics deployed at Thanet, with additional details presented in Appendix 1.

3.1.6. Equipment was temporarily installed on turbine platforms, located at 13 m above sea level, of four different turbines:

a. SCANTER 5000 radar (turbine G01)

3.1.7. The SCANTER radar is a fan beam and solid state radar with an enhanced detection capability in wind farms, able to suppress sea and ground clutter, and rain. In contrast to magnetron-based radars like LAWR 25 (see b. below), solid state radars replace the magnetron with a solid-state, broadband transmitter that outputs a clean, frequency-stable signal. It is coupled to a receiver that uses a more precise band of frequencies, eliminating much of the background noise that would mask the faint echoes from a given target, and it is capable of generating sharp returns.

3.1.8. The SCANTER radar has a high and uniform detection probability curve (DPC) (studied through radar cross sections of similar size to those of seabirds, see Appendix 1). This sensor was applied with observer-aided tracking during daylight hours and calm weather conditions. Data collected by the SCANTER radar within 3 km from the wind farm perimeter and identified to species level have been used to analyse bird macro avoidance.

b. LAWR 25 radar (turbine G05)

3.1.9. The LAWR radar is a fan beam and magnetron-based radar. The LAWR radar, as other magnetro-based radars, is known to be sensitive to sea clutter in sea states higher than Beaufort 2 and has less detection capacity in wind farms than the SCANTER radar. LAWR radars had previously been used in post-construction monitoring programmes in Belgium (Vanermen et al. 2013), at Horns Rev 1 and 2 (Skov et al. 2012a) and at the Dutch OWEZ offshore wind farm (Krijgsveld et al. 2011).

3.1.10. In comparison with the SCANTER radar, the LAWR radar has a variable theoretical DPC, with high detection (>0.67) between 1,250 and 3,000 m from the radar (FEBI 2013). The LAWR 25 radar and supporting equipment was applied with observer-aided tracking during daylight hours and calm weather conditions.

3.1.11. Appendix 1 (Section 4) presents a test undertaken by DHI in 2012 at Blåvand (Denmark), where detection and tracking performance by the SCANTER and LAWR radar data were compared. Although the SCANTER radar demonstrated to have better detection ability with distance and produce outputs of higher resolution, due to the high costs associated with the SCANTER radar, it was decided to deploy one SCANTER radar only and three LAWR radars to complement data collection.

3.1.12. Due to limited data sample size collected by the LAWR radar and the equipment detection limitations inside the wind farm the LAWR radar data collected from turbine G05 was not used to analyse bird macro avoidance (see Appendix 2, Section 5).

c. Vectronix 21 Aero laser rangefinders (turbines G01 and G05)

3.1.13. Comparable to a handheld binocular equipped with a built-in, battery driven laser system.

Rangefinders allow measurement of distance, altitude and direction to a given object.

3.1.14. There is extensive experience using this equipment in offshore and coastal applications. For instance, seabird flight speeds have been studied using rangefinders along the Swedish coast (Pennycuik et al. 2013); in Estonia rangefinders were used to look at factors affecting flight altitude during waterbird migrations (Kahlert et al. 2012); and in the UK (Swansea city), rangefinders were used to study gull flight trajectories (Shepard et al. 2016). In relation to offshore wind farms, rangefinders have previously been used at the German Apha Ventus offshore wind farm, operated from boats to analyse flight height measurements (Mendel et al. 2014). Danish Horns Rev offshore wind farm (operated from offshore platforms) (Skov et al. 2012a) and Rødsand 2 offshore wind farm (operated from the shore) to monitor migratory species after construction (Skov et al. 2012b; Skov and Heinänen 2013). Pre-construction studies at Anholt (Skov et al. 2012c), Kriegers Flak and Danish coastal wind farms have also used rangefinders, operated from boats in the case of Sæby, and from the shore in the case of Smålandsfarvandet to determine flight heights of seabirds (Skov et al. 2012c, Skov et al. 2015, Žydelis et al. 2015a, Žydelis et al. 2015b).

3.1.15. Under optimal conditions, tripod mounted laser rangefinders can be used out to a distance of approximately 1.5 - 2 km for seabird species, depending on the angle of view and on bird flight behaviour (gliding, soaring or flapping). Accordingly, rangefinders were operated by observers during daylight hours from turbines G01 and G05, where the selection of targets was made through the SCANTER and LAWR radars (see below), or through the visual screening of observer's field view if radar equipment was unavailable (see Appendix 2). From both G01 and G05 the turbine tower obstructed the view in the wind farm array to the west of the observers, while turbines located in NW and SW directions from the observers were within the field of view. Thus, movements of seabirds could be followed through a relatively large proportion of the wind farm area around the two platforms. Data collected by rangefinders within 1.5 km have been used to analyse bird macro avoidance and to measure flight heights. Given the range of studies using rangefinders in offshore applications, further validation of the equipment was not considered necessary.

3.1.16. The use of equipment by the study seabird observers is described in Appendix 1, where constraints and limitations are noted. The protocol for data collection is included in Appendix 3.

NIRAS DHI CARBON TRUST

d. Thermal Animal Detection System (TADS) and LAWR radars (turbines F04 and D05)

3.1.17. The implementation of the TADS system has been pioneered by the Department of Wildlife Ecology and Biodiversity at NERI (Desholm 2003, Desholm 2005). It consists of a pan-tilt housing with two thermal night vision cameras, and a dual-function zoom daylight/lowlight colour TV camera. At Thanet, two different TADS camera systems were installed for the duration of the data collection on two separate turbines inside the wind farm, F04 and D05. The TADS software was programmed to connect the cameras with LAWR radars, responsible for detecting bird signals and triggering the TADS system for video recording.

3.1.18. The development of software for integration of radar and camera tracking has been a major component of this study, and testing of the equipment was undertaken before installation at Thanet (see Section 3.2).

3.1.19. Set to a scanning range of 1.5 km, the theoretical DPC for these radars indicates a high detection (>0.67) between 265 and 875 m from the radar. As a result of the connection with the TADS Camera system, when the distance to the bird target became less than approximately 1000 m, the birds position coordinates were transmitted from the radar to the camera using an analogue signal capable to filter sea clutter to some extent, which would subsequently film part or the whole event of the bird passing the wind turbine over a 20 s sequence. Sea clutter still infested the data in many cases, resulting in a high number of false positives, videos recorded with no apparent presence of birds.

3.1.20. It should also be noted that resolution on daylight videos and night videos is significantly different (see Appendix 1), and together with visibility can influence the extent to which birds can be identified to species level. In the case of night videos, it was only possible to identify species at group level.

3.1.21. Daylight data collected by the TADS cameras and LAWR radar from F04 and D05 have been used to analyse meso avoidance redistribution and micro avoidance behaviour within the wind farm.

3.1.22. The LAWR radar and TADS camera system managed to collect daylight data at species level within a range of weather conditions, including sea states from 0 – 7 (Figure 3.3).

3.1.23. Table 3.1 provides an overview of equipment properties and limitations, which are further described in Appendix 1.

Figure 3.3. **Weather conditions (Beaufort sea state) captured by TADS system and LAWR radar data during daytime from turbines F04 and D05 for Northern Gannet and large gulls records.**
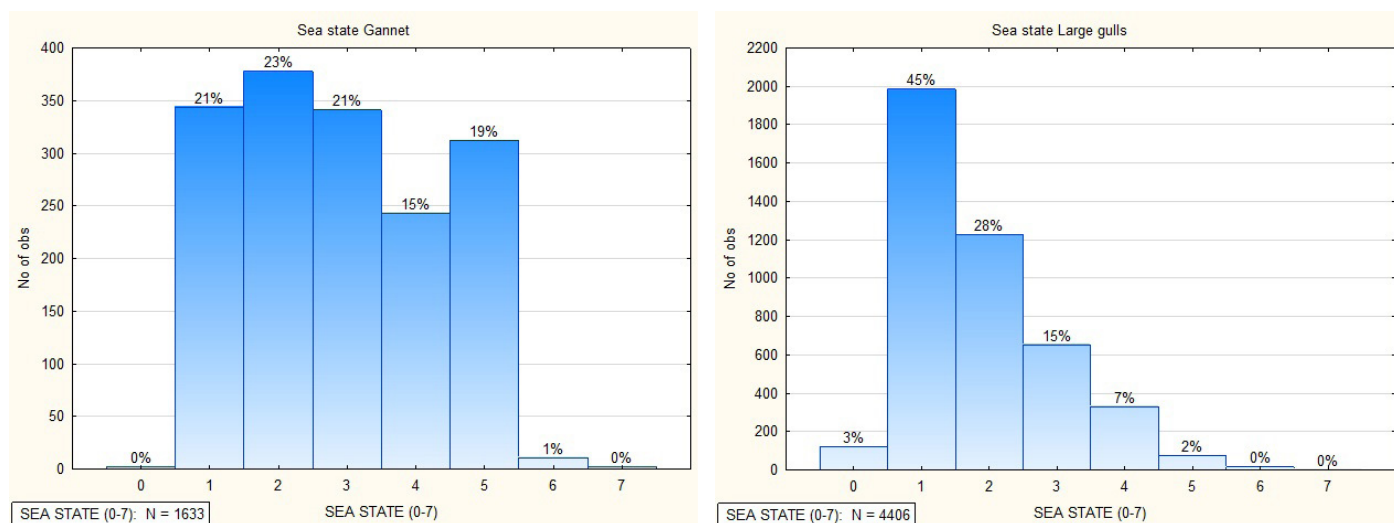
Table 3.1.   Overview of sensor equipment characteristics. Additional information can be found in Appendices 1 (equipment characteristics) and 3 (observer protocol).

Sensor	Detection probability	Application	Assumptions and Limitations
SCANTER 5000 RADAR (TURBINE G01)	Close to 1.0, slightly dropping after 5 km	(Applicable to both SCANTER and LAWR radar on turbines G01 and G05 respectively, see Appendix 1) • For each track, there is an automatic recording of target location and direction in way points • Track followed by technician within 5 km inside / outside the wind farm, identified to species level when target is located within 2-1.5 km from observer (depending on species / visibility conditions) Radar software used to record target info Automatic recording of radar screen images (subject to equipment operational status)	• Scanning Range set to 12 km • High and uniform detection probability throughout studied area both inside and outside the wind farm (macro avoidance analysis is limited to up to 3 km outside the wind farm) • Blind sector between 216° and 296° • Shading inside the wind farm due to the presence of turbine towers is very limited • Data collection (at species level) only possible when observers are deployed • Up to 10 tracks can be followed at any one time • Detection of seabirds typically possible within 5 km, with species identification possible within 2 – 1.5 km, depending on species and visibility conditions • Birds flying at < 10 m altitude within 45 m of the radar cannot be detected both inside and outside the wind farm • Maximum height at which flying seabirds can be detected at 1 km distance is 285 m both inside and outside the wind farm
LAWR 25 radar (turbine G05)	High detection (>0.67) between 1,250 and 3,000 m		• Scanning Range set to 6 km • Detection probability varies throughout scanned area (high detection between 1,250 – 3000 m) • Blind sector between 180° and 280° • Shading inside the wind farm due to the presence of turbine towers is limited • Data collection (at species level) only possible when observers are deployed • Up to 10 targets can be followed at any one time • Detection of seabirds typically possible within 5 km, with species identification possible within 2 – 1.5 km, depending on species and visibility conditions • Performance sensitive to sea clutter in sea states higher than Beaufort 2, resulting in limited or no radar detection being possible by the observer team when using the LAWR 25 radar • Birds flying at <10 m altitude within 85 m of the radar cannot be detected both inside and outside the wind farm • Maximum height at which flying seabirds can be detected at 1 km distance is 175 m both inside and outside the wind farm

Sensor	Detection probability	Application	Assumptions and Limitations
RANGEFINDERS (TURBINES G01 AND G05)]	**Influenced by different factors (aspect of birds and flights, visibility, platform stability)**	• **"Fired" with approx. 3-5 s intervals once target is located out in the field** • **Log in of positions and altitudes undertaken automatically via GPS** • **Rangefinder logbook used to record target info** **Further information can be found in Appendices 1 and 3**	• **Detection range is 1.5 - 2 km, depending on species** • **Blind sector with an amplitude of 90 degrees (varying inside and outside the wind farm depending on turbine where rangefinder is used from, see above)** • **Sensitive to metal interference. Requires calibration to spatially adjust the horizontal positioning of records inside and outside the wind farm (and therefore cannot be used in meso avoidance analysis)** • **Only one target can be followed at any one time** • **Target selection relies on radar detection or visual screening of field view** • **The ability to successfully aim and hit a flying seabird with the laser of the rangefinder is influenced by the stability of the platform, moisture content of the air column and visual interference from rotating turbines when shooting at a target**
THERMAL ANIMAL DETECTION SYSTEM (TADS) (TURBINES F04 AND D05)	**Relies on radar**	*(Applicable to both TADS Camera System and LAWR radars working together)* • **Radar detects target within 1.5 km** • **Radar detection relies on cross-correlation with known bird radar signatures** • **Radar shares coordinates with camera when target is within 1 km** • **Camera follows target, tracking for around 20 s, and videoing part or the whole event of the bird passing the wind turbine**	• **Cameras recording range is 1 km, 20° field of view** • **Each TADS camera cover a total of 4 turbines within high detection zones covered by the radar** • **At the installation turbine itself the camera view is only able to cover part of the rotor, and therefore most birds recorded around the installation turbine are not used in avoidance analysis** • **Very few videos of tracks at distances beyond two rows (1 km) of turbines from the installation turbine** • **Few videos of low flying birds close to the installation turbine**
LAWR 25 RADARS (TURBINES F04 AND D05)	**High detection (>0.67) between 265 and 875 m**	• **Camera programmed to use the thermal night vision cameras during the hours of darkness and switch to using the daylight/lowlight colour TV camera when daylight.** • **Camera software used to record track info** **Automatic recording of radar screen images (subject to equipment operational status)**	• **Scanning range set to 1.5 km** • **Detection probability varies throughout scanned area** • **Birds flying at < 10 m altitude within 85 m of the radar cannot be detected** • **Maximum height at which flying seabirds can be detected at 1 km distance is 175 m** • **Locally around the foundations breaking waves may give rise to clutter affecting radar performance and leading to a high proportion of "false positives", however, analogue signal capable to filter sea clutter to some extent**

NIRAS   DHI   CARBON TRUST

3.2. TESTING AND VALIDATION

3.2.1. Before equipment installation at Thanet in Aug 2014, the connection between the TADS camera system and the LAWR radars was tested in two coastal locations in Denmark; Århus (between April and May 2014) and Ebeltoft harbour, where a wind farm is located along the western pier at a distance of 500-700 m from the radar station (June 2014). The higher density of flying seabirds at Ebeltoft, especially gulls, allowed for detailed testing of detection distances by the camera. The presence of the wind farm also allowed for testing for potential interference between bird detections and turbine towers and blades.

3.2.2. During testing, radar echoes that best characterised a flying bird were characterised from a cross-correlation with known bird radar signatures (Herring Gull) recorded at the test site before deployment of the equipment at Thanet.

a. Communication between TADS Camera System and LAWR 25 radar

3.2.3. As further described in Appendix 1, the communication between the TADS Camera system and the LAWR 25 radar has taken place through the radar-camera tracking unit (TADS Tracker). Compared to manual operation of the TADS camera the software-controlled operation executes much faster with positioning of the camera within 2.3 seconds.

3.2.4. Drone tests carried out under good weather conditions showed detection and tracking of small drone (30 cm) by thermal camera to distances between 710 and 1,000 m. The drone was flying at 30 m height above sea surface at a speed of 25 km/h, and the maximum distance was recorded when the camera tracking facility lost the drone from the viewer.

b. Detection and identification range of TADS camera system under different weather conditions

3.2.5. The detection and identification range of both the TADS visual and thermal cameras for different species of seabirds was assessed at the test site in Ebeltoft. Gulls could be detected at 1,000 m distance through the visual lens and at 800 m through the thermal lens. Identification of gulls to species level was possible at 600 m distance through the visual lens, and between 400 and 500 m through the thermal lens.

3.2.6. The thermal cameras performance degradation due to rain was found to be very range sensitive, whereby there is a dramatic drop off in the 100 - 500 m range. However, tests carried out by the camera provider (FLIR) documented that the thermal IR band offers better range performance compared to the visual band. Additional tests of detection ranges during different conditions were carried out in Denmark on the first generation TADS camera (Thermovision IRMV 320V) in 2002 (Desholm 2003).

3.2.7. It is considered that sea clutter within the wind farm could have been caused by breaking waves around the foundations, leading to the high false positives observed in data collected. However, in comparison to the LAWR radar located at the periphery of the wind farm (turbine G05), sea clutter can be filtered to some extent by the LAWR radar positioned at F04 / D05, as it uses an analogue signal (raw signal).

3.3. EQUIPMENT INSTALLATION, OPERATION & DECOMMISSIONING

a. Equipment installation

3.3.1. The original plan was to complete the installation of the monitoring system in a dedicated one week programme (with a standby week allowed for weather and access issues) between the 14 and 28 July 2014. However, a number of challenges were encountered, including unavailability of vessel for transfers, weather conditions, and delayed receipt of Ofcom licensing approval for all radars. Consequently, the monitoring system was installed at Thanet between the 28 July and 18 August 2014, requiring a total of 10 working days.

NIRAS DHI CARBON TRUST

b. Equipment operation

3.3.2.   Although data collection commenced 1 July 2014 by use of laser rangefinders from turbines G01 and G05 (prior to installation of the radars), data collection by observers using radar equipment (SCANTER and LAWR radar respectively) first started on 28 August 2014 during the observer training offshore, and finalised on 14 April 2016, when observer deployment ceased.

3.3.3.   Collection of radar images (screen dumps) from both radars was, however, undertaken throughout the monitoring period, with some interruptions associated with equipment failure (see Table 3.2 below).

3.3.4.   Automated tracking using the TADS Camera System linked to LAWR radars from turbines F04 and D05 did not commence until 23 October 2014, when remote access to the system was made possible. The collection of screen dumps was also maintained throughout the monitoring period.

3.3.5.   Equipment status was checked twice a day through DHI's network. DHI notifications on equipment disruptions were noted by NIRAS in a fieldwork log, with notable disruptions (over 5 days) of service up to 21 June 2016 summarised in Table 3.2. Given the nature of offshore deployment, it is considered that the equipment has performed as expected, with servicing often constrained due to adverse weather conditions, vessel / technicians availability. The need to ensure that all offshore certificates are in place both for the Personal Protective Equipment (PPE) and staff working offshore has been key determining the timely servicing of equipment, and have in some cases caused delays despite careful monitoring of expiry timelines of certificates.

3.3.6.   The installation of GMS switches in all four turbines, in November 2014, further enabled the remote restarting of the equipment, which proved to be very valuable in cases of equipment hibernating after power cuts, which have often taken place during the regular operation and maintenance activities taking place at Thanet.

Table 3.2.   Main disruptions of the Equipment throughout the monitoring period.

Overall availability*		Disruption	Impact on data collection	Date logged
SCANTER RADAR (G01)	81%	Faulty transformer inside the tower. No power reaching the radar	Unavailability for 17 days	10 – 17 Feb 2015
		Broken controller RxTx, with servicing substantially delayed due to vessel availability and weather conditions	Unavailability for 44 days	24 Mar – 5 May
		Faulty radar module, with servicing delayed due to PPE requiring recertification	Unavailability for 29 days	15 Jun – 13 Jul 2015
		Fault in the external module (IO), servicing delayed due to technician's unavailability	Unavailability for 27 days	21 Jan – 16 Feb 2016
		RST software suffering frequent deactivation, requiring manual resetting	Intermittent collection of screen dumps	Dec 2015 – Jun 2016

* Overall availability based on disruptions recorded on fieldwork log. It does not include disruption due to sea clutter during fieldwork application.

Overall availability*		Disruption	Impact on data collection	Date logged
LAWR RADAR (TURBINE G05)	94%	Power cut affecting equipment connection. Servicing delayed due to technician missing tools. Radar equipped with GSM switch that allowed restarting the computer remotely	Unavailable for 18 days	3 – 20 Nov 2014
		Power cut. Servicing delayed due to unavailability of Vattenfall / Vestas technicians, committed with other tasks and lack of vessel availability (breakdown)	Unavailable for 17 days	26 Feb – 13 Mar 2016
TADS + LAWR (TURBINE F04)	91%	Power cut affecting equipment connection. Servicing delayed due to technician missing tools. Radar equipped with GSM switch that allowed restarting the computer remotely	Unavailable for 18 days	3 – 20 Nov 2014
		Defective battery in one of the radar control boxes. Radar antenna motor was upgraded from 24 rpm to 42 rpm	Unavailable for 14 days	24 Sep – 7 Oct 2015
		Unresponsive camera. Servicing delayed due to PPE requiring recertification	Unavailable for 15 days	29 Jun – 13 Jul 2015
TADS + LAWR (turbine D05)	96%	Power cut affecting equipment connection. Servicing delayed due to technician missing tools. Radar equipped with GSM switch that allowed restarting the computer remotely	Unavailable for 10 days	11 – 20 Nov 2014

3.3.7. Equipment maintenance was scheduled to take place every 6 months, although non-scheduled servicing was often used to check up all four radars and Camera System. During maintenance operations, data automatically recorded by the equipment (i.e. screen dumps from all four radars and video data) were also retrieved, saved in external hard drives and stored / managed in the study's data management system, organised into turbine platform, month and day. The radar and rangefinder track data collected by observers were uploaded to a Drop box account shared with the study team.

3.3.8. In relation to the TADS Camera system, it should be noted that the camera lenses were provided with special coating which minimised the effect of the deposition of salt from the atmosphere, and therefore did not require regular cleaning. Despite the coating, variation in visibility is seen as a function of the occurrence of rain.

c. Equipment decommissioning

3.3.9. As opposed to the installation of the Monitoring System, decommissioning was completed in only two days without any incidents. On the 21 June, decommissioning of the SCANTER radar was completed on turbine G01, when all the equipment was moved onto transfer vessel safely. Although there was then an issue with one of the vessel's engines, this was resolved at sea and the study team proceeded to turbine G05 to uninstall the LAWR radar equipment. This was completed with some of the boxes left on the turbine overnight for collection next day. On the 22 June 2016, equipment from turbines D05 and F04 was fully decommissioned.

3.3.10. Finally, between 23 and 24 June 2016, equipment was packed and shipped to Denmark.

3.4. FIELDWORK EFFORT

3.4.1. The requirement of achieving 250 survey deployment days throughout the duration of the monitoring period (originally spanning from July 2014 to June 2016) was based on experience at Horns Rev wind farm, which had similar reported bird densities as those expected at Thanet, and was considered to provide a sufficient sample size in statistical terms. Survey deployment days refer to those days used to deploy one observer to undertake seabird surveys at Thanet. Given that observers were required to work in pairs, a maximum of four deployments could be achieved on a single day (one team working on each turbine).

3.4.2. As presented in Figure 3.4, the original fieldwork plan devised in March 2014 allocated the number of deployments consistently throughout the monitoring period, with additional effort planned during the summer months, when favourable weather conditions for fieldwork were expected. The original fieldwork plan was subsequently updated on a monthly basis based on number of survey deployments achieved and anticipated windows of suitable weather conditions (see Appendix 5 for a summary of weather and visibility conditions present at Thanet throughout the monitoring period).

Figure 3.4.   **Overview of fieldwork effort from 1 July 2014 - 14 April 2016, and comparison with original fieldwork plan.**
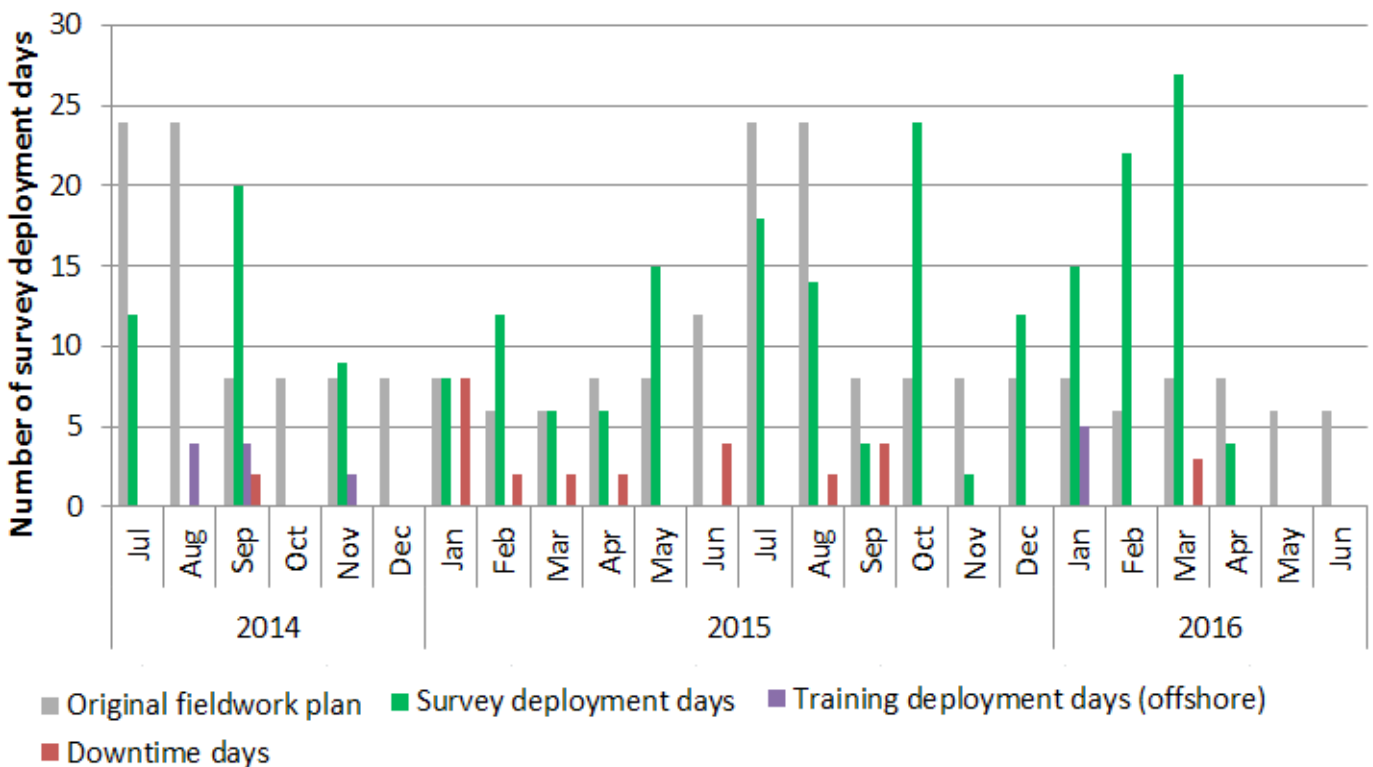
3.4.3. The deployment of observer teams to track birds using radars and rangefinders from turbines G01 and G05 commenced on the 1 July 2014 and continued up until the 14 April 2016, a 22 month period. A strong emphasis was placed on the health and safety of observer teams, particularly as their work involved transferring to and from operational turbines offshore. Close cooperation with Vattenfall ensured that there were no reportable incidents during this study.

3.4.4. Data collection by observers was limited to relatively calm (low wind speed conditions of up to 10 m/s) and clear weather conditions.

3.4.5. Fieldwork was dependent upon:

- the availability of observers, which, in line with health and safety requirements, required at least two observers on each turbine;

- the operational requirements of Thanet, allowing for the availability of seating aboard a crew transfer vessel (CTV);

- sea and weather conditions allowing for the safe transfer of personnel to/from the turbines and their occupation. As a guide, cessation of transfer to/from turbines for the observer teams occurred when the sea state reached "moderate" which typically occurs at Beaufort force 4-5, dependent on local factors such as tidal state.

- equipment status, with fieldwork often cancelled if radars were not operational.

3.4.6. The CTVs available to the study operated on weekdays from Ramsgate, approximately departing at 08.00 am and returning late afternoon (i.e. before 18.00), subject to sea / weather conditions. In order to maximise fieldwork opportunities, the following mitigation measures were implemented by the study team:

- In June 2015, the fieldwork plan was modified to include Mondays, with the selection of suitable weather windows for deployment made by NIRAS.

- Sample size collected up to May 2015 indicated relatively low numbers for Black-legged Kittiwake, and accordingly fieldwork effort was maximised during January – March 2016, considered as the key period for observing this species.

- In February 2016, a CTV was chartered by Vattenfall for the ORJIP observer team to compensate for the operational constraints anticipated for the remainder of the monitoring period, with only one vessel being available from February – July 2016. Weekend deployments were also included in the fieldwork plan to maximise use of the vessel.

3.4.7. Overall, a total of 230 survey deployment days were achieved, in addition to 15 training days undertaken offshore during which data was also collected. Fieldwork effort was shared between both turbine platforms, with 55% of deployments undertaken from turbine G01 and 45% from turbine G05 (see Appendix 4).

3.4.8. A total of 29 downtime days were recorded, represented in Figure 3.4 in red, reflecting the number of days in which observers were mobilised to site, but fieldwork was subsequently cancelled due to unexpected adverse weather conditions or vessel unavailability. Weather played a significant role in fieldwork planning, representing 64% of deployment cancellations (see Appendix 4 for further information).

3.5. SAMPLE SIZE

3.5.1. This section provides an overview of data collected using the monitoring system. A monthly breakdown of data collected is presented in Appendices 6 and 7. Sample size obtained are a result of bird presence, fieldwork effort and equipment performance, see Sections 3.3 and 3.4.

3.5.2. As presented in Appendix 2 (Section 6), several tracks detected could not be identified to species level and used in the data analysis, this may have been due to visibility conditions, distance of the target or loss of a target. On average, at the macro scale, 46% of radar tracks detected could not be identified to the species level, varying significantly across distances considered.

3.5.3. Table 3.3 presents the number of radar tracks collected by observers, and identified to species level, from turbines G01 (by use of SCANTER radar) and G05 (by use of LAWR radar) respectively.

3.5.4. A total of 1,555 radar tracks were collected for the five target species, of which 1,205 were detected and tracked SCANTER radar tracks, showing the superior performance by this radar in comparison with the LAWR radar.

Table 3.3. The number of tracks recorded by radar for each species from turbines G01 (SCANTER radar) and G05 (LAWR radar) between 1 July 2014 and 30 April 2016. Note that LAWR radar data were not used to quantify macro EAR (see Appendix 2, Section 5).

Species	SCANTER radar (turbine G01)	LAWR radar (turbine G05)	Total
Northern Gannet	585	185	770
Black-legged Kittiwake	75	49	124
Lesser Black-backed Gull	138	29	167
Herring Gull	187	36	223
Great Black-backed Gull	220	51	271
Black-headed Gull	11	1	12
Black-throated Diver	1	4	5
Brent Goose	16	1	17
Common Guillemot	36	3	39
Common Gull	50	7	57
Common Scoter	14	1	15
Common Starling	22	0	22
Common Tern	4	0	4
Cormorant	23	3	26
Goldfinch	1	0	1
Great Skua	3	0	3
Grey Heron	1	1	2
Greylag Goose	1	1	2
House Martin	0	1	1

Species	SCANTER radar (turbine G01)	LAWR radar (turbine G05)	Total
Little Gull	0	1	1
Northern Fulmar	3	4	7
Pink-footed Goose	1	4	5
Razorbill	12	42	54
Red-throated Diver	61	21	82
Redwing	4	0	4
Sandwich Tern	24	5	29
Shelduck	2	2	4
Unidentified auk	24	41	65
Unidentified bird	49	1	50
Unidentified diver	3	0	3
Unidentified goose	1	1	2
Unidentified gull	47	26	73
Unidentified tern	0	3	3
Wigeon	1	0	1
Total	1,620	524	2,144

3.5.5. There are different factors that may have influenced the amount of data collected by each radar, including:

- Bird distribution, there may have been more bird activity around the corner of the wind farm at turbine G01 (SCANTER radar) as compared to the eastern side of the wind farm, where turbine G05 is located (LAWR radar);

- Radar detection probability, the SCANTER radar has high detection efficiency for seabirds from the radar up to 10 km distance, whereas the LAWR only has high detection efficiency between 1.2 km and 3.5 km distance (see Appendix 1); and,

- Radar sensitivity to sea clutter, the LAWR radar was often affected by sea clutter during windy conditions, making it very difficult for the observer teams to rely on the radar screen to select and follow targets. This has potentially had an impact on the number of seabird tracks recorded using this radar (see Appendix 1).

3.5.6. Table 3.4 presents the number of rangefinder tracks collected from turbines G01 and G05 respectively, part of which were also detected and tracked by the radar (see tracks between brackets). These only include tracks identified to species level.

3.5.7. A total of 1,818 rangefinder tracks were collected for the five target species, slightly higher than the number of radar tracks collected which may be explained by the use of rangefinder during times when radars were not operative.

Table 3.4. **The number of tracks recorded when using laser rangefinders for each species from turbines G01 and G05 between 1 July 2014 to 30 April 2016. Number of tracks also recorded by radar is indicated in brackets.**

Species	SCANTER radar (turbine G01)	LAWR radar (turbine G05)	Total
Northern Gannet	428 (136)	278 (23)	706
Black-legged Kittiwake	135 (13)	161 (0)	296
Lesser Black-backed Gull	115 (35)	79 (1)	194
Herring Gull	154 (41)	148 (1)	302
Great Black-backed Gull	201 (28)	119 (1)	320
Arctic Skua	2 (0)	1 (0)	3
Black-headed Gull	12 (4)	6 (0)	18
Brent Goose	11 (6)	2 (1)	13
Common Guillemot	10 (0)	5 (0)	15
Common Gull	109 (12)	101 (0)	210
Common Scoter	3 (2)	0 (0)	3
Common Tern	17 (3)	0 (0)	17
Cormorant	13 (8)	7 (0)	20
Fulmar	6 (1)	3 (0)	9
Great Skua	5 (1)	1 (0)	6
Pink-footed Goose	3 (1)	1 (1)	4
Razorbill	13 (0)	7 (3)	20
Red-throated Diver	37 (17)	12 (1)	49
Sandwich Tern	25 (8)	15 (0)	40
Shelduck	1 (1)	1 (0)	2
Unidentified auk	10 (5)	5 (0)	15
Unidentified gull	12 (1)	15 (1)	27
Unidentified tern	1 (0)	0 (0)	1
Wigeon	1 (1)	0 (0)	1
Total	1,324	967	2,291

3.5.8. Table 3.5 provides an overview of videos analysed to inform this Final report, including all daylight videos collected from turbines F04 and D05 by use of the LAWR radar and TADS camera system. In addition, a sample of 48,000 night videos were processed for analysis out of the total number of 459,164 night videos.

NIRAS DHI CARBON TRUST

Table 3.5.   The number of videos recorded by both the TADS camera system and LAWR radar analyseds.

		Turbine D05	Turbine F04	Total
Daylight videos	Total number of videos processed	284,347	274,207	558,554
	Total number of videos with birds	7,882	4,741	12,623
Night videos	Total number of videos processed	21,025	13,378	48,000
	Total number of videos with birds	45	31	76

3.5.9. The table shows that only 2.25% of daylight videos collected by the system had recorded moving birds, indicating a high sensitivity to wave and rain clutter by the system, which led to a high false-positive rate. Species identified in daylight video analysis from turbines F04 and D05 respectively are presented in Table 3.6.

Table 3.6.   The number of daytime tracks recorded by both TADS cameras and LAWR radars on turbines F04 and D05 during the period Oct 2014 to Jun 2016.

Species	Turbine F04	Turbine D05	Total
Northern Gannet	386	1,241	1,627
Black-legged Kittiwake	53	179	232
Herring Gull	125	167	292
Lesser Black-backed Gull	24	34	58
Great Black-backed Gull	105	226	331
Lesser/Great Black-backed Gull	264	553	817
Arctic Skua	0	1	1
Common Crane	2	0	2
Common Eider	3	1	4
Common Gull	53	89	142
Common Scoter	5	6	11
Crow species	1	0	1
Diver species	1	0	1
Goose species	0	1	1
Great Cormorant	0	2	2
Great Skua	0	1	1
Marsh Harrier	1	0	1
Northern Fulmar	1	3	4
Passerine species	1	7	8

NIRAS   DHI   CARBON TRUST

Species	Turbine F04	Turbine D05	Total
Pomarine Skua	1	0	1
Sandwich Tern	0	1	1
Seaduck species	2	1	3
Swallow	0	1	1
Tern spp	13	6	19
Unidentified			
Bird species	16	93	109
Large gull species	1,606	1,551	3,157
Gull species	1,383	2,295	3,678
Small gull species	161	171	332
Seabird species	221	1,073	1,294
Total	4,428	7,703	12,131

3.5.10.   The higher number of birds recorded from turbine D05 may be explained by the proximity of the transformer platform to this turbine, located within 600 m, which was observed to be often used by gulls for resting. It is, however, not clear why the number of Northern Gannets recorded from turbine D05 is higher in comparison to those recorded from turbine F04, the amount observation effort was the same at these turbines.

3.5.11.   Of the sample of night videos processed, the proportion with flying birds indicated very low nocturnal seabird activity in Thanet, with only 0.2% of videos including flying birds.

3.5.12.   Table 3.7 indicates species groups identified in the sample of night videos processed.

Table 3.7.   The number of night time tracks recorded by both the TADS cameras and LAWR radars on turbines F04 and D05 from the sample of videos processed from the period Oct 2014 – Jun 2016.

Species	Turbine F04	Turbine D05	Total
Great Black-backed Gull	0	1	1
Bird species	0	2	2
Large gull species	1	4	5
Gull species	21	15	36
Small gull species	0	4	4
Seabird species	9	19	28
Total	31	45	76

NIRAS DHI CARBON TRUST
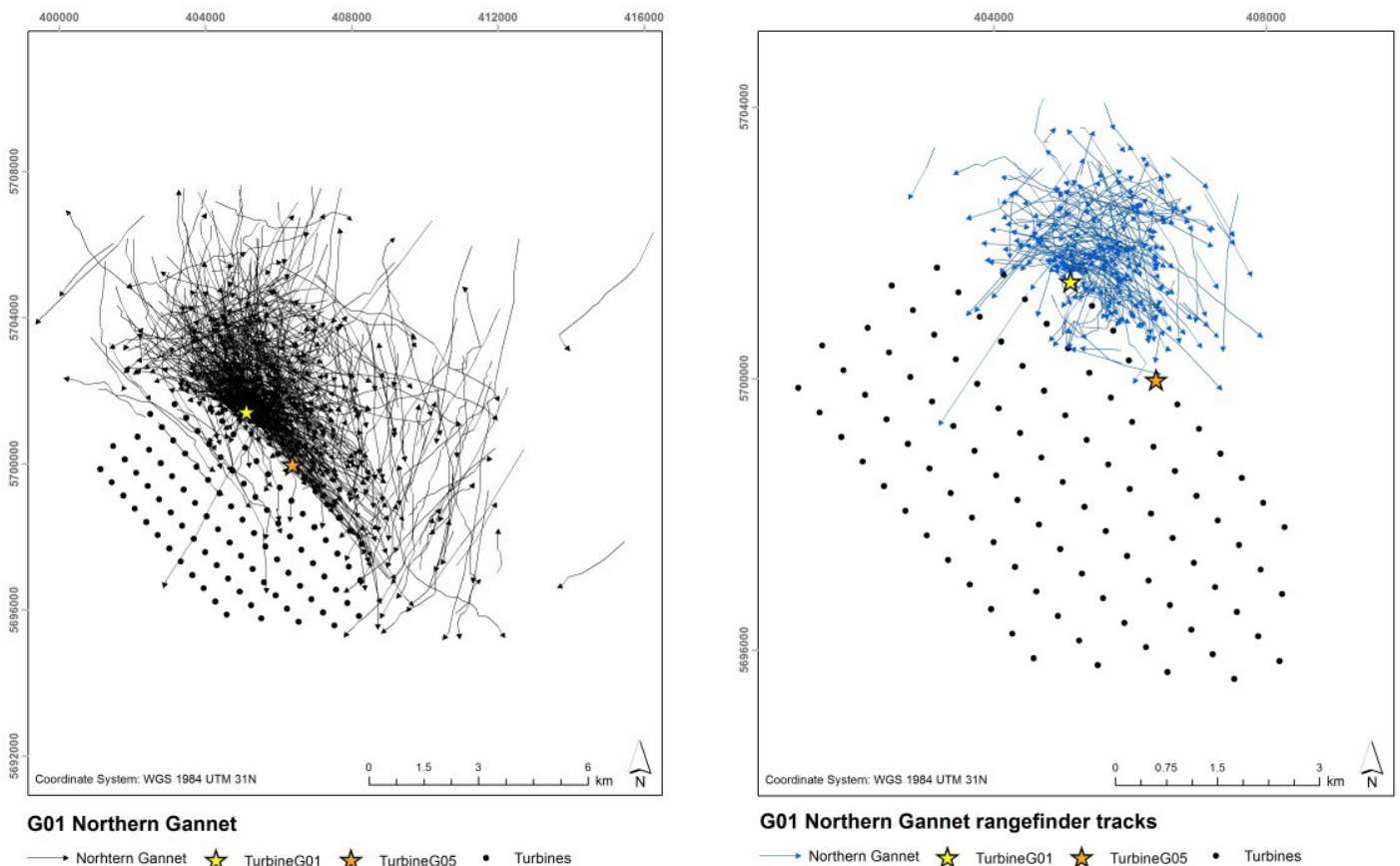
④ ANALYTICAL METHODOLOGY

4.1. BRIEF HISTORY OF METHODOLOGY DEVELOPMENT

4.1.1. As further discussed in Section 7, the application of an avoidance rate factor in collision risk modelling (CRM) has historically been based on post-construction comparisons of the number of collisions recorded or observed using modelling, often based on data from onshore wind farms, and the number of collisions predicted pre-construction (Cook et al. 2014). As a consequence, these avoidance rates may, more accurately, be thought of as correction factors.

4.1.2. EARs derived by this study are considered to represent the likely degree of successful avoidance of an offshore wind farm by a seabird. EARs are also intended to inform how to "correct" CRM, ensuring collision risk accounts for avoidance behaviour (see Section 7). The overall EAR is composed of combining EAR at three different spatial scales: macro avoidance, meso avoidance and micro avoidance (see Section 2.2 for definitions and scope of analysis).

4.1.3. Throughout the duration of this study, the methodology for data analysis and calculation of EARs has evolved considering different options for the treatment of radar / rangefinder track data (see examples in Figure 4.1).

Figure 4.1. Examples of radar (left) and rangefinder (right) tracks collected from turbine G01 identified as Northern Gannets.

ANALYTICAL METHODOLOGY

4.1.4. This section provides an overview of the development of the study's analytical methodology. Additional information on methods considered and options tested can be found in Appendix 8.

a.Analysis of data to inform macro and meso EARs

4.1.5. As mentioned previously, the definitions of the three scales (macro, meso and micro) originally provided by Cook et al. (2014) have been modified in this study in order to be as suitable as possible for the analysis of the study's collected data, and as much as aligned as possible to the assumptions made by the Band model (Band 2007) on bird behaviour. In this study, macro avoidance is defined as bird avoidance responses to the presence of the wind farm occurring beyond its perimeter (and the rotor-swept zone (RSZ) of the outermost turbines), resulting in a redistribution of birds. This encompasses including the area within 500 m of the wind farm that is excluded by Cook et al. (2014) who defined macro-responses to reflect all behavioural responses to the presence of the wind farm that occur at distances greater than 500 m from the base of the outermost turbines.

4.1.6. The original **'Track Abundance Method'** calculated macro EARs by comparing the change of track abundance inside and outside the wind farm, with the track abundance considered outside the wind farm up to 3 km; while meso EARs were estimated by comparing the change in number of trigger points recorded inside and outside the rotor-swept zone (RSZ) + buffer within the wind farm perimeter, with trigger point counts recorded outside the RSZ + buffer.

4.1.7. The track abundance method therefore measured the proportion of birds that avoid the wind farm / RSZ + buffer in relation to those that enter it. Resulting EARs were highly influenced by the size of areas compared, particularly important in meso avoidance analysis where the area inside the RSZ + buffer is much smaller than the area outside the RSZ + buffer (inside the wind farm).

4.1.8. To account for the size of the areas compared, it was agreed that macro and meso EARs should be derived comparing densities of tracks recorded, in relation to a hypothetical situation in the absence of the wind farm in which the same track density would have been encountered across the studied area (i.e. the densities that might be expected in the absence of the wind farm). It was considered that using a hypothetical situation in the absence of the wind farm as a reference would allow to account for 'ponding' effects, i.e. the build-up of bird numbers on the wind farm perimeter observed in macro avoidance data.

4.1.9. Accordingly, the **'Track Density Method'** was adopted to measure the magnitude of change in the total number of seabird tracks in areas compared by assuming an equal density of seabird tracks across the monitored area in the absence of the wind farm.

4.1.10. The first approach to calculating track densities was based on **track counts per km^2,** considered to provide control of the variable size of areas compared. However, the calculation of track densities using track counts per km^2 found results to be highly influenced by the dissimilarity in the size and geometry of areas compared. For instance, in macro avoidance analysis, the relationship between area outside the wind farm and the number of tracks was not found to be proportional, i.e. the number of tracks does not increase proportionally with an increased area size, which may be due to the movement patterns of seabirds and/or ponding effects.

4.1.11. To take account of scaling issues, the application of mirror areas in the analysis of macro avoidance was tested. The sizes of the areas 'outside' the wind farm analysed were reduced to become comparable in size to the smaller area 'inside' the wind farm covered by collected data, i.e. inside areas are mirrored outside. As a side effect of mirroring areas 'inside' the wind farm, a large part of the sampled area 'outside' was excluded from the track density calculations, reducing the reliability of findings. In addition, it was considered that the application of a similar approach in meso avoidance analysis, where the RSZ + buffer

areas are very small in comparison with their surrounding areas within the wind farm, would not be appropriate, and would result in a significant amount of video data discarded from the analysis.

4.1.12.   The second and adopted approach to calculating track densities was based on the use of **track lengths per unit area,** which was considered insensitive to differences in size of areas compared, allowing for a larger proportion of track data to be included in the calculations of both meso and macro EARs. This method is further described in Sections 4.2and 4.3.

b. Analysis of data to inform micro EARs

4.1.13.   The coding of bird behaviour at the micro scale into birds "adjusting" and "not adjusting" to the presence of blades evolved over time based on behavioural responses observed in video evidence, increasing the complexity and scrutiny of evidence recorded.

4.1.14.   Originally, the RSZ + buffer was conceived as a circle, where any birds crossing its extent would be coded as "not adjusting" to the presence of blades. The other codes included "adjusting" and "colliding" (Figure 4.2).

Figure 4.2.   **Original coding of bird behaviour at micro scale; the blue circle represents the RSZ and the red circle represent the RSZ +10m.**

A - Adjusting - Avoids RSZ   **B - Not Adjusting** - Crosses RSZ but survices   **C - Collides**
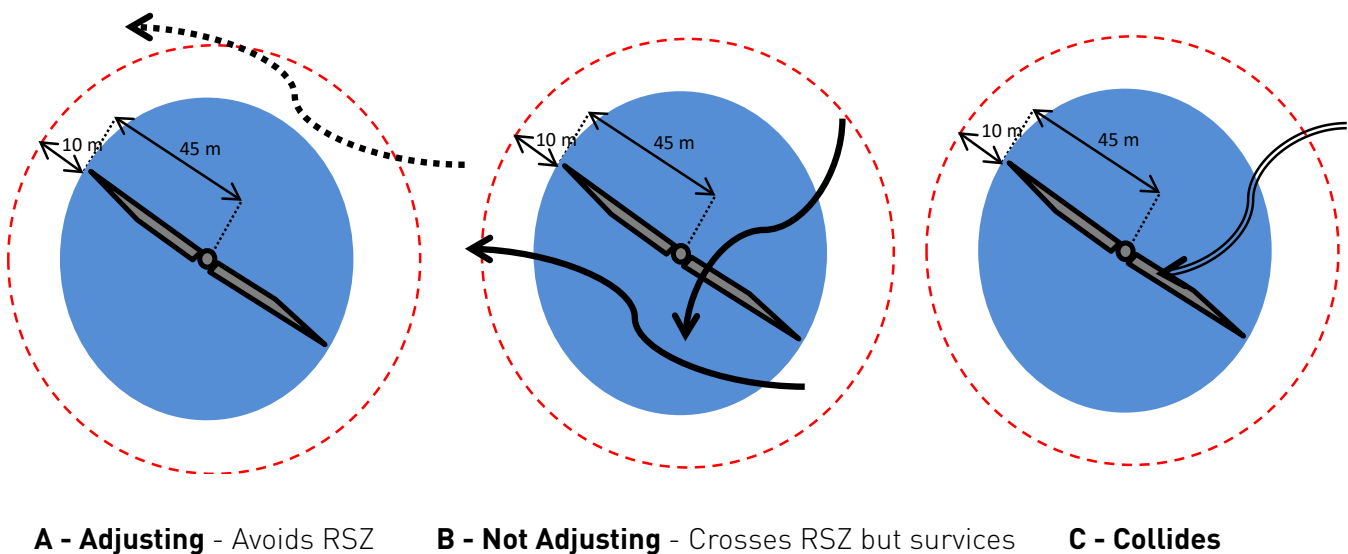
4.1.15.   The increasing number of videos analysed identified additional responses to the presence of turbines, and consideration of rotor orientation was identified as a critical factor on the analysis of behavioural responses. For instance, video evidence showed birds regularly avoid the RSZ (blue circle) by flying parallel to rotor i.e. within the 10 m buffer. Birds were considered as 'not adjusting' when flying through the RSZ and surviving.

4.1.16.   Given that the rotor orientation changes with the wind direction, the coding of micro avoidance behaviour was modified to consider the rotor and RSZ as an ellipse oriented perpendicularly to the wind direction during the time of the intersection of the seabird track, which provides a better representation of actual bird behaviour.

4.1.17.   The codes currently used to describe bird responses at the micro scale are further described in Section 4.4.

4.2. MACRO AVOIDANCE ANALYSIS

4.2.1. To understand why track lengths per unit area can be used to estimate track density and quantify avoidance, it is important to note that the bird flux rate through the RSZ in CRM is defined as the total number of birds passing through the RSZ over a defined period of time. The bird flux rate can be used to estimate predicted number of collisions in the absence of avoidance action:

Cpred = (Flux rate * P_{coll}) + error

4.2.2. The bird flux rate is proportional to the **density of birds** (per unit area) in the airspace occupied by the turbine **(D_A)**, and avoidance can be measured by a reduction in the density of birds in that air space.

EAR = 1 - D_A (with the wind farm) / D_A (in the absence of the wind farm)

4.2.3. The length of a bird track within a unit area **(N)** is considered a measure of track density (see Box 1) that facilitates comparison of track densities in areas of dissimilar size and shape, as required by the conceptual definitions of **macro avoidance** (where the track density in the area inside the wind farm is compared to the track density in the absence of a wind farm, i.e. assuming the same density and same total bird flights in the whole area extending to 3 km outside the wind farm perimeter); and **meso avoidance** (where the track density in the area inside the RSZ + 10 m is compared to the track density in the whole wind farm footprint, i.e. in absence of turbines).

Box 1 – Track length per unit area as a measure of track density

If the bird density is **D_A** (per unit area) then the number of birds in flight in an area **A** is **$D_A A$**.

If their flight tracks were all observed, in unit time the total track length covered would be **$D_A A v$,** where v is the flight speed of the birds.

Track length per unit area (N) would be **N = D_Av.**

Thus track length per unit area (N) is a measure of bird density **(D_A)** which can be derived by dividing by the bird flight speed: **D_A= N / v.**

Within an area **A** of uniform bird density, track length per unit area is:

$\rightarrow$ Total track length within **A** divided by **A**

Mean of track length within each grid cell / area of one grid cell over all the grid cells comprising area A.

ANALYTICAL METHODOLOGY

4.2.4. To facilitate the measurement of track lengths, a grid of equally sized 100m x 100m cells was used to divide the area analysed into "units".

4.2.5. Due to differences in data available for macro avoidance analysis (radar and rangefinder data collected from both turbines G01 and G05) and meso avoidance analysis (radar / TADS data collected from both turbines F04 and D05), the steps followed to measure track length per unit area, and therefore macro and meso EARs are described separately for each dataset. Radar data collected from turbine G05 using the LAWR radar was not considered appropriate for analysis of macro avoidance due to the limited sample size and limitations in equipment detection inside the wind farm. This is further explained in Appendix 2 (Section 5). However, the steps followed to analyse the data are presented below.

a. Radar data collected from turbines G01 (SCANTER 5000) and G05 (LAWR radar)

4.2.6. Data recorded using the SCANTER / LAWR radars include geo-referenced 2-dimensional record (GIS geodatabase) of seabird tracks identified at the species levels by observers, who stored the different entries into the BirdTracker database (see Appendix 1).

4.2.7. To prepare the data for analysis, the following steps were taken:

Creation of unique track IDs per individual species where necessary, as there were cases in which more than one species was recorded within the same track (i.e. when flying as a group).

Filtering of high quality tracks, removing tracks with data errors (e.g. gaps).

Data importation into ArcGIS as a point shapefile, and selection of data associated with the five target species for further analyses. Point data are converted to line shapefiles based on track IDs and point order (using ET Geo Wizards, point to line). All attributes from the point file were joined to the line data attribute table.

Creation of a 100x100 m grid shapefile, clipped by a buffer defining the surveyed area with a max radius of 3 km beyond the wind farm perimeter. Figure 4.3 shows the different areas compared in the analysis. The area covered inside the wind farm from G01 was 6.107 km^2 and from G05 5.780 km^2 (lime green). The area outside the wind farm covered from G01 was 15.883 km^2 and 14.638 km^2 from G05 (turquoise green). Blind sectors (areas shaded by the turbine tower) were also removed.

Creation of a shapefile with radar tracks, characterised by their location, i.e. whether the track is located inside or outside the wind farm or both. Tracks recorded with the rangefinder above the wind farm were listed as outside.

Creation of a shapefile with segmented tracks. The shapefile with radar tracks is overlaid onto the 100x100 m grid shapefile, so that each track is cut into segments within each grid cell ("unit") and the length of each track segment can be calculated (using Geospatial Modelling Environment). Each segment is characterized by two columns that indicate whether they are located inside, outside the wind farm or both.

Creation of a shapefile with segmented tracks. The shapefile with radar tracks is overlaid onto the 100x100 m grid shapefile, so that each track is cut into segments within each grid cell ("unit") and the length of each track segment can be calculated (using Geospatial Modelling Environment). Each segment is characterized by

Figure 4.3. Radar 100x100 m study grids (up to 3 km outside the wind farm) used for calculating mean "track length per unit area" used in calculations of EAR
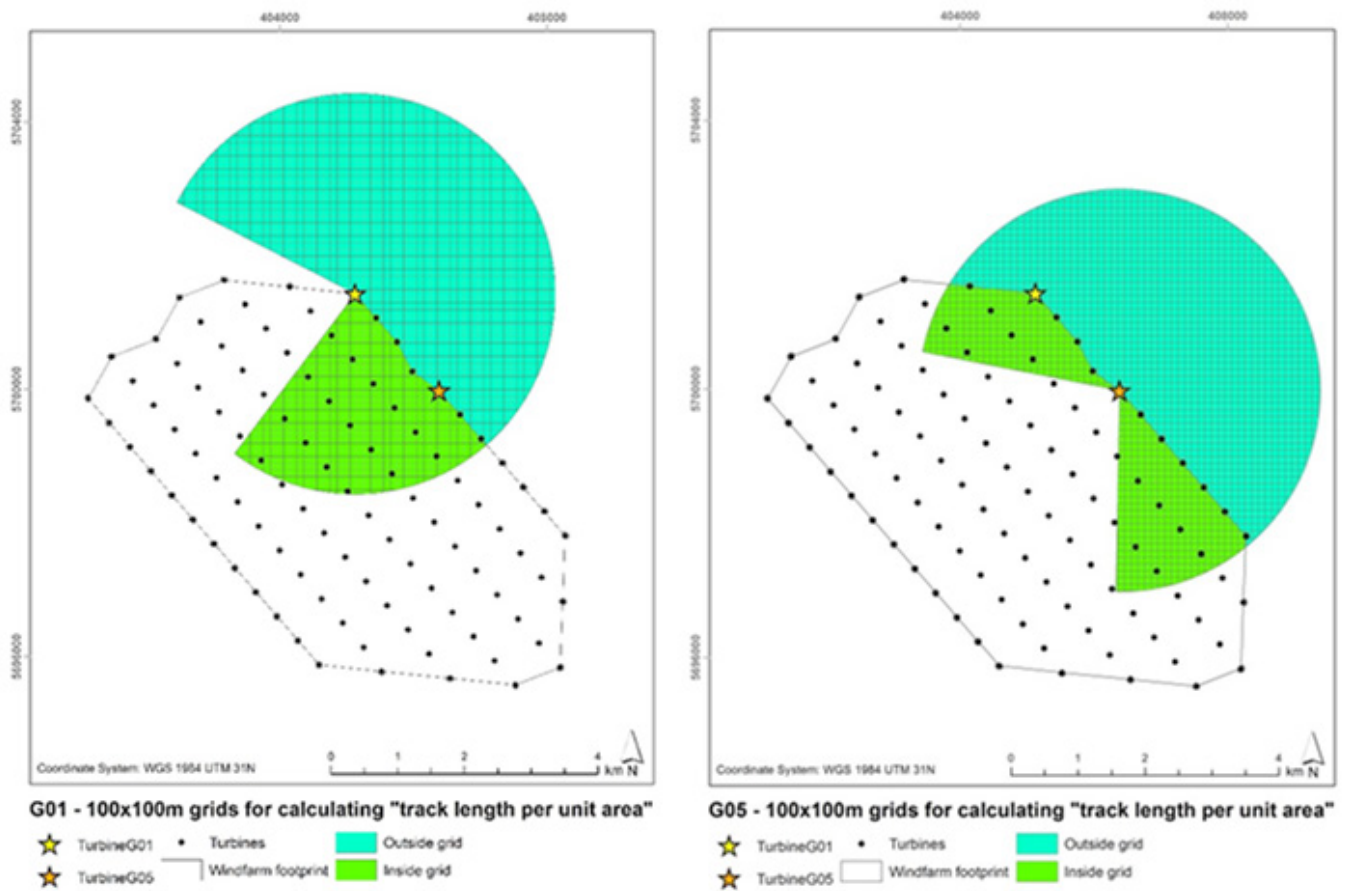
two columns that indicate whether they are located inside, outside the wind farm or both.

4.2.8. The shapefiles produced during data processing and preparation (100x100 m grid file, tracks and segmented tracks) were imported into R to be used in macro EAR estimation (see step c. below).

b. Rangefinder data collected from turbines G01 and G05

4.2.9. Data recorded using rangefinders from turbines G01 and G05 include geo-referenced 3-dimensional records (GIS geodatabase) of seabird tracks identified at species level, indicating whether the track was identified using the radar or not and including flight height (stored in Rangefinder database). Rangefinder tracks also tracked by radars were not included in the macro avoidance analyses.

4.2.10. The following steps were taken to prepare rangefinder data for analysis:

Correction (spatial adjustment) of rangefinder data position. The rangefinder data needs to be corrected for distortion due to the presence of metal constructions of the turbine platforms. The corrections are made with the assistance of fixed calibration points with known positions recorded during fieldwork (see Appendix 3), using the R package 'vec2dtransf' and the affine method (Carrillo 2014).

Conversion of point data to tracks using ArcGIS. The dataset was scanned for positional errors (which can be due to the rangefinder fixing on a turbine or a cloud or any object other than a bird/bird flock) by a visual assessment of daily tracks. Errors, i.e. position which could not be true (e.g. clear spikes, unrealistically long tracks or tracks far away from the observation spots) were removed from the point data and new tracks were created based on the corrected point file. Rangefinder tracks also recorded by the radar were not included in

the macro avoidance analyses to avoid double counting.

Creation of shapefiles. For each rangefinder dataset (collected from turbines G01 and G05 respectively) three shapefiles were created following the same procedure as in the case of radar data. This included:

a) rangefinder track shapefile (with tracks characterised by their location, i.e. whether the track is located inside, outside the wind farm or both)

b) segmented track shapefile

c) 100x100 m grid shapefile, where the area inside the wind farm (lime green) covered from G01 was 1.203 km^2 and 1.968 km^2 from G05. The area outside the wind farm (turquoise green) covered from G01 was 3.745 km^2 and 3.549 km^2 from G05 (Figure 4.4), noting that in this case a 1.5 km range from the turbine locations is used.

Figure 4.4.   Rangefinder 100x100 m study grids (1.5 km range) used for calculating mean "track length per unit area" used in calculations of EARs
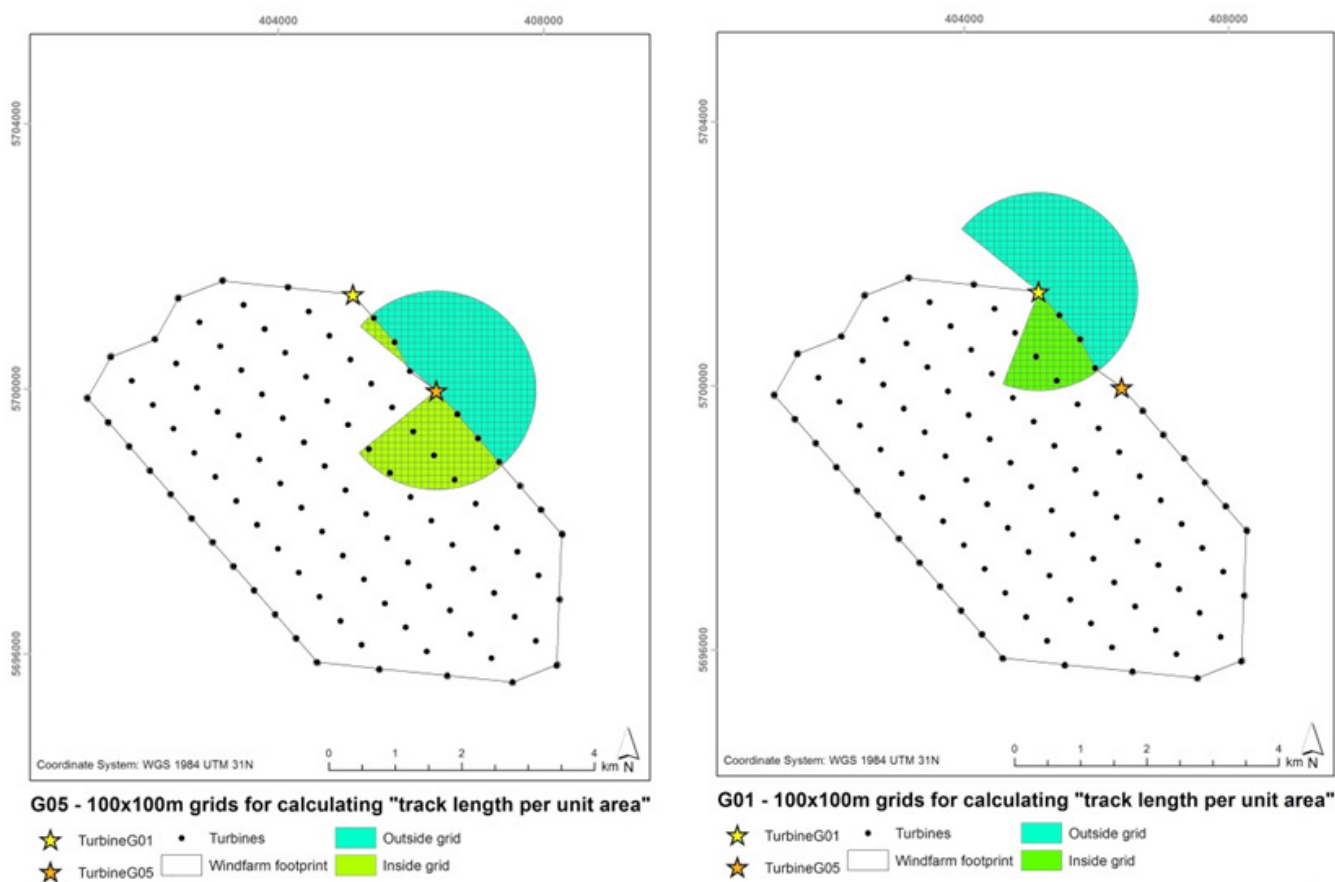
4.2.11.   The shapefiles produced during data processing and preparation (100x100 m grid file, tracks and segmented tracks) were further imported into R (see step c. below).

c. Overall macro EAR

4.2.12.   The first step in the macro EAR calculation conducted in R, is to calculate the (total) track length (i.e. summation of the segmented tracks) in each 100 x 100 m grid cell both inside and outside the wind farm for each sensor and further the mean (total) track length per unit areas (of all grid cells) inside and outside the wind farm (Figure 4.3 and Figure 4.4).

4.2.13. To combine the data from each sensor into an overall macro EAR for each of the target species, the following formula was applied:

$$\text{Overall Macro EAR} = 1 - N_{in} / N_{ref}$$

Where:

N_{in} is the observed mean track length per unit area within the wind farm and sensor specific surveyed area, calculated as mean track lengths per unit area from each sensor (Figure 4.3, Figure 4.4). N_{in} from each sensor were summed in the formula when more than one sensor was included.

N_{ref} is the mean track length per unit area in the absence of the wind farm, a hypothetical situation without a wind farm in which the same bird tracks would have been distributed evenly throughout the studied areas (inside / outside the wind farm). Calculated as:

$$N_{ref} = (N_{in} A_{in} + N_{out} A_{out}) / (A_{in} + A_{out})$$

Where sensor specific $N_{in} A_{in}$ and $N_{out} A_{out}$ were summed in the formula, when more than one sensor was included.

N_{out} is the mean track length per unit area outside the wind farm within the sensor specific surveyed area, calculated as mean track lengths per unit area from each sensor (Figure 4.3, Figure 4.4).

A_{in} is the area within the whole wind farm (not only the surveyed area, i.e. not sensor specific)

A_{out} is the whole area outside the wind farm affected by redistribution of birds due to the presence of wind turbines, i.e. up to 3 km (Figure 4.5).
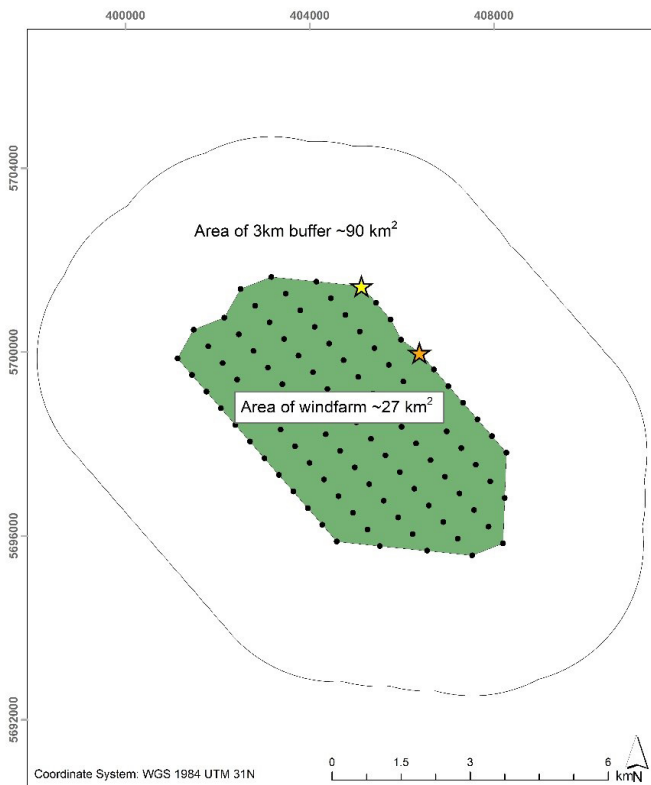

Figure 4.5.   Areas used in the formula for calculating macro EAR

ANALYTICAL METHODOLOGY

4.2.14. Macro EARs were also calculated for each sensor separately to allow for comparison between sensors and the combined macro EAR.

d. Estimating variability

4.2.15. To estimate the variability, i.e. standard deviation, associated with the calculated empirical macro avoidance rate, a bootstrap function (package boot, Canthy 2002) was used for resampling (with replacement) the datasets of complete tracks a thousand times. Within the bootstrap function the track length per unit area was calculated for each bootstrap sample (based on the segmented track data).

4.2.16. Macro EAR for each sensor separately and for all sensors combined was further calculated on each bootstrap sample (simultaneously), based on the calculated track length per unit area. This approach allowed for estimation of standard deviations (variability) around the calculated EARs.

4.2.17. All EARs were calculated using actual data collected, while the standard deviation was derived from the bootstrap samples. This assumes that the available sample is a representative sample of the whole area inside and outside the wind farm, and that the sample size is large enough to complete the analysis.

e. Estimating uncertainty

4.2.18. In addition to the variability associated with the data collected, there are several different sources of uncertainty associated with macro avoidance analysis. A description of assumptions and limitations in chapter 2.2 introduces uncertainty. An option considered to measure these was to extend the confidence limits by an arbitrary value of 10% for each avoidance scale. However, in discussion with the Expert Panel, it was agreed that in order to better quantify uncertainty, the potential sources should be broken down into smaller components to get a more transparent estimate of the uncertainty, and accordingly these have been listed and a value (standard deviation) has been assigned to each separately (Table 4.1).

Table 4.1. **The component sources of uncertainty of the empirical macro avoidance analysis with for each, the standard deviation assigned. The variability was estimated empirically based on bootstrapping while the other components were assumed.**

Sources of uncertainty (term as used in formulas)	Estimate of the uncertainty (assigned standard deviation)
Variability (Variability)	Calculated using bootstrap (see d. above)
Boundary range definition bias (Boundary)	Can be "indicated" by changes observed in values using the 1.5 and 3 km boundary (see Appendix 2, Section 4), and is approximated at 0.1.
Species identification bias (Identification)	SD assigned proportional to level of misidentifications. Approximated to be 0.05 though for Northern Gannet this should be lower (0.01) as this species is comparatively easier to identify than other species.
Spatial adjustment of RF tracks (Adjustment)	Difficult to assess the actual error, with an assumed value of 0.05.
Fishing vessel effect (Fishing)	Difficult to assess although can be assumed to be relatively large for large gulls, with the value of 0.10 considered appropriate.

ANALYTICAL METHODOLOGY

NIRAS DHI CARBON TRUST

Sources of uncertainty (term as used in formulas)	Estimate of the uncertainty (assigned standard deviation)
Large-scale displacement (Displacement)	Considering the study's data indicates redistribution occurs within 3 km (see Appendix 2), uncertainty associated with this can be assumed to be low, with the assumed value of 0.01 considered appropriate. There is no evidence available for the target species that there would be a large scale displacement beyond 3 km, as acknowledged by the recommendation of the UK Statutory Nature Conservation Bodies (SNCBs) for the use of a displacement buffer of 2 km for offshore wind farm assessments (JNCC 2017)[4].
Weather dependent bias (Weather)	Standard uncertainty of 0.10 assumed and "indicated" from weather bias of flight height.
Detection bias (Detection)	(only relevant if LAWR radar data collected from turbine G05 is used)

4.2.19. Individual components identified above were subsequently combined into an overall uncertainty at the macro scale, u_c(macroEAR), using standard rules of uncertainty calculation (Farrance and Frenkel 2012), and the following formula:

$$u_c(macroEAR) = \sqrt{(} u(macroEAR,Variability)^2 + u(macroEAR,Boundary)^2 +$$
$$u(macroEAR,Identification)^2 + u(macroEAR,Adjustment)^2 + u(macroEAR,Fishing)^2 +$$
$$u(macroEAR,Displacement)^2 + u(macroEAR,Weather)^2 + u(macroEAR,Detection)^2$$

4.3. MESO AVOIDANCE ANALYSIS

a. Data collected from turbines F04 and D05 (LAWR radar + TADS Camera System)

4.3.1. Data recorded using the TADS Camera System in connection with the LAWR radar include a record of spatial reference points (coordinates) for each bird captured by the system (hereafter referred to as "trigger points"). Trigger points represent the position at which the radar instructed the camera to lock onto the bird target. It is not necessarily the position at which the bird target is initially videoed by the camera because of (1) a brief (< 1 sec) delay in positioning of the camera and (2) the bird entering the field of view of the video.

4.3.2. Beyond the trigger point the radar may have thereafter lost the bird target at any time and in consequence no further coordinates may have been recorded to depict all/part of the 20 s period that the camera has been able to video record the bird target. Accordingly, meso avoidance analysis is only based on the location of trigger points (inside / outside the RSZ 10 m buffer) and visual assessment of video evidence (i.e. meso avoidance responses are only coded as such when there is an obvious response to the presence of the turbine. For instance, birds flying constantly below the rotor swept zone when crossing the turbine were removed from the analysis), and should be considered as an approximation.

4.3.3. Given that only trigger points can be used, it is necessary to model mean track lengths that represent reality as much as possible. To prepare the data for analysis using the track length per unit method, the following steps were taken:

Coding of trigger points - using the geographical coordinates as well as video evidence, trigger points were coded in relation to their location relative to the RSZ + 10 m buffer (see Section 4.4). Within the wind farm perimeter, trigger points were classified as:

---

[4] JNCC (2017). Joint SNCB Interim Displacement Advice Note. Advice on how to present assessment information on the extent and potential consequences of seabird displacement from Offshore Wind Farm (OWF) developments. January 2017.

NIRAS   DHI   CARBON TRUST

◇ Outside the RSZ + 10 m buffer (there is meso avoidance)

    1 = bird flies between turbines

    2 = bird flies below the rotor

    3 = bird flies above the rotor

◇ Inside the RSZ + 10 m buffer (there is no meso avoidance)

    0 = bird enters the rotor-swept zone + 10 m buffer

Creation of trigger point shapefile - To account for the theoretical DPC associated with the LAWR radar (see Section 3.1), and minimise potential bias, only data recorded in high detection areas were used in the analysis

Figure 4.6. **High detection zones used for meso avoidance analysis, classified as inside area (rotor-swept zone + 10 m) and outside area within the wind farm.**

ANALYTICAL METHODOLOGY
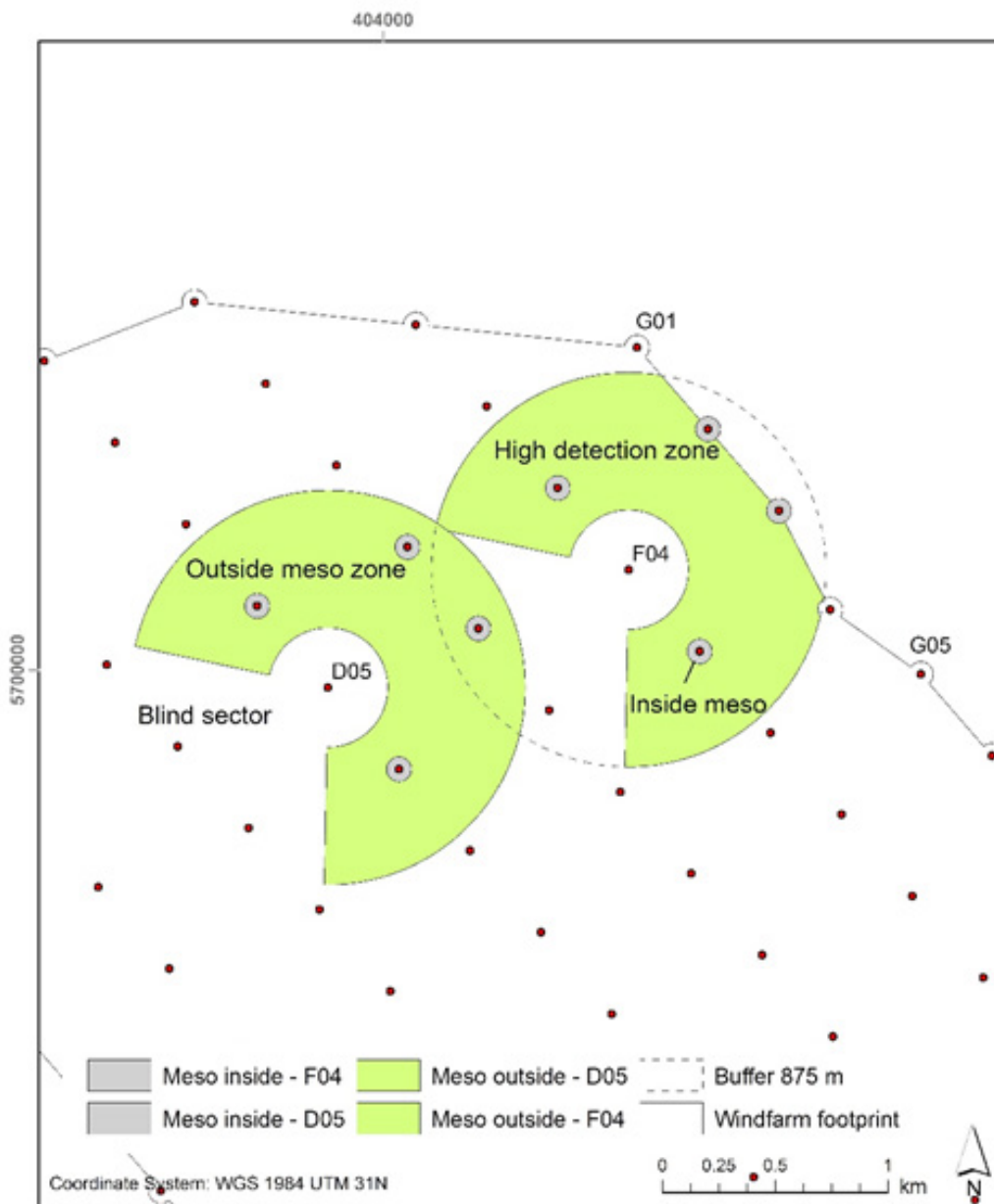
(within 265 and 875 m, corresponding to the upper third (or 67%) of the DPC). The radar blind sectors and area outside the wind farm were removed, as these are not relevant for meso avoidance analysis. As illustrated in Figure 4.6, a total of 4 turbines per camera were included in the meso avoidance analysis, each of them with a RSZ + 10 m area of 0.0095 km^2, the total area within the high detection zones of radars located on turbines F04 and D05 is 1,411 km^2 and 1,572 km^2 respectively.

Calculation of mean track lengths - in the absence of actual radar tracks and to make best use of the limited data available, a mean track length was defined for each trigger point. This approach differed for those trigger points located inside to those located outside the RSZ + 10 m buffer. See Appendix 8 for an overview of the different options tested:

◊ **Inside the RSZ (45 m) + 10 m buffer** – The lengths of tracks recorded in this area are considered comparable to the length of the rangefinder segments used for calculating the flight speed (i.e. finest resolution used for calculating flight speed), and therefore it is assumed that any flights

Box 1 – Calculation of mean track length within the rotor-swept zone (illustration)

Total track length = No of data points in swept area x пR/2

Area = п R^2

Track length per unit area = no of data points in swept area   x   пR/2   / п R^2
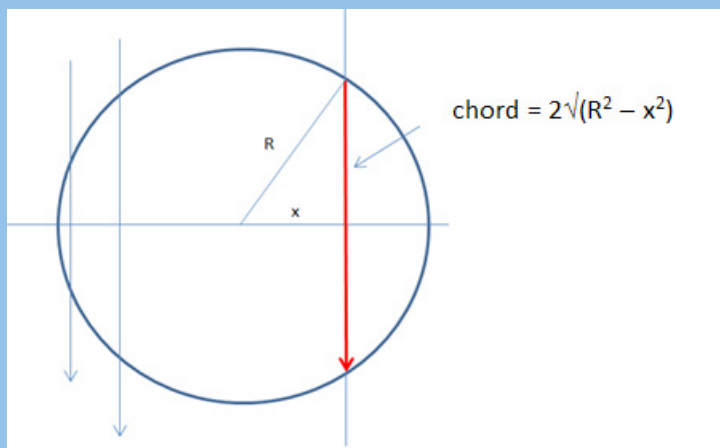
$$\text{chord} = 2\sqrt{(R^2 - x^2)}$$

Mean chord = $\int_{-R}^{R} 2\sqrt{(R^2 - x^2)}\, dx / 2R$

= пR/2

An important assumption is that flight lines are distributed randomly with respect to the centre of the RSZ (i.e. the variable x is distributed uniformly across the width of the circle).

ANALYTICAL METHODOLOGY

NIRAS DHI CARBON TRUST

through this area are straight or linear. The mean track length can therefore be calculated using the formula (see also Box 2 for the mathematical description of mean track lengths):

Mean track length in a circle = πR/2 = 86.4 m

Where R is the radius of the RSZ + 10 m buffer = 45 + 10 = 55 m

◇ **Outside the RSZ + 10 m buffer** – To calculate mean track lengths outside the RSZ + buffer within the wind farm (in the high detection zone of the radars, Figure 4.6), the same approach was followed. A mean track length within a circle with a radius of 875 m (distance to the outermost boundary of the high detection zone, which allows to cover most of the data) was created resulting in 1,374 m long mean tracks. As the high detection zone has a "doughnut" shape and part of the high detection zone is outside the wind farm area, the track lengths are reduced proportionally from the mean track length (65.4% and 58.7% respectively for D05 and F04). The resulting mean track lengths for D05 and F04 were therefore 898 m and 807 m respectively.

Application of speed correction to the tracks outside the RSZ + 10 m buffer – Because it cannot be assumed that birds fly in straight lines in the much larger area outside the RSZ + 10 m buffer within the wind farm, the length of the track needs to be corrected in line with the flight duration. This can be undertaken by using a species-specific flight speed correction factor based on average species-specific flight speed[5] divided by the track speed[6] (see Section 4.7) recorded by the rangefinders.

b. Overall Meso EAR

4.3.4. The calculation of meso avoidance was done using the same approach as for the macro avoidance calculations. First the mean track length per unit are was calculated for the areas inside the RSZ + 10 m buffer, and "outside" areas within the wind farm, defined as the whole high detection zone (including RSZ + buffer areas, as targets located in these areas could be coded as "outside" if they flew below or above the rotors). The following formula was then used in R to estimate meso EAR for each target species (summing up N_{in} and N_{out} from both sensors in the formula):

Overall Meso EAR = 1 - Nin / Nref

Where:

Nin is the mean track length per unit area calculated using recorded trigger points within the RSZ + 10m buffer

Nref is the mean track length per unit area in the absence of the turbines. A hypothetical pre-construction situation in which the same bird tracks would have been distributed evenly throughout the studied areas (inside / outside the RSZ + 10 m buffer within the wind farm). **Nref = (Nin Ain + Nout Aout) / (Ain+Aout)**

Where:

N$_{out}$ is the mean track length per unit area calculated using recorded trigger points within the wind farm footprint but outside the RSZ + 10 m buffer

A$_{in}$ is the total area of the RSZ + 10 m summed up of all wind farm turbines

A$_{out}$ is the whole area inside the wind farm

---

[5] Species-specific flight speed or ground speed is based on the speed required to move between two subsequent recorded positions or nodes.

[6] Track speed accounts for nonlinear flight patterns in long tracks (with more than 5 recorded positions or nodes, on average longer than 1 km) recorded by rangefinder.

NIRAS DHI CARBON TRUST

c. Estimating variability

4.3.5.   A bootstrap function was then used to calculate variability (Standard Deviation) in the same way as done for macro EAR.

d. Estimating uncertainty

4.3.6.   As in the case of empirical macro avoidance analysis, the potential sources of uncertainty associated with meso avoidance analysis have been listed and a value (standard deviation) has been assigned to each separately (Table 4.2). Chapter 2.2 gives a description of the assumptions and limitations.

Table 4.2.   The component sources of uncertainty of empirical meso avoidance analysis with for each, the standard deviation assigned.

Sources of uncertainty (term used in formulas)	Estimate of the uncertainty (assigned standard deviation)
Variability	Calculated using bootstrap (see c. above)
Coding errors (Coding)	Uncertainty is difficult to assess. The value of 0.10 is considered appropriate.
Track length approximation errors (Track length)	Uncertainty is difficult to assess. The value of 0.10 is considered appropriate.
Detection bias (Detection)	A standard uncertainty of 0.1 was assumed. This component is also considered to include uncertainty due to automatic detection, sea clutter effects, potential wind turbine shading, etc.

4.3.7.   Individual components identified above were subsequently combined into an overall uncertainty at the meso scale (uc(mesoEAR)) using standard rules of uncertainty calculation (Farrance and Frenkel 2012), and the following formula:

$$uc(mesoEAR) = \surd \ (u(mesoEAR,Variability)^2 + u(mesoEAR,Coding)^2 + u(mesoEAR,Tracklength)^2 + u(mesoEAR,Detection)^2)$$

4.4.   MICRO AVOIDANCE ANALYSIS

a. Video screening

4.4.1.   While the LAWR radar data collected in combination with the TADS Camera System from turbines F04 and D05 are useful to analyse meso avoidance behaviour, micro avoidance analysis is based on the video evidence only. The following screening process is applied to analyse micro avoidance behaviour and classify trigger point locations used to inform meso avoidance analysis (Section 4.3):

4.4.2.   Initial screening of videos – Movement detected by the LAWR radars other than birds e.g. sea waves, can lead to it being automatically targeted by the camera. Removing such videos from the analysis of bird videos is the purpose of the initial screening exercise. The initial screening is conducted with each 20 s video viewed on VLC Media player using fast forward display. Those videos in which no discernible flying bird(s) are visible due to the absence of bird(s), sitting birds or poor visibility (due to weather or salt/rain on the lens) are removed from further analysis.

4.4.3. Secondary screening of videos - Each video retained following initial screening was taken forward to a 'secondary screening' process during which image quality, species identification, relative position of target tracked and the target's interaction with turbines were documented. During video viewing, a number of different parameters are recorded, described in Table 4.3.

Table 4.3.   Parameters recorded during secondary screening of TADS Camera daylight video by assessor.

Parameters	Comments
Turbine	**Turbine from where the video was recorded i.e. either D05 or F04.**
TrackID	**A unique identification code* for the target being videoed identical to that of its related trigger point. Each code contains in sequence e.g. D05X201510010748(491_508):** **• platform from which the track/video was recorded i.e. D05 or F04** **• year** **• month** **• day** **• time and,** **• trigger point coordinates (in brackets)** **More than one record in the data entry spreadsheet may have the same identification code should one target involve birds of multiple species or differ in behaviour.**
Date	**Date of video**
Species	**Species being tracked by video.**
Species group	**Species group e.g. large gull, small gull, gull, passerine, being tracked by video.**
Number	**Number of birds being tracked by video.**
Age	**Age of bird, if discernible**
Video quality	**The video quality is recorded as either poor (code 3), fair (2) or good (1). A poor image is when the bird cannot be identified to species or species group, if closer enough. A good image is that which equates to what the assessor considers is an image of high definition quality. All other images are classified as of fair quality. All videos in which nothing can be made out due to poor visibility is a separate classification; they are removed from further analysis at initial screening.**
Sea State	**Sea State is assessed from the video.**

* More than one record may exist in the video data entry spreadsheet per video when a target comprises of multiple birds (1) of different species / age groups (i.e. mixed flock) or (2) that differs in behaviour.

NIRAS DHI CARBON TRUST

Parameters	Comments
Behaviour	Behaviour – scored as "micro" if tracks are subjectively assessed from watching the video as being within the rotor-swept zone + 10 m buffer represented as a circle. All other tracks with the exception of collisions, are accredited to "meso".
Meso	Those tracks assigned to meso under "Behaviour" are subjectively assessed from watching the video as either flying above, below the rotor, above the rotor or between turbine rows.
Micro	Those tracks assigned to micro under "Behaviour" are assessed from watching the video as either adjusting or not adjusting to the presence of blades. Number of collisions are also recorded. (see below for an illustrative representation of these codes) .
Collision	Description of collision event should it occur.
Parallel to rotor	Whether bird(s) is flying parallel/alongside to rotor i.e. on a trajectory that will not intersect with the rotor or the airspace directly above or below the rotor.
Behaviour (ESAS)	Behaviour of the bird(s) described using the European Seabirds at Sea (ESAS) standard codes.
Association (ESAS)	Any association of the bird(s) with features (e.g. trawler) described using ESAS codes.
Rotor still	Whether the rotor nearest the bird(s) was static or rotating in the video.
Check position	Video to be re-examined due to uncertainty in bird position i.e. whether to be coded under "Behaviour" as meso or micro.

4.4.4. Tertiary screening/Quality check - On completion of secondary screening, all videos with birds were subjected to tertiary screening/quality check and geo-referencing. This entails:

- **Geo-referencing of videos** - The video and LAWR radar data (trigger point) are combined into a GIS geodatabase with references to the video files using the unique track ID to link all video recordings to a geographic position obtained by the radar. The geo-positioning from the radar has an accuracy of 1-5 m depending on the distance to the target within the wind farm. The length of radar tracks is independent of the 20s fixed time intervals that the cameras are recording each time they are triggered.

- **Re-assessment of behaviour** of those records for which tracks have been scored as either "meso vertical" or "micro" in the secondary screening. On this occasion the track is scored as "micro" only if assessed as displaying micro avoidance in proximity to the rotor or is recorded to cross the rotor-swept zone + 10 m buffer represented as a circle (meso 'non avoidance' area). This is conducted both by checking the videos (bird behaviour and rotor activity), and by assessing the trigger position of the radar track in relation to the orientation of the rotor and the size of the circular buffer zone. Bird behaviour at the micro scale (within the RSZ + 10 m circle) is then analysed in relation to the RSZ + 10 m buffer represented with a dynamic ellipse.

Table 4.4. Parameters recorded during tertiary screening of TADS Camera daylight video by assessor.

Parameters	Comments
Revised Behaviour	Behaviour – scored as "micro" if tracks is subjectively assessed from watching the video as being within the rotor-swept zone + 10 m buffer represented as an ellipse (meso 'non avoidance' area). All other tracks with the exception of collisions, are accredited to "meso".
Revised Meso	Those tracks assigned to horizontal meso avoidance (between turbine rows) under "Behaviour" are not included in the tertiary screening/quality check. The position of all tracks coded as vertical meso avoidance (flying above or below the rotor), are checked against the position of the associated radar track.
Revised Micro	The coding of all tracks assigned to micro under "Behaviour" are checked both visually from watching the videos and in GIS by assessing the position of the radar tracks in relation to the orientation of the rotor (represented as an ellipse) and the size of the circular buffer zone (see below). An additional code is subsequently added for birds avoiding collision by flying along the rotor.
Nearest turbine distance	The nearest turbine to the trigger coordinates of each record is calculated by cross referencing in ArcGIS software the coordinates against a raster map of the distance of the nearest turbine for each 1 m x 1 m grid square.

- **Assessment in relation to the rotor** – Using Thanet weather data (relevant to turbines F04 and D05) and video footage respectively, it is possible to assign video clips to a set of weather conditions and rotor activity status:

    ◊ **Assessment of rotor orientation** – The analysis of weather data, wind speed and direction provide data on the rotor orientation at the time a track / video was recorded. Assessment of radar tracks in relation to rotor orientation is undertaken using GIS. Weather measurement data recorded by Vattenfall from G01 has been used to assess the rotor orientation (informing the sensitivity analysis).

    ◊ **Assessment of rotor activity** – The assessment of turbine activity using video footage can give an indication as to whether the rotor was spinning or not during time of recording.

4.4.5. In contrast with macro and meso avoidance analysis, where only the position of collected data is considered, micro avoidance analysis considers the behavioural reaction of the bird(s) to the orientation of the rotor and the presence of blades when entering the RSZ + 10 m buffer:

- Birds colliding (F)

- Birds not adjusting their flight – crossing the rotor without adjustments but surviving (E)

- Birds adjusting their flight – classified as all birds entering the RSZ + 10 m that have not crossed the rotor without adjusting their flight path or collided with it. This can be birds turning (A) or stopping before crossing the rotor (B, bird observed landing on the sea or avoidance happened at the end of the video sequence), flying on a trajectory within the RSZ + 10 m buffer that will not intersect with the rotor (C), or crossing the rotor with some form of adjustment (D). As the vast majority of recorded seabird flights through the RSZ were of type C, this type of flight behaviour in the RSZ was interpreted as micro avoidance. In those occasions when the rotor is still and a bird is observed crossing the RSZ, birds have been excluded from the analysis, as the Band model accounts for downtime.

Figure 4.7. Illustration of micro avoidance concept and approach to analysis considered in this study. Within the RSZ (blue circle) + 10 m buffer (red circle), black arrows represent bird movement in relation to the rotor (dark blue ellipse + 10 m buffer (red ellipse). The light blue arrow represents wind direction.
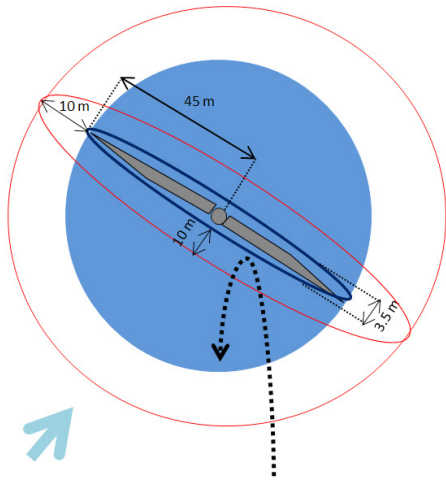
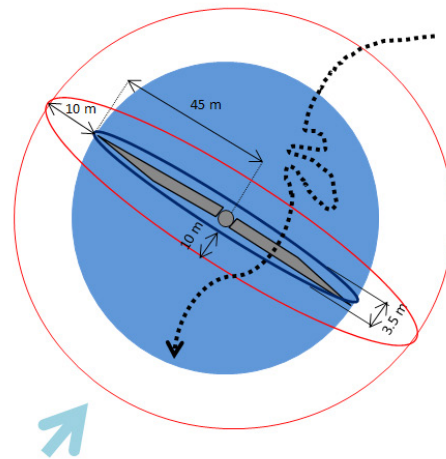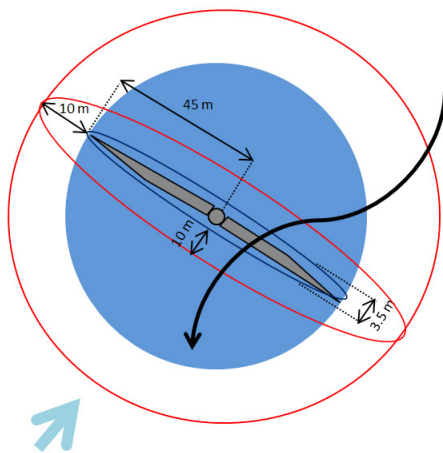**A - Adjusting** - Returns before crossing the rotor, turning 180°
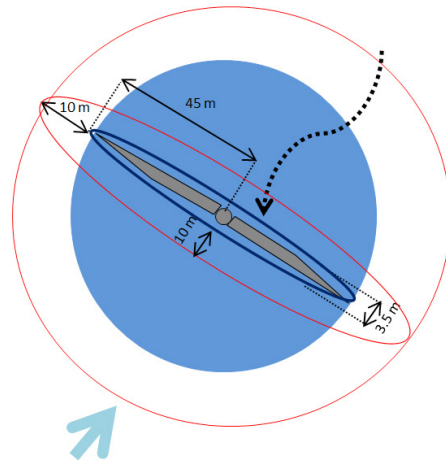
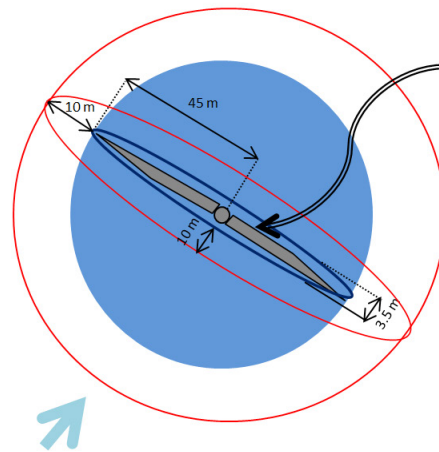**B - Adjusting** - Stops before crossing the rotor
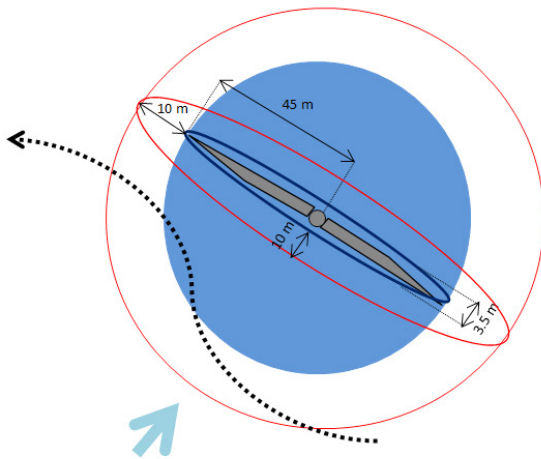
C - Adjusting - Files along the rotor blades

D - Adjusting - Crosses the rotor with adjustments. Bird changes its path in front of rotor to cross between 2 blades.

E - Not Adjusting - Crosses the rotor without adjustments but services

B - Collides

ANALYTICAL METHODOLOGY

4.4.6. Using the coding above, the overall micro EAR was estimated using data for all five target species, and applying the following formula:

$$\text{Overall micro EAR} = \frac{\text{N birds adjusting flight}}{\text{(N birds adjusting+N birds not adjusting+N birds colliding)}}$$

b. Estimating variability

4.4.7. Bootstrapping has been used for resampling the datasets (sampling of our sample with replacement 1,000 or 10,000 times) to estimate the variability, standard deviation, around empirical macro, meso and micro avoidance rates calculated (using the R package "boot").

c. Estimating uncertainty

4.4.8. As in the case of empirical macro and meso avoidance analysis, the potential sources of uncertainty associated with micro avoidance analysis have been listed and a value (standard deviation) has been assigned to each separately (Table 4.5). A description of assumptions and limitations in chapter 2.2 introduces uncertainty.

Table 4.5. **The component sources of uncertainty of empirical micro avoidance analysis with for each, the standard deviation assigned.**

Sources of uncertainty (term used in formulas)	Estimate of the uncertainty (assigned standard deviation)
Variability	**Calculated using bootstrap (see b. above).**
Coding errors (Coding)	**Uncertainty difficult to assess, the value of 0.10 is considered appropriate.**
Species-specific differences (Species-specific)	**An approximate value of 0.02 can be assumed for Northern Gannet and Black-legged Kittiwake based on the different values calculated using observations on all seabird species and on all gull species.**
Detection bias (Detection)	**Standard uncertainty of 0.1 judged from similar detection curves inside/outside and use of doughnut approach. This is considered to also capture unknown uncertainty due to automatic detection, sea clutter, wind turbine shading etc.**

4.4.9. Individual components identified above were subsequently combined into an overall uncertainty at the micro scale (uc(microEAR)) using standard rules of uncertainty calculation (Farrance and Frenkel 2012), and the following formula:

uc(microEAR) = √ (u(microEAR,Variability)^2 + u(microEAR,Coding)^2 + u(microEAR,Species-specific)^2 + u(microEAR,Detection)^2)

4.5 OVERALL AVOIDANCE

a. Formula

The mean overall empirical avoidance was calculated by combining species-specific macro, meso and micro EARs using the following formula, where all three avoidance components are multiplied as non-avoidance and converted to avoidance (Cook et al. 2014, Band 2012):

$$\text{Overall EAR} = 1-((1-\text{macro})\bullet(1-\text{meso})\bullet(1-\text{micro}))$$

b. Estimating uncertainty

4.5.2. In order to quantify uncertainty associated with overall EARs, uc(overallEAR), uncertainty components identified (expressed in the same units) and combined for each scale (see Sections 4.2, 4.3 and 4.4 above) were combined into "overall" standard uncertainty, which is the same as standard deviation, propagated in line with standard rules (Farrance and Frenkel 2012) using the following formula:

$$u_c(\text{overallEAR}) = \text{overallEAR}*\sqrt{\left(\frac{u(\text{macroEAR})}{\text{macroEAR}}\right)^2 + \left(\frac{u(\text{mesoEAR})}{\text{mesoEAR}}\right)^2 + \left(\frac{u(\text{microEAR})}{\text{microEAR}}\right)^2}$$

4.5.3. This formula provides propagated standard deviation for the overall EAR, which can then be used to calculate the 95% confidence limits by:

low 95% limit = overall EAR-(1.96)*(SD)

4.6   NIGHT VIDEO ANALYSIS

4.6.1. In order to sample night videos, a number of dates were selected, focusing on winter months, when abundance of birds, and therefore bird activity was anticipated to be higher. Accordingly, all night videos collected (both during day and night) during the following dates were processed:

Turbine D05	Turbine F04
• 22nd, 23rd, 24th, 26th, 27th, 30th Nov 2014 • 3rd, 8th Jan 2015 • 10th, 13th Apr 2015 • 19th, 20th, 31st Oct 2015 • 1st, 2nd, 22nd, 23rd, 26th Nov 2015 • 1st, 7th, 8th, 9th, 13th, 14th, 15th, 18th, 28th, 31st Dec 2015 • 1st Jan 2016 • 1st, 9th, 11th, 12th, 23rd Feb 2016 • 9th, 10th, 11th, 12th Mar 2016	• 18th, 19th, 20th, 23rd, 24th Nov 2014 • 13th, 15th, 16th, 19th, 24th Dec 2014 • 25th Feb 2015 • 24th, 25th, 27th Mar 2015 • 2nd, 4th, 5th, 10th, 11th, 13th, 30th Apr 2015 • 8th May 2015 • 31st Oct 2015 • 1st, 25th, 26th Nov 2015 • 1st, 9th, 11th, 12th, 14th, 15th, 18th Dec 2015 • 24th Jan 2016 • 9th, 13th, 16th – 29th Feb 2016 • 1st, 3rd Mar 2016

ANALYTICAL METHODOLOGY

4.6.2. These videos were characterised by calm conditions and good visibility, which enhances the detection and species identification distance in the thermal videos. Night time was defined as the timeframe between 30 min after sunset to 30 min before sunrise.

4.6.3. Analysis of videos had two aims:

- Compare bird activity during day and night time, based on the number of videos with birds recorded on a given day during day time and night time respectively

- Code bird behaviour recorded in night videos following the steps applied in the screening of daytime videos (see Section 4.3).

4.6.4. Only one species identification was possible. However, as the sample size of the night videos was small, the analysis was undertaken for all seabird species combined and the analysis of night activity does not distinguish between species.
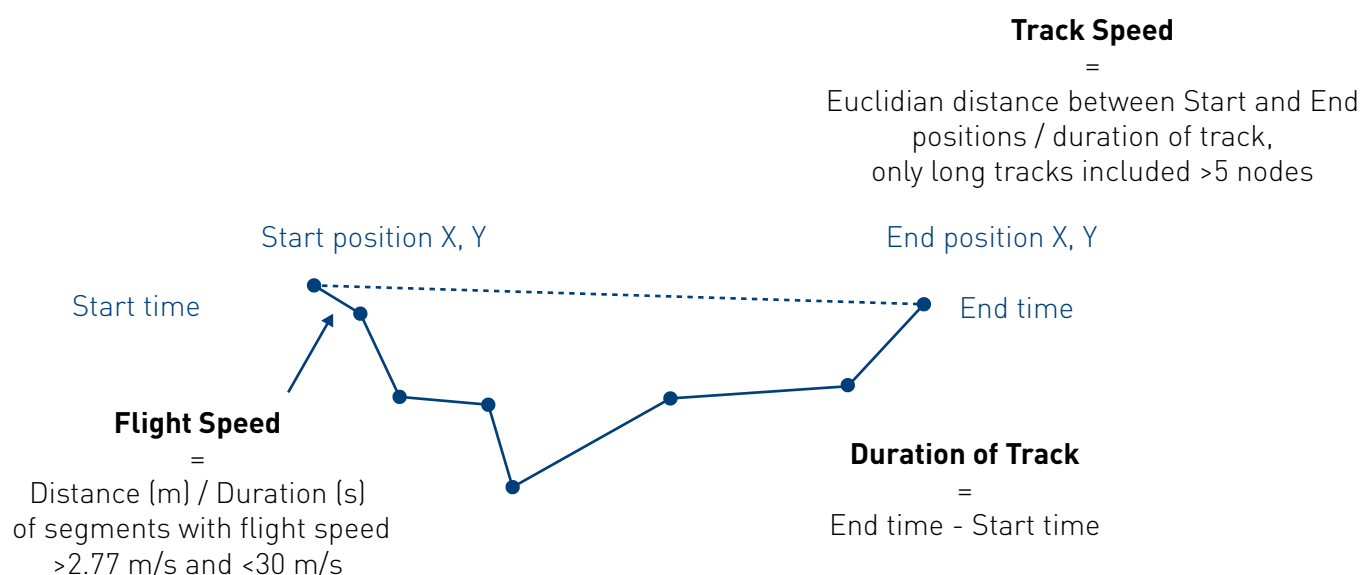
4.7. FLIGHT SPEED ANALYSIS

4.7.1. Average flight speeds per species were calculated using rangefinder data collected from turbines G01 and G05.

4.7.2. Two types of flight speed, considering the horizontal vector, were calculated Figure 4.8:

Flight speed (linear flight speed) - Calculated based on using single segments recorded between two nodes (recorded positions by the rangefinders), where the length of recorded track segments in metres is divided by the flight duration in seconds. Extreme values or birds on the water were removed by selecting only segments with a speed of >2.77 m/s and < 30m/s. The minimum and maximum speeds have been determined arbitrarily in order to avoid extremes and minimise the introduction of potential errors. Regarding the minimum speed, it is judged to represent the slowest possible average speed, even for foraging Northern Gannets. The flight is assumed to be linear between nodes.

Track speed (non-linear flight speed) – Calculated using tracks with more than 5 nodes and a track speed larger than 0 m/s, where the euclidean distance from start to end of the track (m) is divided by the duration of the recording (s). A similar approach based on hourly speed was used by Klaassen et al. (2012), however this temporal scale would be too coarse for data collected by this study. The track speed is used to estimate an actual mean flight duration taking into account that birds are not flying straight all the time.

Figure 4.8. Schematic description of flight speed calculations.

Track Speed
=
Euclidian distance between Start and End positions / duration of track, only long tracks included >5 nodes

Start position X, Y   End position X, Y

Start time   End time

Flight Speed
=
Distance (m) / Duration (s) of segments with flight speed >2.77 m/s and <30 m/s

Duration of Track
=
End time - Start time

4.8. FLIGHT HEIGHT ANALYSIS

4.8.1. Rangefinder height measurements of target species were analysed in order to calculate the proportion of birds flying at rotor height. In addition, the influence of wind conditions on seabird flight altitudes were assessed. The scope of the analysis did not include a development of flight height frequency distributions suitable for the extended Band model.

4.8.2. The altitudes recorded by the rangefinders are recorded in relation to the altitudes of the connected GPS ("baseline" altitude), which are estimated when the rangefinder is initially connected to the GPS on a given fieldwork day, and this altitude is not always correct. Thereafter, the GPS is only storing data, without updating the baseline altitude estimation. Accordingly, the altitude needs to be adjusted so that the baseline altitude is correctly defined.

4.8.3. During fieldwork, observers took calibration measurements of altitude of nearby turbine nacelles with known heights for (baseline) calibration (note that this vertical calibration is a different to the horizontal calibration when spatial adjustment was used). Accordingly, all height recordings were corrected in line with the calibration measurements. As there might be errors[7] in calibration measurements, the range and SD of the calibration altitudes for each survey day were checked, and potential errors (identified when values fell outside the mean +/- SD of calibration measurements) were removed or corrected if the range was very large to avoid any sources of bias.

4.8.4. The final altitude dataset had a mean daily range between lowest and highest calibration heights of 2.5 m and a standard deviation of the calibration heights of 0.87. These values indicate that the fluctuation in measured altitudes was rather small in the dataset used in the analyses. The final species-specific sample sizes used are shown in Section 5.6.

4.8.5. Proportion of birds flying at rotor height was calculated based on all measurement (i.e. several measurements per track).

4.8.6. In order to explain the differences in flight altitude in relation to wind speed and wind direction (relative to the flight direction of the bird) and distance to wind farm boundary, either inside or outside the wind farm footprint, the rangefinder track data was integrated based on closest date and time with measured, turbine specific, wind data from Thanet provided by Vattenfall.

4.8.7. The variable defining flight direction in relation to wind direction indicate whether a bird was flying in:
- head wind (straight against the wind within a range of ±45°),

- tail wind (in the same direction as thew wind within ±45°) or

- cross wind (perpendicular to the wind direction within ±45° from either side).

4.8.8. As the relationships between the response variable (bird altitude) and the predictor variables can be non-linear and the error structure of the data does not typically follow a Gaussian error distribution; a generalised additive modelling framework was used. Further, to account for non-independency (spatial or temporal autocorrelation) of samples within tracks a mixed model was used (GAMM) with a correlation structure. We applied the ARMA (autoregressive-moving-average model) correlation structure. ARMA is a temporal autocorrelation structure were the autoregressive order can be manually specified by adjusting the p-coefficient and moving average by the q-coefficient (see e.g. Zuur et al. 2009). The correlation structure

---

[7] Errors can occur with the Vector if the rangefinder pulse misses the bird and is reflected instead by a foreground or background object. Erroneous observations were easily detected as points on the track that were displaced along the Vector's line of sight. In addition, a KML file for each run was also generated and examined, which allowed displaying the bird's track later in Google Earth, superimposed on a map of the coastline.

ANALYTICAL METHODOLOGY

accounts for non-independence and the autocorrelation in residuals was tested by an autocorrelation function plot (acf). The observer platforms were also included as random terms to account for any non-independences due to a "platform-effect".

4.8.9. The p-value accounting for the residual autocorrelations was chosen (based on the acf graph, i.e. how well it accounted for autocorrelation), and the q-value was kept as the default value which is 0. The correlation structure was defined to be nested within individual tracks (i.e. the correlation structure is restricted to account for correlation within tracks but not between tracks).

4.8.10. The models were fitted in R using the "mgcv" package (Wood 2006). The GAMMs were fitted with altitude as the dependent variable and the predictor variables mentioned above, as smooth terms (using thin plate regression splines, Wood 2006). Flight direction in relation to wind (head, tail or side winds) a factor describing whether the bird was inside or outside the wind farm was included as a categorical variable in the models. To fit the models the most appropriate error distribution was used (most often the gamma error distribution). The degree of smoothing (how closely the model fits the data) was chosen automatically by cross validation in the "mgcv" package, but it was restricted to be no more than 5 (k=5) to avoid potential overfitting.

4.8.11. It should be noted that data used in the analyses were constrained by the limited range of weather conditions during which observers are able to safely access turbines G01 and G05.

ANALYTICAL METHODOLOGY

⑤ RESULTS

5.1. INTRODUCTION

5.1.1. This section presents the results obtained in the quantification of empirical macro, meso and micro avoidance, as well as resulting overall EARs, including assessment of associated uncertainty. Interpretation of bird distribution recorded using radar and rangefinder, and behaviour observed in video evidence (TADS system) is presented in Section 6.

5.1.2. The contribution of each scale to overall estimates is further analysed and discussed, together with an assessment of sensitivity over changes in values. A review of sample size and precision, i.e. how EAR changes when the sample size is reduced is provided in Appendix 9**.**

5.1.3. Results of the analysis of rangefinder data in relation to flight speeds and flight heights are also provided.

5.2. MACRO EAR

5.2.1. The final number of tracks in the final database and the calculated "mean track length per unit

Table 5.1. **Number and track length per unit area for each sensor and target species collected between July 2014 and April 2016 from turbines G01 (where SCANTER was positioned (S)) and G05 (where LAWR radar is positioned (L)). Classification of tracks and their density is presented in relation to their location, either inside the wind farm or outside the wind farm within a 3 km (in the case of radars) and 1.5 km (in the case of rangefinders (RF)). Large gulls refer to all large gull species (LBBG, HG, GBBG) and unidentified large gulls. Please note that G05 radar data are included, although they were not used in the calculation of overall EARs.**

Target species	Sensor and turbine position	Total N tracks	N Tracks inside	N Tracks outside	Track length per unit area inside	SD inside	Track length per unit area outside	SD
Northern Gannet	S G01	583	79	497	9.75	1.47	67.09	3.15
	RF G01	244	15	210	8.15	2.69	44.73	3.48
	L G05	184	2	131	0.16	0.12	20.52	2.04
	RF G05	250	31	209	20.62	2.27	61.70	4.81
Black-legged Kittiwake	S G01	76	19	66	1.52	0.51	6.46	0.95
	RF G01	83	19	80	5.63	1.65	15.88	1.90
	L G05	49	15	44	0.90	0.30	3.83	0.67
	RF G05	159	53	141	13.61	2.48	33.52	3.40

NIRAS DHI CARBON TRUST

Target species	Sensor and turbine position	Total N tracks	N Tracks inside	N Tracks outside	Track length per unit area inside	SD inside	Track length per unit area outside	SD
Lesser Black-backed Gull	S G01	144	21	122	2.73	0.84	14.44	1.33
	RF G01	77	7	75	2.54	1.10	12.22	1.66
	L G05	29	2	21	0.13	0.09	2.61	0.62
	RF G05	78	26	64	6.83	1.74	11.02	1.54
Herring Gull	S G01	187	43	168	4.18	0.85	20.43	1.66
	RF G01	93	17	84	11.98	3.51	17.05	1.94
	L G05	36	5	32	0.49	0.29	3.72	0.75
	RF G05	144	59	124	18.00	2.90	29.13	3.19
Great Black-backed Gull	S G01	220	68	202	5.85	0.80	21.09	1.46
	RF G01	144	33	133	12.09	2.37	24.00	2.32
	L G05	51	20	44	1.78	0.46	4.55	0.77
	RF G05	118	46	97	14.39	2.70	23.59	2.79
Large gulls	S G01	552	132	493	12.76	1.52	56.01	2.56
	RF G01	314	57	292	26.62	4.64	53.27	3.59
	L G05	116	27	97	2.40	0.53	10.87	1.28
	RF G05	341	131	286	39.22	4.36	63.85	4.60

area"with standard deviation (SD, based on bootstrap resampling), are presented in Table 5.1.

5.2.2. All tracks for the five target species collected and the track length per unit area calculated have been mapped and are presented in Section 6.

5.2.3. Estimated macro EARs for each sensor and combined, including with / without G05 LAWR radar data are presented in Table 5.2 and illustrated in Figure 5.1. This is further analysed considering different macro

Table 5.2. **Estimated macro EARs and associated SD for each species, sensors (G01 radar – SCANTER (S); G05 radar – LAWR (L)) and combined sensors with an outer boundary range of 3 km. Highlighted in grey, "No G05 radar data" refers to overall EARs that do not include G05 radar data, and which are recommended to be used in the calculation of overall EARs.**

	Northern Gannet	Black-legged Kittiwake	Herring Gull	Great Black-backed Gull	Lesser Black-backed Gull	All large gulls
Overall Macro EAR	0.816	0.575	0.442	0.469	0.639	0.495
SD	0.023	0.055	0.064	0.054	0.060	0.037
Overall Macro EAR (no G05 radar data)	0.797	0.566	0.422	0.464	0.619	0.481
SD	0.026	0.058	0.067	0.057	0.064	0.038
Macro EAR (S G01 radar)	0.819	0.715	0.749	0.667	0.768	0.723
SD	0.026	0.093	0.049	0.043	0.067	0.031
Macro EAR (L G05 radar)	0.990	0.713	0.834	0.546	0.938	0.731
SD	0.008	0.090	0.096	0.093	0.042	0.054
Macro EAR (G01 RF)	0.776	0.584	0.246	0.431	0.746	0.435
SD	0.072	0.110	0.168	0.101	0.103	0.083
Macro EAR (G05 RF)	0.787	0.530	0.323	0.330	0.321	0.326
SD	0.045	0.077	0.101	0.119	0.160	0.069

Figure 5.1. **Calculated Empirical Macro Avoidance for all target species and large gulls combined with associated bootstrap SD (error bars), for all sensors combined, all sensors leaving G05 out and individually for each sensor. The outer macro avoidance area boundary was defined as 3 km.**
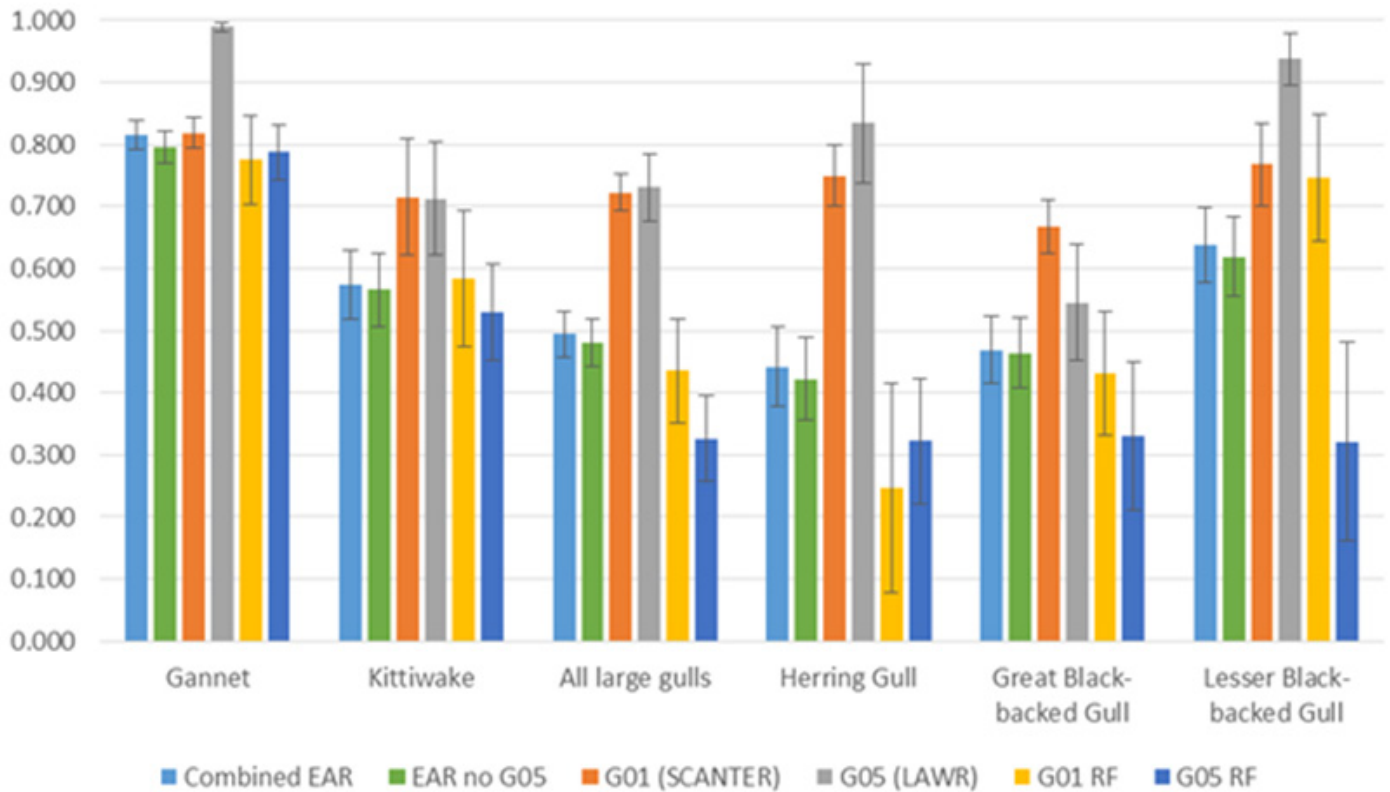
avoidance boundaries in Appendix 2, Section 4.

5.2.4. Results show that the EARs derived using data collected by the LAWR radar at G05 are higher than both the EARs from radar/rangefinder at G01 and from the rangefinder from G05 for all target species.

5.2.5. Results for Northern Gannets are considered consistent between three of the sensors (G01 radar / rangefinder, and G05 rangefinder) which produce similar macro EARs, while the results for the other species differ to some extent between sensors. The rangefinder data resulted in lower estimates which might be due to two reasons, both linked to the detection range of 1.5 km. One potential reason is that because birds do not penetrate deep into the wind farm the density increases faster inside when the range is smaller (1.5 km compared to 3 km), and the 1.5 km is potentially too small for capturing the re-distribution range. Another reason could be that the identification of species is biased for a 3 km range. Therefore using both ranges, 1.5 km for rangefinders and 3 km for radars is considered to be a compromise of defining the redistribution range correctly and identifying the species correctly. It should be noted that a range of 3 km was used for both radar and rangefinder data when calculating the macro EAR across sensors.

5.2.6. The sample sizes for the large gulls and Black-legged Kittiwake is much lower than for the Northern Gannet and therefore also the variability is larger. It should also be noted that the sensitivity of the overall avoidance rate to the macro avoidance rates is low (see Section 5.6) and therefore some variability in the results will not have a major influence on the overall EARs.

5.2.7. As indicated in Appendix 2, Section 4, it is recommended that LAWR radar data collected from turbine G05 are not used in the calculation of overall macro EARs due to

    I. Limitations of equipment detection over distance, with a potential under representation of bird movements within 1.2 km / beyond 2.7 km of the sensor both inside and outside the wind farm; and,

II. Limitations of the equipment performance during windy conditions that led to small sample sizes collected.

5.2.8. Accordingly, the values used to estimate overall macro EARs are the following, based on the combination of rangefinder data collected from both turbines G01 and G05, and SCANTER radar data collected from turbine G01, these are presented with the standard deviation (variability estimated on bootstrap samples):

- Northern Gannet: 0.797 (SD 0.026)

- Black-legged Kittiwake: 0.566 (SD 0.058)

- All large gulls: 0.481 (SD 0.038)

- Herring Gull: 0.422 (SD 0.067)

- Great Black-backed Gull: 0.464 (SD 0.057)

- Lesser Black-backed Gull: 0.619 (SD 0.064)

5.2.9. In addition to the estimated variability (SD), the quantification of combined uncertainty on overall

Table 5.3.   Combined standard deviation (=standard uncertainty) calculated based on combining all uncertainty components at the macro scale.

| Uncertainty/variability components	Northern Gannet SD	Black-legged Kittiwake SD	Large gulls SD	Lesser Black-backed Gull SD	Herring Gull SD	Great Black-Backed Gull SD
Variability	0.026	0.058	0.038	0.064	0.067	0.057
Boundary range definition bias (Boundary)	0.1	0.1	0.1	0.1	0.1	0.1
Species identification bias (Identification)	0.01	0.05	0.01	0.05	0.05	0.05
Spatial adjustment of RF tracks (Adjustment)	0.05	0.05	0.05	0.05	0.05	0.05
Fishing vessel effect (Fishing)	n/a	n/a	0.1	0.1	0.1	0.1
Large-scale displacement (Displacement)	0.01	0.01	0.01	0.01	0.01	0.01
Weather dependent bias (Weather)	0.10	0.10	0.10	0.10	0.10	0.10
COMBINED MACRO SD	0.153	0.169	0.191	0.198	0.199	0.196

macro EARs is presented in Table 5.3 following the approach discussed in section 4.2(e).

5.3. MESO EAR

5.3.1. Trigger points used to derive mean track lengths for meso avoidance analysis are shown in Figure 5.2. These trigger points represent the initial position for the videos as recorded by the radars. In total 12,573 trigger points were recorded (including all species), and of these, 11,577 (or 92%) were located within the high detection zone and included in further analyses.

Figure 5.2. **Number of trigger points recorded from D05 and F04 and georeferenced. Points include records of birds flying below the rotor-swept zone and showing no adjustment in flight behaviour (not included in meso EAR calculations).**

NIRAS DHI CARBON TRUST
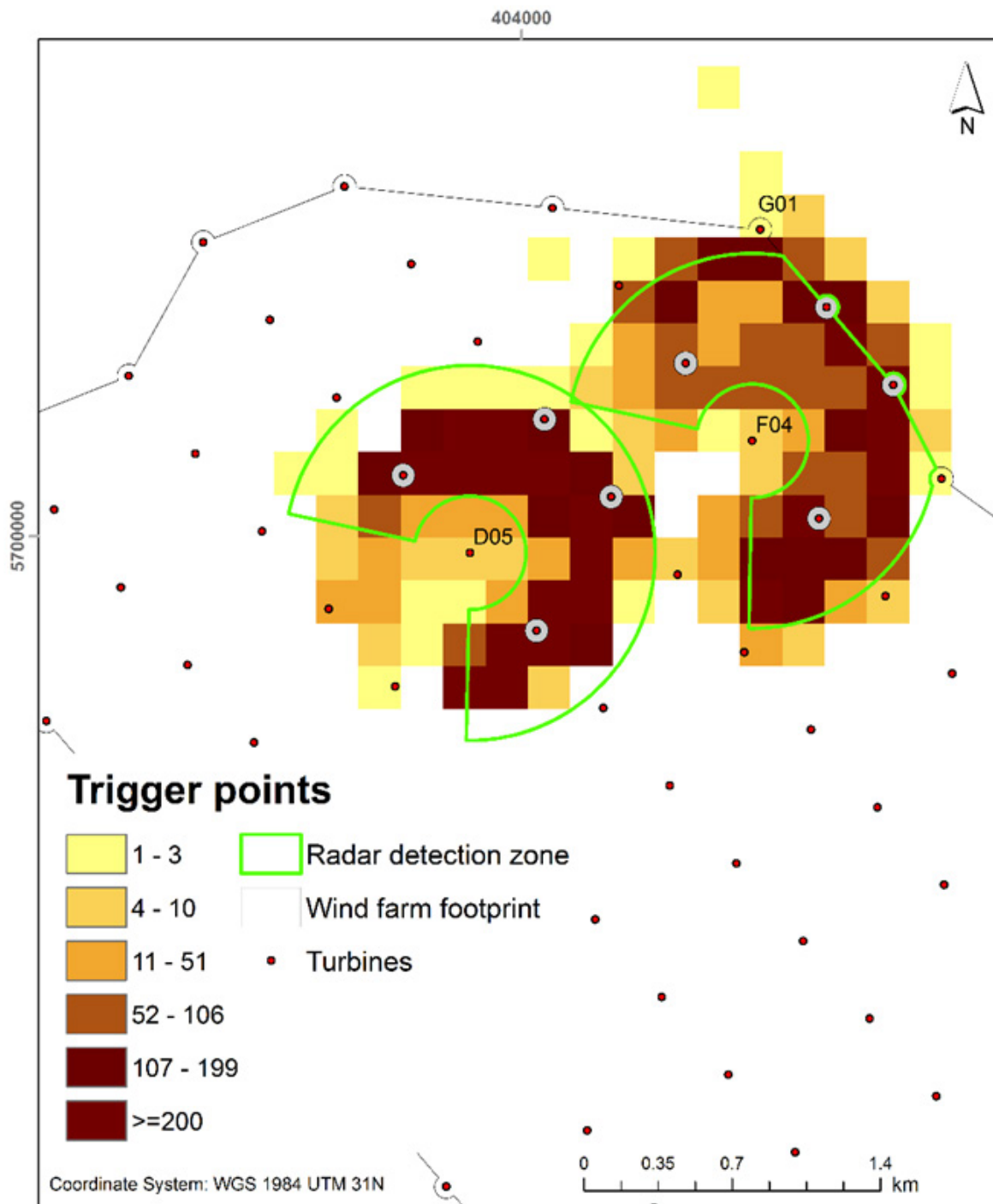
5.3.2. Bird behaviour observed in videos were coded according to the protocol described in Section 4.3, resulting in the following:

Table 5.4. **Meso avoidance behaviour recorded by the TADS Cameras on D05 and F04 from 24 Oct 2014 to 22 Jun 2016. Only tracks in the high detection zone are included.**

Species	Meso avoidance		
	Flies between turbines rows	Flies below rotor	Flies above rotor
Northern Gannet	1,473	12	0
Black-legged Kittiwake	203	2	0
Great Black-backed Gull	292	2	0
Lesser Black-backed Gull	51	0	0
Lesser/Great Black-backed Gull	1,060	10	3
Herring Gull	270	2	0
Large gulls	4,143	33	7
Small gull	419	0	0
Gull unid.	3254	6	2
Seabird unid.	1178	3	0

5.3.3. Following the coding of bird behaviour in videos, codes were used to classify trigger points and associated tracks both inside and/or outside the RSZ using a circular 10 m buffer. In general, low proportions of the classified video tracks were recorded inside the RSZ and buffer. For Northern Gannet 2.2% of the video tracks were recorded inside, while the proportion for the gull species varied from 1.1% for the Herring Gull to 2.8% for the Black-legged Kittiwake and 4.9% for the Great Black-backed Gull (Table 5.6).

NIRAS DHI CARBON TRUST

Table 5.5. **Classification of video tracks inside the RSZ + 10 m buffer ("in") and total number of tracks in the high detection zone outside the RSZ + 10 m buffer, using data collected from TADS Camera System + LAWR radar on turbines D05 and F04 from 24 Oct 2014 – 22 Jun 2016. Lesser/ Great Black-backed gulls include the species-specific counts for both species. Large gulls include Lesser Black-backed Gull, Herring Gull and Great Black-backed Gull, unidentified Lesser Black-backed/Great Black-backed Gull and unidentified large gulls. Northern Gannet (GX), Black-legged Kittiwake (KI), Herring Gull (HG), Lesser Black-backed Gull (LBBG), Great Black-backed Gull (GBBG).**

GX		KI		Large gulls		HG		LBBG/GBBG		GBBG	
In	Total	In	Total	In	Total	In	Total	In	Total	In	Total
33	1518	6	211	110	4300	3	276	36	1110	15	309

5.3.4. Table 5.6 presents the estimated meso EARs and associated SD.

Table 5.6. **Estimated empirical meso avoidance rates and bootstrap standard deviations. Large gulls include Lesser Black-backed Gull, Herring Gull and Great Black-backed Gull, unidentified Lesser Black-backed/Great Black-backed Gull and unidentified large gulls. Northern Gannet (GX), Black-legged Kittiwake (KI), Herring Gull (HG), Lesser Black-backed Gull (LBBG), Great Black-backed Gull (GBBG)G).**

MESO	GX	KI	Large gulls	HG	LBBG/GBBG	GBBG
EAR	0.9205	0.9160	0.9134	0.9614	0.8937	0.8423
SD	0.0137	0.0339	0.0080	0.0221	0.0174	0.0394

5.3.5. In addition to the estimated variability (SD), the quantification of a combined uncertainty on overall meso EARs is presented in Table 5.7.

Table 5.7.   Combined standard deviation (=standard uncertainty) calculated based on combining all uncertainty components at the meso scale.

Uncertainty/variability components	Northern Gannet SD	Black-legged Kittiwake SD	Large gulls SD	Lesser Black-backed Gull SD	Herring Gull SD	Great Black-Backed Gull SD
Variability	0.014	0.034	0.008	0.017	0.022	0.039
Coding errors (Coding)	0.1	0.1	0.1	0.1	0.1	0.1
Track length approximation errors (Tracklength)	0.1	0.1	0.1	0.1	0.1	0.1
Detection bias (Detection)	0.1	0.1	0.1	0.1	0.1	0.1
COMBINED MESO SD	0.174	0.177	0.173	0.174	0.175	0.177

5.4. MICRO EAR

5.4.1. Table 5.8 presents micro avoidance coding results, considering target species and unidentified gull species samples collected from 24 October 2014 to 22 June 2016. The interpretation of behaviour observed is presented in Section 6.

Table 5.8.   Coding of micro avoidance behaviour applied to TADS Camera data collected from turbines D05 and F04 from 24 Oct 2014 to 22 Jun 2016. Species and combined species groups used in the analysis of micro avoidance are marked in bold.

Species	Adjusting			Not adjusting	Collision	Total
	Turns before crossing	Stops before crossing	Crosses with adjustment			
Northern Gannet	4	0	28	1	0	33
Black-legged Kittiwake	0	1	4	0	1	6
Great Black-backed Gull	1	0	12	2	0	15
Lesser Black-backed Gull	0	0	1	0	0	1
Lesser/Great Black-backed Gull (not including species-specific)	6	0	15	1	1	23
Herring Gull	1	0	2	0	0	3
Large gull unid.	9	4	60	0	1	74
Large gulls	17	4	90	3	2	116
Small gull	1	1	3	1	0	6
Gull unid.	9	6	82	2	3	102
Seabird spp.	1	0	29	2	0	32
Other species of seabirds	0	0	2	0	0	4
All species of seabirds	32	12	238	9	6	299

5.4.2. A micro EAR (and associated SD) was calculated separately for large gulls as well as for all recorded seabirds within the RSZs (Table 5.9).

Table 5.9. Estimated empirical micro avoidance for all seabirds combined and separately for large gulls combined, and bootstrap standard deviations.

MICRO	Large gulls	All seabirds
EAR	0.9565	0.9500
SD	0.0190	0.0128

5.4.3. In addition to the estimated variability (SD), the quantification of combined uncertainty on overall micro EARs is presented in Table 5.7.

Table 5.10. Combined standard deviation (=standard uncertainty) calculated based on combining all uncertainty components at the micro scale.

Uncertainty/variability components	Northern Gannet SD	Black-legged Kittiwake SD	Large gulls SD	Lesser Black-backed Gull SD	Herring Gull SD	Great Black-Backed Gull SD
Variability	0.013	0.013	0.019	0.019	0.019	0.019
Coding errors (Coding)	0.05	0.05	0.05	0.05	0.05	0.05
Species-specific differences (Species-specific)	0.02	0.02	0.02	0.02	0.02	0.02
Detection bias (Detection)	0.1	0.1	0.1	0.1	0.1	0.1
COMBINED MESO SD	0.114	0.114	0.115	0.115	0.115	0.115

5.5. OVERALL EAR

5.5.1. Overall EARs per species are presented in Table 5.11, for each species the following data has been used:

- Northern Gannet and Black-legged Kittiwake – based on species-specific macro and meso EARs + micro EAR calculated across all seabird species

- Herring Gull and Great Black-backed Gull – based on species-specific macro and meso EARs together + micro EAR calculated across large gulls

- Lesser Black-backed Gull – based on species-specific macro EAR + combined meso EAR for Lesser/ Great Black-backed Gulls + micro EAR calculated across all large gulls

- Large gulls - based on combined large gull estimates for macro, meso and micro EARs

Table 5.11. Estimated overall EAR and standard deviations (SD), which reflect the propagated variability estimated based on the bootstrap samples.

	Northern Gannet	Black-legged Kittiwake	Herring Gull	Great Black-backed Gull	Lesser Black-backed Gull	All large gulls
Overall Macro EAR	0.999	0.998	0.998	0.998	0.999	0.996
SD	0.0003	0.001	0.0009	0.0009	0.0007	0.0019

5.5.2. In addition to the SD associated with data variability, calculated using the bootstrap resampling done for each EAR component (macro, meso and micro), the quantification of uncertainty on overall EARs (propagation of uncertainty) is presented in Table 5.12.

Table 5.12. Combined standard deviation (=standard uncertainty) calculated based on combining and propagating the uncertainties estimated at each avoidance scale

	Northern Gannet SD	Black-legged Kittiwake SD	Large gulls SD	Lesser Black-backed Gull SD	Herring Gull SD	Great Black-Backed Gull SD
Overall uncertainty (SD)	0.003	0.006	0.007	0.006	0.005	0.011
lower 95% confidence limit	0.994	0.987	0.985	0.987	0.989	0.975
upper 95% confidence limit (if>1, then 1)	1	1	1	1	1	1

NIRAS DHI CARBON TRUST

5.6. IMPORTANCE OF EACH SCALE ON OVERALL EARS AND SENSITIVITY TO CHANGES

5.6.1. To assess the sensitivity to each of the avoidance rate components, or importance of each scale, sensitivity tests were run to compare the change in overall EAR when individual avoidance components were changed by ±0.1 or ±0.3 EAR units (i.e. changing for example Northern Gannet macro EAR from 0.797 to 0.497), or by changing all components at the same time in the same direction.

5.6.2. The overall EAR is most sensitive to changes in micro EAR when keeping the other two components fixed (Figure 5-3 to 5-8). However, the change in overall EAR was small when changing a single component with 0.3 units (which can be regarded as a large change.
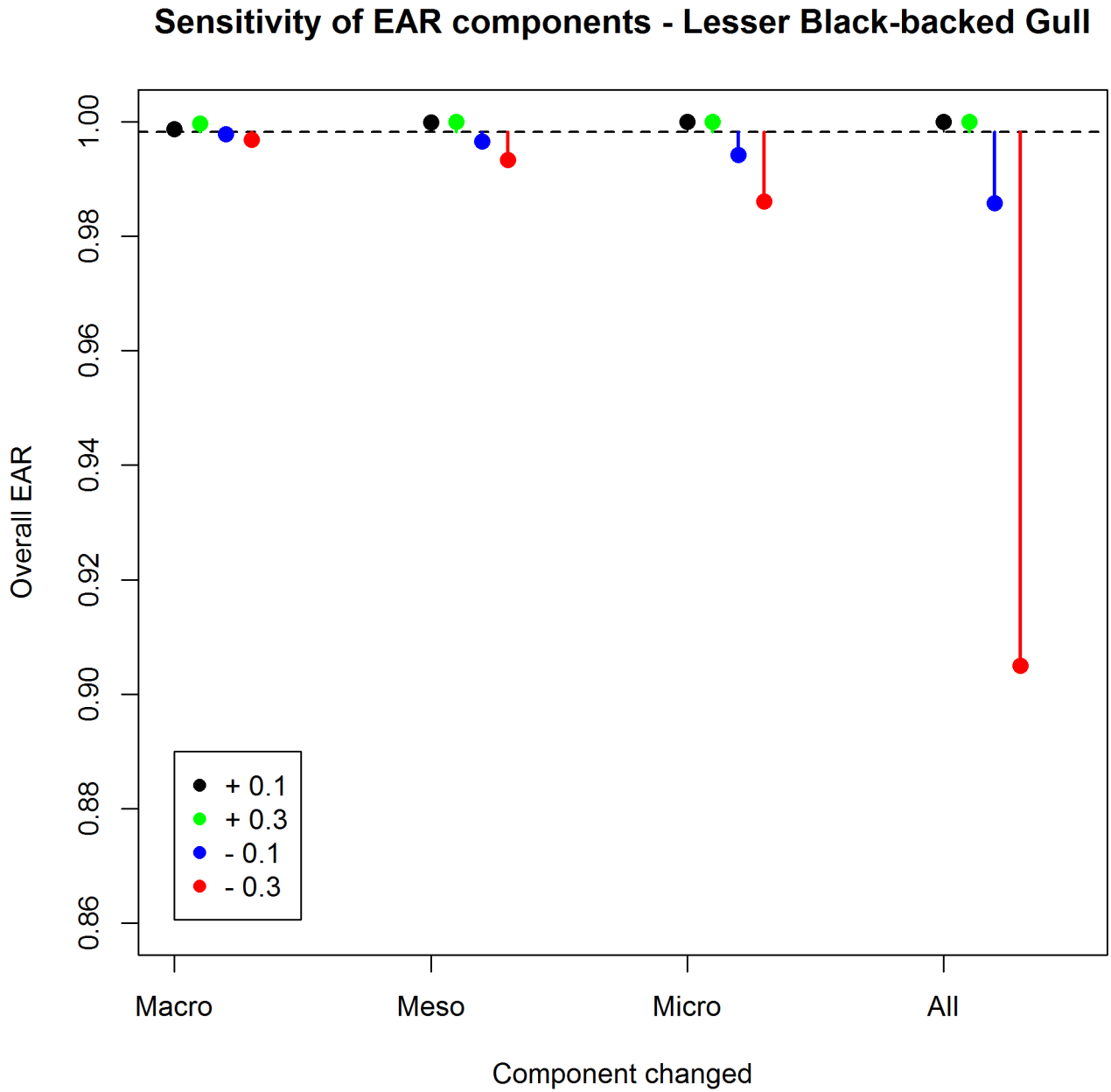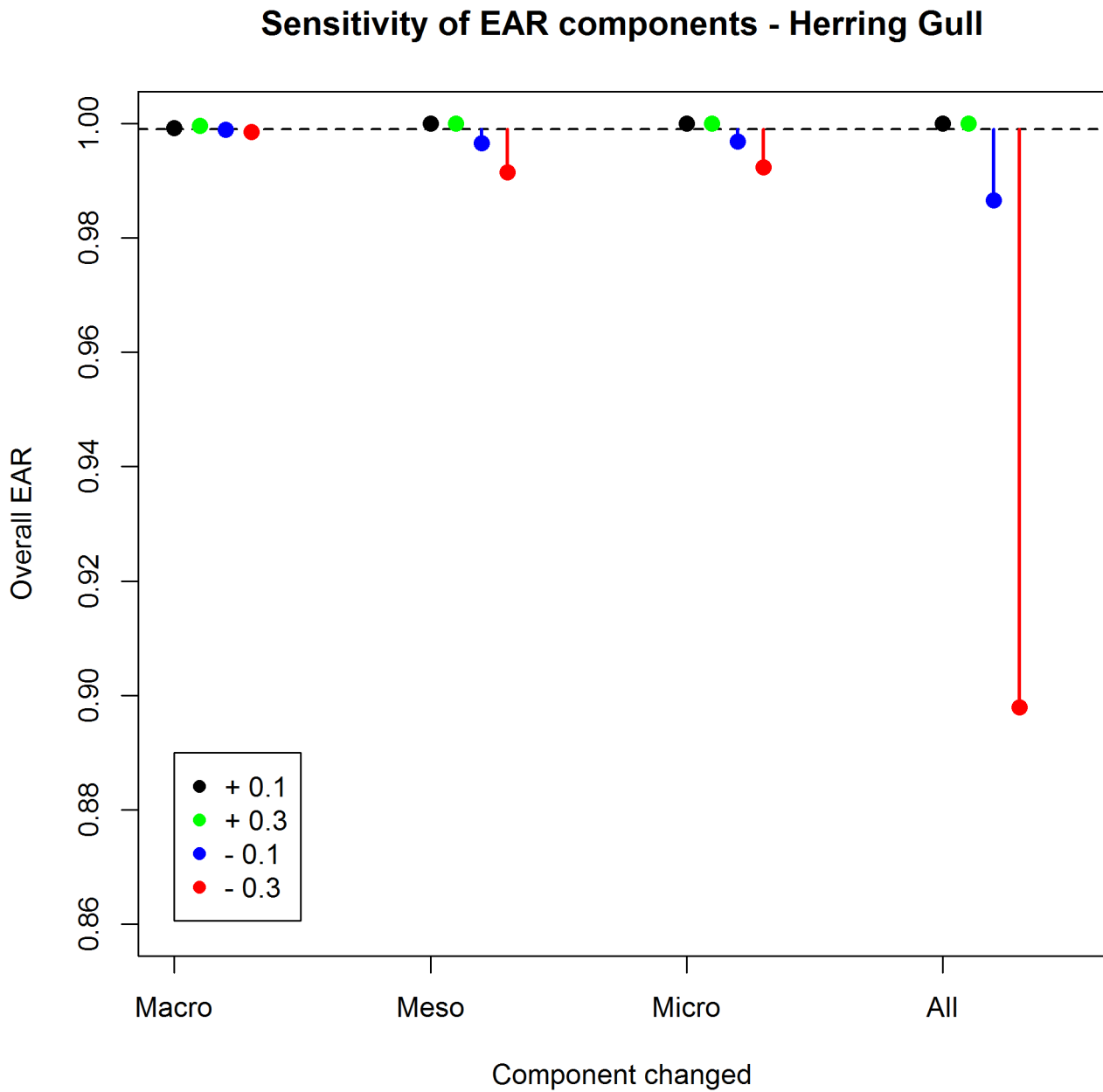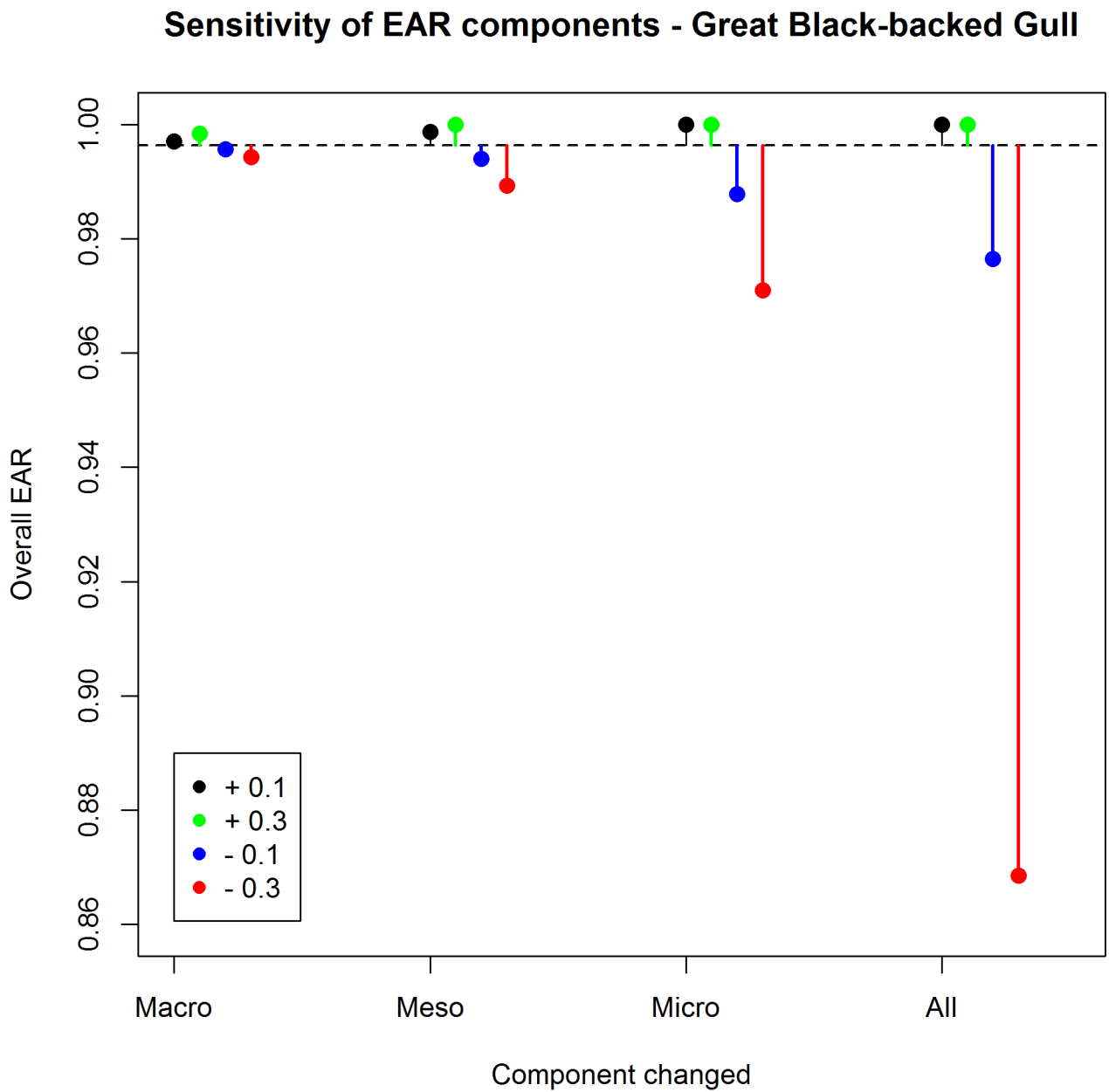
Figure 5.3. Sensitivity test of changing each EAR component (Macro, Meso or Micro) at a time or all at the same time (All) with either ±0.1 (black and blue dots) or ±0.3 (green and red dots). The overall Northern Gannet EAR is indicated with a dashed black line.
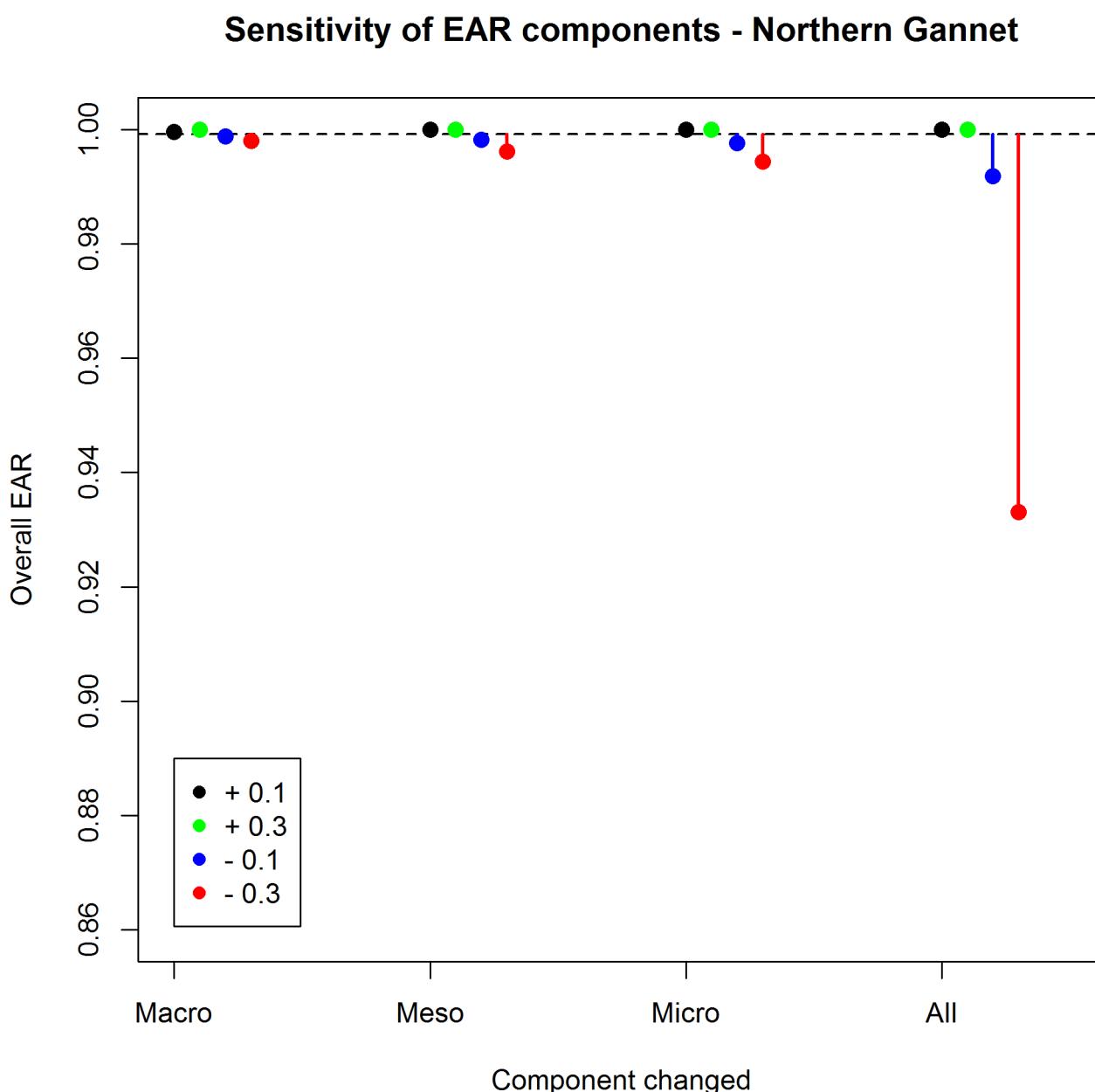
5.6.3. As illustrated in Figure 5.3, when decreasing the micro EAR by 0.3 the change in overall EAR was only 0.0049. But, when decreasing all components with 0.3 units at the same time in the same direction (i.e. reducing all of them) the overall EAR dropped by 0.0661 units for Northern Gannet. A similar pattern can be seen for the other species as well (Figure 5.4, Figure 5.5, Figure 5.6, Figure 5.7, Figure 5.8).

Figure 5.4. Sensitivity test of changing each EAR component (Macro, Meso or Micro) at a time or all at the same time (All) with either ±0.1 (black and blue dots) or ±0.3 (green and red dots). The overall Black-legged Kittiwake EAR is indicated with a dashed black line.
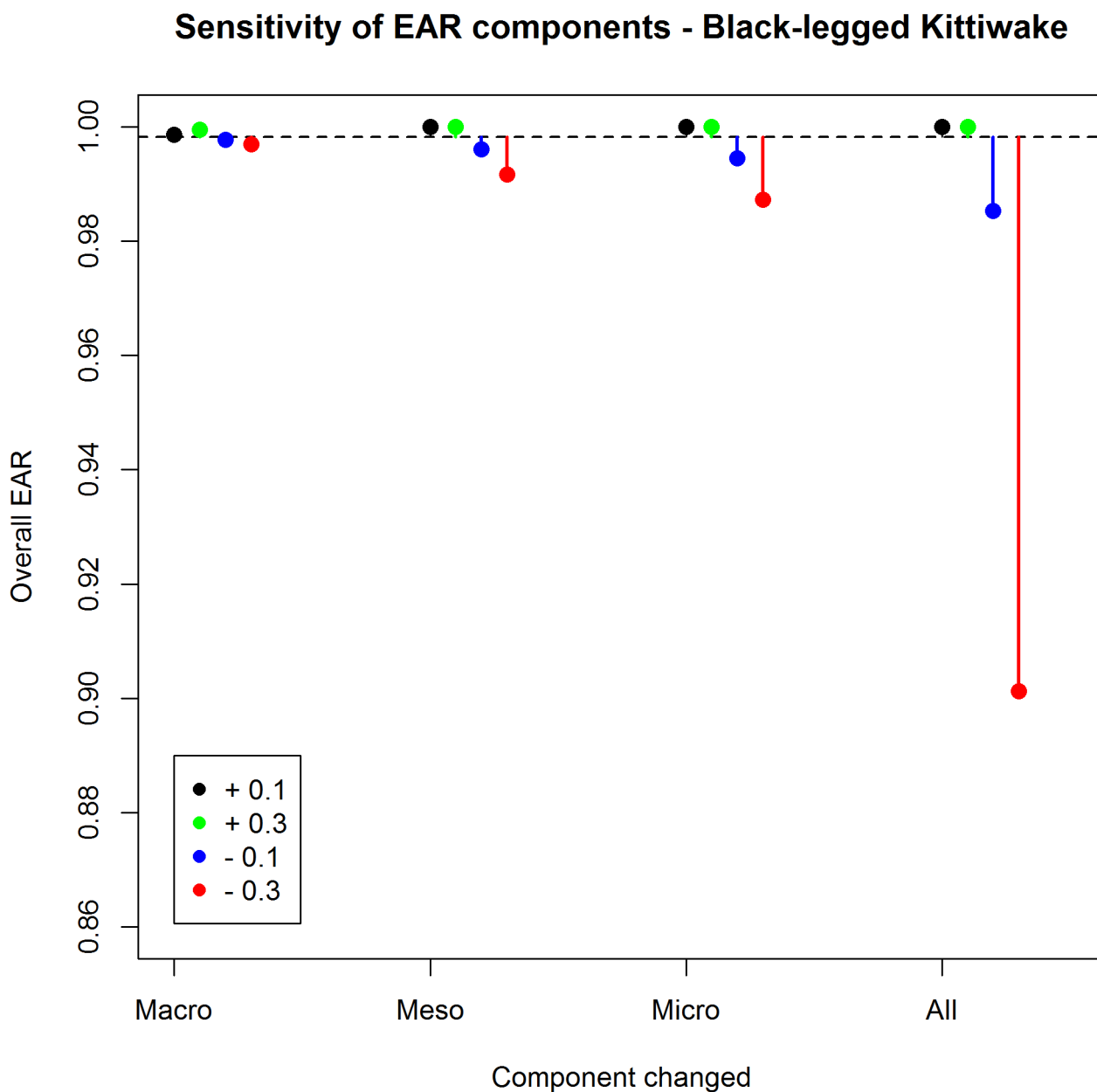
Figure 5.5. Sensitivity test of changing each EAR component (Macro, Meso or Micro) at a time or all at the same time (All) with either ±0.1 (black and blue dots) or ±0.3 (green and red dots). The overall Lesser Black-backed Gull EAR is indicated with a dashed black line.

Figure 5.6. Sensitivity test of changing each EAR component (Macro, Meso or Micro) at a time or all at the same time (All) with either ±0.1 (black and blue dots) or ±0.3 (green and red dots). The overall Herring Gull EAR is indicated with a dashed black line.

Figure 5.7. Sensitivity test of changing each EAR component (Macro, Meso or Micro) at a time or all at the same time (All) with either ±0.1 (black and blue dots) or ±0.3 (green and red dots). The overall Great Black-backed Gull EAR is indicated with a dashed black line.

Figure 5.8. Sensitivity test of changing each EAR component (Macro, Meso or Micro) at a time or all at the same time (All) with either ±0.1 (black and blue dots) or ±0.3 (green and red dots). The overall large gull EAR is indicated with a dashed black line.
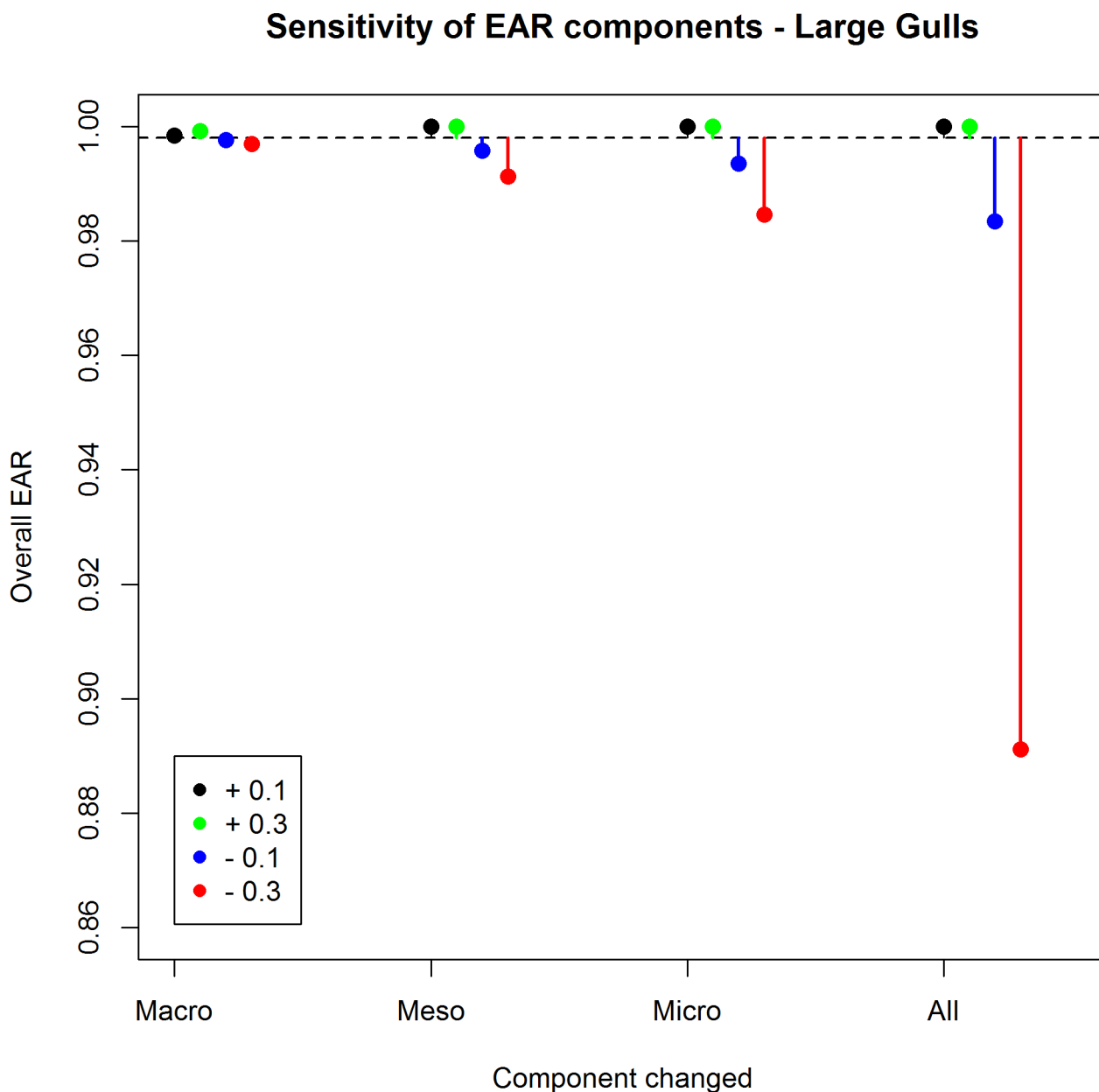
5.6.4. The sensitivity test indicates that even large changes or errors in macro EAR results in small changes in the overall EAR. Only if there are large errors in all components and in the same direction, the change in overall EAR is notable.

5.6.5. Matrices with different values assigned to each component are presented in Section 7 to provide context to the estimated EARs in relation to other studies and possible ranges.

5.7. FLIGHT SPEED

5.7.1. The calculated flight speeds (based on all rangefinder data, both inside and outside the wind farm perimeter are listed in Table 5.13. These values were used to correct mean track lengths calculated in meso avoidance analysis outside the RSZ + 10 m buffer (see Section 4.3).

Table 5.13. Species-specific and turbine-specific (based on data collected from turbines G01 and G05 respectively) flight speeds (m/s) and correction factors for mean random track length (SD is shown in brackets).

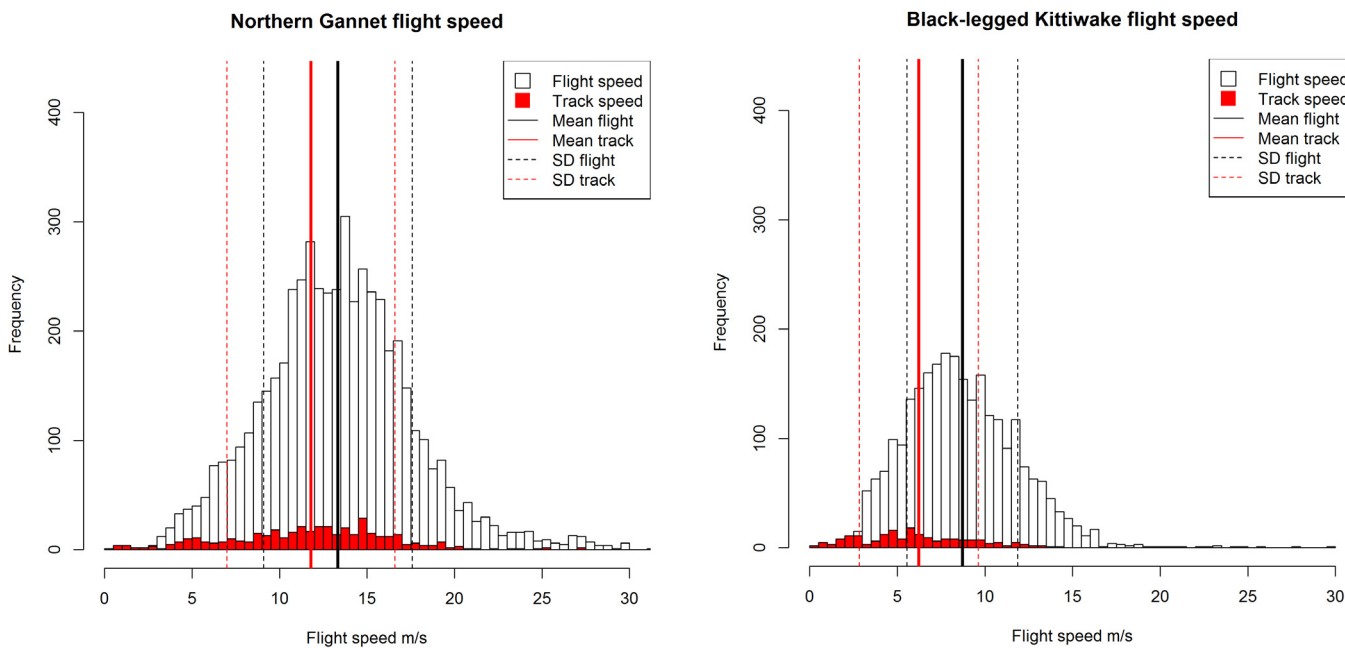| Data	Parameter	Northern Gannet	Black-legged Kittiwake	Large gulls	Lesser Black-backed Gull	Herring Gull	Great Black-backed Gull
Turbine G01	Flight speed	13.32 (4.57)	8.33 (2.96)	10.42 (3.92)	10.89 (4.17)	10.28 (3.70)	9.59 (3.61)
	Track speed	11.78 (5.14)	6.19 (3.65)	8.56 (4.31)	8.66 (2.85)	8.65 (4.13)	7.88 (5.11)
	Correction factor	1.13 (0.63	1.35 (0.93)	1.22 (0.77)	1.26 (0.64)	1.19 (0.71)	1.22 (0.91)
Turbine G05	Flight speed	13.34 (3.92)	8.91 (3.25)	9.62 (3.51)	9.54 (3.63)	9.38 (3.30)	9.93 (3.67)
	Track speed	11.78 (4.39)	6.24 (3.21)	7.72 (3.449	7.72 (3.24)	7.90 (3.46)	7.466 (3.56)
	Correction factor	1.13 (0.54)	1.43 (0.90)	1.25 (0.72)	1.24 (0.70)	1.19 (0.67)	1.33 (0.80)
Combined	Flight speed	13.33 (4.24)	8.71 (3.16)	9.80 (3.63)	10.13 (3.93)	9.68 (3.47)	9.78 (3.65)
	Track speed	11.78 (4.80)	6.22 (3.40)	7.95 (3.92)	8.10 (3.11)	8.13 (3.69)	7.69 (4.47)
	Correction factor	1.13 (0.59)	1.40 (0.92)	1.23 (0.76)	1.25 (0.68)	1.19 (0.69)	1.27 (0.88)

5.7.2. As exemplified by Northern Gannet data represented in Figure 5-9, in comparison to data collected outside the wind farm, there was less rangefinder data collected inside the wind farm. Accordingly, for the purposes of flight speed calculation, all suitable rangefinder tracks (those which were not also recorded by the radar) were used. The species-specific flight speeds for all target species are visualized in Figure 5-10. No statistical analysis has been possible to assess for a difference, if any, between flight speed inside and outside the wind farm as too few data were collected inside the wind farm.
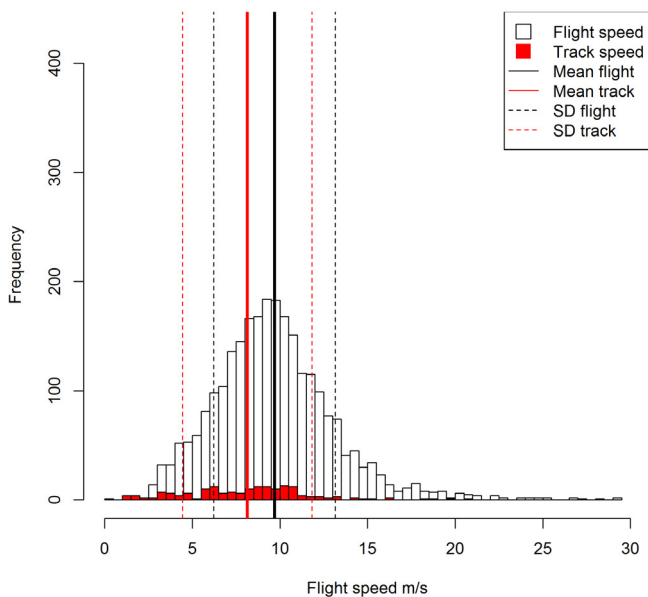
NIRAS DHI CARBON TRUST

Figure 5.9.   Flight and track speed distribution for Northern Gannet inside the wind farm only (to the left) and all suitable data both inside and outside the wind farm combined (to the right).
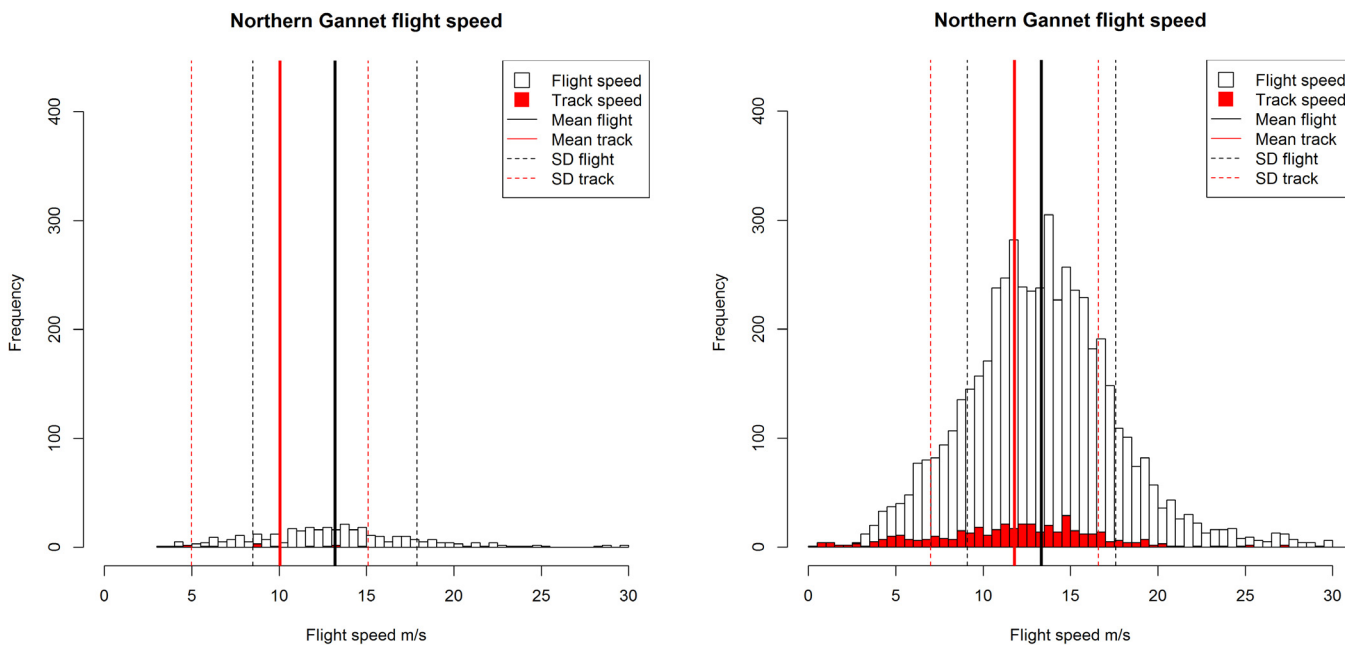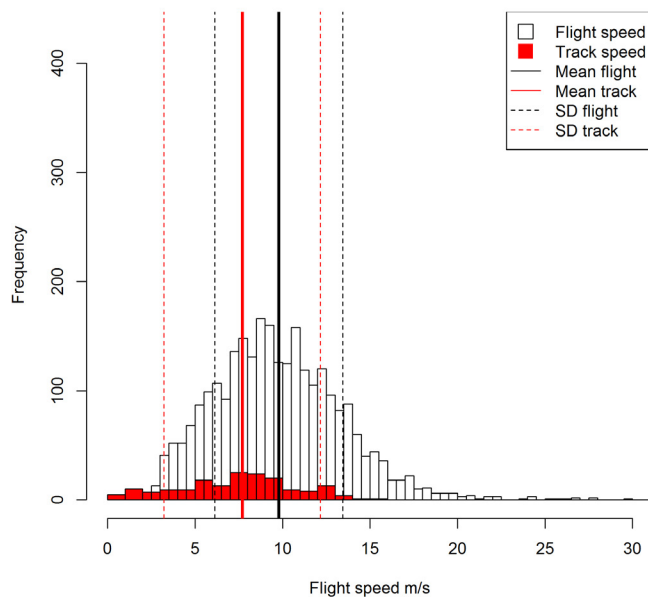

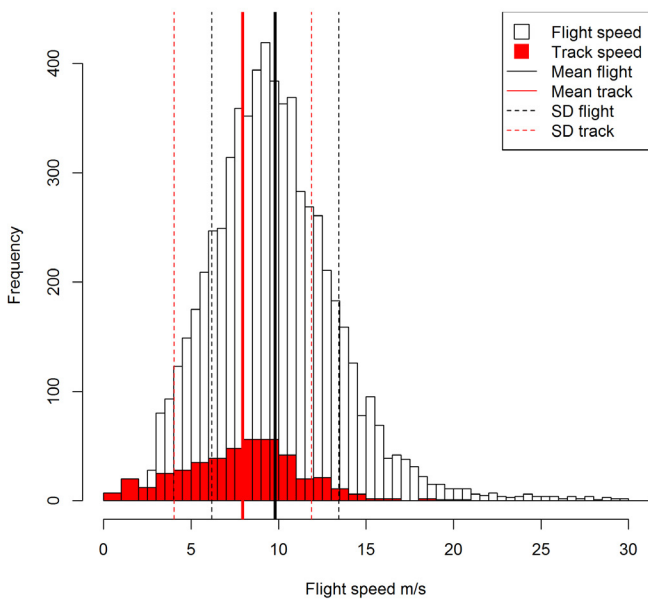**Figure 5.10.   Species-specific flight and track speeds measured using rangefinders at G01 and G05 combined.**
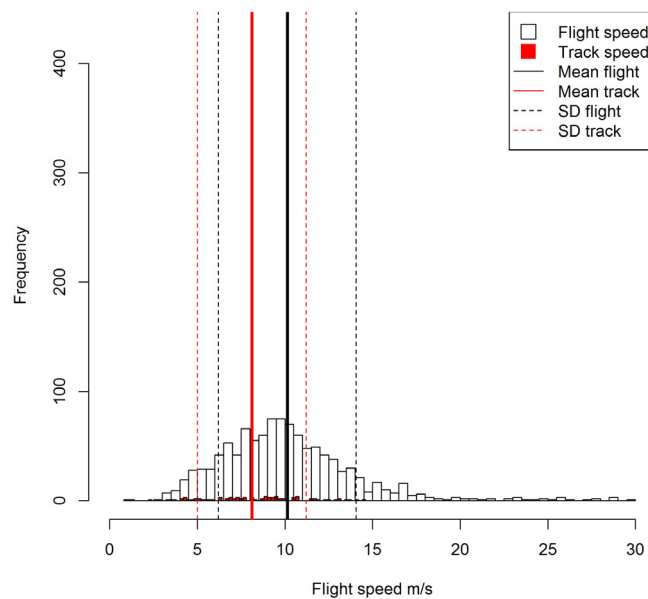
5.8. FLIGHT HEIGHT DISTRIBUTION, INFLUENCE OF WIND AND WIND FARM

5.8.1. Flight height has been calculated using a subset of the rangefinder data. The subset used had high quality geospatial reference and included species ID. 10% of the sub-set of rangefinder data tracks were followed by radar, 86.7% of these were from G01. The small percentage (13.3%) of data that is from the G05 radar was a consequence of the limitations described in Appendix 1 (section 3.3) when the observer team were using the LAWR radar. The proportion of birds flying at rotor height was calculated for each species (Table 5.14).

5.8.2. Northern Gannet was observed to mostly fly below rotor height while Black-legged Kittiwake and large gull species were mostly recorded flying at rotor height.

Table 5.14.   Proportion of birds flying at rotor height based on rangefinder data. Calculated based on all measurements, number of tracks are also indicated in brackets.

Species	% at rotor height	Sample size (n tracks)
Northern Gannet	27%	5773 (662)
Black-legged Kittiwake	77%	2778 (265)
Lesser Black-backed Gull	66%	1159 (174)
Great Black-backed Gull	78%	2724 (284)
Herring Gull	73%	2817 (282)

5.8.3. Species-specific flight heights are visualised in Figures 5-11, 5-17, 5-20 and 5-23.

5.8.4. The flight height distributions collected at the two different wind farm turbines (G01 and G05) are highly consistent (see Figure 5-12, 5-15, 5-18, 5-21 and 5-24).

5.8.5. The Northern Gannet was the species with the average lowest flight height, whereas all gull species had relatively high mean flight heights, with Great Black-backed Gull recording flying higher than the other species (Table 5.14).

5.8.6. The explanatory variables assessed in the GAMM model showed that relationships between wind, inside/outside wind farm, distance to wind farm and flight height were not very strong. However, there were some significant although weak patterns (Tables 5-9 to 5-13).

5.8.7. In general, it was observed that birds fly slightly lower in head wind in comparison with tail and cross winds, statistically significant for Northern Gannet and Black-legged Kittiwake.

5.8.8. No statistical analysis has been possible to assess for flight height variation with distance to the wind farm.

5.8.9. Northern Gannets, Black-legged Kittiwakes and Lesser Black Backed Gulls also fly slightly higher (statistically significant) inside the wind farm in comparison to outside, which has also been observed by for example Krijgsveld et al. (2011). The median flight height of Northern Gannets outside the wind farm was 15 m in comparison to 21 m inside the wind farm, and the median flight height of Lesser Black-backed Gulls was 28 m outside the wind farm versus 40 m inside the wind farm. The difference in flight height of Black-legged Kittiwakes was very small. The median flight height was 33 m inside compared to 34 m outside the wind farm. However, due to the slightly higher 1st quartile the mean flight height was 1 m higher inside than outside the wind farm.

5.8.10. The responses to wind speed were generally weak and varying. All response curves (the relationship between altitude and the predictor variable) are shown for Northern Gannet in Figure 5.13, for Black-legged Kittiwake in Figure 5.16, for Lesser Black backed Gull in Figure 5.19, for Herring Gull in Figure 5.22 and for Great Black-backed Gull in Figure 5.25. Findings are further discussed in Section 6.

Figure 5.11. **Histogram of flight height distribution of Northern Gannet (upper left) and boxplots comparing heights at the two platforms (upper right), for different wind direction (lower left) and outside and inside the wind farm footprint (lower right). The red line indicates 25 m, which is the lowest tip of the rotor at the Thanet wind farm. The "boxes" in the box plots indicates the first quartile (bottom of the box), the third quartile (top of the box) and the thick black line indicates the median value. The error bars indicate the range (minimum and maximum excluding outliers) and the open circles indicate outliers.**
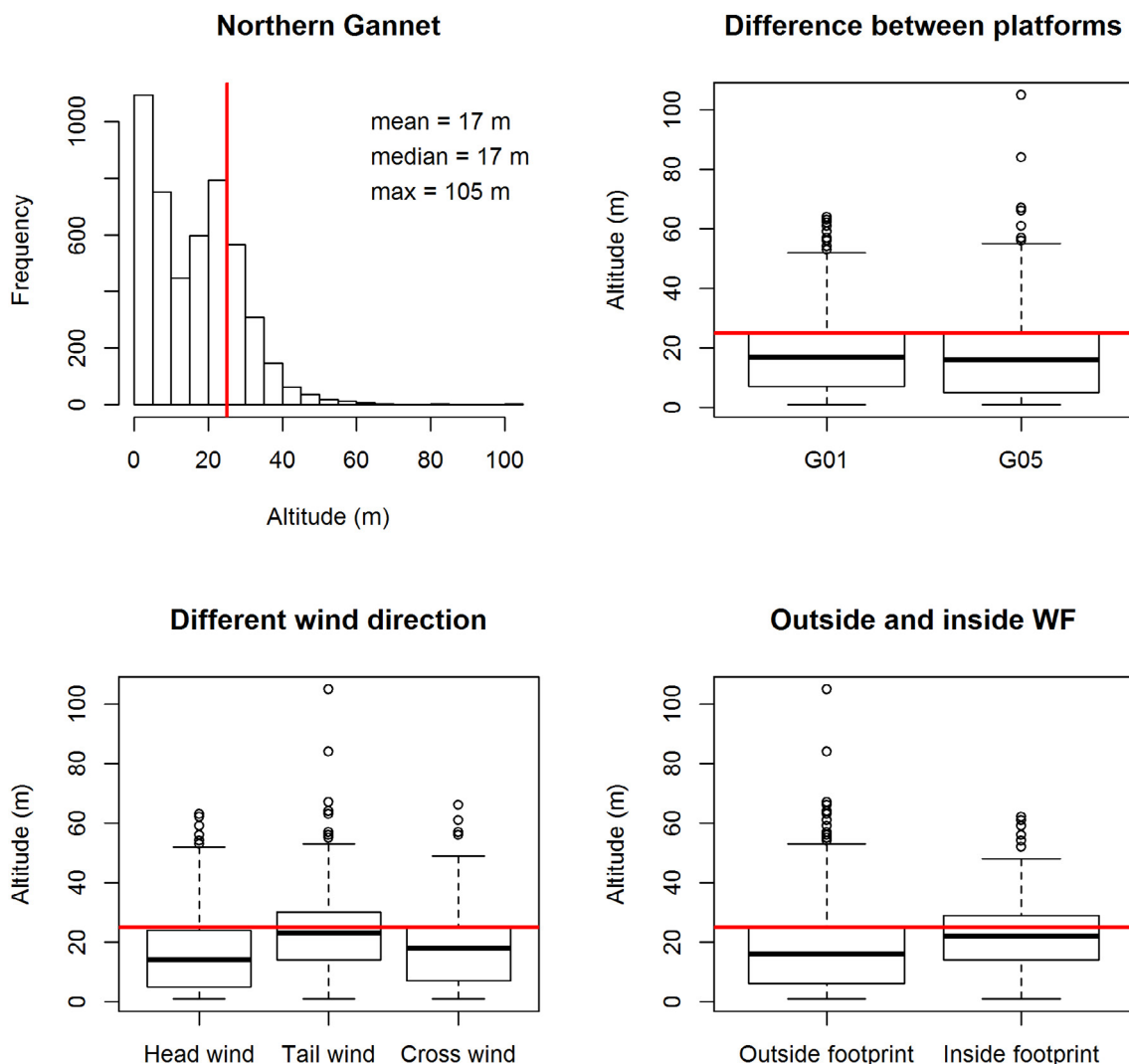
Figure 5.12. **Northern Gannet flight height distribution by platform, sample sizes indicated in the title, number of height recordings and number of tracks in parenthesis.**
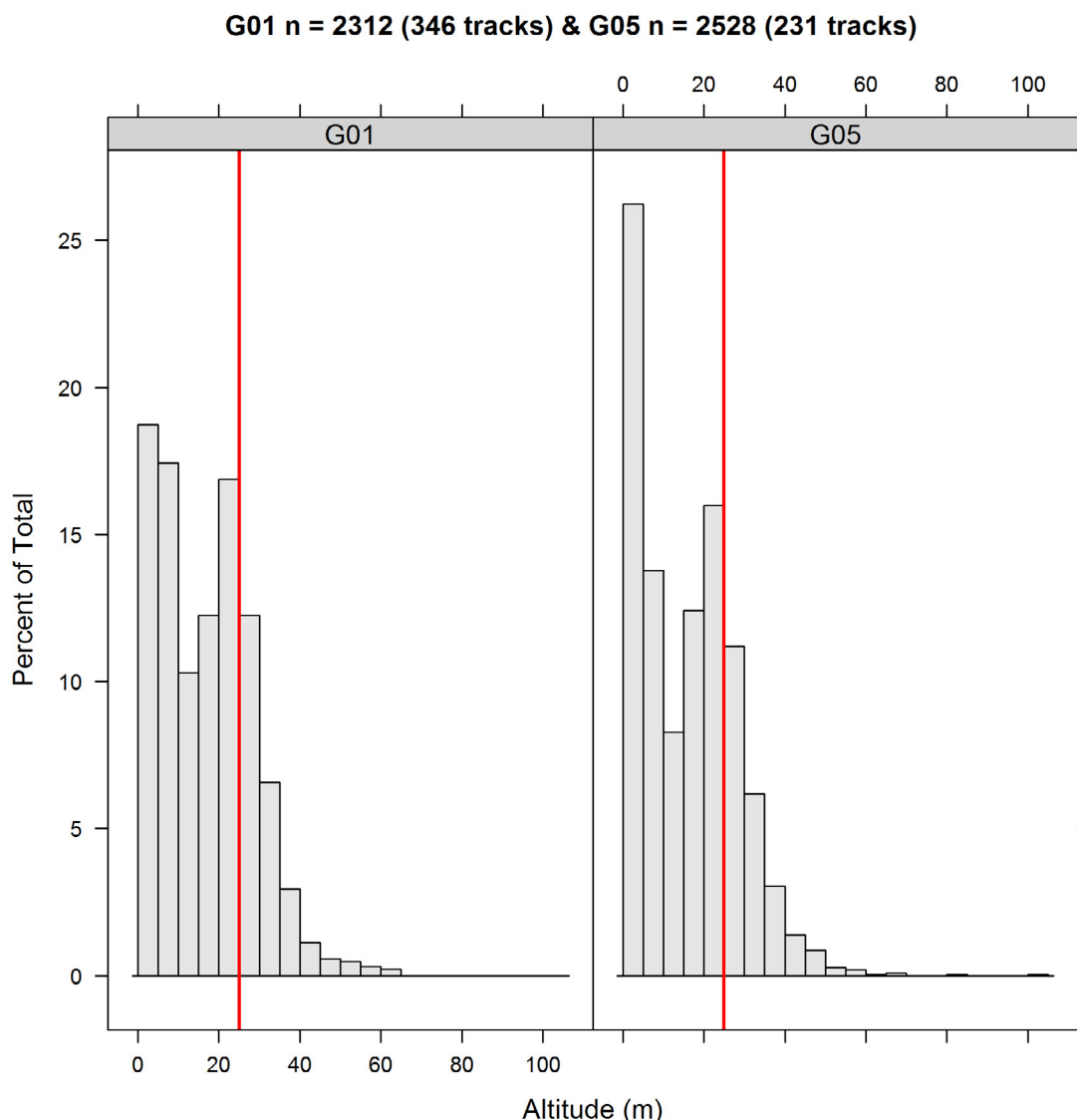

Table 5.15. **Significance and t-values/f-values for the fixed parametric and smooth terms included in the GAMMs for Northern Gannet. Number of samples used in the analysis is shown on the bottom row.**

		t - value	p -value
Parametric	tail wind	<0.001	<0.001
	cross wind	<0.001	<0.001
	inside wind farm	0.01	0.01
Smooth	Distance to wind farm perimeter: outside wind farm	1.786	0.135
	Distance to wind farm perimeter: inside wind farm	6.951	<0.001
	Wind speed: head wind	7.575	<0.01
	Wind speed: tail wind	2.206	0.138
n of samples	4840		

Figure 5.13. Response curves of the GAMM for Northern Gannet. The response is indicated on the Y-axis in the scale of the linear predictor (higher values indicate higher altitude) and range of the predictors are indicated on the x-axis. The degree of smoothing of the continuous variables are displayed in the title of the Y-axis. The grey area and dotted lines indicate 95% confidence intervals.
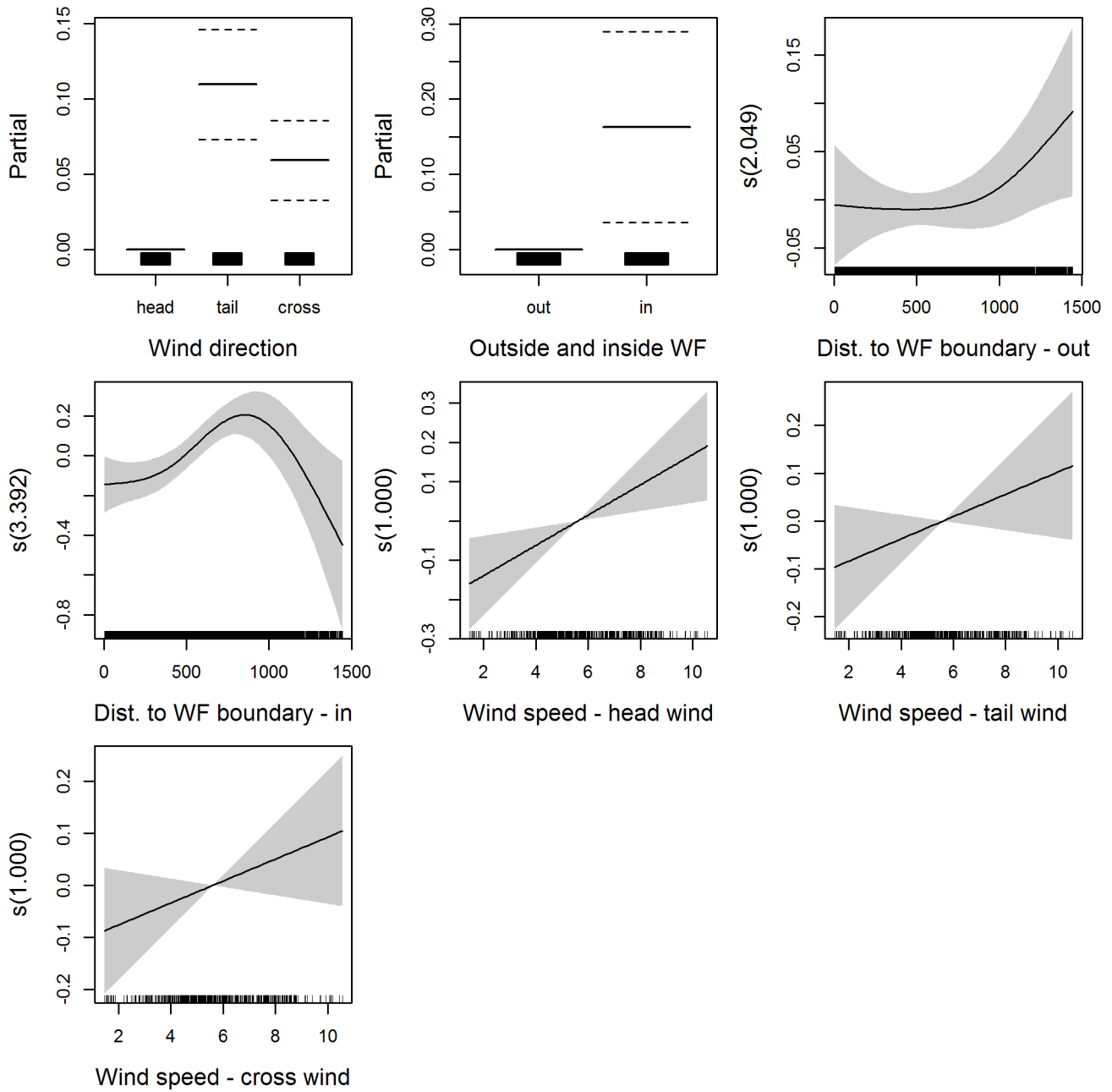
Figure 5.14.   Flight height distribution of Black-legged Kittiwake (upper left) and boxplots comparing heights at the two platforms (upper right), for different wind direction (lower left) and outside and inside the wind farm footprint (lower right. The red line indicates 25 m, which is the lowest tip of the rotor at the Thanet wind farm. The "boxes" in the box plots indicates the first quartile (bottom of the box), the third quartile (top of the box) and the thick black line indicates the median value. The error bars indicate the range (minimum and maximum excluding outliers) and the open circles indicate outliers.
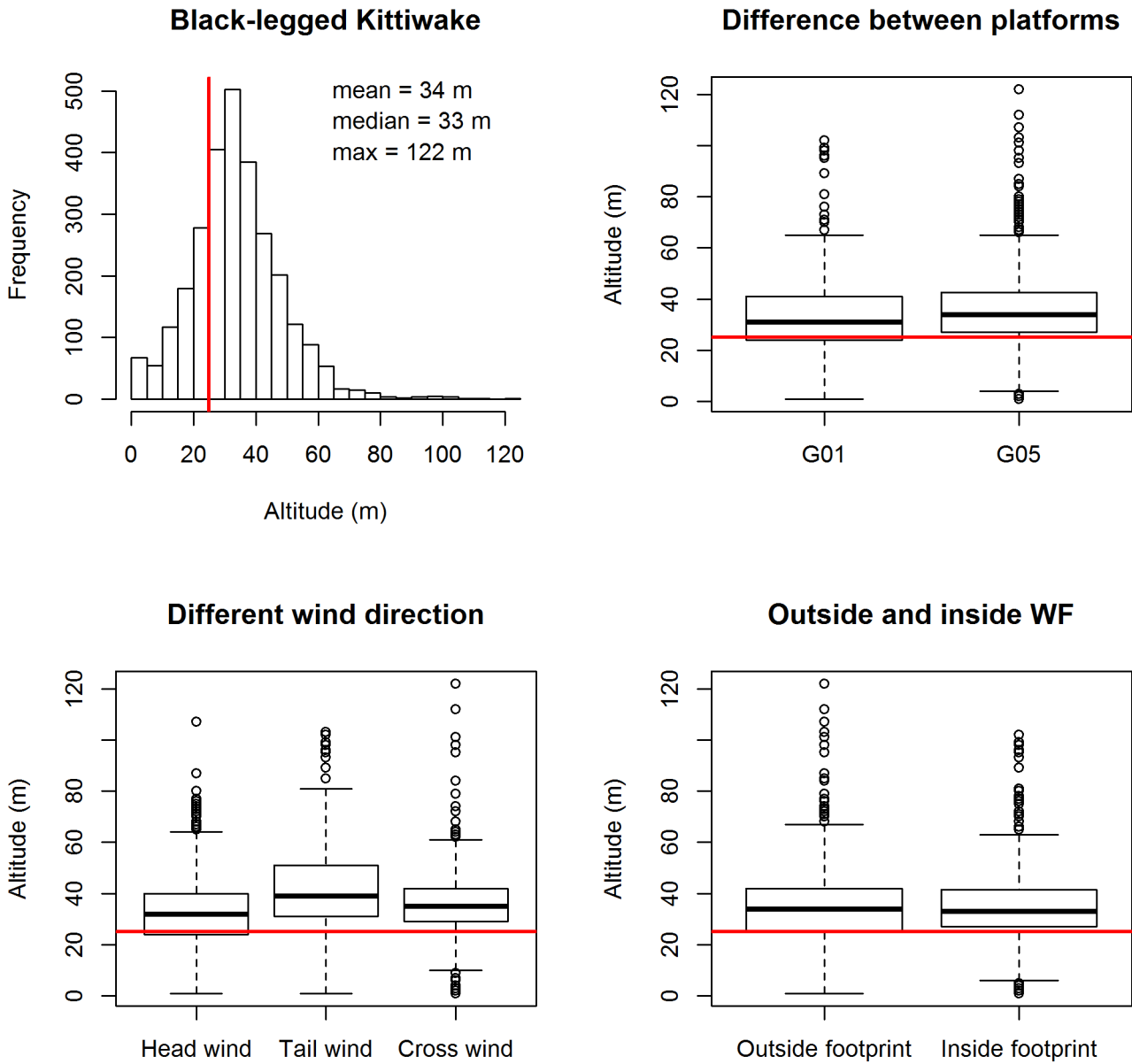
Figure 5.15. Black-legged Kittiwake flight height distribution by platform, sample sizes indicated in the title, number of height recordings and number of tracks in parenthesis.

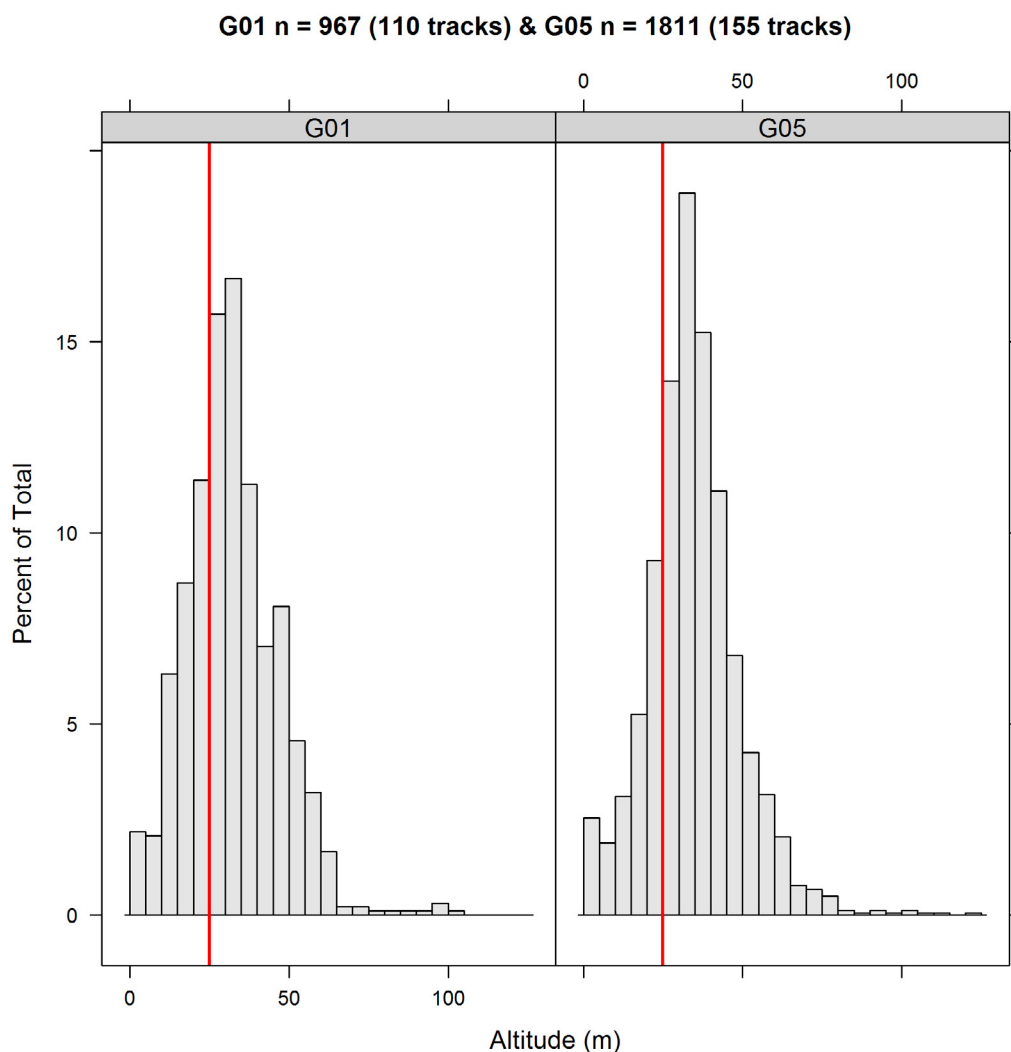**G01 n = 967 (110 tracks) & G05 n = 1811 (155 tracks)**

Table 5.16. Significance and t-values/f-values for the fixed parametric and smooth terms included in the GAMMs for Black-legged Kittiwake. Number of samples used in the analysis is shown on the bottom row.

		t - value	p -value
Parametric	tail wind	3.313	<0.001
	cross wind	2.105	<0.05
	inside wind farm	3.001	<0.01
Smooth	Distance to wind farm perimeter: outside wind farm	2.897	0.089
	Distance to wind farm perimeter: inside wind farm	3.660	0.056
	Wind speed: head wind	1.470	0.225
	Wind speed: tail wind	1.065	0.302
	Wind speed: cross wind	1.434	0.231
n of samples	2778		

Figure 5.16. **Response curves of the GAMM for Black-legged Kittiwake. The response is indicated on the Y-axis in the scale of the linear predictor (higher values indicate higher altitude) and range of the predictors are indicated on the x-axis. The degree of smoothing of the continuous variables are displayed in the title of the Y-axis. The grey area and dotted lines indicate 95% confidence intervals.**
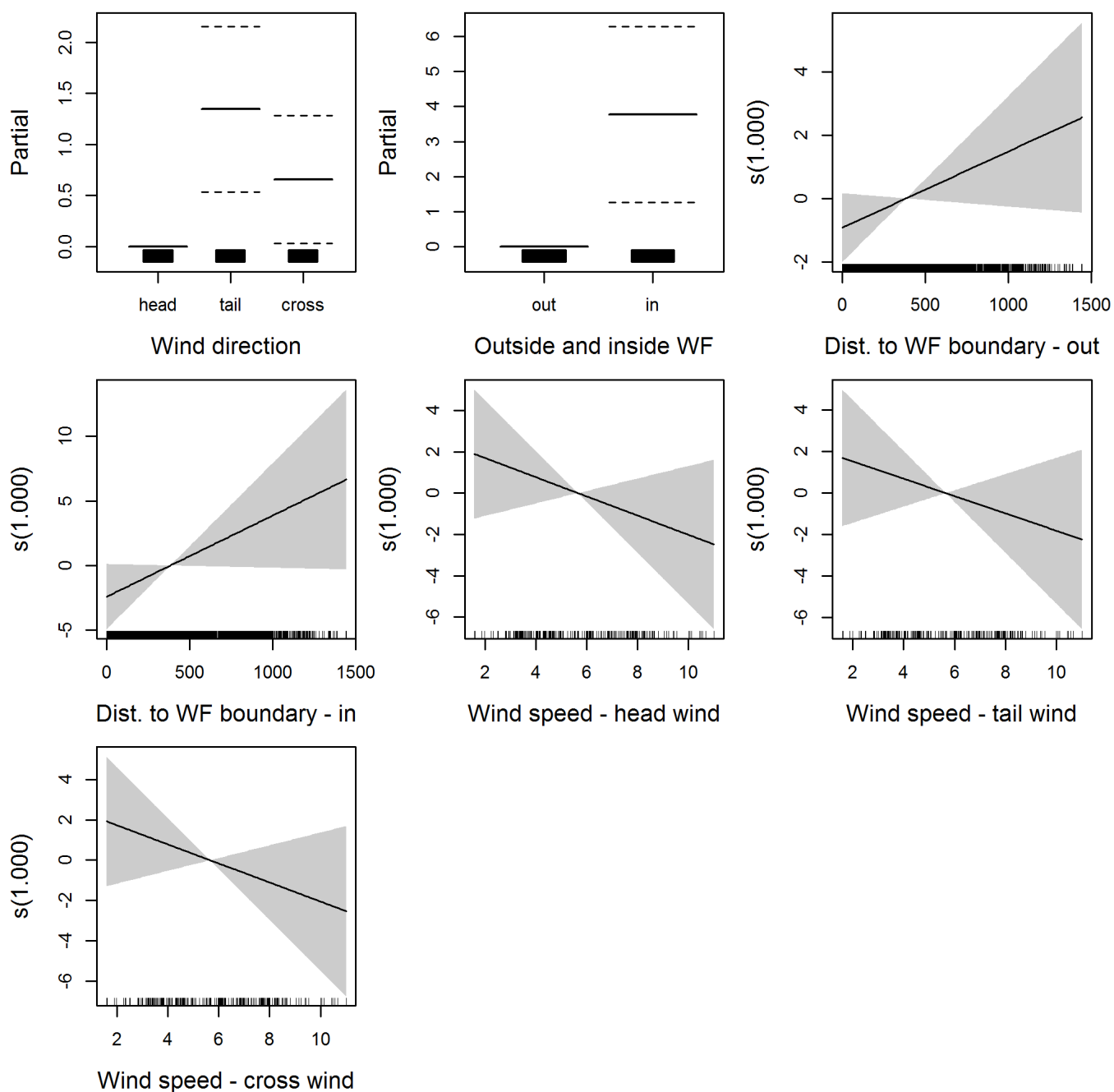
Figure 5.17. Flight height distribution of Lesser Black-backed Gull (upper left) and boxplots comparing heights at the two platforms (upper right), for different wind direction (lower left) and outside and inside the wind farm footprint (lower right. The red line indicates 25 m, which is the lowest tip of the rotor at the Thanet wind farm. The "boxes" in the box plots indicates the first quartile (bottom of the box), the third quartile (top of the box) and the thick black line indicates the median value. The error bars indicate the range (minimum and maximum excluding outliers) and the open circles indicate outliers.
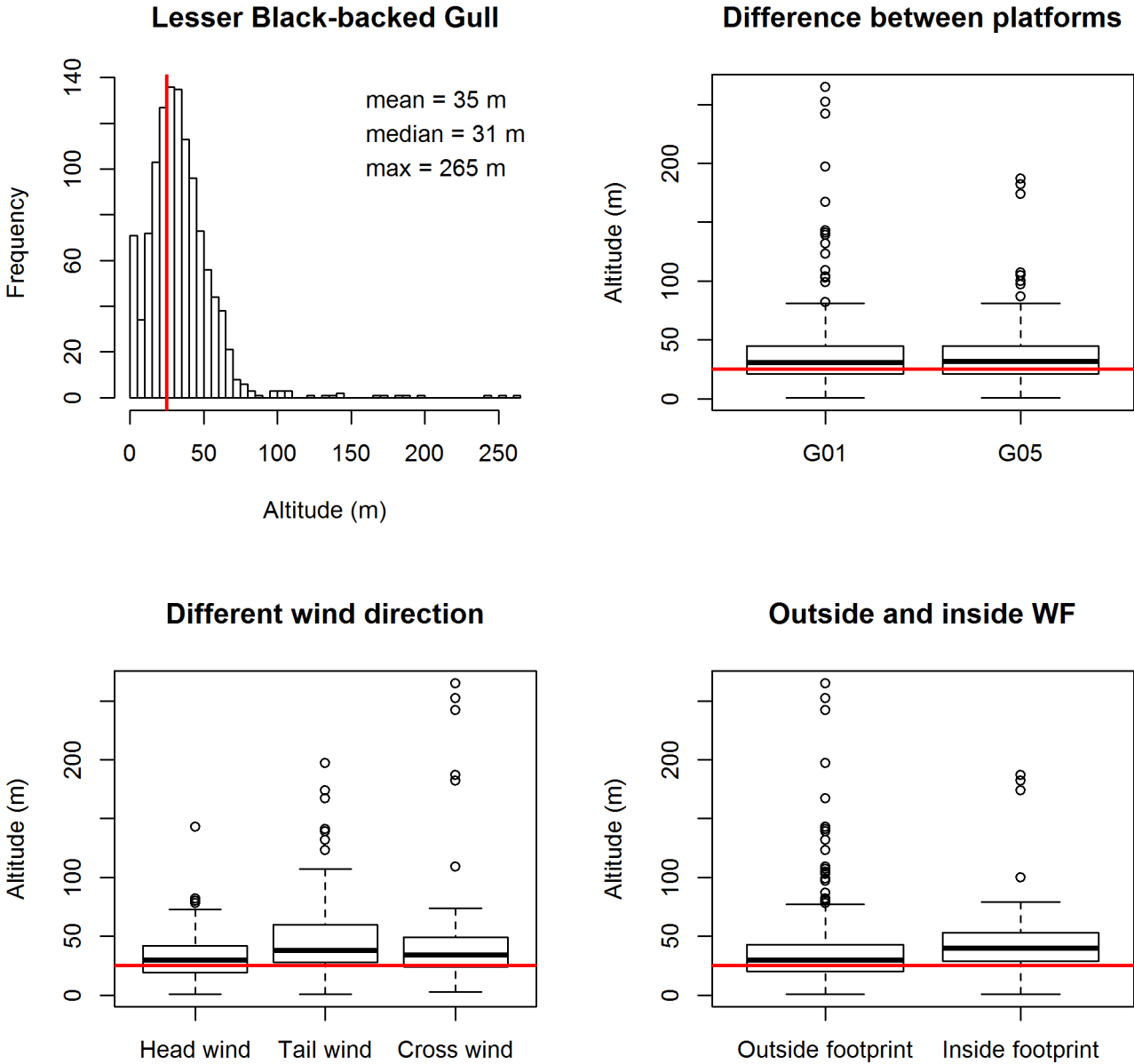
Figure 5.18.   Lesser Black-backed Gull flight height distribution by platform, sample sizes indicated in the title, number of height recordings and number of tracks in parenthesis.
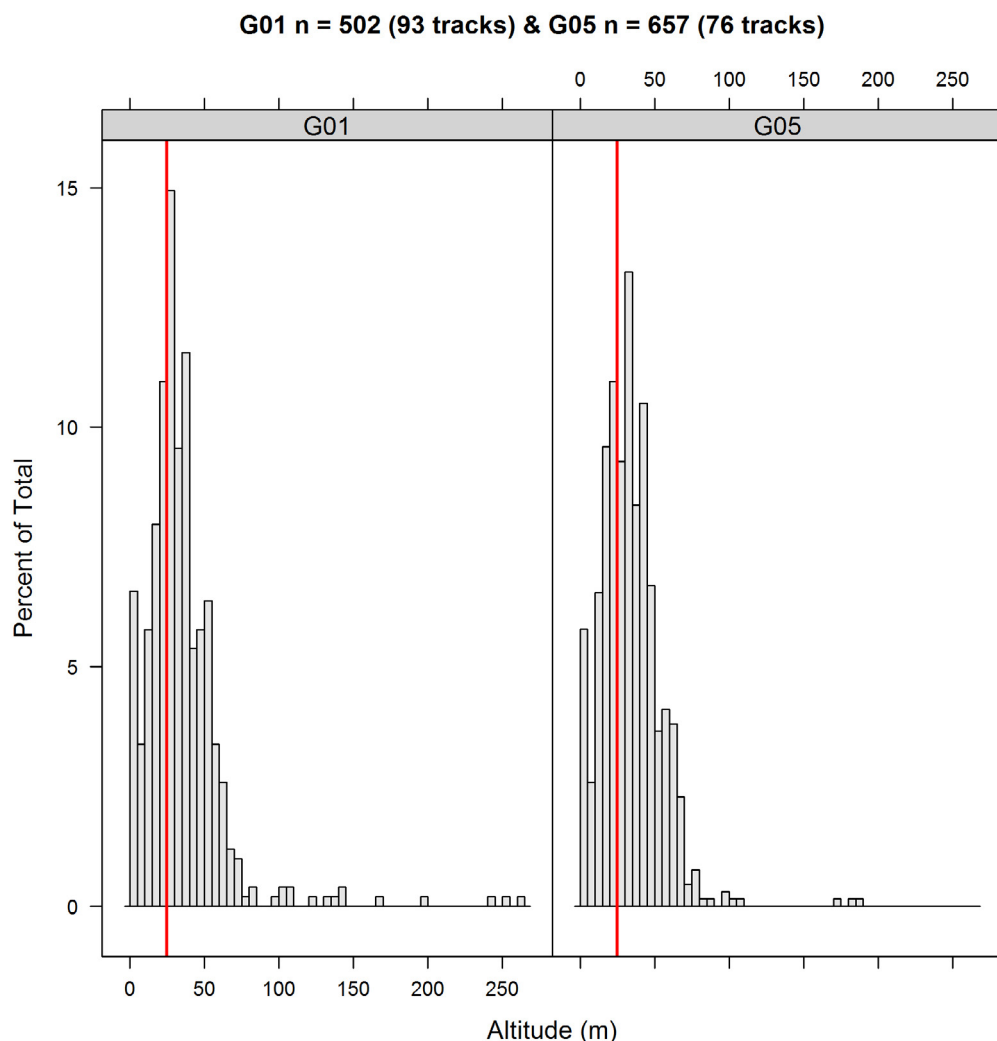

Table 5.17.   Significance and t-values/f-values for the fixed parametric and smooth terms included in the GAMMs for Lesser Black-backed Gull. Number of samples used in the analysis is shown on the bottom row.

		t – value	p -value
Parametric	**tail wind**	1.605	0.109
	cross wind	2.918	<0.01
	inside wind farm	2.753	<0.01
Smooth	**Distance to wind farm perimeter: outside wind farm**	5.203	0.016
	Distance to wind farm perimeter: inside wind farm	16.857	<0.001
	Wind speed: head wind	2.731	0.099
	Wind speed: tail wind	4.282	<0.05
	Wind speed: cross wind	1.478	0.224
n of samples	1159		

Figure 5.19. Response curves of the GAMM for Lesser Black-backed Gull. The response is indicated on the Y-axis in the scale of the linear predictor (higher values indicate higher altitude) and range of the predictors are indicated on the x-axis. The degree of smoothing of the continuous variables are displayed in the title of the Y-axis. The grey area and dotted lines indicate 95% confidence intervals.
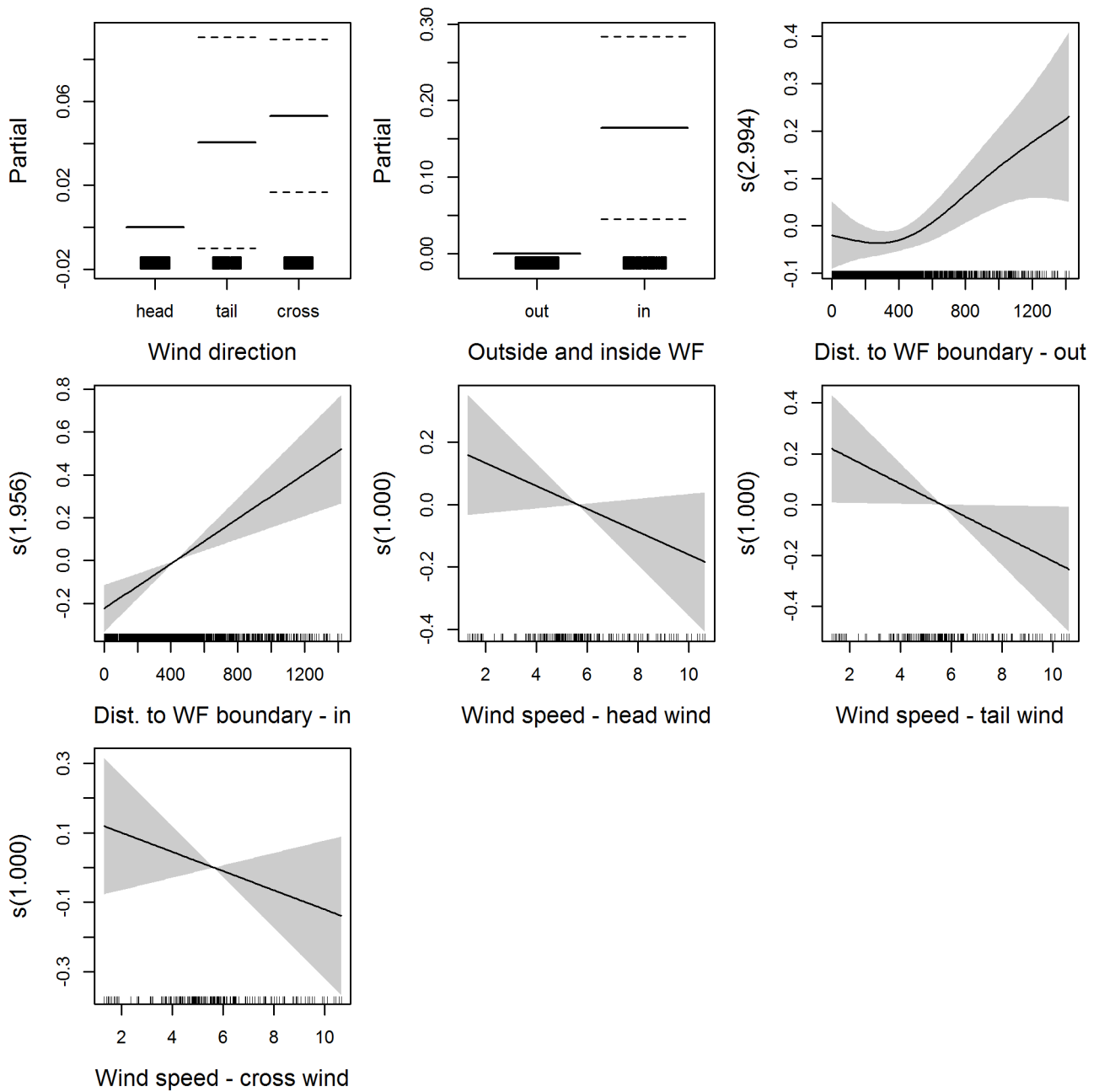
Figure 5.20. Flight height distribution of Herring Gull (upper left) and boxplots comparing heights at the two platforms (upper right), for different wind direction (lower left) and outside and inside the wind farm footprint (lower right. The red line indicates 25 m, which is the lowest tip of the rotor at the Thanet wind farm. The "boxes" in the box plots indicates the first quartile (bottom of the box), the third quartile (top of the box) and the thick black line indicates the median value. The error bars indicate the range (minimum and maximum excluding outliers) and the open circles indicate outliers.
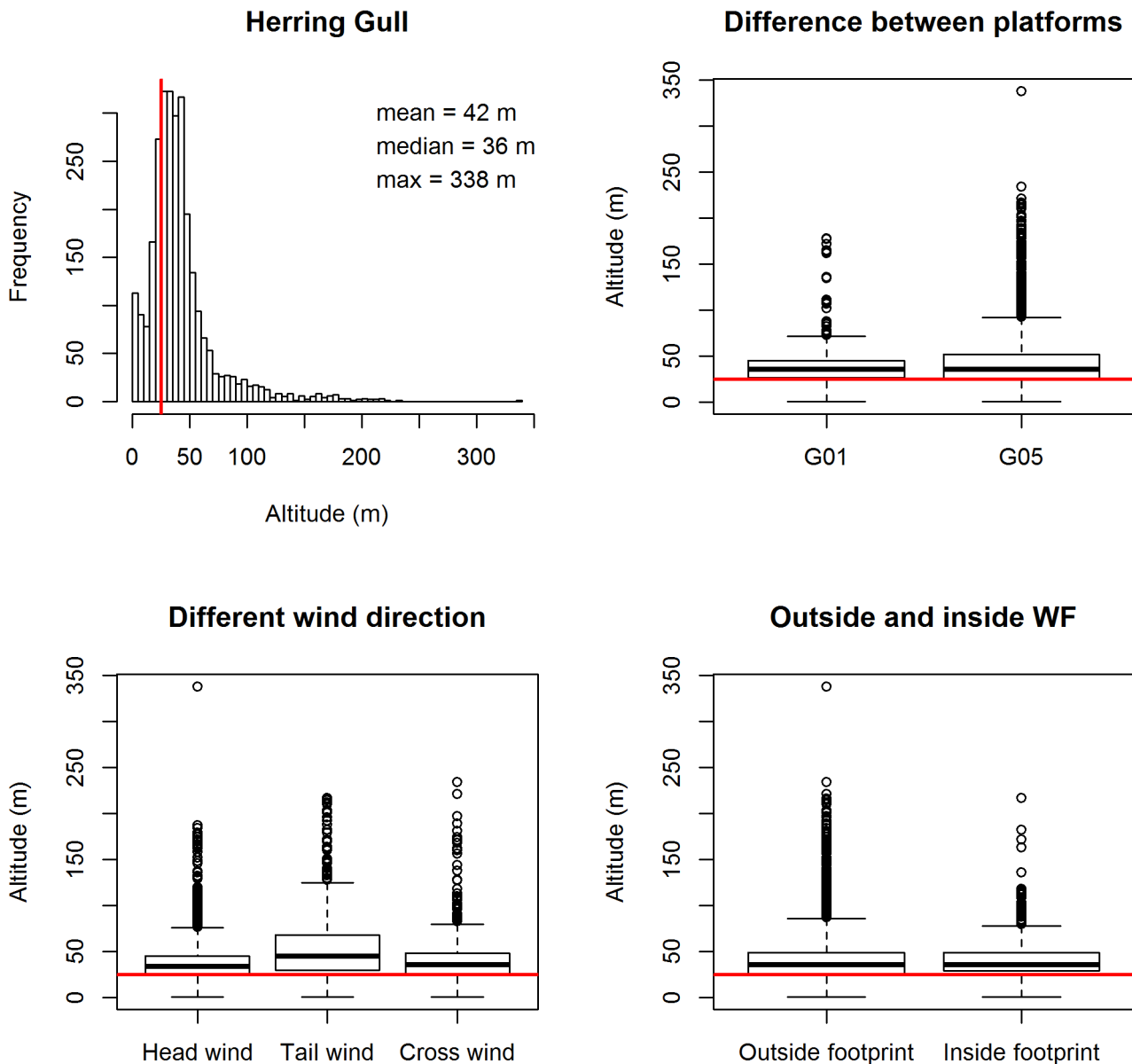
Figure 5.21. Herring Gull flight height distribution by platform, sample sizes indicated in the title, number of height recordings and number of tracks in parenthesis.
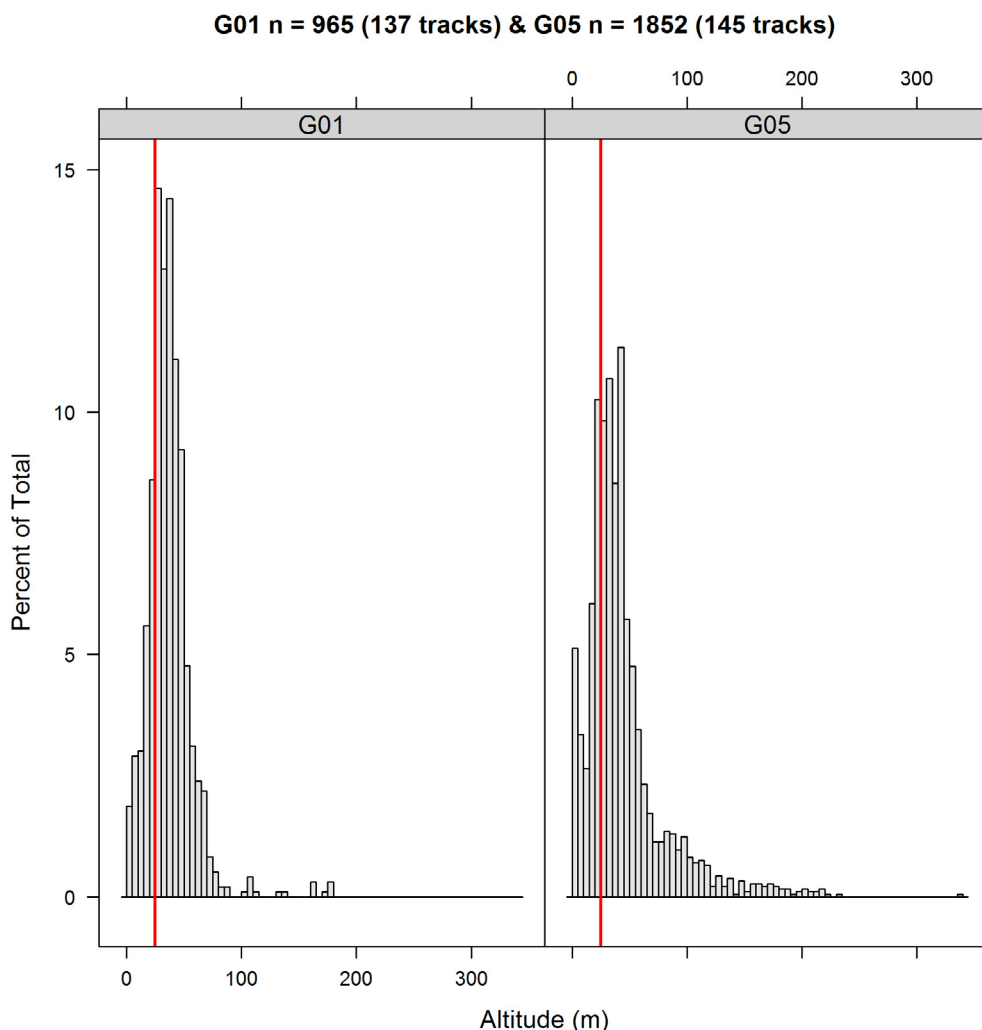

Table 5.18. Significance and t-values/f-values for the fixed parametric and smooth terms included in the GAMMs for Herring Gull. Number of samples used in the analysis is shown on the bottom row.

		t – value	p –value
Parametric	tail wind	0.651	0.515
	cross wind	-0.548	0.584
	inside wind farm	-1.544	0.123
Smooth	Distance to wind farm perimeter: outside wind farm	0.184	0.668
	Distance to WF perimeter: inside wind farm	0.450	0.502
	Wind speed: head wind	8.142	<0.001
	Wind speed: tail wind	7.888	<0.01
	Wind speed: cross wind	6.287	<0.01
n of samples	2817		

Figure 5.22. Response curves of the GAMM for Herring Gull. The response is indicated on the Y-axis in the scale of the linear predictor (higher values indicate higher altitude) and range of the predictors are indicated on the x-axis. The degree of smoothing of the continuous variables are displayed in the title of the Y-axis. The grey area and dotted lines indicate 95% confidence intervals.
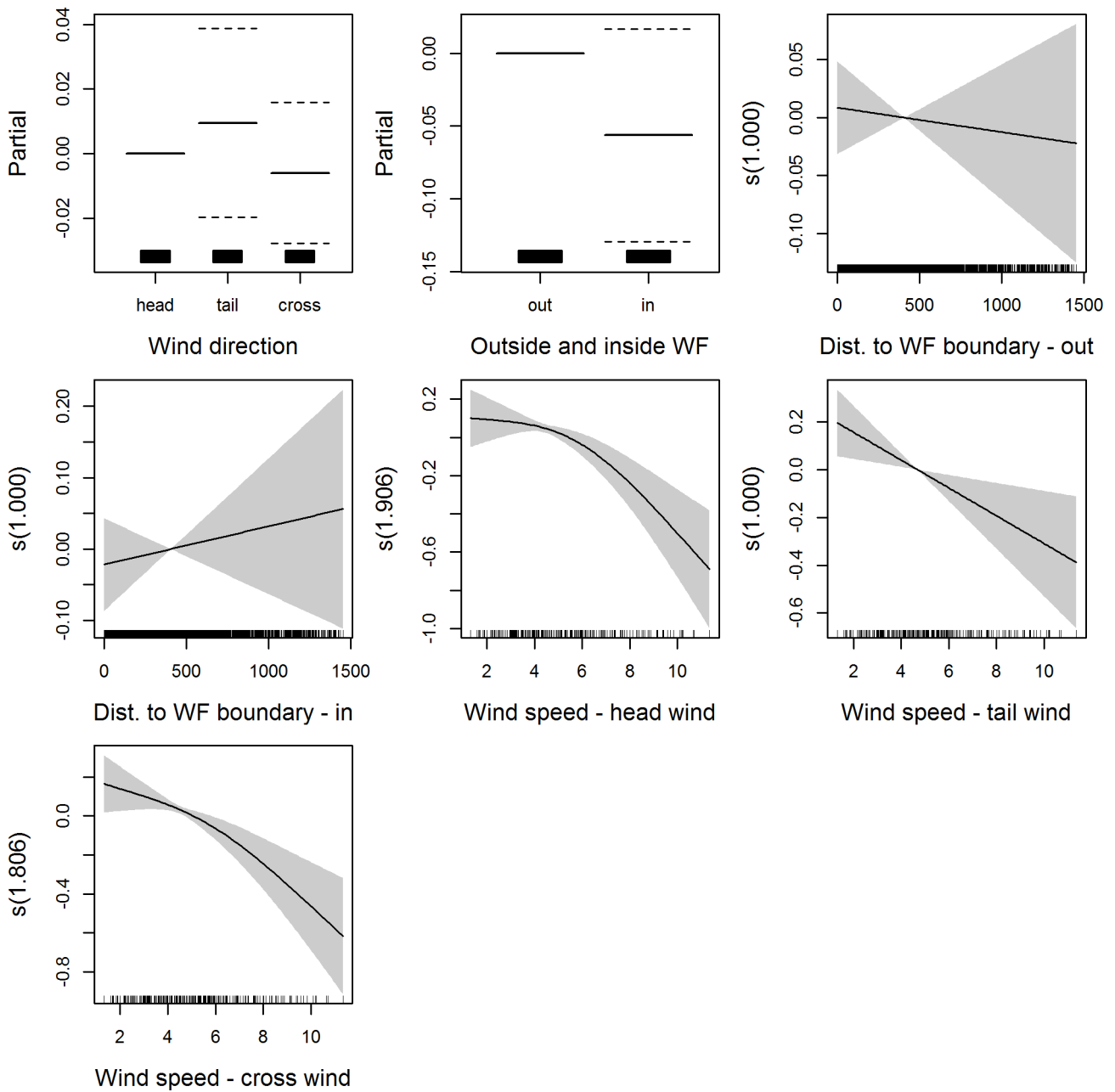
Figure 5.23. Flight height distribution of Great Black-backed Gull (upper left) and boxplots comparing heights at the two platforms (upper right), for different wind direction (lower left) and outside and inside the wind farm footprint (lower right. The red line indicates 25 m, which is the lowest tip of the rotor at the Thanet wind farm. The "boxes" in the box plots indicates the first quartile (bottom of the box), the third quartile (top of the box) and the thick black line indicates the median value. The error bars indicate the range (minimum and maximum excluding outliers) and the open circles indicate outliers.
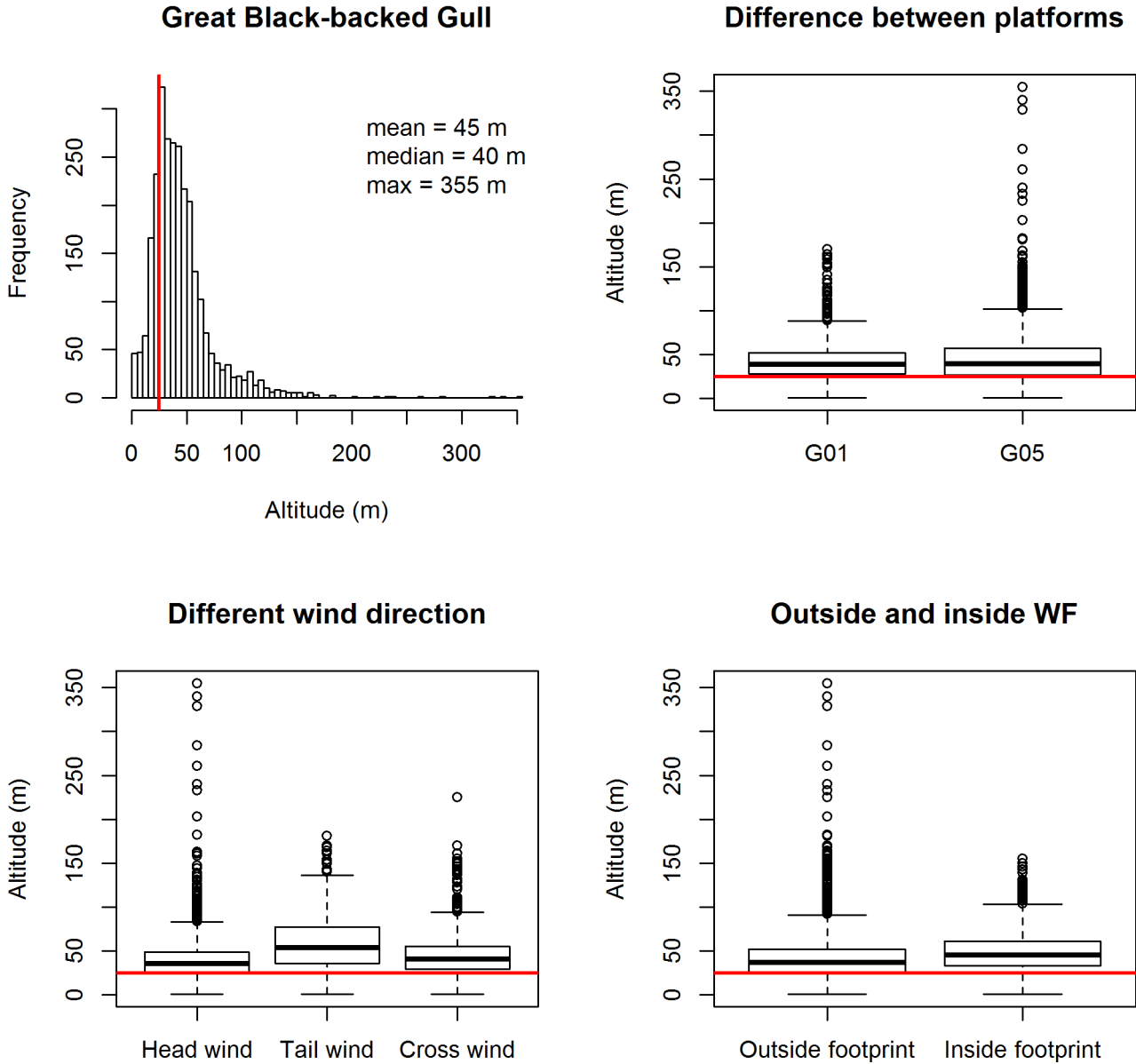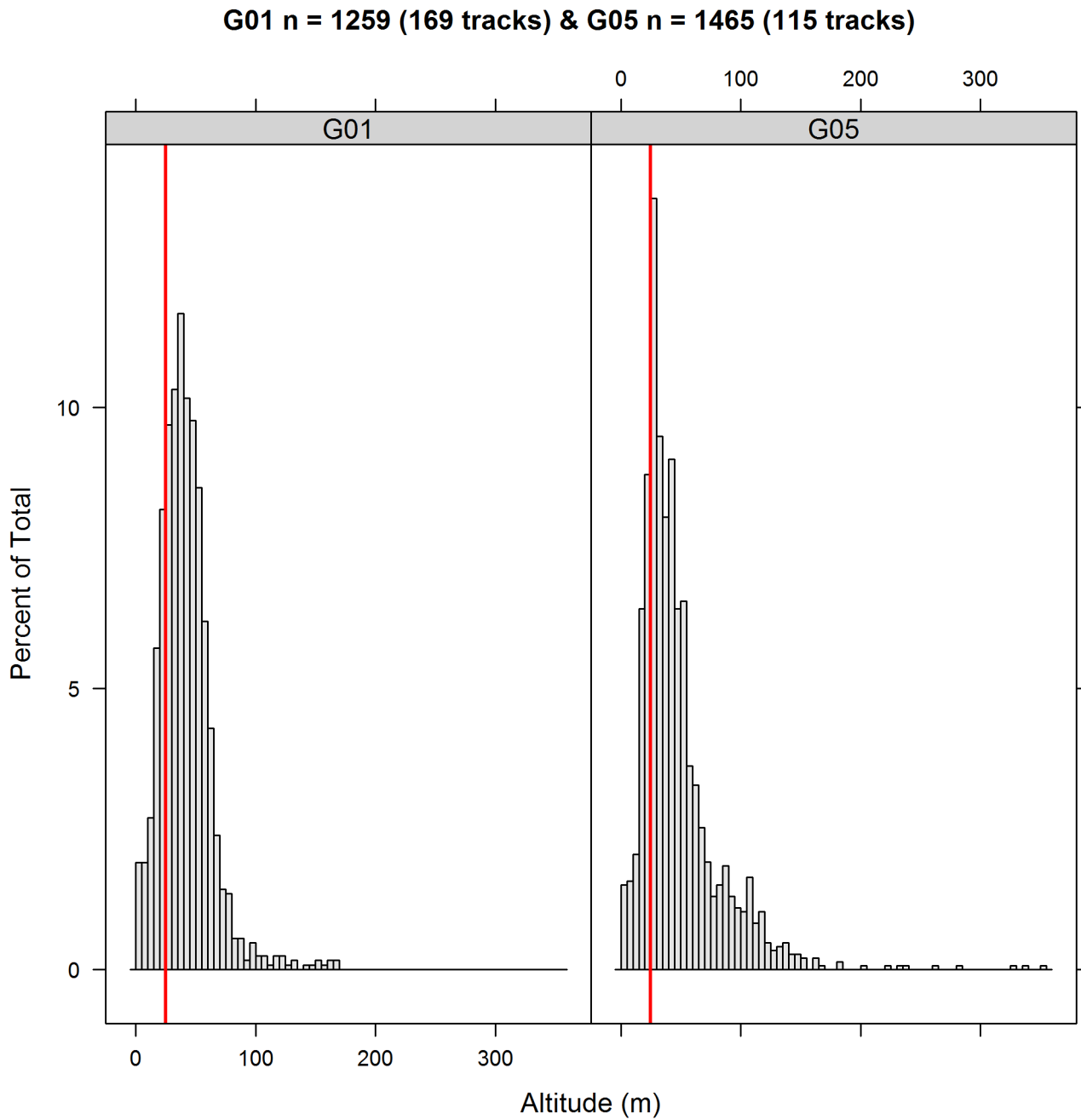
Figure 5.24. **Great Black-backed Gull flight height distribution by platform, sample sizes indicated in the title, number of height recordings and number of tracks in parenthesis.**

Table 5.19. Significance and t-values/f-values for the fixed parametric and smooth terms included in the GAMMs for Great Black-backed Gull. Number of samples used in the analysis is shown on the bottom row.

RESULTS		t – value	p –value
Parametric	tail wind	1.683	0.093
	cross wind	2.092	0.037
	inside wind farm	-1.411	0.158
Smooth	Distance to wind farm perimeter: outside wind farm	0.342	0.559
	Distance to WF perimeter: inside wind farm	0.114	0.735
	Wind speed: head wind	1.397	0.142
	Wind speed: tail wind	1.328	0.249
	Wind speed: cross wind	1.866	0.172
n of samples	2724		

Figure 5.25. Response curves of the GAMM for Great Black-backed Gull. The response is indicated on the Y-axis in the scale of the linear predictor (higher values indicate higher altitude) and range of the predictors are indicated on the x-axis. The degree of smoothing of the continuous variables are displayed in the title of the Y-axis. The grey area and dotted lines indicate 95% confidence intervals. s.
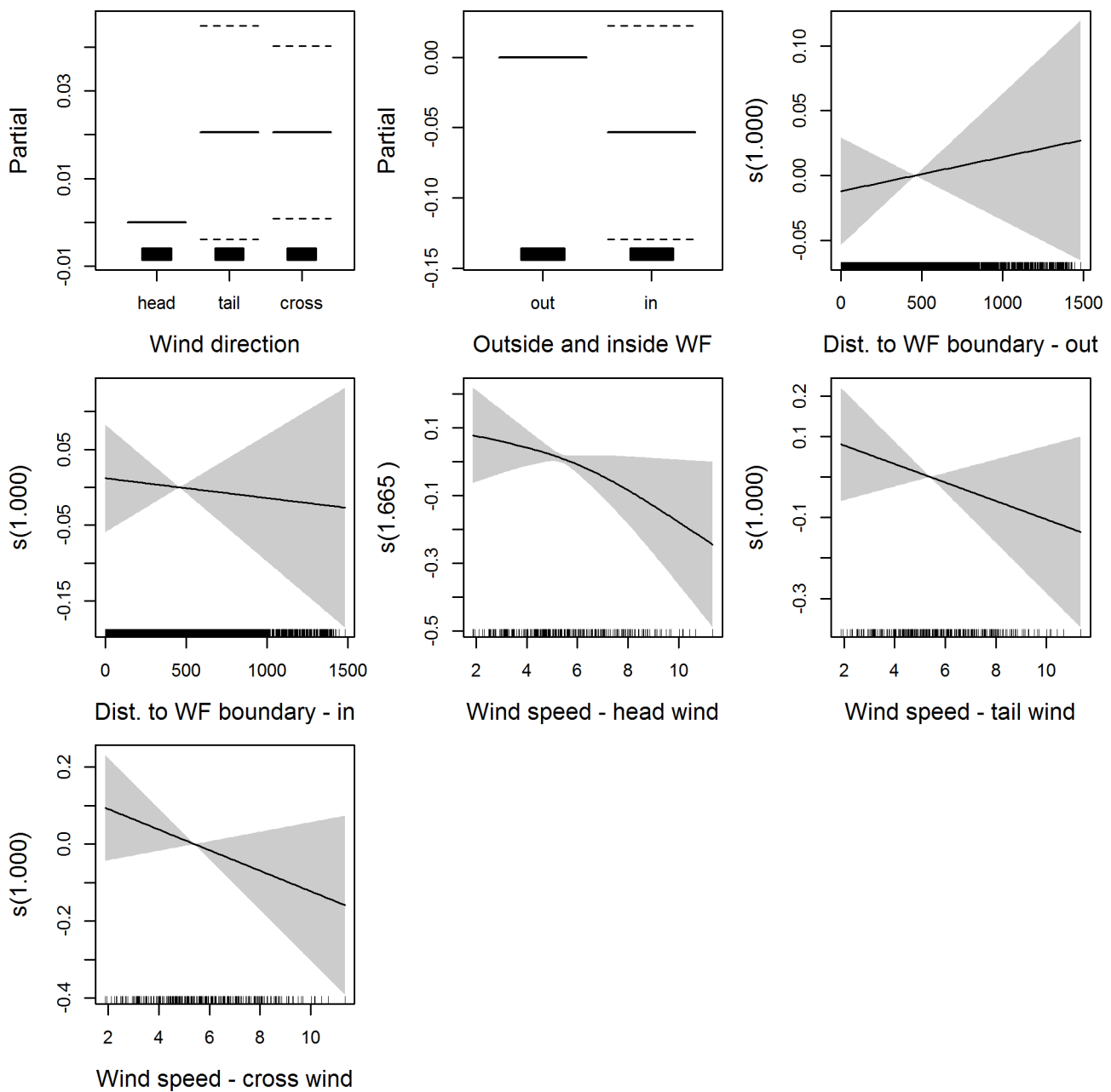
6 INTERPRETATION OF BIRD BEHAVIOUR OBSERVED

6.1. INTRODUCTION

6.1.1. This section presents the interpretation of bird behaviour based on the distribution of tracks collected by the radar and rangefinders, as well as a summary of observations recorded through video evidence at Thanet.

6.1.2. Reference to other studies have been included, although the variation in methods applied means that comparison of results between wind farms is challenging. For instance, many studies are purely based on the assessment of changes in densities recorded based on ship surveys, while others rely on radar and visual observations of flight tracks. In addition, there is a great variety of factors that may affect changes in densities / flight tracks observed, such as weather conditions, population changes unrelated to the wind farm or food availability, which are difficult to disentangle.
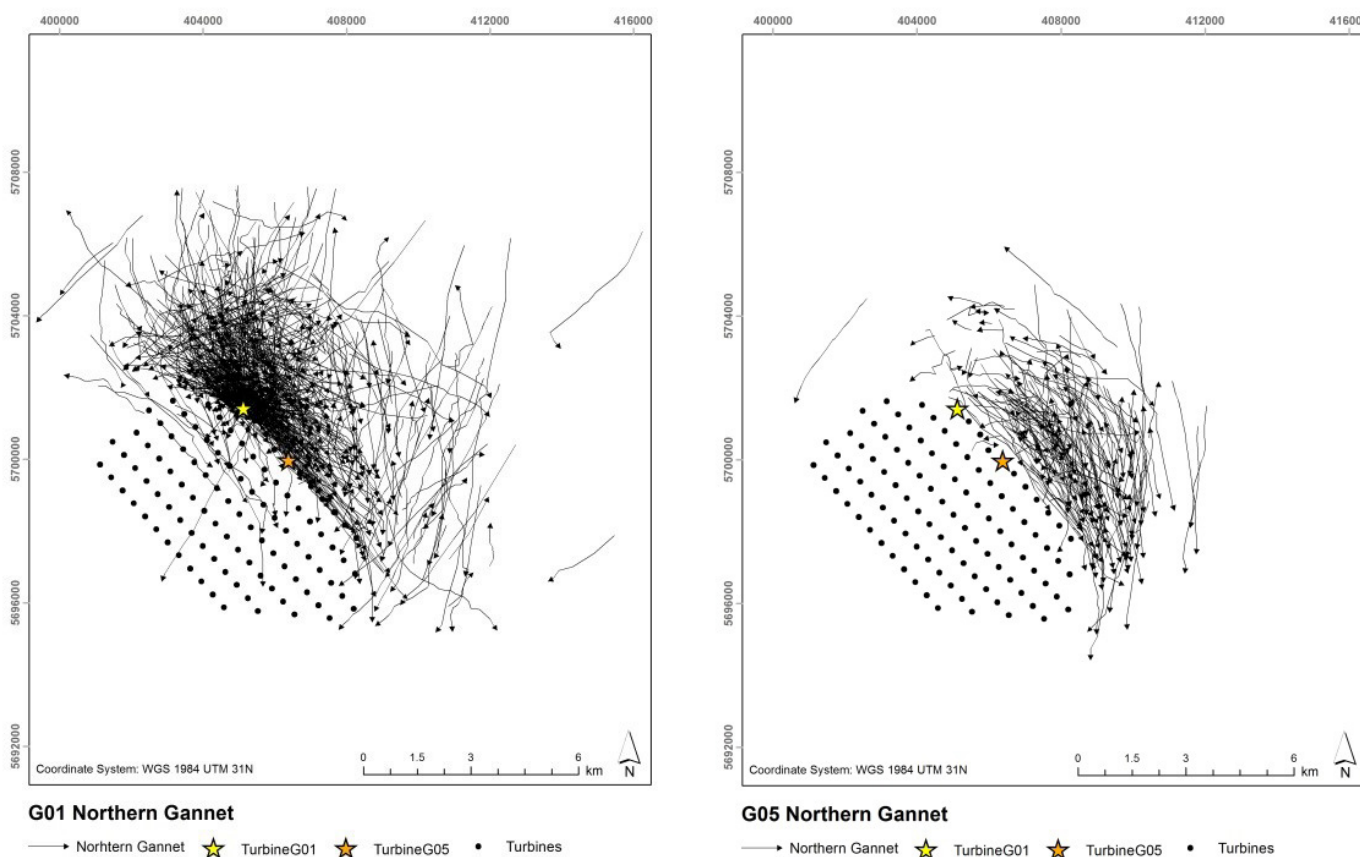
6.2. NORTHERN GANNET

6.2.1. There is a general lack of evidence regarding Northern Gannets' avoidance behaviour around offshore wind farms at the macro scale, particularly in relation to certain circumstances, such as during foraging or commuting activity, and or during migration. There is also uncertainty on the extent to which Northern Gannets may habituate to the presence of wind turbines (Furness 2016). In her review, Krijgsveld (2014) indicated that seven out of seven reports addressing seabird behaviour around offshore wind farms reported avoidance by Northern Gannets. As part of a study undertaken at the Dutch Offshore Wind farm Egmond aan Zee, Krijgsveld et al. (2011) reported that Northern Gannet showed the highest level of avoidance at the macro scale, with only 3% of all Northern Gannets found flying inside the wind farm, and 14% at the edge of the wind farm. Similarly, Rehfisch et al. (2014) reported a high macro avoidance rate (95%) for Northern Gannet based on digital aerial post-construction surveys at the Greater Gabbard Offshore Wind Farm. At the Dutch Blight Band wind farm, Vanermen et al. (2014) reported strong avoidance by Northern Gannet, with an 85% decrease in abundance in the impact area after wind farm construction.

6.2.2. In this study, Northern Gannet was overall the most numerous tracked species, with a total of 1,317 tracks collected in total within 3 km of Thanet by all sensors on turbines G01 and G05, of which 585 were collected by the SCANTER radar from turbine G01.

6.2.3. Collected tracks are mapped in Figure 6.1, where it can be interpreted that Northern Gannets are avoiding the wind farm, but not completely.

NIRAS   DHI   CARBON TRUST

Figure 6.1.   Northern Gannets flight tracks collected using the SCANTER radar and LAWR radar from turbines G01 (left) and G05 (right) respectively.


6.2.4.   High number of tracks were recorded just outside the wind farm, and judged by the track density recorded by the SCANTER radar from turbine G01, the avoidance pattern results in a concentration of Northern Gannets within 1.5 km distance from the edge of the wind farm, and the track density decreasing farther away, which could be interpreted as returning to a baseline density value. Whether this concentration at the edge of the wind farm is a phenomenon introduced by the wind farm can only be assumed, as other local factors may have played a role (see Section 2.2, where studies in which redistribution close to the wind farm edge has also been observed are listed).

6.2.5.   The number of tracks recorded from turbine G05 was much lower, which can be associated to the constraints associated with the use of this piece of equipment (see Appendix 2) from where only two tracks were recorded inside the wind farm.

6.2.6.   The density of tracks (based on the track length per unit method) is mapped in Figure 6.2

NIRAS DHI CARBON TRUST

Figure 6.2.   Northern Gannets track density (calculated through track length per unit area method) based on all data collected using the SCANTER radar and LAWR radar from turbines G01 (left) and G05 (right) respectively.
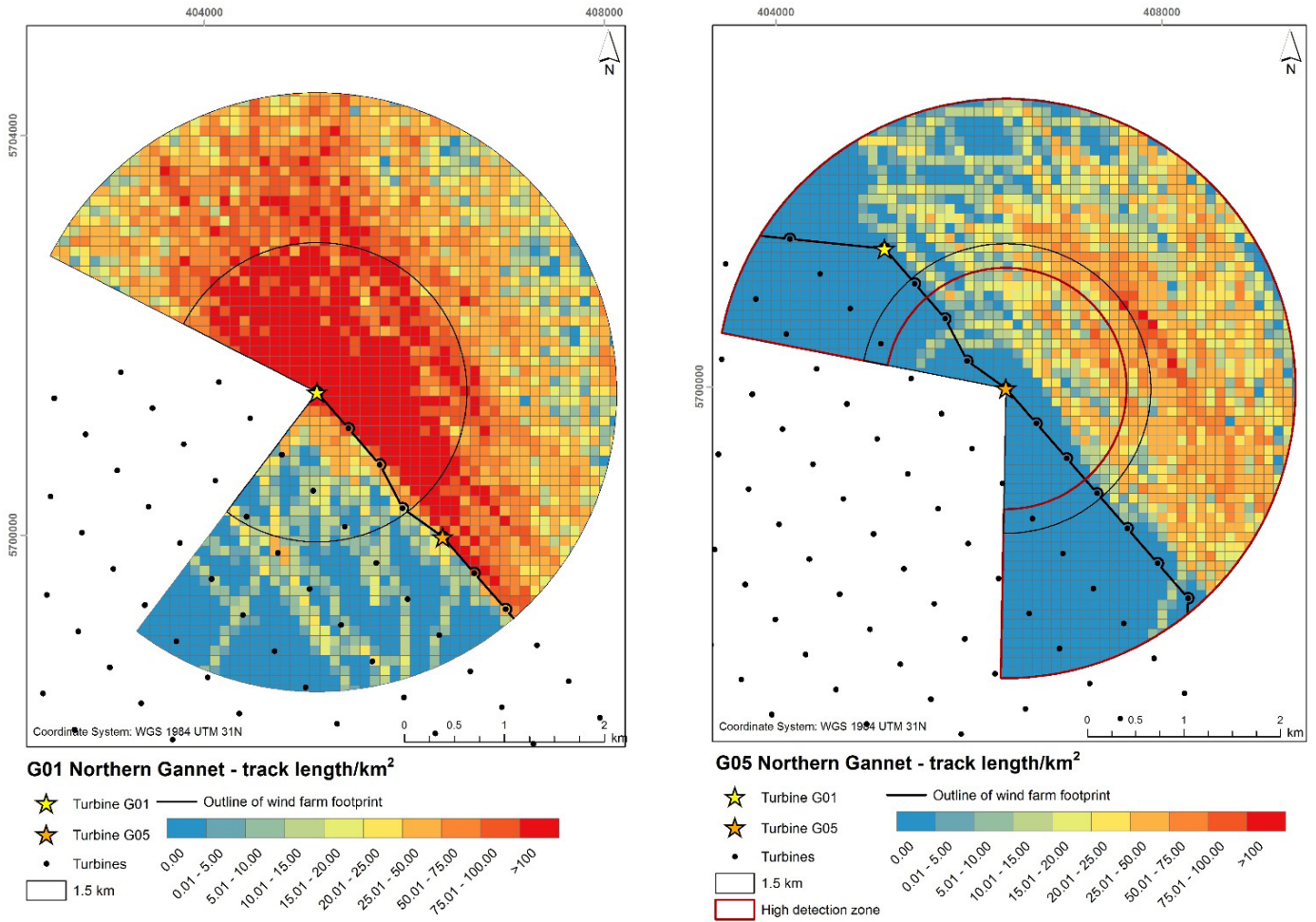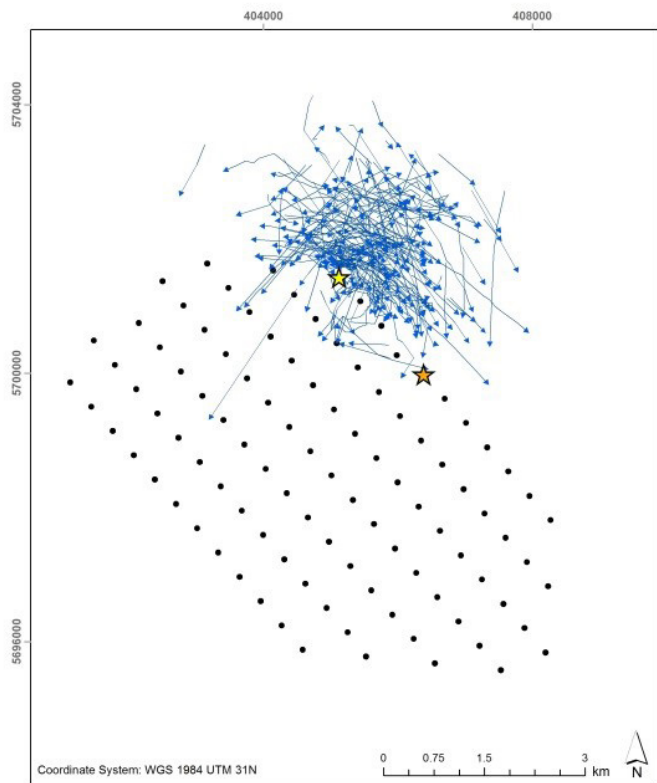

6.2.7.   At the same time, data collected by rangefinders within 1.5 km from both turbines G01 and G05, show similar patterns to those observed from turbine G01 (Figure 6.3). The quantification of empirical macro avoidance in this case (RF Macro EAR = G01 0.776/G05 0.787) can be considered in line with the interpretation of redistribution observed by mapped data.

6.2.8.   In relation to flight direction, Northern Gannets were mainly observed flying to the southeast, throughout the year (Figure 6.4). This directional movement may indicate that gannets recorded at the Thanet site were mainly performing larger scale feeding movements rather than seasonal migration or local feeding movements.
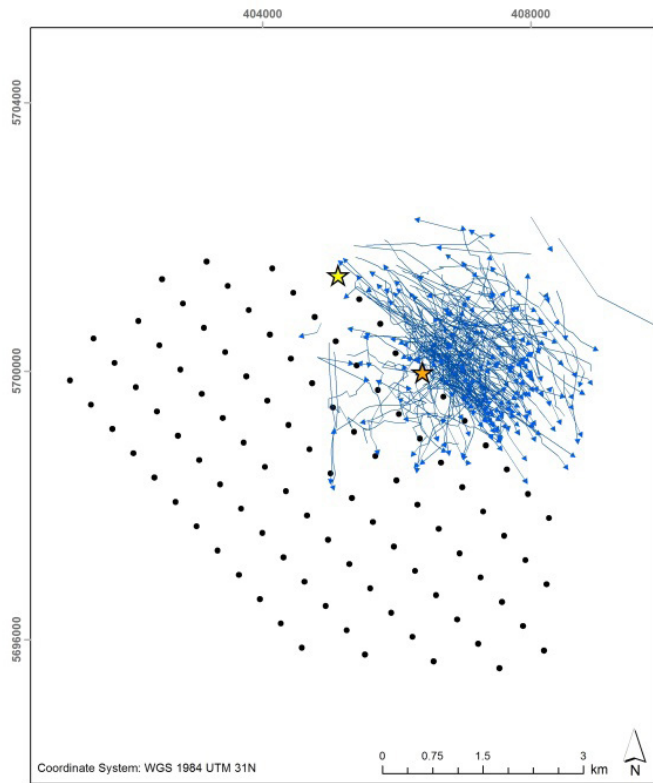
Figure 6.3. Northern Gannets flight tracks (upper) collected using rangefinders from turbines G01 (left) and G05 (right) respectively, and estimated track density, calculated applying the track length per unit method (lower).
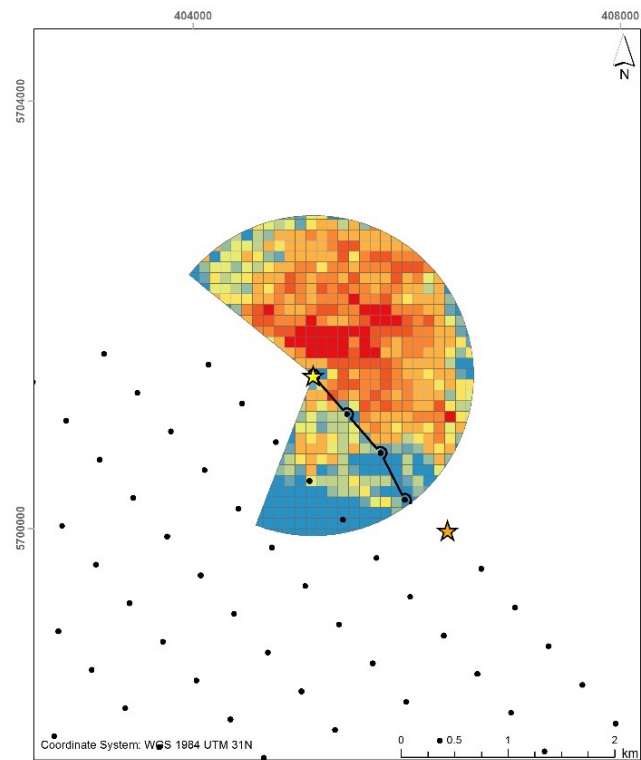
INTERPRETATION OF BIRD BEHAVIOUR OBSERVED

Figure 6.4.   Recorded flight directions, number of samples (x and y axis) per direction. Mean value is noted with a black line, accompanied by associated confidence limits.
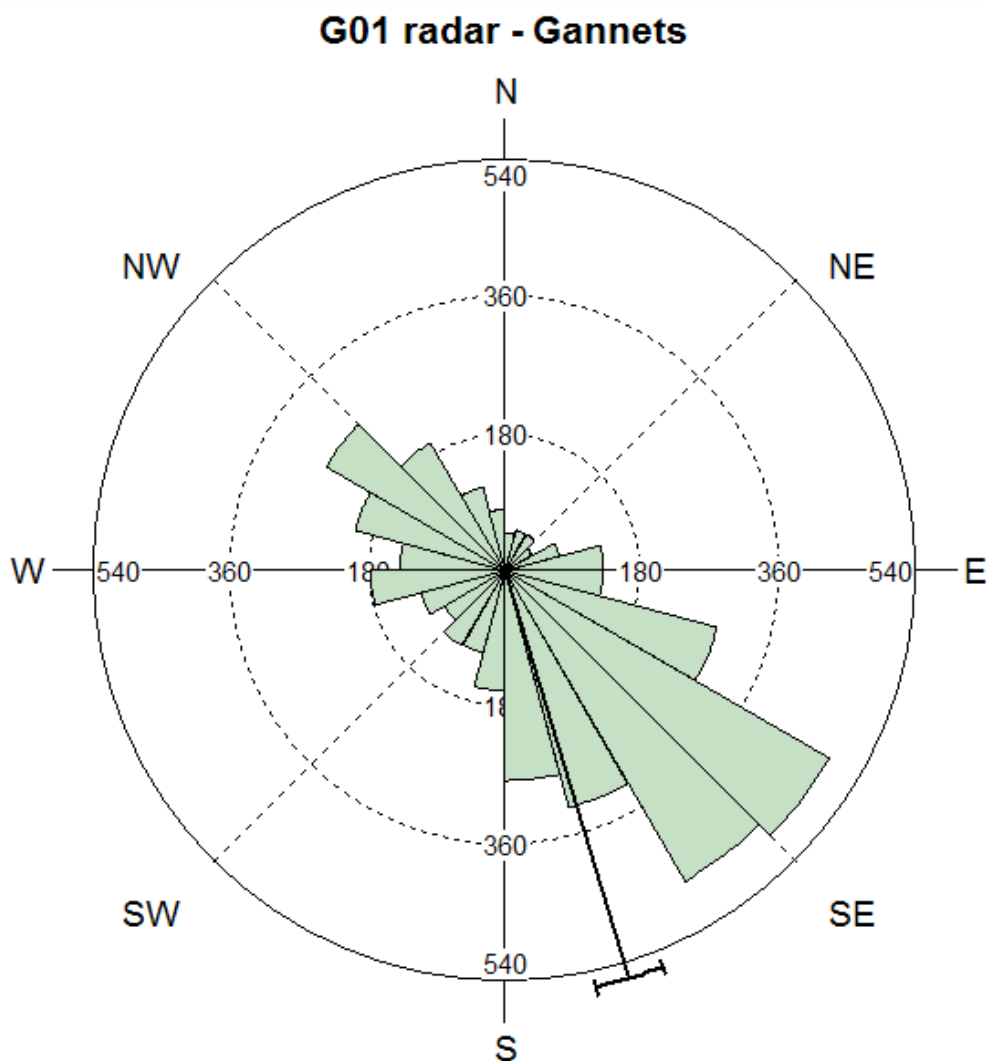
6.2.9.   No apparent differences between seasons could be observed (Figure 6.5), a potential explanation for this could be that the birds are following a regular foraging route. Similar patterns are observed in data collected by all sensors (see Appendix 2, Section 2).

6.2.10.   The median flight height of Northern Gannets in the study area was estimated at 17 m, i.e. below rotor height, and overall, the study recorded 27% of Northern Gannets flying at rotor height (see Section 5.6). Interestingly, the flight height distribution observed was bimodal (see Section 5.6) with peaks at below 10 m and at 20-25m. The same pattern was recorded from both platforms (G01 / G05), indicating a consistent pattern.

6.2.11. Cleasby et al. (2015) showed highly similar patterns based on telemetry data, recording a bimodal flight height distribution for Northern Gannet, with a median flight height of commuting birds at 12 m and feeding birds at 27 m. Similarly, at the German Apha Ventus offshore wind farm, Northern Gannets were observed to prefer flight heights between 10 to 20 m (Mendel et al. 2014). Other studies, however, present varying proportions of flights at rotor height. For instance, evidence from visual surveys conducted in the UK assessed flight height of 44,851 birds at 27 sites, suggesting that 12.6% (95% CI 6.2 to 20%) of flight occurred at collision risk height (Johnston et al. 2014a,b). The highest proportion of birds flying at rotor height was recorded in a radar study in Denmark, and was based on tracks of 143 birds, 44% of Northern Gannet flight were found to occur at collision risk height (Krijgsveld et al. 2005). Visual assessments made at OWEZ (Krisjgsveld et al. 2011) reported general flight altitudes below 10 m, with some foraging birds reaching altitudes up to 50 m when reaching for food, with a proportion of 30% of birds flying at rotor height (no sample size stated) (Krijgsveld et al. 2011).

Figure 6.5. Mean flight direction of Northern Gannet recorded from turbine G01 using the SCANTER radar.

INTERPRETATION OF BIRD BEHAVIOUR OBSERVED
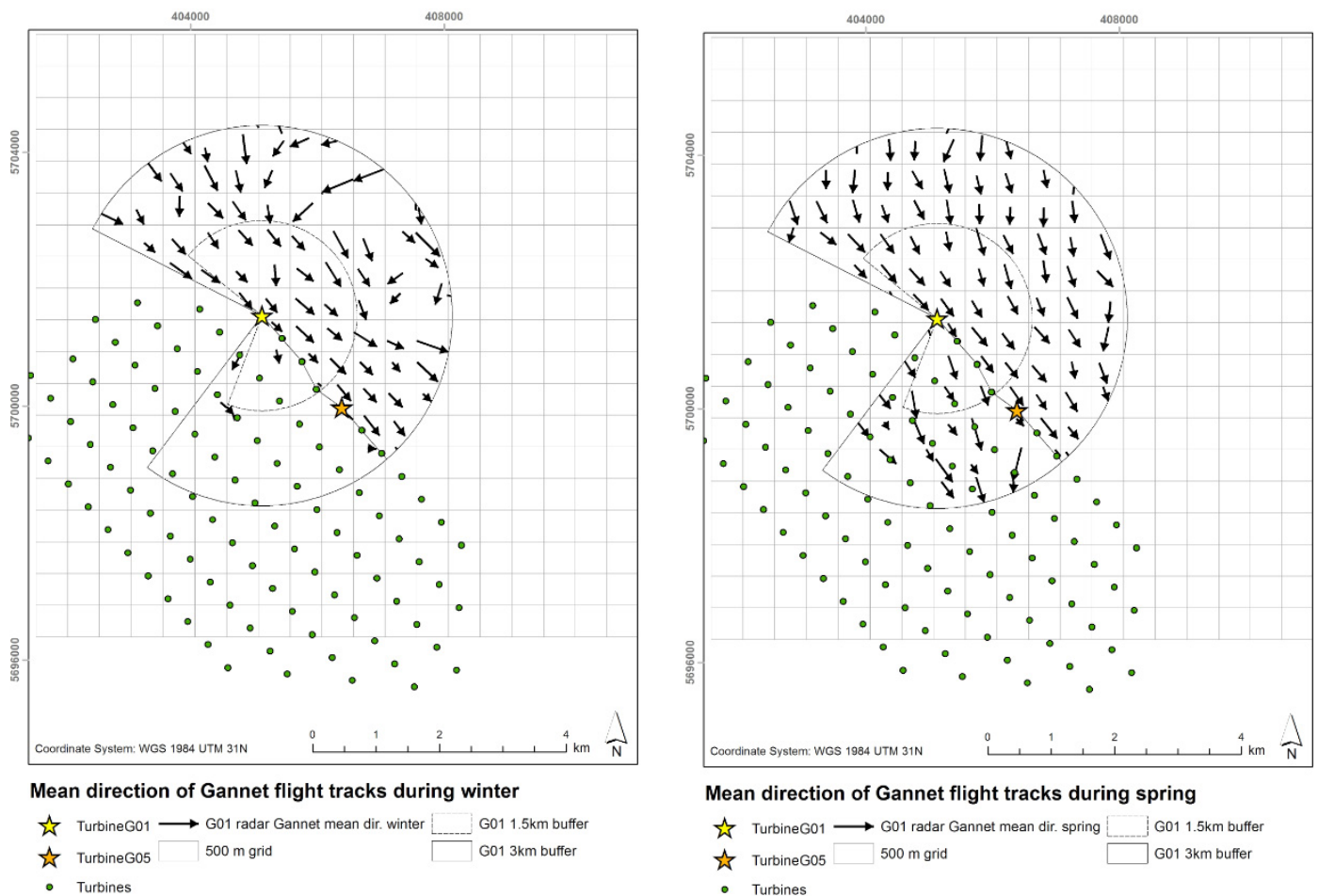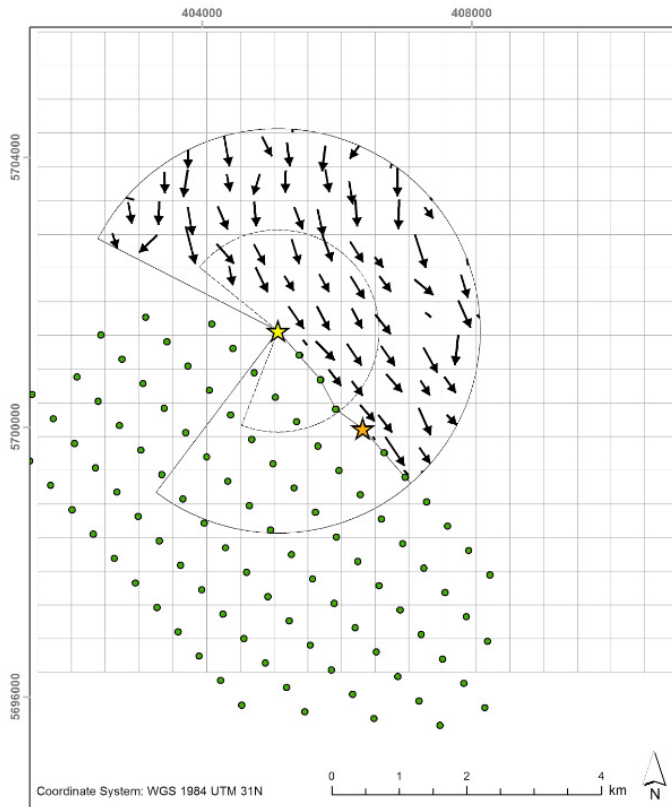
Mean direction of Gannet flight tracks during summer

☆ TurbineG01 → G01 radar Gannet mean dir. summer | G01 1.5km buffer
☆ TurbineG05 □ 500 m grid | G01 3km buffer
• Turbines
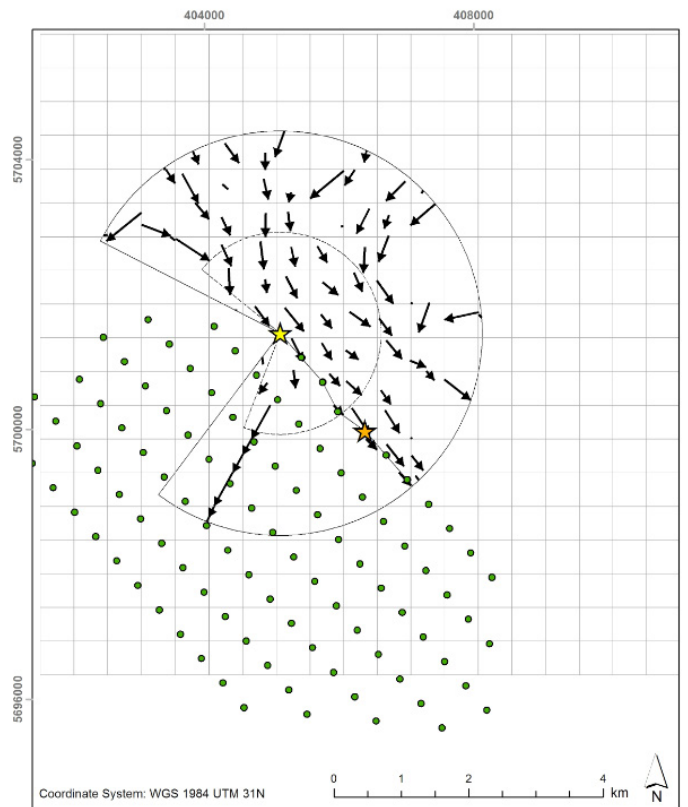
Mean direction of Gannet flight tracks during autumn

☆ TurbineG01 → G01 radar Gannet mean dir. autumn | G01 1.5km buffer
☆ TurbineG05 □ 500 m grid | G01 3km buffer
• Turbines

6.2.13. The flight speeds recorded in this study are similar to what has been recorded by some other studies as well. GPS data reported in other studies are generally, however, large scaled and therefore also include "transition flights" from colonies to feeding grounds, long sustained directional flights, in comparison to the rangefinder dataset used in this study. Pettex et al. (2012) reported a mean flight speed of about 13.5 m/s in comparison to 13.3 m/s measured in this study.

6.2.14. At the meso scale, 0.6% of recorded seabirds displayed meso avoidance by adjusting vertically and fly below or above the RSZ, while the proportion including low-flying seabirds with no obvious vertical adjustment observed was 1.6%. A 3.3% of videos showed Northern Gannets foraging inside the wind farm.

6.2.15. Of the birds observed entering the RSZ + 10 m buffer (n=299), 11.0% were identified as Northern Gannets, and most of micro avoidance responses recorded for this species (84.8%) were crossings with adjustments, mainly through flying along the plane of the spinning rotor. As seen from the frequency distribution of sea states during which Northern Gannets were recorded in the wind farm, the species was observed commonly in sea states 1 to 5 and less commonly in sea states 0, 6 and 7 (Figure 3.3). Measurements of sea states in Thanet are not available, yet the pattern suggests that gannets entered the wind farm in all weather conditions.

INTERPRETATION OF BIRD BEHAVIOUR OBSERVED

6.3. BLACK-LEGGED KITTIWAKE

6.3.1.   The literature review conducted by Furness (2016) found little evidence regarding avoidance of Black-legged Kittiwakes to offshore wind farms (i.e. macro avoidance), with the studies of Vanermen et al. (2017) and Mendel et al. (2014) being amongst the few where avoidance was documented. The review by Krijgsveldt (2014) reports that smaller gull species show variation in behaviour towards the wind farms, with results varying between studies, showing both avoidance of, indifference and attraction to wind farms. As an example, at Offshore Wind farm Egmond aan Zee, Black-legged Kittiwake were relatively abundant within the wind farm (Krijgsveld et al. 2011).

6.3.2.   In comparison with Northern Gannet, the number of Black-legged Kittiwake tracks collected was lower, with a total of 367 tracks collected using all sensors.

6.3.3.   Collected and mapped radar data (Figure 6.6, Figure 6.7 and Figure 6.8) can be interpreted to indicate avoidance at the macro scale, with an aggregation of birds just outside the wind farm (similarly to distributions recorded for Northern Gannet), and relatively few Black-legged Kittiwakes tracked beyond 1.5 km by the radars.

6.3.4.   The difference between tracks recorded inside and outside the wind farm was minor between radars, however, interestingly, all tracks collected from turbine G05 moving towards the wind farm were either moving straight in or out from the wind farm.

Figure 6.6.   **Black-legged Kittiwake flight tracks collected using the SCANTER radar and LAWR radar from turbines G01 (left) and G05 (right) respectively.**

INTERPRETATION OF BIRD BEHAVIOUR OBSERVED
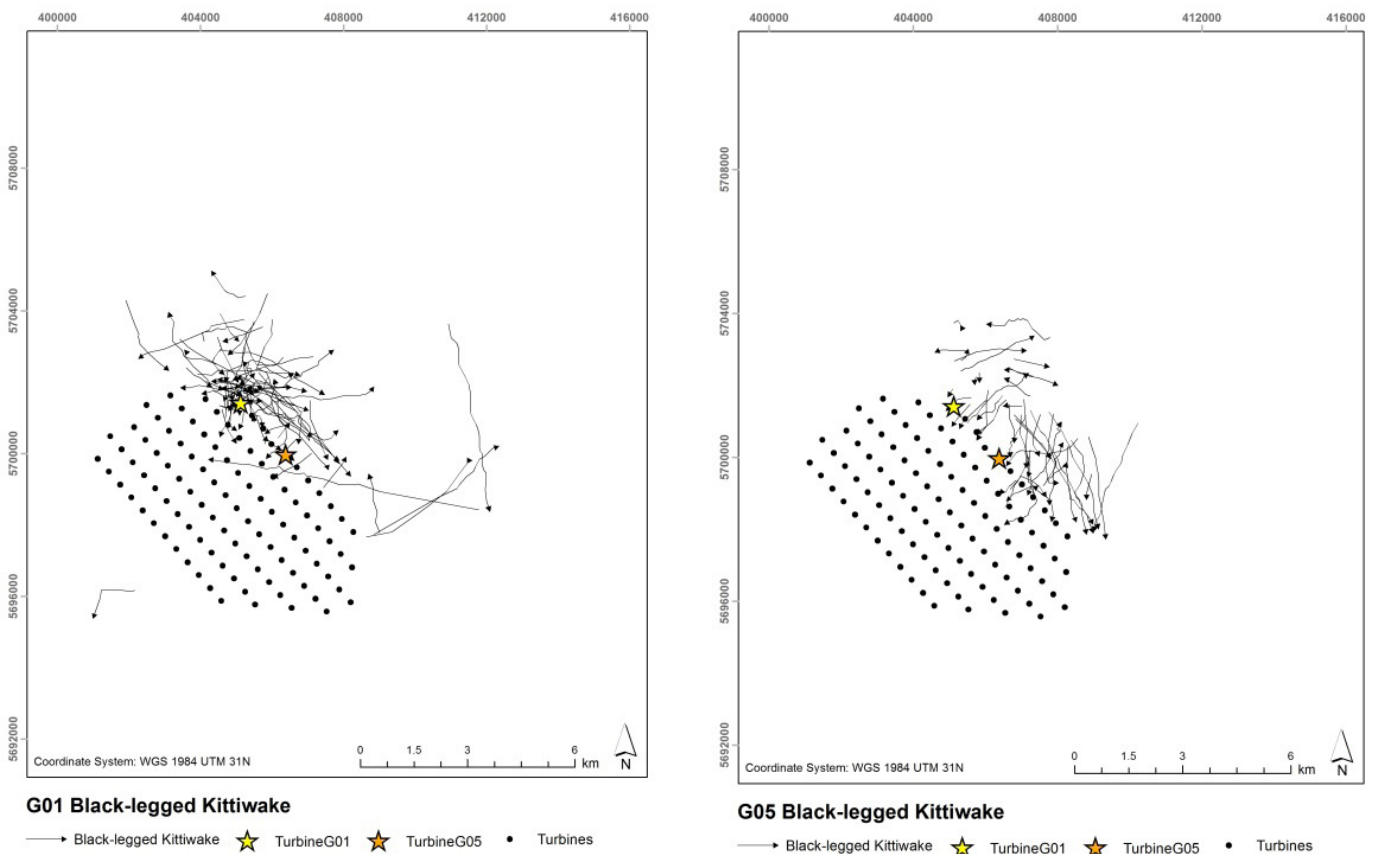
Figure 6.7. **Black-legged Kittiwake track density (calculated through track length per unit area method) based on all data collected using the SCANTER radar and LAWR radar from turbines G01 (left) and G05 (right) respectively.**
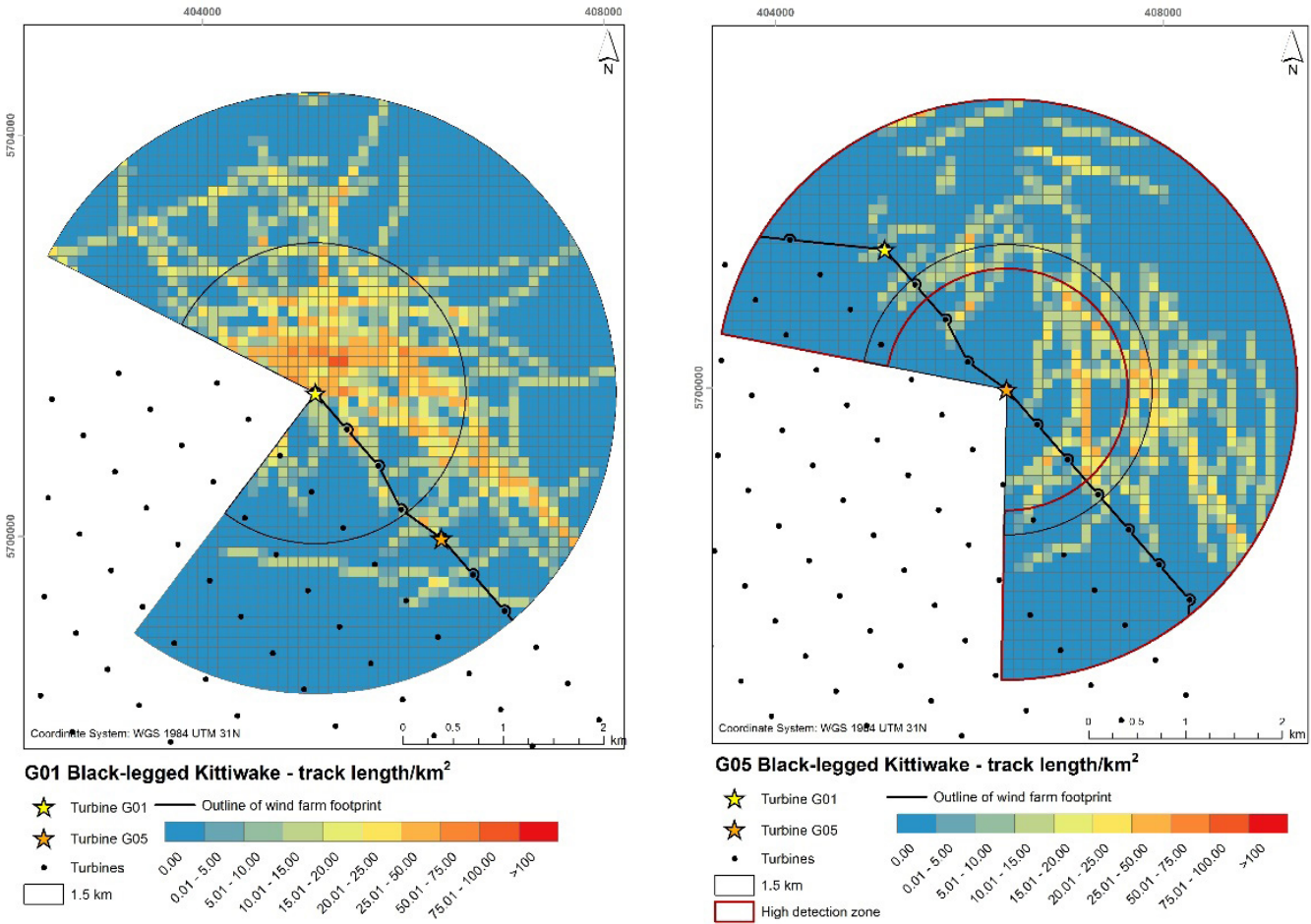
6.3.5. The mapped patterns of rangefinder track data were not very different from data collected by the SCANTER radar at G01, however, more rangefinder tracks were collected from turbine G05 (Figure 6.8).

6.3.6. The macro EAR estimated for Black-legged Kittiwake (Macro EAR = 0.566) is indicating an avoidance behaviour, although many studies are indicating no avoidance behaviour.

6.3.7. Regarding flight direction, the range of directions recorded from turbine G01 is presented in Figure 6.9, showing that mean flight direction were predominantly to the south – southeast.

6.3.8. Similarly, as illustrated in Figure 6.10, flight directions recorded from turbine G05 also showed some variation, although south – southeast direction were the predominant ones.

Figure 6.8. **Black-legged Kittiwake flight tracks (upper) collected using rangefinders from turbines G01 (left) and G05 (right) respectively, and estimated track density, calculated applying the track length per unit method (lower).**

G01 Black-legged Kittiwake rangefinder tracks

G05 Black-legged Kittiwake rangefinder tracks

G01 RF Black-legged Kittiwake - Track length/km^2

G05 RF Black-legged Kittiwake - Track length/km^2

INTERPRETATION OF BIRD BEHAVIOUR OBSERVED

Figure 6.9.   Flight directions for Black-legged Kittiwake recorded from turbine G01.

Mean direction of Kittiwake flight tracks in 500 m grid cells

G01 radar - Kittiwake

Mean direction of Kittiwake flight tracks in 500 m grid cells
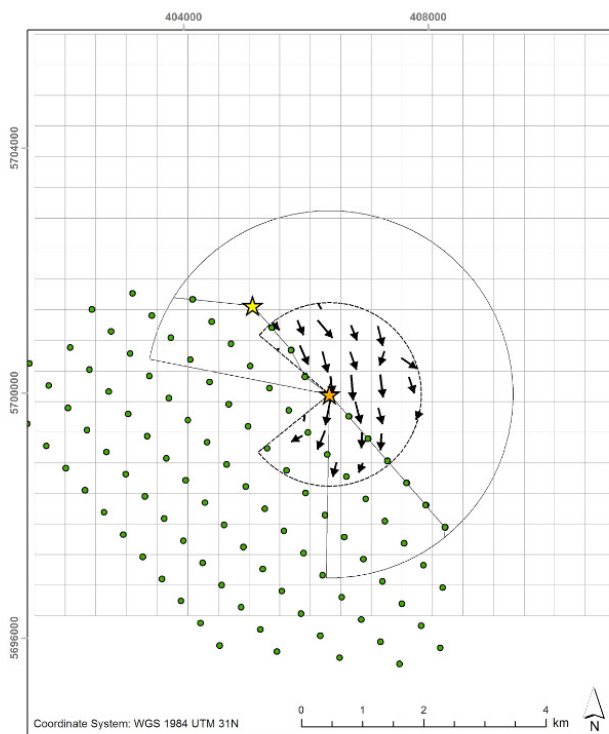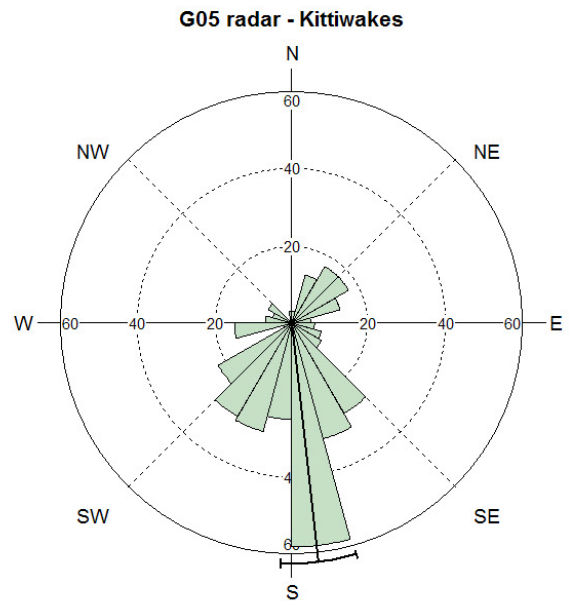
G01 rangefinder - Kittiwakes

INTERPRETATION OF BIRD BEHAVIOUR OBSERVED

Figure 6.10.   Flight directions for Black-legged Kittiwake recorded from turbine G05.

INTERPRETATION OF BIRD BEHAVIOUR OBSERVED

6.3.9. The median flight height recorded in this study was 33 m and therefore within rotor height for most turbine types. The proportion of birds flying at rotor height was found to be around 77% (see Section 5.6). The reported flight heights in literature is diverse and according to the review by Furness et al. (2013) varies in different studies between 0-38% at rotor height, which is lower than indicated by the current study. At the German Alpha Ventus offshore wind farm, Black-legged Kittiwakes were observed to prefer flight heights between 10 to 20 m (Mendel et al. 2014). Evidence from visual surveys in proposed development areas in the UK assessed flight height of 62,975 Kittiwakes suggesting that 15% (11.7-17.3% CI) of flight occurred at collision risk height (Johnston et al. 2014a,b). Other reports indicate this proportion varies between 4 – 18 %. In contrast, other radar studies show higher proportions, e.g. based on tracks of 2,459 birds, but excluding birds following fishing boats, estimated 38% at collision risk height (Krijgsveld et al. 2005), and 45% (sample size not stated but possibly including the previous data) (Krijgsveld et al. 2011).

6.3.10. GPS flight speed for Black-legged Kittiwake is reported by for example Kotzerka et al. (2010) and Elliot et al. (2014), 9.2 m/s and 10.6 m/s respectively. This is slightly higher than measured in the current study, 8.7 m/s (however with a large variation, see Section 5.5, Figure 5.10). This may be partly explained by foraging activity, often observed in videos recorded, with 4.2% of daylight videos showing Black-legged Kittiwakes foraging inside the wind farm.

6.3.11. At the meso scale, 0.6% of recorded seabirds displayed meso avoidance by adjusting vertically and fly below or above the RSZ, while the proportion including low-flying seabirds with no obvious vertical adjustment observed was 1.6%.

6.3.12. Of the birds observed entering the RSZ + 10 m buffer (n=299), 2.0% were identified as Black-legged Kittiwakes, and most of micro avoidance responses recorded for this species, four of these were crossings with adjustments.

6.4. LARGE GULLS

6.4.1. The observation of large gulls' response to offshore wind farms has been diverse, although in general, strong avoidance has not been reported from any site according to Krijgsveldt's review (2014). For instance, at OWEZ, large gulls seemed relatively indifferent to the presence of the offshore wind farm, with distribution mainly influenced by occurrence of fishing vessels (Krijgsveld et al. 2011; Hartman et al. 2012). Krijgsveld et al. 2005 showed that flight behaviour and abundance of gulls around the Egmond aan Zee wind farm were strongly associated with fishing vessels (70-80% of recorded birds). This was true for both smaller and larger species, although results suggested that larger gulls were more often associated with fishing vessels than smaller species.

6.4.2. Similarly, the relatively high degree of macro avoidance recorded for large gulls in this study (macro EAR ranging from 0.442 in Herring Gull to 0.619 in Lesser Black-backed Gul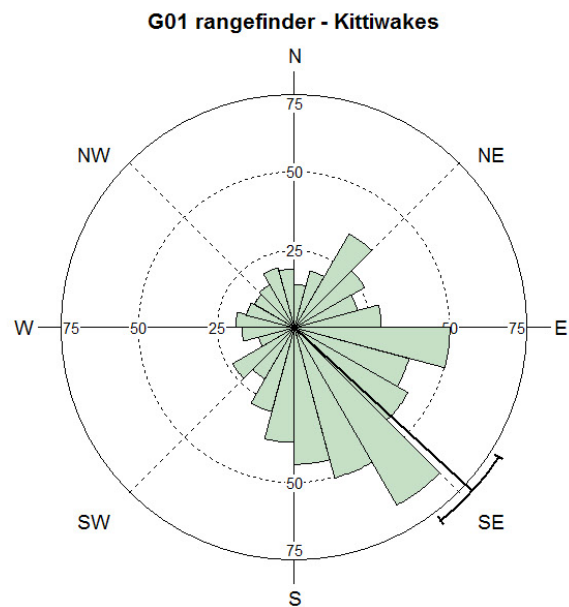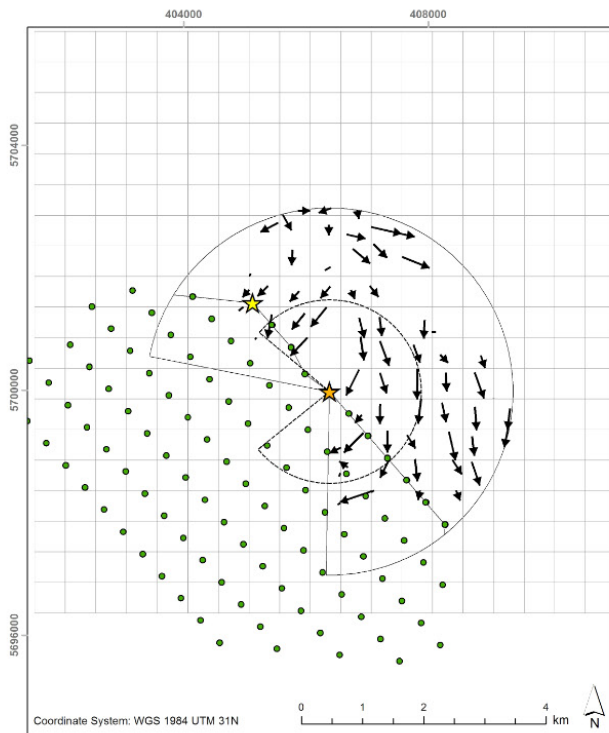l) needs to be interpreted with care, as local conditions have a strong influence on bird distribution and bird behaviour. For example, fishing vessels were at times observed by the Seabird Observers to be operating in close proximity to the wind farm i.e. within 3 km, which often attracted several tens of large gulls foraging on fishing vessel discards. Such foraging opportunities potentially resulted in the redistribution of large gulls such that a proportion originally inside the wind farm would aggregate in the short term around the fishing vessel outwith the wind farm. The influence of fishing activity on bird behaviour was not recorded systematically during fieldwork, and has not been analysed in relation to macro avoidance. Accordingly, whether the regular occurrence of fishing vessels outside wind farms is common to other sites should be considered when interpreting the study's data and application of results. It was also noted by the Seabird Observers that the transformer station inside the wind farm was a focal point of attraction for roosting large gulls.

6.4.3. As seen from the frequency distribution of sea states during which large gulls were recorded in the wind farm, these species were observed commonly in sea states 1 to 3 and less commonly in sea states 0 and sea states higher than 3 (Figure 3.3). Measurements of sea states in Thanet are not available, yet as seen in Appendix 4 wind speeds above 8 m/s were dominating during the non-breeding seasons which suggests that large gulls mainly entered the wind farm in relatively calm conditions.

a. Lesser Black-Backed Gull

6.4.4. The sample size for Lesser Black-backed Gull was the smallest of all target species, with a total of 325 tracks collected by the sensors located on the turbines G01 and G05, most tracks collected by the SCANTER radar on turbine G01.

6.4.5. The behavioural patterns observed from turbine G01 are similar when radar and rangefinder data are compared Figure 6.11, Figure 6.12 and Figure 6.13).

Figure 6.11. **Lesser Black-backed gull flight tracks collected using the SCANTER radar and LAWR radar from turbines G01 (left) and G05 (right) respectively.**
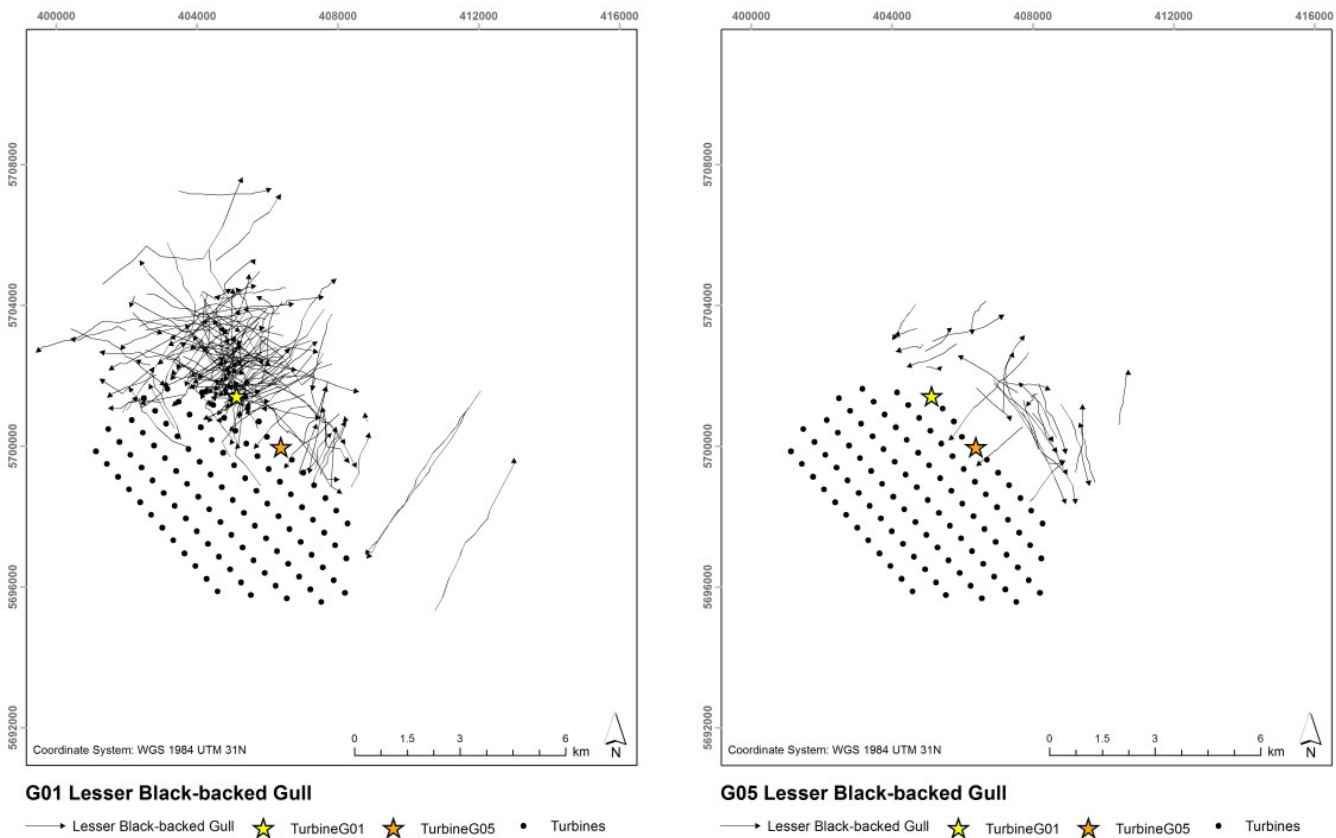
6.4.6. From turbine G05, there seems to be less avoidance (although it should be noted that sample size from this turbine is smaller), in comparison to data collected from turbine G01 by SCANTER, which is also indicated by the estimated mean track length per unit area. A change in behaviour between platforms could potentially also be due to for example feeding behaviour or distribution of fishing vessels.

6.4.7. The tracks recorded inside the wind farm from G01 were mostly recorded between the two outermost rows of turbines. The tracks recorded inside the wind farm recorded from turbine G05 were all perpendicular to the wind farm outline.
The distribution pattern observed by rangefinders is similar to that provided by the radar data, indicating avoidance and a peak density just outside the wind farm footprint (Figure 6.13).

INTERPRETATION OF BIRD BEHAVIOUR OBSERVED

Figure 6.12. Lesser Black-backed gull track density (calculated through track length per unit area method) based on data collected using the SCANTER radar and LAWR radar from turbines G01 (left) and G05 (right) respectively.

INTERPRETATION OF BIRD BEHAVIOUR OBSERVED

Figure 6.13. Lesser Black-backed gull flight tracks (upper) collected using rangefinders from turbines G01 (left) and G05 (right) respectively, and estimated track density, calculated applying the track length per unit method (lower)

INTERPRETATION OF BIRD BEHAVIOUR OBSERVED

6.4.8. Furness et al. (2013) indicate there is a large variation in defined percentage of Lesser Black-backed Gulls flying at rotor height, varying between 25.2 and 90% in different studies. For instance, 28.2% is reported by Johnston et al. (2014a, b), and the GPS study conducted by Ross-Smith et al. (2016) suggests lower proportions, showing that Lesser Black-backed Gulls tagged at Suffolk flew lower near shore than offshore, where 61.4% of birds were found flying below 20 m. At the German Alpha Ventus offshore wind farm, less than half of individual measurements for Lesser-black Backed Gull comprised heights above 30 m (Mendel et al. 2014). Higher proportions have, however, been reported by Krijgsveld et al. (2005), with 55% of Lesser Black-backed Gull flights detected by radar recorded to be at collision risk height (sample of 2470 observations). Krijgsveld et al. (2011) reported variable flight altitudes, with local foraging gulls flying at average altitudes of 50 m above sea level, or 20 m when foraging behind ships, and calculated that 60% of the birds were flying at collision risk height (no sample size reported).

6.4.9. In this study, Lesser Black-backed Gull was found to fly on average at rotor height, with a median flight height of 31 m, and 67% of individuals flying at rotor height, similar to some of the studies described above.

6.4.10. The GPS flight speed for Lesser-black Backed gull reported by Klaassen et al. (2012) was 10.7 m/s, similar to the speed measured in this study which was 10.1 m/s.

b. Great Black-Backed Gull

6.4.11. The sample size for Great Black-backed Gull was the largest among the large gull species; in total, 562 tracks were collected by the sensors located on the turbines G01 and G05.

6.4.12. As in the case of the other target species, there seem to be an aggregation of birds close to the wind farm.

6.4.13. Weak avoidance patterns are indicated by the SCANTER radar and rangefinder data collected from turbine G01, similar to the pattern generated by rangefinder tracks from G05. However, the LAWR radar data collected from turbine G05 produced different patterns, with reduced avoidance, although most of the tracks recorded inside the wind farm were located between the two outermost turbine rows (Figure 6.14 and Figure 6.15).

Figure 6.14.   Great Black-backed gull flight tracks collected using the SCANTER radar and LAWR radar from turbines G01 (left) and G05 (right) respectively.
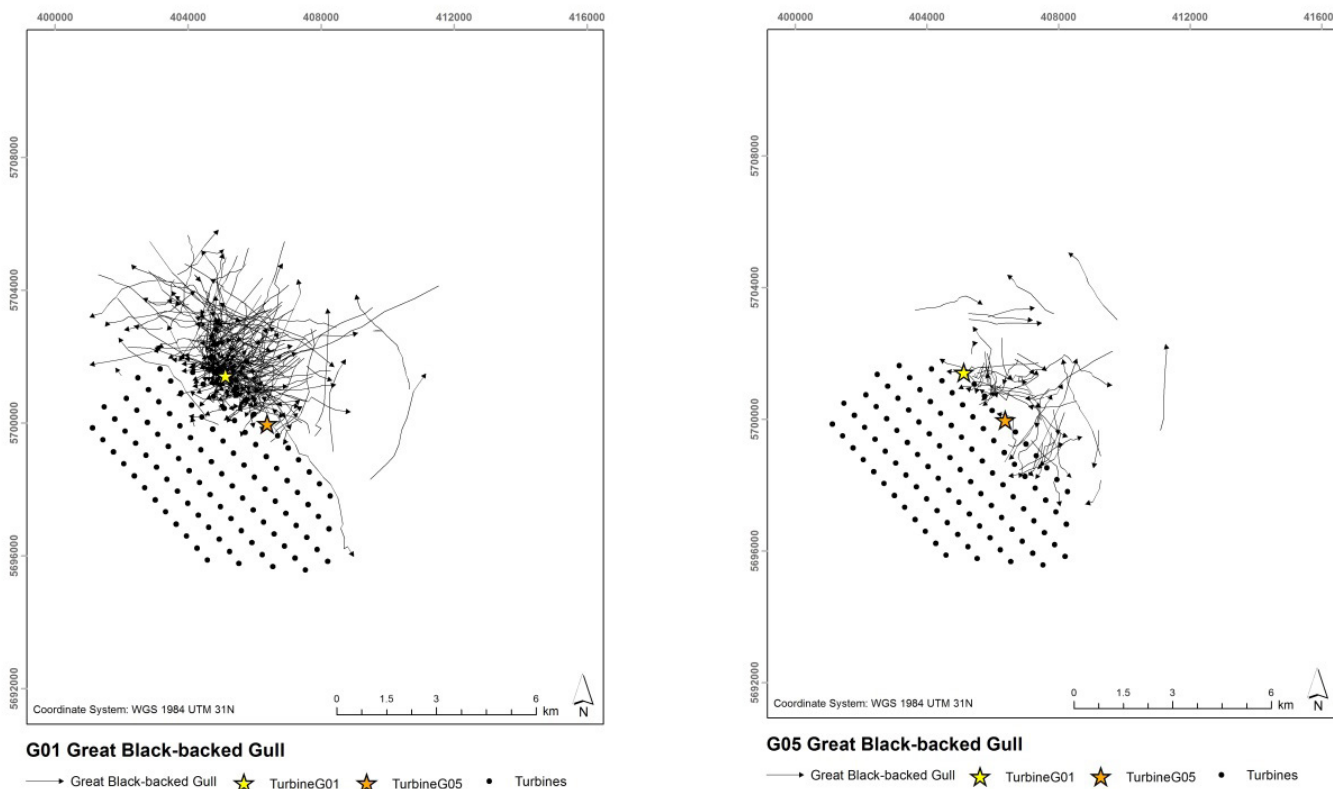
Figure 6.15.   Great Black-backed gull track density (calculated through track length per unit area method) based on data collected using the SCANTER radar and LAWR radar from turbines G01 (left) and G05 (right) respectively.

INTERPRETATION OF BIRD BEHAVIOUR OBSERVED
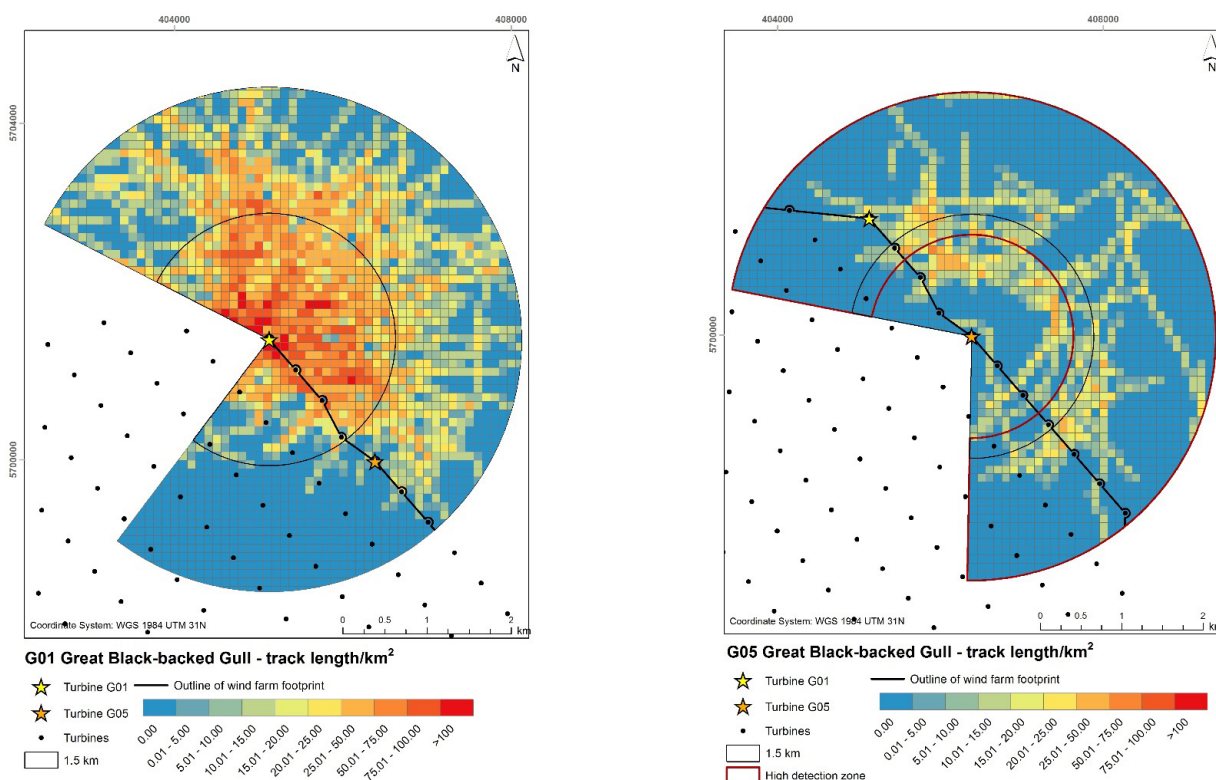
Figure 6.16.   Great Black-backed gull flight tracks (upper) collected using rangefinders from turbines G01 (left) and G05 (right) respectively, and estimated track density, calculated applying the track length per unit method (lower)

INTERPRETATION OF BIRD BEHAVIOUR OBSERVED
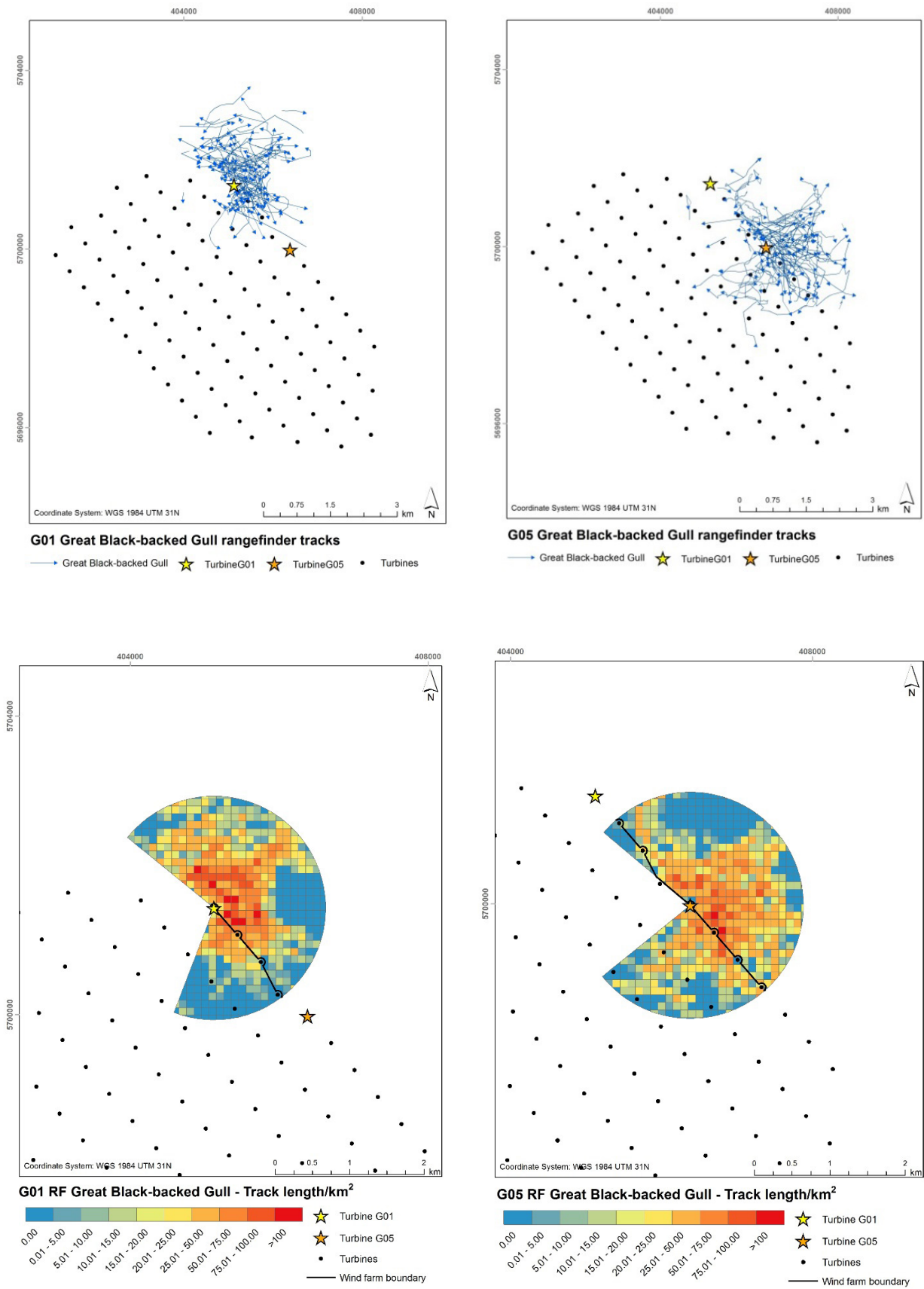
6.4.14. In the review made by Furness (2016), the reported proportion of birds flying at rotor height varied between 6-57%, varying between survey methods. For instance, evidence from visual surveys in proposed development areas in the UK assessed flight height of 8,911 Great Black-backed Gulls suggested that 36.5% (95% CI 20.0-52.0) of flight occurred at collision risk height (Johnston et al. 2014a, b). Boat surveys suggested values between 23% - 56%; while the radar study by Krijgsveld et al. (2005) reported 57% of Lesser Black-backed gull flights detected by radar to be at collision risk height (sample of 143 observations, excluding birds following fishing boats which tended to be flying low). Krijgsveld et al. (2011) reported 60% at collision risk height from further radar studies at the same site but with no sample size reported.

6.4.15. Great Black-backed Gull had the highest recorded median flight height in this study, 40 m, which is in line with the height mean flight height recorded for large gulls by Krijgsveld et al (2005), 36 m, but higher than many other studies. The proportion of birds flying at rotor height reached 81%.

6.4.16. Flight speed based on GPS measurements (Gyimesi et al. 2017) from two different studies was 12.5 m/s and 10.7 while the flight speed recorded in the current study was 9.8 m/s.

c. Herring Gull

6.4.17. In total, 483 Herring Gull tracks were captured by the sensors located on turbines G01 and G05. Similar numbers of tracks were captured by the SCANTER radar (G01) and two rangefinders (G01 and G05), whereas few were captured by the LAWR radar (turbine G05). This was a pattern was reflected across the four target species of gull.

6.4.18. The pattern observed for Herring Gull tracks generated by the SCANTER radar indicates an avoidance (Figure 6.17, Figure 6.18) while the rangefinder data from both turbines G01 and G05 indicate limited avoidance (Figure 6.19). However, in the latter case, most of the gulls inside the wind farm were recorded between the two outermost turbine rows, i.e. Herring Gulls did not seem to penetrate deep into the wind farm. At the same time, it should be noted that only few Herring Gulls were tracked by the LAWR radar from turbine G05. All tracks entering the wind farm were all perpendicular to the wind farm outline.

6.4.19. In contrast with the avoidance behaviour interpreted at Thanet, Vanermen et al. (2014) reported significant attraction of Herring Gull towards the Bligh Bank wind farm.

NIRAS DHI CARBON TRUST

Figure 6.17. **Herring gull flight tracks collected using the SCANTER radar and LAWR radar from turbines G01 (left) and G05 (right) respectively.**
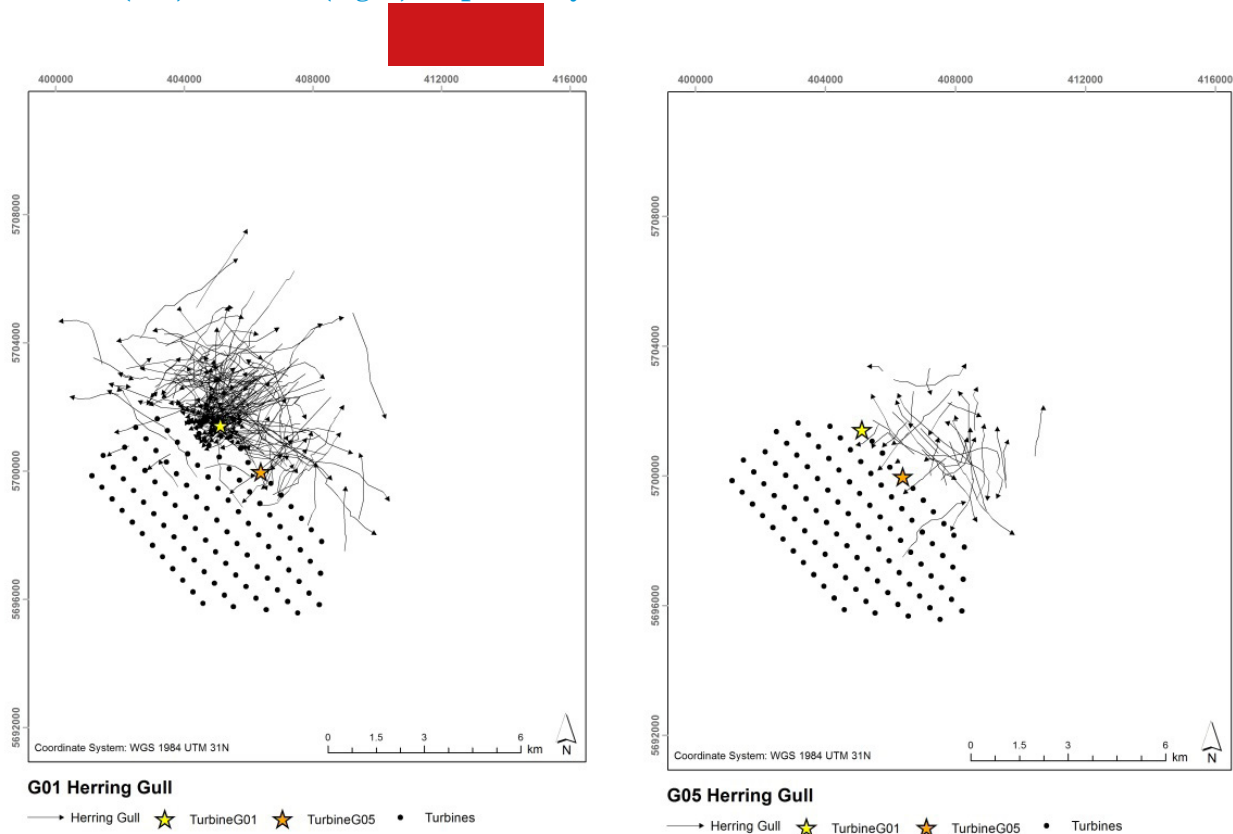
Figure 6.18. **Herring gull track density (calculated through track length per unit area method) based on data collected using the SCANTER radar and LAWR radar from turbines G01 (left) and G05 (right) respectively.**
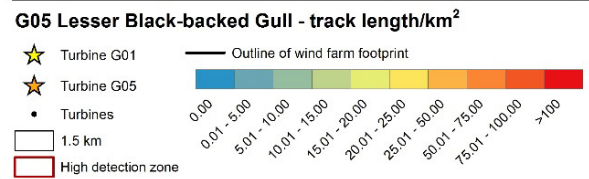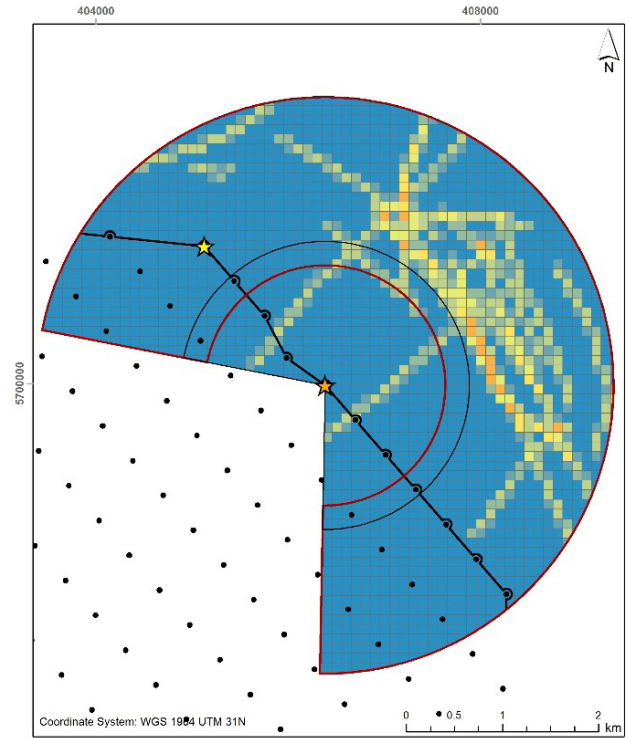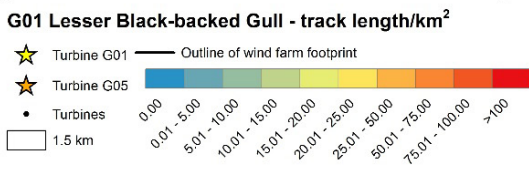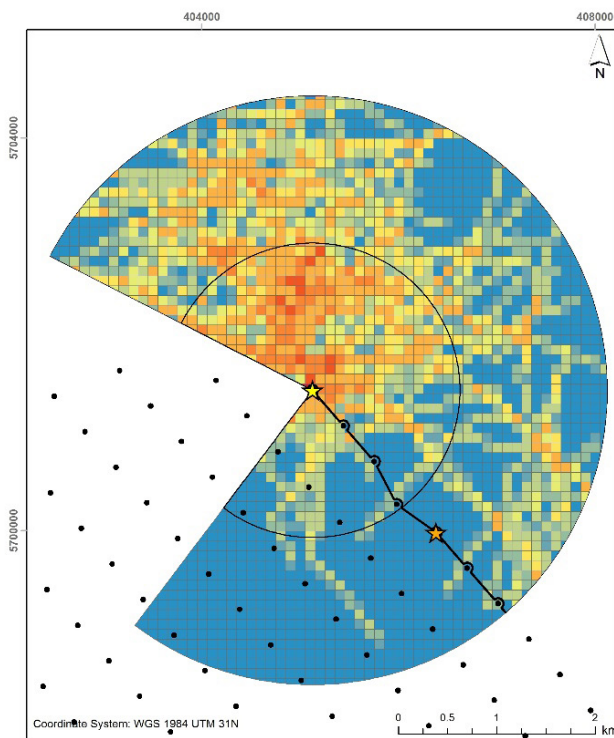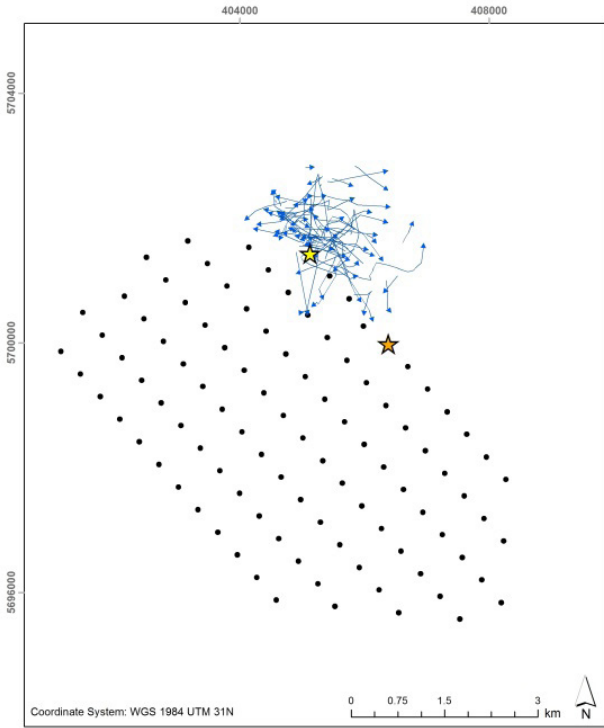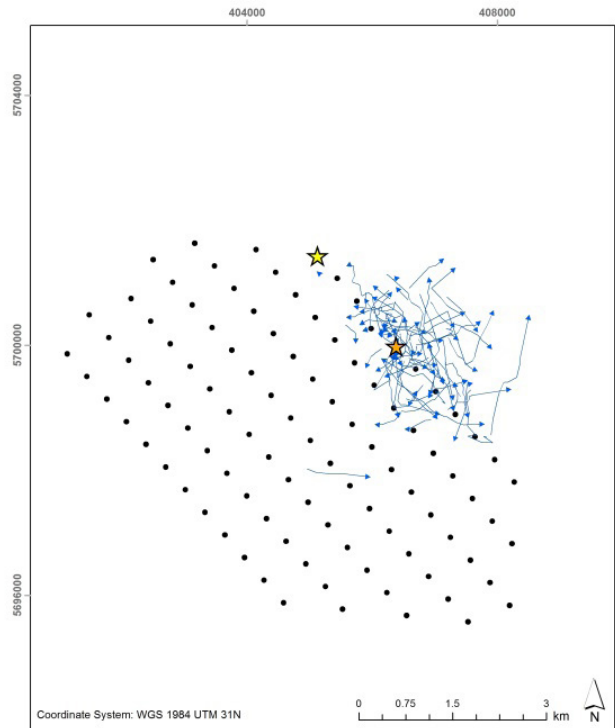
INTERPRETATION OF BIRD BEHAVIOUR OBSERVED
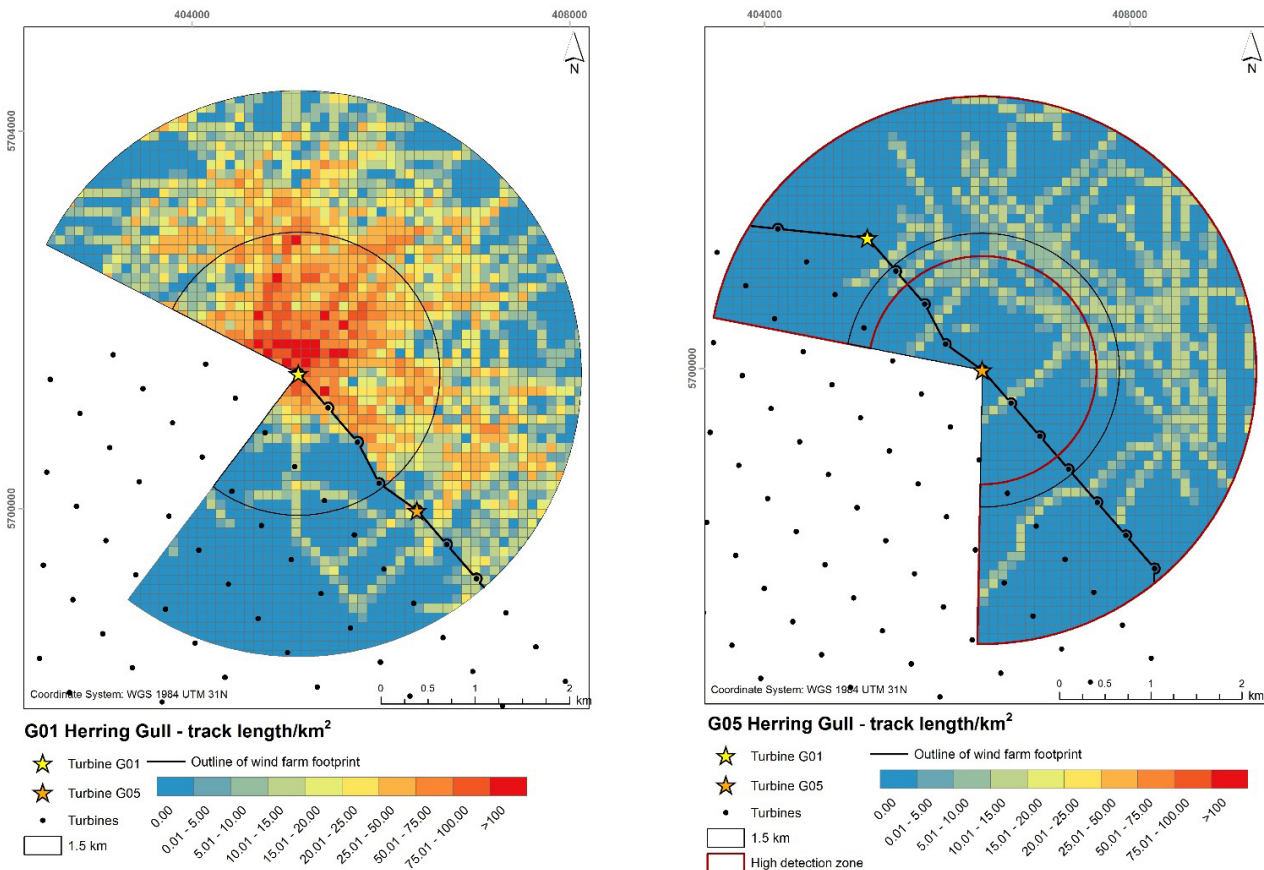
Figure 6.19. Herring gull flight tracks (upper) collected using rangefinders from turbines G01 (left) and G05 (right) respectively, and estimated track density, calculated applying the track length per unit method (lower).
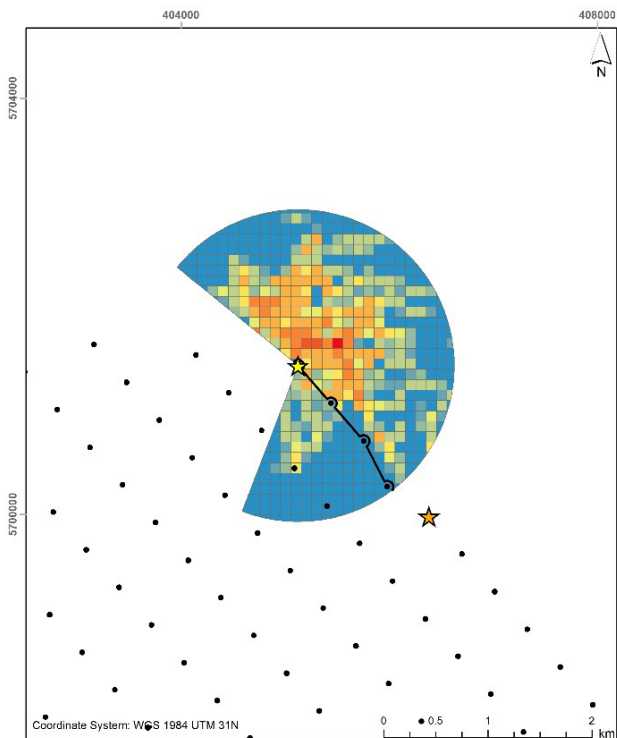

INTERPRETATION OF BIRD BEHAVIOUR OBSERVED
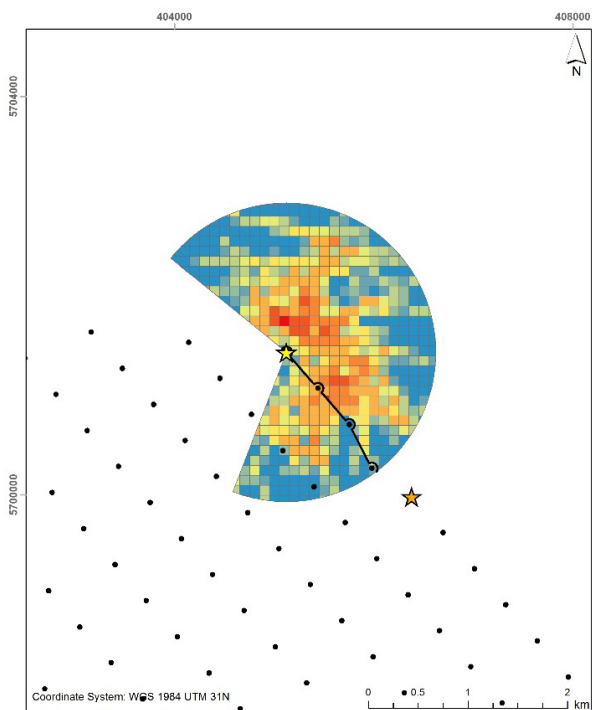
6.4.20. The median flight track recorded for Herring Gull was 36 m, which is the same as the mean value reported by Krijgsveld et al. (2005) for all gull species combined, and values reported at the German Alpha Ventus offshore wind farm, where large gull species were observed to fly higher than average, with median flight heights for herring gull between 30 – 35 m (Mendel et al. 2014). Approximately 77% of birds were found flying at rotor height.

6.4.21. The recoded flight speed was 9.7 m/s and slightly lower as the speed reported by Pennycuick (1987), which was 11.3 m/s.

In relation to flight directions, large gull observations showed a high level of variability, as illustrated in Figure 6.20.

Figure 6.20.   Recorded flight directions for large gulls, number of samples (x and y axis) per direction. Mean value is noted with a black line, accompanied by associated confidence limits.

INTERPRETATION OF BIRD BEHAVIOUR OBSERVED
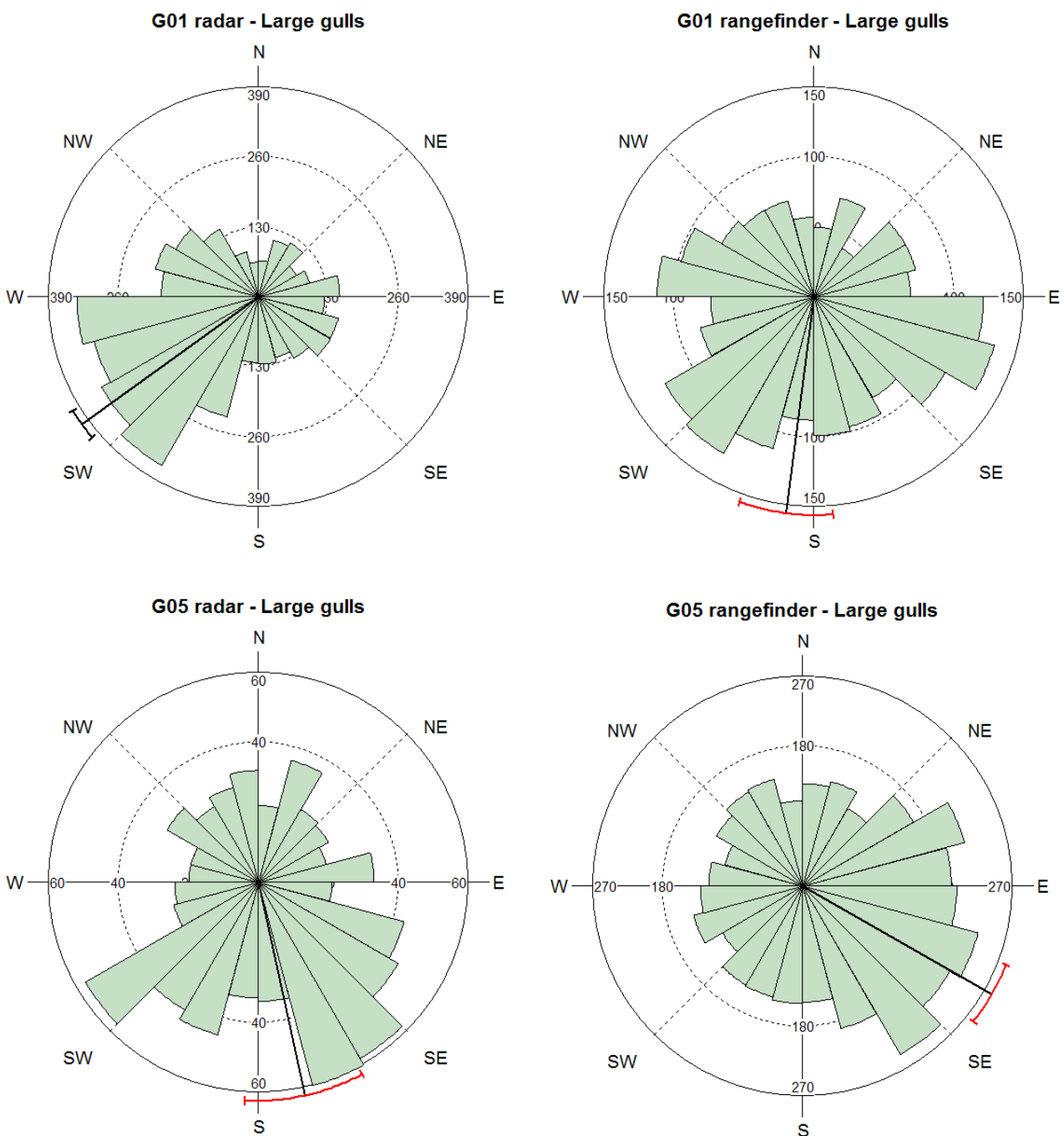
6.4.22. At the meso scale, 0.6% of recorded seabirds displayed meso avoidance by adjusting vertically and fly below or above the RSZ, while the proportion including low-flying seabirds with no obvious vertical adjustment observed was 1.6%. A 1.5% of daylight videos showed large gulls foraging inside the wind farm, and a significant proportion (n=383) of daylight videos showed large gulls in association the turbines and transformer platform.

6.4.23. Of the birds observed entering the RSZ + 10 m buffer (n=299), 38.7% were identified as large gulls, and most of micro avoidance responses recorded for these species (95.7%) were crossings with adjustments, mainly birds flying along the plane of the spinning rotor (Table 5.8). According to Cook et al. (2014) previously 3000 hours of effort at 16 individual turbines had only resulted in 45 records of birds within the close vicinity of the rotor swept zone, 42 of these was defined as showing some sort of avoidance behaviour.

6.5. COLLISIONS

6.5.1. An overview of the recorded collision events during the 20 months of camera-monitoring in Thanet is provided in Table 6.1. Further details of these events are provided below.

Table 6.1.   Overview of collision events recorded by TADS cameras between November 2014 and June 2016.

Species	Date	Camera platform	Turbine at which collision was recorded	Angle of approach to rotor plane	Altitude	Position on blade	Wind speed (m/s)	Sea state	Visibility (km)
Black-legged Kittiwake (adult)	1 Nov 2014	F04	F03	Perpendicular	50 m	Central part	7	1	10
Lesser/ Great Black-backed Gull (adult)	24 Nov 2014	D05	D06	Oblique	80 m	Central part	5	1	10
Unidentified gull sp.	28 Nov 2014	D05	D04	Oblique	120 m	Tip of blade	8	2	2
Large gull sp.	21 Aug 2015	D05	D06	Oblique	70 m	Tip of blade	6	2	5
Large gull sp.	12 Dec 2015	D05	D06	Oblique	80 m	Central part	8	2	5
Unidentified gull sp.	10 Feb 2016	D05	D06	Oblique	30 m	Tip of blade	8	2	5

- Collision of an adult Black-legged Kittiwake at F04 on the 1 November 2014 was observed to occur after the bird was hovering and trying to adjust the flight path in front of the RSZ.

- Collision of a Lesser or Great Black-backed Gull at D05 on the 24 November 2014 was observed following repeated to-and-from movements between two RSZs.

- Collision recording of an unidentified gull at D05 on 28 November 2014 showed the bird dropping from top position to the sea.

- Collision recording of an unidentified large gull at D05 on 12 December 2015 showed the bird dropping from central position to the sea.

- Collision recording of an unidentified gull at D05 on 10 February 2016 showed the bird dropping from lower part of rotor to the sea.

6.5.2. Given the lack of evidence on offshore collisions from previous studies, video data collected by the study provide a useful source of evidence on bird behaviour around RSZ and collision events.

6.6. COMPARISON BETWEEN DAY AND NIGHT ACTIVITY/ BEHAVIOUR

6.6.1. As presented in Table 6.2, the comparison of bird activity during the day and night indicated overall low levels of nocturnal activity with some variation. The definition night time is defined in paragraph4.6.2 .

6.6.2. The sample size of night videos is, however, relatively low, which most likely is a consequence of the low nocturnal activity.

Table 6.2. **Comparison of daylight and night activity based on the total number of videos collected during selected dates.**

Date	Daylight videos with birds	Night videos with birds	%	Date	Daylight videos with birds	Night videos with birds	%
Turbine D05				Turbine F04			
Nov 2014**	517	22	4%	Nov 2014**	202	10	5%
Jan 2015*	40	0	0%	Dec 2014**	518	3	1%
Apr 2015*	59	0	0%	Feb 2015*	64	0	0%
Oct 2015*	43	4	9%	Mar 2015*	44	1	2%
Nov 2015**	133	0	0%	Apr 2015**	120	2	2%
Dec 2015**	715	6	1%	May 2015*	17	0	0%
Jan 2016*	66	1	1%	Oct 2015*	5	0	0%
Feb 2016**	139	3	2%	Nov 2015*	29	1	3%
Mar 2016*	122	7	8%	Dec 2015**	300	13	4%
				Jan 2016*	6	0	0%
				Feb 2016**	471	3	1%
				Mar 2016*	60	0	0%
Total	**1,834**	**41**	**2.2%**	**Total**	**1,836**	**33**	**1.8%**
*based on videos collected from < 5 dates **based on videos collected from ≥ 5 dates							

INTERPRETATION OF BIRD BEHAVIOUR OBSERVED

NIRAS DHI CARBON TRUST

6.6.3. The average proportion of nocturnal activity indicates that bird activity during night is lower than 3%, although given the potential limitations associated with the data should be considered as anecdotal evidence. The GPS study conducted by Ross-Smith et al. (2016) showed that there was low flying activity recorded at night, suggesting a small risk of interaction with offshore developments after dark. In addition, in this study, Lesser Black-backed Gulls were observed flying lower at night than during the day.

6.6.4. Tagging studies of Northern Gannet (Garthe et al. 1999, 2012, Hamer et al. 2000, 2007), Lesser Black-backed Gull (Klaassen et al. 2012et al.) and Black-legged Kittiwake (Hamer et al. 1993, Daunt et al. 2002, Kotzerka et al. 2010, Orben et al. 2015) also corroborate low nocturnal activity by seabirds. However, the body of evidence mainly used to inform CRM is the expert view of Hüppop (2004) on levels of nocturnal flight activity for a range of marine bird species, varying between 20 – 50%, which seems conservative given the evidence collected in this and other studies (see Section 7.5).

6.6.5. Although coding bird behaviour in night videos was constrained by the quality of the image and distance of birds, there were no seabirds observed inside the RSZ, and most of the avoidance responses recorded were seabirds flying between rotors, Table 6.3.

Table 6.3.   Comparison of behaviour coded in daylight and night videos respectively

Video type		Meso avoidance	
	Files between turbines rows	Files below rotor	Files above rotor
Daylight video	7023	960	44
Night video	69	5	-

6.6.6. The limited level of flight activity at night was further indicated by the fact that 26% of night time videos (n=26) were recordings of sitting seabirds.

NIRAS   DHI   CARBON TRUST

7 INFORMING COLLISION RISK ASSESSMENT

7.1. INTRODUCTION

7.1.1.   Consenting decisions on offshore wind developments rely on evidence provided by environmental statements, which are usually required to include a quantitative estimate of collision risk for all bird species present on the site, and assess the significance of that collision risk on the respective bird populations (Band 2012). In this context, collision risk assessment is undertaken by the use of Collision Risk Modelling (CRM), which provides an estimate of the potential number of bird collisions likely to occur at a proposed wind farm.

7.1.2.   This section provides an overview on the use of collision risk models and application of avoidance rates, presenting recommendations on the use of evidence derived by this study.

7.2. COLLISION RISK MODELLING

7.2.1.   There are a variety of different collision risk models available (Masden and Cook 2016). However, particularly in the UK, and more widely in Europe, the most commonly applied model is the Band model (Band 2012)[8], which was specifically designed for onshore projects and the survey data that are typically acquired in these locations. Offshore, many seabirds fly at relatively low heights over the sea surface. The height distribution is species-specific and may depend on species ecology and the site.

7.2.2.   There are two versions of this model, "basic" and "extended", the latter taking more account of the flight height distribution of birds and the differential risk to those birds across the rotor-swept zone (RSZ).

7.2.3.   As illustrated in Figure 7.1, both versions of the model (basic / extended) calculate a predicted collision rate based on data relevant to the wind farm design and productivity, and information about birds at the proposed wind farm site. Band first estimates the collision risk in the absence of avoidance behaviour. An avoidance rate is then applied to take account of the likely degree of successful avoidance (see Section 7.3). All the parameters informing the model are referred to as model "input parameters".

---

[8] The "Band model" was originally developed for onshore wind turbines and promoted as guidance by Scottish Natural Heritage, has undergone several iterations with the most recent associated with the Strategic Ornithological Support Services (SOSS) (Band 2012).

NIRAS DHI CARBON TRUST

Figure 7.1.   The collision risk model (Band 2012) and its key input parameters
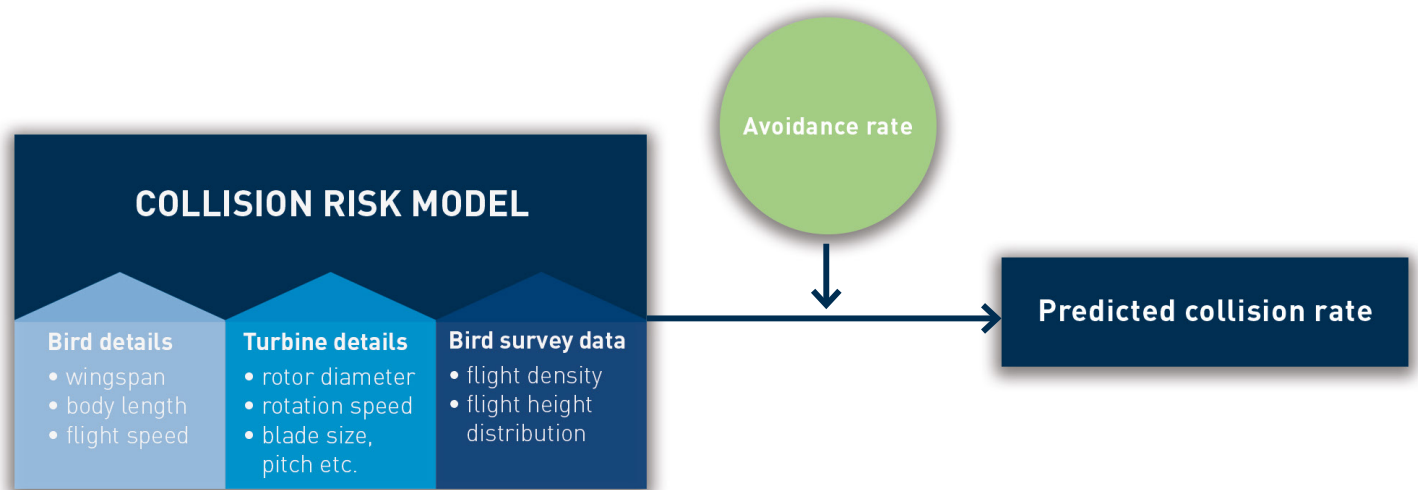
7.2.4.   Calculating a collision mortality rate involves the following stages (Band 2012):

Stage A: Assemble data on the **number of flights which**, in the absence of birds being displaced, taking other avoiding action or being attracted to the wind farm, are potentially at risk from wind farm turbines;

Stage B: Use that flight activity data to estimate the **potential number of birds flying through the rotor-swept zone** throughout a given time unit (bird flux rate);

Stage C: Calculate the **probability of a bird being hit by the wind farm rotor blades** given that it passes through the rotor-swept zone. This is based on the technical specifications of the turbines (breadth and pitch of turbine blades and rotation speed) and the morphology of the bird (e.g. wing aspect), speed and flight behaviour (flapping or soaring of the bird).

Stage D: Multiply these to yield the **potential collision mortality rate** for the bird species in question, allowing for the proportion of time that turbines are not operational, assuming current bird use of the site and that no avoiding action is taken;

Stage E: Allow for the proportion of birds likely to avoid the wind farm or its turbines, either because they have been displaced from the site or because they take evasive action, multiplying the potential collision mortality rate by an avoidance rate. Band (2012) recommends using an appropriate range of avoidance rates to cover any uncertainties involved in their estimation.

Stage F: Express the variability (inherent heterogeneity of the environment) or uncertainty (lack of data or incomplete knowledge) surrounding such a collision risk estimate. The main sources of uncertainty are listed in Table 7.1, related to flight activity, model simplifications and turbine design, which need to be separately identified. In addition, collision risk estimates should be presented based on a range of assumptions on avoidance. Calculated risks should accordingly be held as an indication of the risk rather than an exact figure.

Table 7.1.   Main sources of uncertainty in collision risk estimates using the Band model. Source: Band (2012), Masden and Cook (2016).

Uncertainty related to flight activity
• survey data is sampled, often both in time and space, and usually exhibits a high degree of variability. Mean estimates can only be representative of flight activity   • survey data is unavailable for certain conditions, including night time and storm conditions   • natural variability in bird populations, over time and space, for ecological reasons   • flight height information may be subject to observer bias
Uncertainty related to model simplifications (see Subsection c. below)
• the collision risk model uses a simplified geometry for turbine blades and bird shape   • it only considers flights parallel to the wind, i.e. perpendicular to rotation of the turbine   • it does not include any risk of collision with turbine towers   • bird parameters (length, wingspan, flight speed) have a range, they are not fixed   • bird speed is not a constant but is dependent on wind speed as well as other factors
Uncertainty related to the turbine design
• details of blade dimension and pitch may be unavailable at the time of making the estimate   • turbines deployed may differ from those used in the collision risk analysis
Uncertainty related to bird behaviour
• insufficient knowledge about bird displacement and attraction effects   • there is limited firm information on bird avoidance behaviour at sea

7.2.5.   The two versions of the Band model provide four different options for calculating collision risk (of which options 1, 2 and 3 are the most frequently used).

a. Basic model

7.2.6.   The basic version of the model (Band 2000; Band, Madders and Whitfield 2007) considers the collision risk to birds flying at risk height to be uniform within the RSZ of turbines:

Option 1 - Uses the proportion of birds at risk height as derived from pre-construction site surveys.

Option 2 - Uses the proportion of birds at risk height as derived from a generic flight height distribution provided by data collected across multiple sites.

7.2.7.   In practice, birds are unlikely to be evenly distributed across the RSZ of a turbine (Johnston et al. 2014a), as the flight height of seabirds are often skewed towards lower heights. There are three consequences of a skewed distribution of flights with height:

- The proportion of birds flying at risk height decreases as the height above sea level of the rotor's lower blade tip is increased for the same rotor;

- Less birds will collide with the rotor than if the birds were evenly distributed across the rotor swept area, as birds will be distributed towards the bottom of the circle described by the rotor (i.e. rotor swept area) where the risk of collision is less than what it is closer to the rotor hub (centre);

- The collision risk for birds passing through the lower parts of a rotor is less than the average collision risk for the whole rotor.

b. Extended model

7.2.8. The extended version of the model (Band 2012) is built on the basic model, and makes use, where available, of data on the distribution of bird heights; in particular to enable use of the data on flight heights of birds at sea compiled for SOSS (Strategic Ornithological Support Services for the UK offshore wind industry) by Cook et al. (2012). It combines Stages B, C and D described above, merged in a single calculation.

Option 3 – Uses a generic flight height distribution to estimate collision risk at different points within the turbines' RSZ. As birds are typically clustered to the lower edges of the RSZ (Johnston et al. 2014a), option 3 often results in lower estimates of collision rates.

Option 4 – Uses flight height distribution generated from site surveys.

7.2.9. Although the extended model is believed to reduce the uncertainty associated with flight heights (Table 7.1), Band (2012) further recommends allowing ±20% error for these.

c. Model update to incorporate variability and uncertainty

7.2.10. Masden (2015) reflects on the estimation of model uncertainty and application to collision risk estimates (Stage F), considering that the approach is relatively simplistic, as it combines different sources of variability / uncertainty, which can only be applied when these sources are independent of one another. In addition, Stage F is not integrated into the model itself but applied post hoc.

7.2.11. In practice, the application of stage F has been observed to be rather limited, resulting in CRM rarely stating the error associated to collision estimates, and therefore failing to represent the complexity of the situation (Masden 2015).

7.2.12. Given that the benefit of incorporating variability / uncertainty into the modelling process has been considered beneficial, Masden (2015) proposed a model update to incorporate these using a simulation approach, which would in principle allow for a better understanding of uncertainty associated with predicted collisions and providing confidence limits. The model has not yet been validated, and may be further progressed in the future.

d. Limitations and assumptions

7.2.13. CRMs have a number of limitations that are important to recognise in order to ensure that collision risk estimates are used appropriately. In relation to the Band model, the following have been identified by Masden and Cook (2016):

Correlation between collision risk and abundance of birds. The Band model, as well as other CRMs, assume a linear relationship between collision risk and bird abundance. However, there are factors not captured by the Band models like species-specific behaviour, turbine layout and wind conditions which may play an important role in determining the average bird flight speed and hence flux of birds in a wind farm (de Lucas et al. 2008).

Collision probability. The probability for a bird to collide while crossing the rotor-swept zone (P_{coll}) is estimated by combining the bird's flight speed, morphology and measurements of the rotation speed and rotor blades (Band 2012). The probability of collision estimated by the Band model for seabirds typically ranges between 5% and 15%. Perpendicular crossing of the spinning rotor by target species has been observed 15 times during this study (see Section 5.4), and in six of these events the bird collided. This means that the probability of colliding while crossing the rotor-blades is likely to be higher than assumed. Reasons for this might be that the Band model assumes birds to always fly in a perpendicular direction to the rotor (Band 2012), and assumes that birds cross the rotor at mean instantaneous flight speed.

Correlation between the predicted number of collisions and the bird flux rate. The Band model assumes a constant flux of birds through the wind farm, often based on pre-construction densities, and assuming mean flight speeds through the wind farm as linear flight patterns. If a large scale displacement occurs after construction or population sizes changes due to other reasons, the pre-construction density might be unrealistically high (or low) in comparison to that experienced in the wind farm after construction.

Linear flight pattern at a fixed speed in a fixed direction. In order to calculate the bird flux rate, the band model uses linear flight patterns at fixed speeds and directions, determined by different studies undertaken outside wind farms (e.g. Alerstam et al. 2007). This assumption is considered simplistic and unrealistic as shown by the study's data. Table 7.2 shows the difference between average flight speeds calculated from single segments and entire tracks (tracks with more than 5 nodes) of the ORJIP rangefinder track data collected at Thanet both inside and outside the wind farm. The comparison shows that seabirds do not fly in a straight line and therefore spend a longer time inside the wind farm than would be the case if bird flights would be straight, meaning that the flux rate[9] is likely to be lower than assumed by the Band model, which would result in a lower predicted collision rate. Appendix 10 presents a sensitivity test on how the flux factor in the Band model changes when the flight speed and pre-construction densities are altered. 7.3. Avoidance

Table 7.2.   Species-specific mean flight speeds (m/s) measured from single rangefinder segments and mean track speeds (m/s) measured over entire rangefinder tracks in Thanet (SD is shown in brackets).

	Northern Gannet	Black-legged Kittiwake	Large gulls
Flight speed	13.33 (4.24)	8.71 (3.16)	9.80 (3.63)
Track speed	11.78 (4.80)	6.22 (3.40)	7.95 (3.92)

7.3. AVOIDANCE

7.3.1. A key assumption in the model is that birds do not avoid wind turbines, leading to a significant over-estimate of the likely collision rate. It is currently considered appropriate to assume that 2%, or fewer, of the collisions predicted by the model are likely to occur in practice. In order to understand how bird avoidance behaviour is accounted for in CRM, it is necessary to make a distinction between avoidance behaviour[10] and avoidance rates:

---

[9] In the current version of the Band model the flux is determined from two parameters provided by the user; the density and the speed. As a consequence, with a lower speed due to a longer residence time in the wind farm the flux rate will descend.

[10] The introduction of offshore wind farms can also result in the attraction of birds to the site, defined as an increase in numbers of birds within the wind farm area post-construction and can arise though several means: turbines acting as a resting platform, providing feeding opportunities through changes in local hydrography, seabed morphology or by acting as an artificial reef.

NIRAS DHI CARBON TRUST

a. Avoidance behaviour

7.3.2. Avoidance behaviour can be defined as any action taken by a bird, when close to an operational wind farm, which prevents collision (SNH 2010). Such action may be taken early enough to avoid entering into the wind farm (macro avoidance), or taken within the wind farm, avoiding the RSZ (meso avoidance) or individual blades (micro avoidance).

7.3.3. At the same time, behavioural displacement operates at a different level, with the introduction of the wind farm altering the birds' habitat use, e.g. used for feeding or resting due to the presence of a wind farm. This may be manifested as a reduction in the number of birds flying into the area of the wind farm to look for food however this does not necessarily mean that birds will no longer enter the wind farm (SNH 2010).

b. Avoidance rates

7.3.4. Avoidance rates are applied to take account of the fact that many birds may either avoid the wind farm entirely as a consequence of being displaced, or responding with some form of avoidance behaviour, as described above (SNH 2010). They are expressed as a fraction, and are typically high, in the order of 0.98 (e.g. Cook et al. 2015). Avoidance rates can be determined in two different ways:

Option A - Using observed collision rates - Derived by comparing observed collision rates to the number of collisions that would be expected in the absence of avoidance behaviour, considering all bird movements within the perimeter of the wind farm. Band (2012) provides a method for their calculation, recommending the use of the same input parameters used to calculate the collision estimates:

$$AR = 1 - (C_{obs}/C_{pred})$$

$$C_{pred} = (Flux\ rate * P_{coll}) + error$$

Where:

*C$_{pred}$ - predicted number of collisions in the absence of avoidance action
*C$_{obs}$ - observed number of collisions
*Flux rate - total number of birds passing through the RSZ
*P$_{coll}$ - probability of a bird colliding with a turbine, specific to the morphology and speed of bird species and design of turbines (Cook et al. 2011)

7.3.5. Given that avoidance rates calculated using this approach use the model outputs (i.e. Cpred) in addition to accounting for avoidance behaviour, these avoidance rates include the inherent uncertainty and variability associated with the model (see Section 7.2, Table 7.1), and is specific to the specific model parameters used. As a consequence, avoidance rates calculated following this approach may, more accurately, be thought of as correction factors for the model.

7.3.6. The use of avoidance rates derived by collision rates, have the following implications (Cook et al. 2014):

   I. Given the **lack of evidence of collision rates offshore**, terrestrial survey data is used. However, it is acknowledged that flight behaviour may differ between onshore and offshore environments (Cook et al. 2014). For instance, gulls can adjust their flight mode in response to airflow patterns in order to minimize their energy expenditure. In addition, avoidance rates rely on accurate measurement of collision mortality (i.e. Cobs), which are, however, modelled and have associated uncertainty, as injured birds may for example die well away from turbines (Band, Madders and Whitfield, 2007)

   II. Terrestrial surveys are usually carried out within 2 km of the wind farm, rarely employing distance correction, potentially **underestimating the flux rates of birds** (population estimates) and consequently underestimating both collision and avoidance rates.

III. In practice both P_{coll} and the flux rate are likely to be **subject to error** – P_{coll} in relation to the model input parameters, and flux rate in relation to estimates of the total number of birds passing through the wind farm. This is often constrained by the application of mean flight speeds assuming linear flight patterns and short observation periods that need to be subsequently extrapolated. It should be noted that these potential sources of error are very difficult to distinguish.

IV. The extended model accounts for a changing risk of collision with height based on a detailed flight height distribution, this means that the risk of colliding is smaller and therefore **different avoidance rates** have to be applied for the basic and extended versions in order to derive the same number of observed collisions in both series of back-calculations.

Option B - Based on actual observations of birds' behaviour – There have been a number of studies on visual and/or radar observations (Desholm et al. 2006, Everaert & Stienen 2007, Blew et al. 2008, Krijgsveld et al. 2011, Cook et al. 2012, Trinder 2012, Moray Offshore Renewables Limited 2012, Smartwind/Forewind 2013, Everaert 2014). However, the number of these aiming at calculating avoidance rates is very limited. Given the variety of approaches used to measure avoidance, in particular the distances involved, quantifications are often inconsistent and difficult to compare (Cook et al. 2012).

7.3.7. The use of avoidance rates derived by actual birds' behaviour have the following implications (Cook et al. 2014):

I. Observations may still need **careful interpretation** given the varying drivers behind certain distributions / behaviours.

II. Observations made post-construction do not take account of the proportion of birds which have shown behavioural displacement, and moved away from the wind farm site, thereby reducing levels of flight activity and collision risk, which may lead to an **over-estimate of likely collision risk** (SNH 2010) if flux estimates are based on densities of flying birds pre-construction, i.e. resulting in more precautionary avoidance rates.

III. Given that extended model is an updated model version accounting for a skewed flight distribution, the same avoidance rates can be applied to the basic and extended versions of the Band CRM. However, if empirical offshore flight height recordings are applied with the Band CRM more accurate collision rates will be estimated using the extended model.

IV. Key CRM model parameters applied with empirically derived avoidance rates should reflect empirical flight speed in offshore wind farms and flight height recorded at sea outside offshore wind farms.

c. Avoidance rates currently used

7.3.8. Cook et al. (2014) reviewed the information available on seabird behaviour around wind farms (Desholm et al. 2006, Everaert & Stienen 2007, Blew et al. 2008, Krijgsveld et al. 2011, Everaert 2014 among others) and likely avoidance rates, recognising that there is no information on actual mortality rates at offshore wind farms. Although Band (2012) recommends that the avoidance rates used for collision risk estimates should be based on actual avoidance behaviour offshore, including both at macro and micro scales, the lack of data offshore has meant that calculation of avoidance rates has tended to rely on post-construction comparisons of the number of collisions recorded or observed at onshore wind farms and the number of collisions predicted offshore before construction (Smartwind/Forewind 2013, Cook et al. 2014), following the methodology described under Option A above, which is supported by SNH (SNH 2010).

7.3.9. In order to make use of best available data and facilitate their application in offshore wind applications, Cook et al. (2014) calculated generic avoidance rates for use in the basic and extended versions of the model. These generic avoidance rates are based on data combining collision rates and passage rates through wind farms obtained from 20 different sites (17 of which located onshore and 3 of which

located offshore). The UK Statutory Nature Conservation Bodies (SNCBs; JNCC et al. 2014) support the recommended avoidance rates (AR) presented by Cook et al. (2014) in relation to four of the five priority species (the exception being Black-legged Kittiwake). These are presented within Table 7.3 together with the avoidance rates recommended by UK SNCBs for Black-legged Kittiwake. No recommendation regarding avoidance rates for use with the extended Band model has been made for Northern Gannet and Black-legged Kittiwake due to a lack of species-specific data.

Table 7.3.   Basic and Extended Band model avoidance rates (± 2SD) derived by Cook et al. (2014) and supported by the UK SNCBs for use the Band model (JNCC et al. 2014).

Species	Avoidance rates for use in basic Band model	Avoidance rates for use in extended Band model
Northern Gannet	**0.989 (± 0.002)**	**Not available**
Lesser Black-backed Gull	**0.995 (± 0.001)**	**0.989 (± 0.002)**
Herring Gull	**0.995 (± 0.001)**	**0.990 (± 0.002)**
Great Black-backed Gull	**0.995 (± 0.001)**	**0.989 (± 0.002)**
Black-legged Kittiwake	**0.989 (± 0.002)**	**Not available**

7.3.10.   The difference between avoidance rates recommended for use in the basic and extended Band model is because the avoidance rates are back-calculated based on collisions and the collision risk is lower for the extended model which uses a detailed flight height distribution. Therefore, a lower avoidance rates is needed for predicting the "observed" (estimated) number of collisions.

7.3.11.   Cook et al. (2014) also provide a thorough sensitivity analysis on many of the key input parameters to the generic avoidance rates, concluding that the uncertainty surrounding the corpse correction factor (see Option A above, described in 7.3.4), flight speed, rotor speed and flux rate is the most influential.

7.3.12.   It should also be noted that Band (2012) recommends that avoidance rates derived using collision rates should be used with the same model input parameters like flight speed and height and turbine parameters that informed the calculation of the collision rate as described in Option A above. described in 7.3.4 In practice, however, the use of generic avoidance rates means that these values are used independently of other input parameters (e.g. turbine parameters) that are fed into the model (for the calculation of "uncorrected" collision rates). Accordingly, this is a source of uncertainty that is not possible to quantify, but potentially large.

7.4. EMPIRICAL AVOIDANCE RATES (EARS)

7.4.1.   The overall **EARs** derived in this study are based on an empirically derived foundation of evidence of bird behaviour offshore, and detailed empirical data on each component of avoidance (micro, meso and macro), as Band (2012) recommends. In addition, the EARs are independent of model input parameters for the Band model. Thus, EARs are considered to be able to provide more accurate collision estimates in both basic and extended versions of the Band model provided that empirical data on bird flight speed in the wind farm and bird flight height are used as input parameters to the model.

NIRAS **DHI** **CARBON TRUST**

7.4.2. Table 7.4 provides a summary of the main sources of uncertainty in the calculated study's EARs.

7.4.3. To account for these sources of uncertainty, they have been categorised, quantified and combined based on the author's expert judgement (see Section 5).

7.4.4. The mean values of overall EARs obtained are presented in Table 7.5, and in every case, are higher than the avoidance rates currently recommended by the regulators to be used in the Band model.

Table 7.4.   Main sources of uncertainty associated with the study's EARs.

Uncertainty related to bird behaviour

- **Avoidance behaviour is only considered up to 3 km outside the wind farm**

- **Potential displacement or barrier effects beyond 3 km outside the wind farm have not been considered**

- **Driving mechanisms behind observed patterns of macro avoidance are unknown**

Uncertainty related to data collection

- **Data informing EARs calculation have been collected on one site only, and is unavailable for certain conditions, including night time, and is limited for higher sea states and poor visibility conditions**

- **Data is sampled (does not provide accurate passage rates of birds through the wind farm as a factor of time), exhibiting a relatively high degree of variability and may be subject to potential bias due to distance of targets and visibility conditions**

- **Equipment performance and detection probability in relation to distance are assumed to be similar across the studied areas (i.e. in areas compared)**

Uncertainty related to data analysis

a) Macro
- **Assumes that the track density in the absence of the wind farm would have been uniform across the wind farm and within the area outside the wind farm up to 3 km**

- **Assumes that the bird flight speed is the same within the wind farm as within the area outside the wind farm up to 3 km**

b) Meso
- **Behavioural responses and distance to RSZ are assessed visually, and may be subject to bias**

- **Track lengths informing empirical meso EARs are not available and can only be considered as an approximation. These are calculated assuming straight flight lines across the RSZ + 10 m buffer within the wind farm. The track lengths outside the RZS are estimated as mean track length in a circle, adjusted by proportion of the circle not surveyed as well as for non-linear flight patterns (based on comparing flight speed to track speed)**

c) Micro
- **Behavioural responses to the rotor are assessed visually, and may be subject to bias**

- **Due to limited sample size, species-specific micro EARs cannot be calculated**

NIRAS DHI CARBON TRUST

Table 7.5. Extended Band model avoidance rates (± 2SD, or approximate 95% confidence intervals) supported by the UK SNCBs for use in the Band model (JNCC et al. 2014), compared with the study's EARs. In relation to the latter, the combined overall uncertainty (SD) and 95% confidence limits are indicated including both variability and a range of uncertainty components.

Species	Avoidance rates for use in Basic Band model	Avoidance rates for use in Extended Band model	Study EARs	Combined 95% confidence limits	Combined SD
Northern Gannet	0.989 (± 0.002)	Not available	0.999	0.994-1.000	0.003
Lesser Black-backed Gull	0.995 (± 0.001)	0.989 (± 0.002)	0.998	0.987-1.000	0.006
Herring Gull	0.995 (± 0.001)	0.990 (± 0.002)	0.999	0.989-1.000	0.005
Great Black-backed Gull	0.995 (± 0.001)	0.989 (± 0.002)	0.996	0.975-1.000	0.011
Black-legged Kittiwake	0.989 (± 0.002)	Not available	0.998	0.987-1.000	0.006

7.4.5. There is inconsistency in the macro EARs reported for large gulls and Black-legged Kittiwake using different monitoring equipment and described by other studies. As a result there is still uncertainty in the level of macro avoidance. However, macro avoidance has the least influence on the overall EARs estimated for large gulls and Black-legged Kittiwake (see Section 5.6), and the uncertainty associated with the overall EARs for these species can therefore be considered as modest.

7.4.6. Both avoidance rates currently used and EARs derived in this study include sources of uncertainty, which, as suggested by Band (2012, p. 28) "are likely to dwarf the errors and uncertainties arising from an inexact collision model or variability in survey data". Accordingly, it is considered more appropriate to use a range of values and apply CRMs that allow to account for uncertainty (e.g. Madsen 2016).

7.4.7. Table 7.6 - Table 7.10 present a range of overall EAR values for each target species, where the micro avoidance rate is kept fixed and macro avoidance (columns) and meso avoidance (rows) rates are allowed to vary. Macro and meso avoidance rates reported by Krijgsveld et al. 2011 (which is the study most comparable to this study; no other study has reported meso avoidance) are also indicated in the tables (matrices), and therefore helps the reader to assess how the EAR compare to that specific study. It is however important to note that no other studies have applied the same methodology as in this study. Krijgsveld et al. (2011) reported a macro avoidance rate of 0.18 for gulls as a group and 0.64 for Northern Gannets and a meso of 0.66 for all species combined. Assuming the same micro EAR as obtained in this study and including the values by Krijgsveld et al. 2011 would result in an EAR within the combined confidence limits of the estimated EAR for Northern Gannets in this study (Table 7.6). For Kittiwake and Herring Gull an estimate based on the macro and meso rates by Krijgsveld et al. 2011 is slightly outside the confidence limits of this study (with a difference of about 0.001, Table 7.7, Table 7.9), while for the other species it is within the lower 95% confidence limits by this study (Table 7.8, Table 7.10).

7.4.8. Most macro avoidance estimates or "classification" of avoidance (into avoidance, no response/ non-avoidance, or attraction) in other studies, are based on survey data and comparing bird abundance or densities inside a wind farm footprint with an area outside the wind farm or within a control area. Often, a buffer of e.g. 500 m around the wind farm is included as being part of the footprint (in this study all birds outside the perimeter of the outermost turbine row including the RSZ, is considered as outside). Based on these studies many of the results indicate that gulls do not show an avoidance behaviour (macro avoidance)

towards the wind farm footprint (Dierschke et al. 2016). A recent study by Vanermen et al. (2017) also indicated an attraction or "no-response" of large gulls to the wind farm based on ship survey data. However, they also report results on GPS tagging data indicating that birds are less active inside the wind farm where they spend a lot of time roosting on wind turbine foundations. The results also indicate that the birds inside the wind farm favour the edge of the wind farm (i.e. they seem to avoid penetrating deep into the wind farm).

7.4.9.   If birds inside the wind farm are not flying they could be regarded as "avoiding", because they are not at risk, especially as bird densities (as used in the Band model) are considered to be birds in flight at any time (i.e. a reduction in flight activity could therefore be considered as an avoidance behaviour). For example, if there are 10 birds inside the wind farm and 10 birds outside the wind farm within an equally sized and shaped area, it would indicate that there is no avoidance because this number is equal and the areas are also equal. If for example, at any time 44% of the birds outside the wind farm are in flight and only 15% inside the wind farm are in flight, this corresponds to 1.5 birds inside and 4.4 birds outside (or in total 5.9 out of the 20 birds in flight at any time). If the outside is considered as the "normal" proportion of birds in flight at any time then there is a 66% decrease of activity inside the wind farm. This is important, as tracking of birds in flight (for example with radars and rangefinders) would, in this example, indicate an avoidance because of the 66% decrease in flight activity inside the wind farm. However, when both flying and sitting birds are considered the above example would indicate no avoidance response because there are still an equal number of birds i.e. 10, both inside and outside of the wind farm.

7.4.10.   The GPS tagging data presented by Vanermen et al. (2017) is the only evidence provided to date that birds do not fly as much in a wind farm. However, there is likely a large site-specific variability. For example, the intensity of fishing vessel activity within the vicinity of wind farms can be expected to influence bird abundance and distribution across the area, with large gulls attracted to any fishery discards. It is however also important to note that the availability of fishery discards is likely to be limited to outside the wind farm therefore influencing the numbers of birds at risk.

7.4.11.   Very few studies report specifically on meso-avoidance rates, only two offshore studies according to the review by Cook et al. 2014. The study by Krijgsveld et al. (2011) indicated a meso avoidance rate of 0.66 (by comparing number of birds within 50 m from a turbine to elsewhere within the wind farm). The flight duration (track length) within the turbine zone and outside is however not accounted for and therefore this meso avoidance rate might potentially be too conservative. The other offshore study mentioned by Cook et al. (2014) is the study by Skov et al. (2012) at Horns Rev, where none of 408 large gulls tracked were recorded within 50 m from a turbine, indicating a very high meso avoidance rate. The overall conclusion drawn by Cook et al. (2014) regarding micro avoidance, i.e. that very few birds enter the micro zone (or when a last reaction to individual turbines are needed) indicate that birds are already strongly avoiding at the meso scale (or macro), i.e. indicating a strong meso avoidance rate, in line with the estimates by this study.

7.4.12.   Similarly, for meso avoidance, very few studies report on empirical derived micro avoidance rates. Krijgsveld et al. (2011) report a value of 0.93, but they also indicate that this value probably is conservative because they consider the RSZ as circular and many of the birds within the RSZ flew in parallel with the rotor blades. Desholm et al. (2005) reported that less than 1% of geese and ducks flew within the RSZ (or at any risk of colliding). An example of a back-calculated avoidance rate, based on recorded and estimated number of collisions, reported for large gulls is 0.953 (Everaert 2014), which is very similar to the micro avoidance rate reported in this study (0.957). Overall, the patterns obtain in this study is in line with other studies.

7.4.13.   Following the evidence presented in this section it is considered that EARs are a better reflection of actual bird avoidance behaviour than that provided by avoidance rates currently used, and are more suitable for application with the un-corrected model outputs when using the basic and extended Band model.

Table 7.6. EARs for Northern Gannet resulting from the micro avoidance rate as calculated by this study and for a range of macro and meso avoidance rates.

Northern Gannet - Macro avoidance rate										
Meso avoidance rate	-0.15	-0.10	0.00	0.10	0.15	0.20	0.25	0.30	0.35	0.40
0.660	0.9805	0.9813	0.9830	0.9847	0.9856	0.9864	0.9873	0.9881	0.9890	0.9898
...										
0.850	0.9914	0.9918	0.9925	0.9933	0.9936	0.9940	0.9944	0.9948	0.9951	0.9955
0.855	0.9917	0.9920	0.9928	0.9935	0.9938	0.9942	0.9946	0.9949	0.9953	0.9957
0.860	0.9920	0.9923	0.9930	0.9937	0.9941	0.9944	0.9948	0.9951	0.9955	0.9958
0.865	0.9922	0.9926	0.9933	0.9939	0.9943	0.9946	0.9949	0.9953	0.9956	0.9960
0.870	0.9925	0.9929	0.9935	0.9942	0.9945	0.9948	0.9951	0.9955	0.9958	0.9961
0.875	0.9928	0.9931	0.9938	0.9944	0.9947	0.9950	0.9953	0.9956	0.9959	0.9963
0.880	0.9931	0.9934	0.9940	0.9946	0.9949	0.9952	0.9955	0.9958	0.9961	0.9964
0.885	0.9934	0.9937	0.9943	0.9948	0.9951	0.9954	0.9957	0.9960	0.9963	0.9966
0.890	0.9937	0.9940	0.9945	0.9951	0.9953	0.9956	0.9959	0.9962	0.9964	0.9967
0.895	0.9940	0.9942	0.9948	0.9953	0.9955	0.9958	0.9961	0.9963	0.9966	0.9969
0.900	0.9943	0.9945	0.9950	0.9955	0.9958	0.9960	0.9963	0.9965	0.9968	0.9970
0.905	0.9945	0.9948	0.9953	0.9957	0.9960	0.9962	0.9964	0.9967	0.9969	0.9972
0.910	0.9948	0.9951	0.9955	0.9960	0.9962	0.9964	0.9966	0.9969	0.9971	0.9973
0.915	0.9951	0.9953	0.9958	0.9962	0.9964	0.9966	0.9968	0.9970	0.9972	0.9975
0.920	0.9954	0.9956	0.9960	0.9964	0.9966	0.9968	0.9970	0.9972	0.9974	0.9976
0.925	0.9957	0.9959	0.9963	0.9966	0.9968	0.9970	0.9972	0.9974	0.9976	0.9978
0.930	0.9960	0.9962	0.9965	0.9969	0.9970	0.9972	0.9974	0.9976	0.9977	0.9979
0.935	0.9963	0.9964	0.9968	0.9971	0.9972	0.9974	0.9976	0.9977	0.9979	0.9981
0.940	0.9966	0.9967	0.9970	0.9973	0.9975	0.9976	0.9978	0.9979	0.9981	0.9982
0.945	0.9968	0.9970	0.9973	0.9975	0.9977	0.9978	0.9979	0.9981	0.9982	0.9984
0.950	0.9971	0.9973	0.9975	0.9978	0.9979	0.9980	0.9981	0.9983	0.9984	0.9985
0.955	0.9974	0.9975	0.9978	0.9980	0.9981	0.9982	0.9983	0.9984	0.9985	0.9987
0.960	0.9977	0.9978	0.9980	0.9982	0.9983	0.9984	0.9985	0.9986	0.9987	0.9988
0.965	0.9980	0.9981	0.9983	0.9984	0.9985	0.9986	0.9987	0.9988	0.9989	0.9990
0.970	0.9983	0.9984	0.9985	0.9987	0.9987	0.9988	0.9989	0.9990	0.9990	0.9991
0.975	0.9986	0.9986	0.9988	0.9989	0.9989	0.9990	0.9991	0.9991	0.9992	0.9993
0.980	0.9989	0.9989	0.9990	0.9991	0.9992	0.9992	0.9993	0.9993	0.9994	0.9994
0.985	0.9991	0.9992	0.9993	0.9993	0.9994	0.9994	0.9994	0.9995	0.9995	0.9996
0.990	0.9994	0.9995	0.9995	0.9996	0.9996	0.9996	0.9996	0.9997	0.9997	0.9997
0.995	0.9997	0.9997	0.9998	0.9998	0.9998	0.9998	0.9998	0.9998	0.9998	0.9999

Micro AR = 0.950		Lower 95% confidence limit			Combined standard deviation			EAR calculated by this study	

NIRAS DHI CARBON TRUST

Northern Gannet - Macro avoidance rate											
Meso avoidance rate	**0.45**	**0.50**	**0.55**	**0.60**	**0.65**	**0.70**	**0.75**	**0.80**	**0.85**	**0.90**	**0.95**
0.660	0.9907	0.9915	0.9924	0.9932	0.9941	0.9949	0.9958	0.9966	0.9975	0.9983	0.9992
...											
0.850	0.9959	0.9963	0.9966	0.9970	0.9974	0.9978	0.9981	0.9985	0.9989	0.9993	0.9996
0.855	0.9960	0.9964	0.9967	0.9971	0.9975	0.9978	0.9982	0.9986	0.9989	0.9993	0.9996
0.860	0.9962	0.9965	0.9969	0.9972	0.9976	0.9979	0.9983	0.9986	0.9990	0.9993	0.9997
0.865	0.9963	0.9966	0.9970	0.9973	0.9976	0.9980	0.9983	0.9987	0.9990	0.9993	0.9997
0.870	0.9964	0.9968	0.9971	0.9974	0.9977	0.9981	0.9984	0.9987	0.9990	0.9994	0.9997
0.875	0.9966	0.9969	0.9972	0.9975	0.9978	0.9981	0.9984	0.9988	0.9991	0.9994	0.9997
0.880	0.9967	0.9970	0.9973	0.9976	0.9979	0.9982	0.9985	0.9988	0.9991	0.9994	0.9997
0.885	0.9968	0.9971	0.9974	0.9977	0.9980	0.9983	0.9986	0.9989	0.9991	0.9994	0.9997
0.890	0.9970	0.9973	0.9975	0.9978	0.9981	0.9984	0.9986	0.9989	0.9992	0.9995	0.9997
0.895	0.9971	0.9974	0.9976	0.9979	0.9982	0.9984	0.9987	0.9990	0.9992	0.9995	0.9997
0.900	0.9973	0.9975	0.9978	0.9980	0.9983	0.9985	0.9988	0.9990	0.9993	0.9995	0.9998
0.905	0.9974	0.9976	0.9979	0.9981	0.9983	0.9986	0.9988	0.9991	0.9993	0.9995	0.9998
0.910	0.9975	0.9978	0.9980	0.9982	0.9984	0.9987	0.9989	0.9991	0.9993	0.9996	0.9998
0.915	0.9977	0.9979	0.9981	0.9983	0.9985	0.9987	0.9989	0.9992	0.9994	0.9996	0.9998
0.920	0.9978	0.9980	0.9982	0.9984	0.9986	0.9988	0.9990	0.9992	0.9994	0.9996	0.9998
0.925	0.9979	0.9981	0.9983	0.9985	0.9987	0.9989	0.9991	0.9993	0.9994	0.9996	0.9998
0.930	0.9981	0.9983	0.9984	0.9986	0.9988	0.9990	0.9991	0.9993	0.9995	0.9997	0.9998
0.935	0.9982	0.9984	0.9985	0.9987	0.9989	0.9990	0.9992	0.9994	0.9995	0.9997	0.9998
0.940	0.9984	0.9985	0.9987	0.9988	0.9990	0.9991	0.9993	0.9994	0.9996	0.9997	0.9999
0.945	0.9985	0.9986	0.9988	0.9989	0.9990	0.9992	0.9993	0.9995	0.9996	0.9997	0.9999
0.950	0.9986	0.9988	0.9989	0.9990	0.9991	0.9993	0.9994	0.9995	0.9996	0.9998	0.9999
0.955	0.9988	0.9989	0.9990	0.9991	0.9992	0.9993	0.9994	0.9996	0.9997	0.9998	0.9999
0.960	0.9989	0.9990	0.9991	0.9992	0.9993	0.9994	0.9995	0.9996	0.9997	0.9998	0.9999
0.965	0.9990	0.9991	0.9992	0.9993	0.9994	0.9995	0.9996	0.9997	0.9997	0.9998	0.9999
0.970	0.9992	0.9993	0.9993	0.9994	0.9995	0.9996	0.9996	0.9997	0.9998	0.9999	0.9999
0.975	0.9993	0.9994	0.9994	0.9995	0.9996	0.9996	0.9997	0.9998	0.9998	0.9999	0.9999
0.980	0.9995	0.9995	0.9996	0.9996	0.9997	0.9997	0.9998	0.9998	0.9999	0.9999	1.0000
0.985	0.9996	0.9996	0.9997	0.9997	0.9997	0.9998	0.9998	0.9999	0.9999	0.9999	1.0000
0.990	0.9997	0.9998	0.9998	0.9998	0.9998	0.9999	0.9999	0.9999	0.9999	1.0000	1.0000
0.995	0.9999	0.9999	0.9999	0.9999	0.9999	0.9999	0.9999	1.0000	1.0000	1.0000	1.0000
Micro AR = 0.950		EAR calculated using the macor and meso avoidance rate estimated by Krijgsveld et al. 2011 Note that the same methodology was not used in that study									

NIRAS   DHI   CARBON TRUST

Table 7.7. EARs for Black-legged Kittiwake resulting from the micro avoidance rate as calculated by this study and for a range of macro and meso avoidance rates.

Black-legged Kittiwake – Macro avoidance rate										
Meso avoidance rate	**-0.15**	**-0.10**	**0.00**	**0.10**	**0.15**	**0.20**	**0.25**	**0.30**	**0.35**	**0.40**
0.660	0.9805	0.9813	0.9830	0.9847	0.9856	0.9864	0.9873	0.9881	0.9890	0.9898
...										
0.850	0.9914	0.9918	0.9925	0.9933	0.9936	0.9940	0.9944	0.9948	0.9951	0.9955
0.855	0.9917	0.9920	0.9928	0.9935	0.9938	0.9942	0.9946	0.9949	0.9953	0.9957
0.860	0.9920	0.9923	0.9930	0.9937	0.9941	0.9944	0.9948	0.9951	0.9955	0.9958
0.865	0.9922	0.9926	0.9933	0.9939	0.9943	0.9946	0.9949	0.9953	0.9956	0.9960
0.870	0.9925	0.9929	0.9935	0.9942	0.9945	0.9948	0.9951	0.9955	0.9958	0.9961
0.875	0.9928	0.9931	0.9938	0.9944	0.9947	0.9950	0.9953	0.9956	0.9959	0.9963
0.880	0.9931	0.9934	0.9940	0.9946	0.9949	0.9952	0.9955	0.9958	0.9961	0.9964
0.885	0.9934	0.9937	0.9943	0.9948	0.9951	0.9954	0.9957	0.9960	0.9963	0.9966
0.890	0.9937	0.9940	0.9945	0.9951	0.9953	0.9956	0.9959	0.9962	0.9964	0.9967
0.895	0.9940	0.9942	0.9948	0.9953	0.9955	0.9958	0.9961	0.9963	0.9966	0.9969
0.900	0.9943	0.9945	0.9950	0.9955	0.9958	0.9960	0.9963	0.9965	0.9968	0.9970
0.905	0.9945	0.9948	0.9953	0.9957	0.9960	0.9962	0.9964	0.9967	0.9969	0.9972
0.910	0.9948	0.9951	0.9955	0.9960	0.9962	0.9964	0.9966	0.9969	0.9971	0.9973
0.915	0.9951	0.9953	0.9958	0.9962	0.9964	0.9966	0.9968	0.9970	0.9972	0.9975
0.920	0.9954	0.9956	0.9960	0.9964	0.9966	0.9968	0.9970	0.9972	0.9974	0.9976
0.925	0.9957	0.9959	0.9963	0.9966	0.9968	0.9970	0.9972	0.9974	0.9976	0.9978
0.930	0.9960	0.9962	0.9965	0.9969	0.9970	0.9972	0.9974	0.9976	0.9977	0.9979
0.935	0.9963	0.9964	0.9968	0.9971	0.9972	0.9974	0.9976	0.9977	0.9979	0.9981
0.940	0.9966	0.9967	0.9970	0.9973	0.9975	0.9976	0.9978	0.9979	0.9981	0.9982
0.945	0.9968	0.9970	0.9973	0.9975	0.9977	0.9978	0.9979	0.9981	0.9982	0.9984
0.950	0.9971	0.9973	0.9975	0.9978	0.9979	0.9980	0.9981	0.9983	0.9984	0.9985
0.955	0.9974	0.9975	0.9978	0.9980	0.9981	0.9982	0.9983	0.9984	0.9985	0.9987
0.960	0.9977	0.9978	0.9980	0.9982	0.9983	0.9984	0.9985	0.9986	0.9987	0.9988
0.965	0.9980	0.9981	0.9983	0.9984	0.9985	0.9986	0.9987	0.9988	0.9989	0.9990
0.970	0.9983	0.9984	0.9985	0.9987	0.9987	0.9988	0.9989	0.9990	0.9990	0.9991
0.975	0.9986	0.9986	0.9988	0.9989	0.9989	0.9990	0.9991	0.9991	0.9992	0.9993
0.980	0.9989	0.9989	0.9990	0.9991	0.9992	0.9992	0.9993	0.9993	0.9994	0.9994
0.985	0.9991	0.9992	0.9993	0.9993	0.9994	0.9994	0.9994	0.9995	0.9995	0.9996
0.990	0.9994	0.9995	0.9995	0.9996	0.9996	0.9996	0.9996	0.9997	0.9997	0.9997
0.995	0.9997	0.9997	0.9998	0.9998	0.9998	0.9998	0.9998	0.9998	0.9998	0.9999

Micro AR = 0.950		Lower 95% confidence limit			Combined standard deviation			EAR calculated by this study		

NIRAS DHI CARBON TRUST

Black-legged Kittiwake - Macro avoidance rate											
Meso avoidance rate	0.45	0.50	0.55	0.60	0. 65	0.70	0.75	0.80	0.85	0.90	0.95
0.660	0.9907	0.9915	0.9924	0.9932	0.9941	0.9949	0.9958	0.9966	0.9975	0.9983	0.9992
...											
0.850	0.9959	0.9963	0.9966	0.9970	0.9974	0.9978	0.9981	0.9985	0.9989	0.9993	0.9996
0.855	0.9960	0.9964	0.9967	0.9971	0.9975	0.9978	0.9982	0.9986	0.9989	0.9993	0.9996
0.860	0.9962	0.9965	0.9969	0.9972	0.9976	0.9979	0.9983	0.9986	0.9990	0.9993	0.9997
0.865	0.9963	0.9966	0.9970	0.9973	0.9976	0.9980	0.9983	0.9987	0.9990	0.9993	0.9997
0.870	0.9964	0.9968	0.9971	0.9974	0.9977	0.9981	0.9984	0.9987	0.9990	0.9994	0.9997
0.875	0.9966	0.9969	0.9972	0.9975	0.9978	0.9981	0.9984	0.9988	0.9991	0.9994	0.9997
0.880	0.9967	0.9970	0.9973	0.9976	0.9979	0.9982	0.9985	0.9988	0.9991	0.9994	0.9997
0.885	0.9968	0.9971	0.9974	0.9977	0.9980	0.9983	0.9986	0.9989	0.9991	0.9994	0.9997
0.890	0.9970	0.9973	0.9975	0.9978	0.9981	0.9984	0.9986	0.9989	0.9992	0.9995	0.9997
0.895	0.9971	0.9974	0.9976	0.9979	0.9982	0.9984	0.9987	0.9990	0.9992	0.9995	0.9997
0.900	0.9973	0.9975	0.9978	0.9980	0.9983	0.9985	0.9988	0.9990	0.9993	0.9995	0.9998
0.905	0.9974	0.9976	0.9979	0.9981	0.9983	0.9986	0.9988	0.9991	0.9993	0.9995	0.9998
0.910	0.9975	0.9978	0.9980	0.9982	0.9984	0.9987	0.9989	0.9991	0.9993	0.9996	0.9998
0.915	0.9977	0.9979	0.9981	0.9983	0.9985	0.9987	0.9989	0.9992	0.9994	0.9996	0.9998
0.920	0.9978	0.9980	0.9982	0.9984	0.9986	0.9988	0.9990	0.9992	0.9994	0.9996	0.9998
0.925	0.9979	0.9981	0.9983	0.9985	0.9987	0.9989	0.9991	0.9993	0.9994	0.9996	0.9998
0.930	0.9981	0.9983	0.9984	0.9986	0.9988	0.9990	0.9991	0.9993	0.9995	0.9997	0.9998
0.935	0.9982	0.9984	0.9985	0.9987	0.9989	0.9990	0.9992	0.9994	0.9995	0.9997	0.9998
0.940	0.9984	0.9985	0.9987	0.9988	0.9990	0.9991	0.9993	0.9994	0.9996	0.9997	0.9999
0.945	0.9985	0.9986	0.9988	0.9989	0.9990	0.9992	0.9993	0.9995	0.9996	0.9997	0.9999
0.950	0.9986	0.9988	0.9989	0.9990	0.9991	0.9993	0.9994	0.9995	0.9996	0.9998	0.9999
0.955	0.9988	0.9989	0.9990	0.9991	0.9992	0.9993	0.9994	0.9996	0.9997	0.9998	0.9999
0.960	0.9989	0.9990	0.9991	0.9992	0.9993	0.9994	0.9995	0.9996	0.9997	0.9998	0.9999
0.965	0.9990	0.9991	0.9992	0.9993	0.9994	0.9995	0.9996	0.9997	0.9997	0.9998	0.9999
0.970	0.9992	0.9993	0.9993	0.9994	0.9995	0.9996	0.9996	0.9997	0.9998	0.9999	0.9999
0.975	0.9993	0.9994	0.9994	0.9995	0.9996	0.9996	0.9997	0.9998	0.9998	0.9999	0.9999
0.980	0.9995	0.9995	0.9996	0.9996	0.9997	0.9997	0.9998	0.9998	0.9999	0.9999	1.0000
0.985	0.9996	0.9996	0.9997	0.9997	0.9997	0.9998	0.9998	0.9999	0.9999	0.9999	1.0000
0.990	0.9997	0.9998	0.9998	0.9998	0.9998	0.9999	0.9999	0.9999	0.9999	1.0000	1.0000
0.995	0.9999	0.9999	0.9999	0.9999	0.9999	0.9999	0.9999	1.0000	1.0000	1.0000	1.0000

Micro AR = 0.950		EAR calculated using the macor and meso avoidance rate estimated by Krijgsveld et al. 2011 Note that the same methodology was not used in that study

INFORMING COLLISION RISK ASSESSMENT

NIRAS DHI CARBON TRUST

Table 7.8.   EARs for Lesser Black-backed Gull resulting from the micro avoidance rate as calculated by this study and for a range of macro and meso avoidance rates.

Lesser Black-backed Gull - Macro avoidance rate										
Meso avoidance rate	-0.15	-0.10	0.00	0.10	0.15	0.20	0.25	0.30	0.35	0.40
0.660	0.9832	0.9839	0.9854	0.9868	0.9876	0.9883	0.9890	0.9898	0.9905	0.9912
...										
0.850	0.9926	0.9929	0.9936	0.9942	0.9945	0.9948	0.9952	0.9955	0.9958	0.9961
0.855	0.9928	0.9931	0.9938	0.9944	0.9947	0.9950	0.9953	0.9956	0.9959	0.9963
0.860	0.9931	0.9934	0.9940	0.9946	0.9949	0.9952	0.9955	0.9958	0.9961	0.9964
0.865	0.9933	0.9936	0.9942	0.9948	0.9951	0.9954	0.9956	0.9959	0.9962	0.9965
0.870	0.9936	0.9939	0.9944	0.9950	0.9952	0.9955	0.9958	0.9961	0.9964	0.9966
0.875	0.9938	0.9941	0.9946	0.9952	0.9954	0.9957	0.9960	0.9962	0.9965	0.9968
0.880	0.9941	0.9943	0.9948	0.9954	0.9956	0.9959	0.9961	0.9964	0.9966	0.9969
0.885	0.9943	0.9946	0.9951	0.9955	0.9958	0.9960	0.9963	0.9965	0.9968	0.9970
0.890	0.9946	0.9948	0.9953	0.9957	0.9960	0.9962	0.9965	0.9967	0.9969	0.9972
0.895	0.9948	0.9950	0.9955	0.9959	0.9962	0.9964	0.9966	0.9968	0.9971	0.9973
0.900	0.9951	0.9953	0.9957	0.9961	0.9963	0.9966	0.9968	0.9970	0.9972	0.9974
0.905	0.9953	0.9955	0.9959	0.9963	0.9965	0.9967	0.9969	0.9971	0.9973	0.9975
0.910	0.9955	0.9957	0.9961	0.9965	0.9967	0.9969	0.9971	0.9973	0.9975	0.9977
0.915	0.9958	0.9960	0.9963	0.9967	0.9969	0.9971	0.9973	0.9974	0.9976	0.9978
0.920	0.9960	0.9962	0.9966	0.9969	0.9971	0.9972	0.9974	0.9976	0.9978	0.9979
0.925	0.9963	0.9965	0.9968	0.9971	0.9973	0.9974	0.9976	0.9977	0.9979	0.9981
0.930	0.9965	0.9967	0.9970	0.9973	0.9974	0.9976	0.9977	0.9979	0.9980	0.9982
0.935	0.9968	0.9969	0.9972	0.9975	0.9976	0.9978	0.9979	0.9980	0.9982	0.9983
0.940	0.9970	0.9972	0.9974	0.9977	0.9978	0.9979	0.9981	0.9982	0.9983	0.9985
0.945	0.9973	0.9974	0.9976	0.9979	0.9980	0.9981	0.9982	0.9983	0.9985	0.9986
0.950	0.9975	0.9976	0.9979	0.9981	0.9982	0.9983	0.9984	0.9985	0.9986	0.9987
0.955	0.9978	0.9979	0.9981	0.9983	0.9984	0.9985	0.9985	0.9986	0.9987	0.9988
0.960	0.9980	0.9981	0.9983	0.9985	0.9985	0.9986	0.9987	0.9988	0.9989	0.9990
0.965	0.9983	0.9983	0.9985	0.9986	0.9987	0.9988	0.9989	0.9989	0.9990	0.9991
0.970	0.9985	0.9986	0.9987	0.9988	0.9989	0.9990	0.9990	0.9991	0.9992	0.9992
0.975	0.9988	0.9988	0.9989	0.9990	0.9991	0.9991	0.9992	0.9992	0.9993	0.9994
0.980	0.9990	0.9991	0.9991	0.9992	0.9993	0.9993	0.9994	0.9994	0.9994	0.9995
0.985	0.9993	0.9993	0.9994	0.9994	0.9995	0.9995	0.9995	0.9995	0.9996	0.9996
0.990	0.9995	0.9995	0.9996	0.9996	0.9996	0.9997	0.9997	0.9997	0.9997	0.9997
0.995	0.9998	0.9998	0.9998	0.9998	0.9998	0.9998	0.9998	0.9998	0.9999	0.9999

Micro AR = 0.950		Lower 95% confidence limit			Combined standard deviation			EAR calculated by this study		

NIRAS   DHI   CARBON TRUST

Lesser Black-backed Gull - Macro avoidance rate										
Meso avoidance rate	0.45	0.50	0.55	0.60	0. 65	0.70	0.75	0.80	0.85	0.90	0.95
0.660	0.9920	0.9927	0.9934	0.9942	0.9949	0.9956	0.9963	0.9971	0.9978	0.9985	0.9993
...											
0.850	0.9965	0.9968	0.9971	0.9974	0.9977	0.9981	0.9984	0.9987	0.9990	0.9994	0.9997
0.855	0.9966	0.9969	0.9972	0.9975	0.9978	0.9981	0.9984	0.9988	0.9991	0.9994	0.9997
0.860	0.9967	0.9970	0.9973	0.9976	0.9979	0.9982	0.9985	0.9988	0.9991	0.9994	0.9997
0.865	0.9968	0.9971	0.9974	0.9977	0.9980	0.9983	0.9985	0.9988	0.9991	0.9994	0.9997
0.870	0.9969	0.9972	0.9975	0.9978	0.9980	0.9983	0.9986	0.9989	0.9992	0.9994	0.9997
0.875	0.9970	0.9973	0.9976	0.9979	0.9981	0.9984	0.9987	0.9989	0.9992	0.9995	0.9997
0.880	0.9972	0.9974	0.9977	0.9979	0.9982	0.9985	0.9987	0.9990	0.9992	0.9995	0.9997
0.885	0.9973	0.9975	0.9978	0.9980	0.9983	0.9985	0.9988	0.9990	0.9993	0.9995	0.9998
0.890	0.9974	0.9976	0.9979	0.9981	0.9983	0.9986	0.9988	0.9991	0.9993	0.9995	0.9998
0.895	0.9975	0.9977	0.9980	0.9982	0.9984	0.9986	0.9989	0.9991	0.9993	0.9995	0.9998
0.900	0.9976	0.9979	0.9981	0.9983	0.9985	0.9987	0.9989	0.9991	0.9994	0.9996	0.9998
0.905	0.9978	0.9980	0.9982	0.9984	0.9986	0.9988	0.9990	0.9992	0.9994	0.9996	0.9998
0.910	0.9979	0.9981	0.9983	0.9985	0.9986	0.9988	0.9990	0.9992	0.9994	0.9996	0.9998
0.915	0.9980	0.9982	0.9984	0.9985	0.9987	0.9989	0.9991	0.9993	0.9995	0.9996	0.9998
0.920	0.9981	0.9983	0.9985	0.9986	0.9988	0.9990	0.9991	0.9993	0.9995	0.9997	0.9998
0.925	0.9982	0.9984	0.9985	0.9987	0.9989	0.9990	0.9992	0.9994	0.9995	0.9997	0.9998
0.930	0.9983	0.9985	0.9986	0.9988	0.9989	0.9991	0.9992	0.9994	0.9995	0.9997	0.9998
0.935	0.9985	0.9986	0.9987	0.9989	0.9990	0.9992	0.9993	0.9994	0.9996	0.9997	0.9999
0.940	0.9986	0.9987	0.9988	0.9990	0.9991	0.9992	0.9994	0.9995	0.9996	0.9997	0.9999
0.945	0.9987	0.9988	0.9989	0.9991	0.9992	0.9993	0.9994	0.9995	0.9996	0.9998	0.9999
0.950	0.9988	0.9989	0.9990	0.9991	0.9992	0.9994	0.9995	0.9996	0.9997	0.9998	0.9999
0.955	0.9989	0.9990	0.9991	0.9992	0.9993	0.9994	0.9995	0.9996	0.9997	0.9998	0.9999
0.960	0.9991	0.9991	0.9992	0.9993	0.9994	0.9995	0.9996	0.9997	0.9997	0.9998	0.9999
0.965	0.9992	0.9992	0.9993	0.9994	0.9995	0.9995	0.9996	0.9997	0.9998	0.9998	0.9999
0.970	0.9993	0.9994	0.9994	0.9995	0.9995	0.9996	0.9997	0.9997	0.9998	0.9999	0.9999
0.975	0.9994	0.9995	0.9995	0.9996	0.9996	0.9997	0.9997	0.9998	0.9998	0.9999	0.9999
0.980	0.9995	0.9996	0.9996	0.9997	0.9997	0.9997	0.9998	0.9998	0.9999	0.9999	1.0000
0.985	0.9996	0.9997	0.9997	0.9997	0.9998	0.9998	0.9998	0.9999	0.9999	0.9999	1.0000
0.990	0.9998	0.9998	0.9998	0.9998	0.9998	0.9999	0.9999	0.9999	0.9999	1.0000	1.0000
0.995	0.9999	0.9999	0.9999	0.9999	0.9999	0.9999	0.9999	1.0000	1.0000	1.0000	1.0000
Micro AR = 0.950		EAR calculated using the macor and meso avoidance rate estimated by Krijgsveld et al. 2011 Note that the same methodology was not used in that study									

INFORMING COLLISION RISK ASSESSMENT

NIRAS   DHI   CARBON TRUST

Table 7.9.   EARs for Herring Gull resulting from the micro avoidance rate as calculated by this study and for a range of macro and meso avoidance rates.

Herring Gull – Macro avoidance rate										
Meso avoidance rate	-0.15	-0.10	0.00	0.10	0.15	0.20	0.25	0.30	0.35	0.40
0.660	0.9832	0.9839	0.9854	0.9868	0.9876	0.9883	0.9890	0.9898	0.9905	0.9912
...										
0.850	0.9926	0.9929	0.9936	0.9942	0.9945	0.9948	0.9952	0.9955	0.9958	0.9961
0.855	0.9928	0.9931	0.9938	0.9944	0.9947	0.9950	0.9953	0.9956	0.9959	0.9963
0.860	0.9931	0.9934	0.9940	0.9946	0.9949	0.9952	0.9955	0.9958	0.9961	0.9964
0.865	0.9933	0.9936	0.9942	0.9948	0.9951	0.9954	0.9956	0.9959	0.9962	0.9965
0.870	0.9936	0.9939	0.9944	0.9950	0.9952	0.9955	0.9958	0.9961	0.9964	0.9966
0.875	0.9938	0.9941	0.9946	0.9952	0.9954	0.9957	0.9960	0.9962	0.9965	0.9968
0.880	0.9941	0.9943	0.9948	0.9954	0.9956	0.9959	0.9961	0.9964	0.9966	0.9969
0.885	0.9943	0.9946	0.9951	0.9955	0.9958	0.9960	0.9963	0.9965	0.9968	0.9970
0.890	0.9946	0.9948	0.9953	0.9957	0.9960	0.9962	0.9965	0.9967	0.9969	0.9972
0.895	0.9948	0.9950	0.9955	0.9959	0.9962	0.9964	0.9966	0.9968	0.9971	0.9973
0.900	0.9951	0.9953	0.9957	0.9961	0.9963	0.9966	0.9968	0.9970	0.9972	0.9974
0.905	0.9953	0.9955	0.9959	0.9963	0.9965	0.9967	0.9969	0.9971	0.9973	0.9975
0.910	0.9955	0.9957	0.9961	0.9965	0.9967	0.9969	0.9971	0.9973	0.9975	0.9977
0.915	0.9958	0.9960	0.9963	0.9967	0.9969	0.9971	0.9973	0.9974	0.9976	0.9978
0.920	0.9960	0.9962	0.9966	0.9969	0.9971	0.9972	0.9974	0.9976	0.9978	0.9979
0.925	0.9963	0.9965	0.9968	0.9971	0.9973	0.9974	0.9976	0.9977	0.9979	0.9981
0.930	0.9965	0.9967	0.9970	0.9973	0.9974	0.9976	0.9977	0.9979	0.9980	0.9982
0.935	0.9968	0.9969	0.9972	0.9975	0.9976	0.9978	0.9979	0.9980	0.9982	0.9983
0.940	0.9970	0.9972	0.9974	0.9977	0.9978	0.9979	0.9981	0.9982	0.9983	0.9985
0.945	0.9973	0.9974	0.9976	0.9979	0.9980	0.9981	0.9982	0.9983	0.9985	0.9986
0.950	0.9975	0.9976	0.9979	0.9981	0.9982	0.9983	0.9984	0.9985	0.9986	0.9987
0.955	0.9978	0.9979	0.9981	0.9983	0.9984	0.9985	0.9985	0.9986	0.9987	0.9988
0.960	0.9980	0.9981	0.9983	0.9985	0.9985	0.9986	0.9987	0.9988	0.9989	0.9990
0.965	0.9983	0.9983	0.9985	0.9986	0.9987	0.9988	0.9989	0.9989	0.9990	0.9991
0.970	0.9985	0.9986	0.9987	0.9988	0.9989	0.9990	0.9990	0.9991	0.9992	0.9992
0.975	0.9988	0.9988	0.9989	0.9990	0.9991	0.9991	0.9992	0.9992	0.9993	0.9994
0.980	0.9990	0.9991	0.9991	0.9992	0.9993	0.9993	0.9994	0.9994	0.9994	0.9995
0.985	0.9993	0.9993	0.9994	0.9994	0.9995	0.9995	0.9995	0.9995	0.9996	0.9996
0.990	0.9995	0.9995	0.9996	0.9996	0.9996	0.9997	0.9997	0.9997	0.9997	0.9997
0.995	0.9998	0.9998	0.9998	0.9998	0.9998	0.9998	0.9998	0.9998	0.9999	0.9999

Micro AR = 0.950		Lower 95% confidence limit			Combined standard deviation		EAR calculated by this study		

NIRAS   DHI   CARBON TRUST

Herring Gull - Macro avoidance rate										
Meso avoidance rate	0.45	0.50	0.55	0.60	0.65	0.70	0.75	0.80	0.85	0.90	0.95
0.660	0.9920	0.9927	0.9934	0.9942	0.9949	0.9956	0.9963	0.9971	0.9978	0.9985	0.9993
...											
0.850	0.9965	0.9968	0.9971	0.9974	0.9977	0.9981	0.9984	0.9987	0.9990	0.9994	0.9997
0.855	0.9966	0.9969	0.9972	0.9975	0.9978	0.9981	0.9984	0.9988	0.9991	0.9994	0.9997
0.860	0.9967	0.9970	0.9973	0.9976	0.9979	0.9982	0.9985	0.9988	0.9991	0.9994	0.9997
0.865	0.9968	0.9971	0.9974	0.9977	0.9980	0.9983	0.9985	0.9988	0.9991	0.9994	0.9997
0.870	0.9969	0.9972	0.9975	0.9978	0.9980	0.9983	0.9986	0.9989	0.9992	0.9994	0.9997
0.875	0.9970	0.9973	0.9976	0.9979	0.9981	0.9984	0.9987	0.9989	0.9992	0.9995	0.9997
0.880	0.9972	0.9974	0.9977	0.9979	0.9982	0.9985	0.9987	0.9990	0.9992	0.9995	0.9997
0.885	0.9973	0.9975	0.9978	0.9980	0.9983	0.9985	0.9988	0.9990	0.9993	0.9995	0.9998
0.890	0.9974	0.9976	0.9979	0.9981	0.9983	0.9986	0.9988	0.9991	0.9993	0.9995	0.9998
0.895	0.9975	0.9977	0.9980	0.9982	0.9984	0.9986	0.9989	0.9991	0.9993	0.9995	0.9998
0.900	0.9976	0.9979	0.9981	0.9983	0.9985	0.9987	0.9989	0.9991	0.9994	0.9996	0.9998
0.905	0.9978	0.9980	0.9982	0.9984	0.9986	0.9988	0.9990	0.9992	0.9994	0.9996	0.9998
0.910	0.9979	0.9981	0.9983	0.9985	0.9986	0.9988	0.9990	0.9992	0.9994	0.9996	0.9998
0.915	0.9980	0.9982	0.9984	0.9985	0.9987	0.9989	0.9991	0.9993	0.9995	0.9996	0.9998
0.920	0.9981	0.9983	0.9985	0.9986	0.9988	0.9990	0.9991	0.9993	0.9995	0.9997	0.9998
0.925	0.9982	0.9984	0.9985	0.9987	0.9989	0.9990	0.9992	0.9994	0.9995	0.9997	0.9998
0.930	0.9983	0.9985	0.9986	0.9988	0.9989	0.9991	0.9992	0.9994	0.9995	0.9997	0.9998
0.935	0.9985	0.9986	0.9987	0.9989	0.9990	0.9992	0.9993	0.9994	0.9996	0.9997	0.9999
0.940	0.9986	0.9987	0.9988	0.9990	0.9991	0.9992	0.9994	0.9995	0.9996	0.9997	0.9999
0.945	0.9987	0.9988	0.9989	0.9991	0.9992	0.9993	0.9994	0.9995	0.9996	0.9998	0.9999
0.950	0.9988	0.9989	0.9990	0.9991	0.9992	0.9994	0.9995	0.9996	0.9997	0.9998	0.9999
0.955	0.9989	0.9990	0.9991	0.9992	0.9993	0.9994	0.9995	0.9996	0.9997	0.9998	0.9999
0.960	0.9991	0.9991	0.9992	0.9993	0.9994	0.9995	0.9996	0.9997	0.9997	0.9998	0.9999
0.965	0.9992	0.9992	0.9993	0.9994	0.9995	0.9995	0.9996	0.9997	0.9998	0.9998	0.9999
0.970	0.9993	0.9994	0.9994	0.9995	0.9995	0.9996	0.9997	0.9997	0.9998	0.9999	0.9999
0.975	0.9994	0.9995	0.9995	0.9996	0.9996	0.9997	0.9997	0.9998	0.9998	0.9999	0.9999
0.980	0.9995	0.9996	0.9996	0.9997	0.9997	0.9997	0.9998	0.9998	0.9999	0.9999	1.0000
0.985	0.9996	0.9997	0.9997	0.9997	0.9998	0.9998	0.9998	0.9999	0.9999	0.9999	1.0000
0.990	0.9998	0.9998	0.9998	0.9998	0.9998	0.9999	0.9999	0.9999	0.9999	1.0000	1.0000
0.995	0.9999	0.9999	0.9999	0.9999	0.9999	0.9999	0.9999	1.0000	1.0000	1.0000	1.0000
Micro AR = 0.950		EAR calculated using the macor and meso avoidance rate estimated by Krijgsveld et al. 2011. Note that the same methodology was not used in that study									

NIRAS   DHI   CARBON TRUST

Table 7.10. EARs for Great Black-backed Gull resulting from the micro avoidance rate as calculated by this study and for a range of macro and meso avoidance rates.

Great Black-backed Gull - Macro avoidance rate										
Meso avoidance rate	-0.15	-0.10	0.00	0.10	0.15	0.20	0.25	0.30	0.35	0.40
0.660	0.9832	0.9839	0.9854	0.9868	0.9876	0.9883	0.9890	0.9898	0.9905	0.9912
...										
0.830	0.9916	0.9920	0.9927	0.9934	0.9938	0.9942	0.9945	0.9949	0.9952	0.9956
0.835	0.9918	0.9922	0.9929	0.9936	0.9940	0.9943	0.9947	0.9950	0.9954	0.9957
0.840	0.9921	0.9924	0.9931	0.9938	0.9942	0.9945	0.9948	0.9952	0.9955	0.9959
0.845	0.9923	0.9927	0.9933	0.9940	0.9943	0.9947	0.9950	0.9953	0.9957	0.9960
0.850	0.9926	0.9929	0.9936	0.9942	0.9945	0.9948	0.9952	0.9955	0.9958	0.9961
0.855	0.9928	0.9931	0.9938	0.9944	0.9947	0.9950	0.9953	0.9956	0.9959	0.9963
0.860	0.9931	0.9934	0.9940	0.9946	0.9949	0.9952	0.9955	0.9958	0.9961	0.9964
0.865	0.9933	0.9936	0.9942	0.9948	0.9951	0.9954	0.9956	0.9959	0.9962	0.9965
0.870	0.9936	0.9939	0.9944	0.9950	0.9952	0.9955	0.9958	0.9961	0.9964	0.9966
0.875	0.9938	0.9941	0.9946	0.9952	0.9954	0.9957	0.9960	0.9962	0.9965	0.9968
0.880	0.9941	0.9943	0.9948	0.9954	0.9956	0.9959	0.9961	0.9964	0.9966	0.9969
0.885	0.9943	0.9946	0.9951	0.9955	0.9958	0.9960	0.9963	0.9965	0.9968	0.9970
0.890	0.9946	0.9948	0.9953	0.9957	0.9960	0.9962	0.9965	0.9967	0.9969	0.9972
0.895	0.9948	0.9950	0.9955	0.9959	0.9962	0.9964	0.9966	0.9968	0.9971	0.9973
0.900	0.9951	0.9953	0.9957	0.9961	0.9963	0.9966	0.9968	0.9970	0.9972	0.9974
0.905	0.9953	0.9955	0.9959	0.9963	0.9965	0.9967	0.9969	0.9971	0.9973	0.9975
0.910	0.9955	0.9957	0.9961	0.9965	0.9967	0.9969	0.9971	0.9973	0.9975	0.9977
0.915	0.9958	0.9960	0.9963	0.9967	0.9969	0.9971	0.9973	0.9974	0.9976	0.9978
0.920	0.9960	0.9962	0.9966	0.9969	0.9971	0.9972	0.9974	0.9976	0.9978	0.9979
0.925	0.9963	0.9965	0.9968	0.9971	0.9973	0.9974	0.9976	0.9977	0.9979	0.9981
0.930	0.9965	0.9967	0.9970	0.9973	0.9974	0.9976	0.9977	0.9979	0.9980	0.9982
0.935	0.9968	0.9969	0.9972	0.9975	0.9976	0.9978	0.9979	0.9980	0.9982	0.9983
0.940	0.9970	0.9972	0.9974	0.9977	0.9978	0.9979	0.9981	0.9982	0.9983	0.9985
0.945	0.9973	0.9974	0.9976	0.9979	0.9980	0.9981	0.9982	0.9983	0.9985	0.9986
0.950	0.9975	0.9976	0.9979	0.9981	0.9982	0.9983	0.9984	0.9985	0.9986	0.9987
0.955	0.9978	0.9979	0.9981	0.9983	0.9984	0.9985	0.9985	0.9986	0.9987	0.9988
0.960	0.9980	0.9981	0.9983	0.9985	0.9985	0.9986	0.9987	0.9988	0.9989	0.9990
0.965	0.9983	0.9983	0.9985	0.9986	0.9987	0.9988	0.9989	0.9989	0.9990	0.9991
0.970	0.9985	0.9986	0.9987	0.9988	0.9989	0.9990	0.9990	0.9991	0.9992	0.9992
0.975	0.9988	0.9988	0.9989	0.9990	0.9991	0.9991	0.9992	0.9992	0.9993	0.9994
0.980	0.9990	0.9991	0.9991	0.9992	0.9993	0.9993	0.9994	0.9994	0.9994	0.9995
0.985	0.9993	0.9993	0.9994	0.9994	0.9995	0.9995	0.9995	0.9995	0.9996	0.9996
0.990	0.9995	0.9995	0.9996	0.9996	0.9996	0.9997	0.9997	0.9997	0.9997	0.9997
0.995	0.9998	0.9998	0.9998	0.9998	0.9998	0.9998	0.9998	0.9998	0.9999	0.9999

| Micro AR = 0.950 | | Lower 95% confidence limit | | | Combined standard deviation | | | EAR calculated by this study | | |

INFORMING COLLISION RISK ASSESSMENT

NIRAS DHI CARBON TRUST

Meso avoidance rate	0.45	0.50	0.55	0.60	0.65	0.70	0.75	0.80	0.85	0.90	0.95
Great Black-backed Gull - Macro avoidance rate											
0.660	0.9920	0.9927	0.9934	0.9942	0.9949	0.9956	0.9963	0.9971	0.9978	0.9985	0.9993
...											
0.830	0.9960	0.9963	0.9967	0.9971	0.9974	0.9978	0.9982	0.9985	0.9989	0.9993	0.9996
0.835	0.9961	0.9965	0.9968	0.9972	0.9975	0.9979	0.9982	0.9986	0.9989	0.9993	0.9996
0.840	0.9962	0.9966	0.9969	0.9972	0.9976	0.9979	0.9983	0.9986	0.9990	0.9993	0.9997
0.845	0.9963	0.9967	0.9970	0.9973	0.9977	0.9980	0.9983	0.9987	0.9990	0.9993	0.9997
0.850	0.9965	0.9968	0.9971	0.9974	0.9977	0.9981	0.9984	0.9987	0.9990	0.9994	0.9997
0.855	0.9966	0.9969	0.9972	0.9975	0.9978	0.9981	0.9984	0.9988	0.9991	0.9994	0.9997
0.860	0.9967	0.9970	0.9973	0.9976	0.9979	0.9982	0.9985	0.9988	0.9991	0.9994	0.9997
0.865	0.9968	0.9971	0.9974	0.9977	0.9980	0.9983	0.9985	0.9988	0.9991	0.9994	0.9997
0.870	0.9969	0.9972	0.9975	0.9978	0.9980	0.9983	0.9986	0.9989	0.9992	0.9994	0.9997
0.875	0.9970	0.9973	0.9976	0.9979	0.9981	0.9984	0.9987	0.9989	0.9992	0.9995	0.9997
0.880	0.9972	0.9974	0.9977	0.9979	0.9982	0.9985	0.9987	0.9990	0.9992	0.9995	0.9997
0.885	0.9973	0.9975	0.9978	0.9980	0.9983	0.9985	0.9988	0.9990	0.9993	0.9995	0.9998
0.890	0.9974	0.9976	0.9979	0.9981	0.9983	0.9986	0.9988	0.9991	0.9993	0.9995	0.9998
0.895	0.9975	0.9977	0.9980	0.9982	0.9984	0.9986	0.9989	0.9991	0.9993	0.9995	0.9998
0.900	0.9976	0.9979	0.9981	0.9983	0.9985	0.9987	0.9989	0.9991	0.9994	0.9996	0.9998
0.905	0.9978	0.9980	0.9982	0.9984	0.9986	0.9988	0.9990	0.9992	0.9994	0.9996	0.9998
0.910	0.9979	0.9981	0.9983	0.9985	0.9986	0.9988	0.9990	0.9992	0.9994	0.9996	0.9998
0.915	0.9980	0.9982	0.9984	0.9985	0.9987	0.9989	0.9991	0.9993	0.9995	0.9996	0.9998
0.920	0.9981	0.9983	0.9985	0.9986	0.9988	0.9990	0.9991	0.9993	0.9995	0.9997	0.9998
0.925	0.9982	0.9984	0.9985	0.9987	0.9989	0.9990	0.9992	0.9994	0.9995	0.9997	0.9998
0.930	0.9983	0.9985	0.9986	0.9988	0.9989	0.9991	0.9992	0.9994	0.9995	0.9997	0.9998
0.935	0.9985	0.9986	0.9987	0.9989	0.9990	0.9992	0.9993	0.9994	0.9996	0.9997	0.9999
0.940	0.9986	0.9987	0.9988	0.9990	0.9991	0.9992	0.9994	0.9995	0.9996	0.9997	0.9999
0.945	0.9987	0.9988	0.9989	0.9991	0.9992	0.9993	0.9994	0.9995	0.9996	0.9998	0.9999
0.950	0.9988	0.9989	0.9990	0.9991	0.9992	0.9994	0.9995	0.9996	0.9997	0.9998	0.9999
0.955	0.9989	0.9990	0.9991	0.9992	0.9993	0.9994	0.9995	0.9996	0.9997	0.9998	0.9999
0.960	0.9991	0.9991	0.9992	0.9993	0.9994	0.9995	0.9996	0.9997	0.9997	0.9998	0.9999
0.965	0.9992	0.9992	0.9993	0.9994	0.9995	0.9995	0.9996	0.9997	0.9998	0.9998	0.9999
0.970	0.9993	0.9994	0.9994	0.9995	0.9995	0.9996	0.9997	0.9997	0.9998	0.9999	0.9999
0.975	0.9994	0.9995	0.9995	0.9996	0.9996	0.9997	0.9997	0.9998	0.9998	0.9999	0.9999
0.980	0.9995	0.9996	0.9996	0.9997	0.9997	0.9997	0.9998	0.9998	0.9999	0.9999	1.0000
0.985	0.9996	0.9997	0.9997	0.9997	0.9998	0.9998	0.9998	0.9999	0.9999	0.9999	1.0000
0.990	0.9998	0.9998	0.9998	0.9998	0.9998	0.9999	0.9999	0.9999	0.9999	1.0000	1.0000
0.995	0.9999	0.9999	0.9999	0.9999	0.9999	0.9999	0.9999	1.0000	1.0000	1.0000	1.0000

Micro AR = 0.950

EAR calculated using the macor and meso avoidance rate estimated by Krijgsveld et al. 2011
Note that the same methodology was not used in that study

NIRAS   DHI   CARBON TRUST

7.5. INFORMING CRM INPUT PARAMETERS

7.5.1. As indicated in Section 7.2, illustrated by Figure 7.1: The collision risk model (Band 2012) and its key input parameters, in addition to overall avoidance rates the Band (2012) collision risk model requires detailed data in relation to:

- **Design parameters** (blade width, blade length, blade pitch, rotor speed, hub height) and wind farm productivity (% time);

- The **flux of birds** for the species in question (density per km^2, flight speed, proportion at rotor height, nocturnal flight activity);

- **Biometric data** (wing span, body length) and data on flight height, flight speed and diurnal/nocturnal activity; and

7.5.2. In addition, the extended version of the Band Model (2012) requires data on flight heights, as a frequency distribution of heights at high resolution, which is used to partition the flux of birds through the various parts of the RSZ as a means to estimate rates of collision of low flying species with higher precision.

7.5.3. This study provides important and enhanced input for some of the required data used in the Band model, including species-specific data on flight speeds, species-specific evidence on flight heights that can inform flight height distributions, and empirical evidence on nocturnal activity.

a. Species-specific flight speed

7.5.4. At present, flight speed data for use in CRM relies on published data based on very small sample sizes. If data is lacking for a specific-species, it is recommended to use data from a surrogate (similar) species instead (SNH 2014).

7.5.5. The rangefinder track data recorded in Thanet offer species-specific empirical data on flight speeds and track speeds (limited to the length of tracks, Table 7-6) from large numbers of individuals, albeit in non-adverse weather conditions. As such, the data are a valuable source of information on more realistic mean flight speeds and associated variability in offshore wind farms necessary for improving estimates of the flux of birds for the species in question. It should be noted that currently only one flight speed is used in the Band model and is used for calculating both the flux and collision risk when flying through the rotor. For the flux calculation, the track speed is more appropriate and for flight speed through the rotor the flight speed is better to use.

Table 7.11. **Species-specific mean flight speeds (m/s) often used in CRM, and those measured from single rangefinder segments recorded at Thanet (SD is shown in brackets).**

Species	Flight speed commonly used (no. of tracks)	Flight speed estimated by the study
Northern Gannet	14.9* (32)	13.33 (4.24) [n=683]
Black-legged Kittiwake	13.1** (2)	8.71 (3.16) [n= 287]
Lesser Black-Backed Gull	13.1** (11)	
Great Black-backed Gull	13.7** (4)	9.80 (3.63)*** [n=790]
Herring Gull	12.8** (18)	

NIRAS DHI CARBON TRUST

* Pennycuick (1997)
** Alestarm et al. (2007)
*** Estimated with data for all large gulls combined

b. Species-specific flight heights

7.5.6. Given that the risk of collision is associated with the flight height (risk is only considered present at flight heights between the lowest and highest points of the rotors), CRMs can be informed by the proportion of birds flying within that risk height.

7.5.7. Most of the existing evidence on seabird flight heights comes from observers on boats, assigning birds to height categories, which can be used to generate flight height distributions (Johnston et al. 2014). However, height estimates from boat surveys are subjective (Camphuysen et al. 2004) and their accuracy has not been assessed (Johnston et al. 2014). Other methods for obtaining these include the use of vertical radars (which does not allow species identification), rangefinders, or more recently applied aerial and LiDAR surveys.

7.5.8. The rangefinder track data collected at Thanet (outside the wind farm footprint) provide detailed data that can be used to develop flight height distributions for use in the Extended Band Model. Generic flight height distributions can be estimated from the rangefinder data using a non-linear smoothing algorithm (see e.g. Johnston et al. 2014).

c. Nocturnal activity

7.5.9. There is considerable uncertainty about levels of bird flight activity by night. Garthe and Hüppop (2004) offer an expert view on levels of nocturnal flight activity for a range of marine bird species, expressed in terms of a 1-5 ranking of the likely level of nocturnal activity in comparison with observed levels of daytime activity:

Species	Review by Garthe and Hüppop (2004) Nocturnal flight activity
Northern Gannet	2 (25%)
Black-legged Kittiwake	3 (50%)
Lesser Black-Backed Gull	3 (50%)
Greater Black-backed Gull	3 (50%)
Herring Gull	3 (50%)

Previous studies only managed to capture very small sample sizes (Desholm 2005), and therefore, the thermal video data collected by this study provide an unprecedented body of evidence on nocturnal flight activity by seabirds in an offshore wind farm, indicating very low activity during dark hours throughout the annual cycle. Based on the thermal videos processed, there is an indication that nocturnal flight activity may only constitute a negligible proportion of total flight activity of target species (most likely < 3%). However, given limitation in sample size of night videos, it is suggested to only use this evidence as anecdotal.

8 RECOMMENDATIONS FOR FUTURE WORK

8.1. SCOPE OF FUTURE STUDIES

8.1.1. Based on the study's agreed scope, associated limitations and remaining gaps in our understanding of bird behaviour around offshore wind farm, a number of additional areas of work have been identified and are recommended to be prioritised in future studies. These include:

- Studies to focus on bird avoidance behaviour at the meso and micro scales, as these have been identified as the most influential components in the estimation of overall EARs. Additional research on seabird distribution and behaviour inside offshore wind farms would therefore be beneficial. Such studies would ideally endeavour to acquire adequate sample sizes to allow the determination of species-specific micro avoidance.

- Studies to focus on the vertical component of avoidance behaviour at the meso scale. Additional studies aiming at collection of 3-D tracks around the RSZ would advance our understanding and quantification of vertical meso avoidance.

- Studies on macro avoidance to focus on capturing a range of weather and visibility conditions (including poor visibility and adverse weather conditions), as well as behaviour throughout the year. Deployment of monitoring equipment at other sites would also allow to better understand variability.

- Studies to focus on capturing the influence of other local factors on seabird behaviour around offshore wind farms, such as proximity to breeding colonies or presence and patterns of fishing activities.

- Studies to look into implications of seabird avoidance behaviour at demographic level, and that attempt to capture displacement to some extent.

- Studies to focus on the effect of distance to wind turbines on seabird flight height and speed.

- Studies to focus on comparisons between the proportion of flying to sitting seabirds inside and outside wind farms.

- Studies to focus on using military grade rangefinders at sites other than Thanet to measure the flight heights of Black-legged Kittiwakes.

- Studies to focus on improving the estimation of P_{Coll} in the Band model to better reflect the observed probability for seabirds to collide while crossing the spinning rotor.

- Studies to further explore Band (2012) and its input parameters for compatibility with empirically estimated, behaviour-based, avoidance rates.

8.1.2. Data collected by this study may be further explored to contribute to some of the areas listed above. For example:

- The database on radar images (screen dumps), which have been collected in parallel to the observer-aided tracking contain information on unspecified tracks of seabirds, and may represent a useful contribution to an assessment of seabird redistribution during adverse weather conditions and night time.

- Information on weather and visibility conditions present during data collection is available and could be used to further analyse the influence of these conditions on seabird behaviour.

- Only 48,000 night videos have been processed as part of this study, and although their processing is time consuming, particularly given the high false positive rate obtained, there may be additional video evidence on bird nocturnal activity in the remaining 411,164 night videos that have not been processed, and may be worth pursuing.

8.2. EQUIPMENT SET-UP AND PROTOCOLS FOR OBSERVATION

8.2.1. Based on lessons learned during the study's design and equipment operation, the following recommendations can be made in relation to equipment set-up and protocols used to obtain data on seabird distribution and behaviour around offshore wind farms:

- Recording bird activity at the macro scale. Two different types of radars have been applied in this study. The SCANTER-5000 radar used by observers from turbine G01 is a high-performance solid state radar with Doppler, while the three other radars used by observers from turbine G05 and as a basis for the radar-camera units on turbines D05 and F04 are standard magnetron-based marine radars (LAWR 25). The differences in detection probability, weather sensitivity and shading effects from turbines between the two types of radars have been compared during the study (see Appendix 2). These comparisons underlined the superior performance of the SCANTER radar compared to the magnetron-based radars in relation to the following features:

  ◊ Long detection distance
  ◊ Even detection probability within scanned range
  ◊ Low sensitivity to wave clutter
  ◊ Low sensitivity to rain clutter
  ◊ Limited interference from turbines

- Recording bird activity inside the wind farm. Although the high false-positive rate of the magnetron-based radars coupled to the cameras due to sensitivity to wave and rain clutter did allow for an estimate of meso and micro avoidance behaviour, tracking of seabird movements in and around the RSZ was hampered by the high level of wave-induced noise on the radar recordings. The SCANTER radar would constitute a more efficient, albeit also significantly more expensive alternative to be used with the cameras in order to obtain detailed tracking in the RSZ.

- There are different methods that can be used to record bird distribution and behaviour around offshore wind farms, the choice of these should, however, depend on the aims of a given study and the spatio-temporal range of conditions that want to be captured. For instance, a range of other studies has assessed macro avoidance behaviour either as a barrier effect or as displacement (see review by Cook et al. 2014). Examples include:

  ◊ post-construction monitoring studies at Horns Rev 1 (Vattenfall) and Nysted (EON), which estimated avoidance of long-distance migrants based on behavioural changes pre- and post-construction, and avoidance was assessed qualitatively (Petersen et al.et al. 2006).
  ◊ studies at Horns Rev 1 and Nysted by Blew et al. (2008) and the post-construction monitoring study at Horns Rev 2 (DONG Energy, Skov et al.et al. 2012), which assessed macro avoidance based on differences in measured mean number of tracks inside/outside the wind farm without consideration of detection bias by the radars and potential shading due to the turbines.
  ◊ post-construction monitoring study at Egmond aan Zee (Shell-NordzeeWind-Nuon, Krijgsveld et al. 2011), which dealt with the distance bias by comparing areas inside and around the wind farm that had comparable levels of detection loss (distance from radar) and dealt with the shading effect by correcting for detection loss in certain sectors of the wind farm. Macro avoidance was estimated by Krijgsveld et al. (2011) by comparing total number of recorded tracks inside/outside the wind farm corrected for relative surface area within and outside the wind farm.

- Development of sensor technologies for measuring micro and meso avoidance. Figure 8.1 and Figure 8.2 present the spatio-temporal coverage of the study's equipment in relation to previous studies and future technologies that may be developed or are in development. The development of the integrated radar-camera unit in ORJIP has solved the challenge of continuous data collection in an offshore wind farm in all weather conditions.

Figure 8.1. Spatio-temporal coverage of the study's equipment during *calm weather conditions* in relation to technologies previously used and those that may be developed in the future.
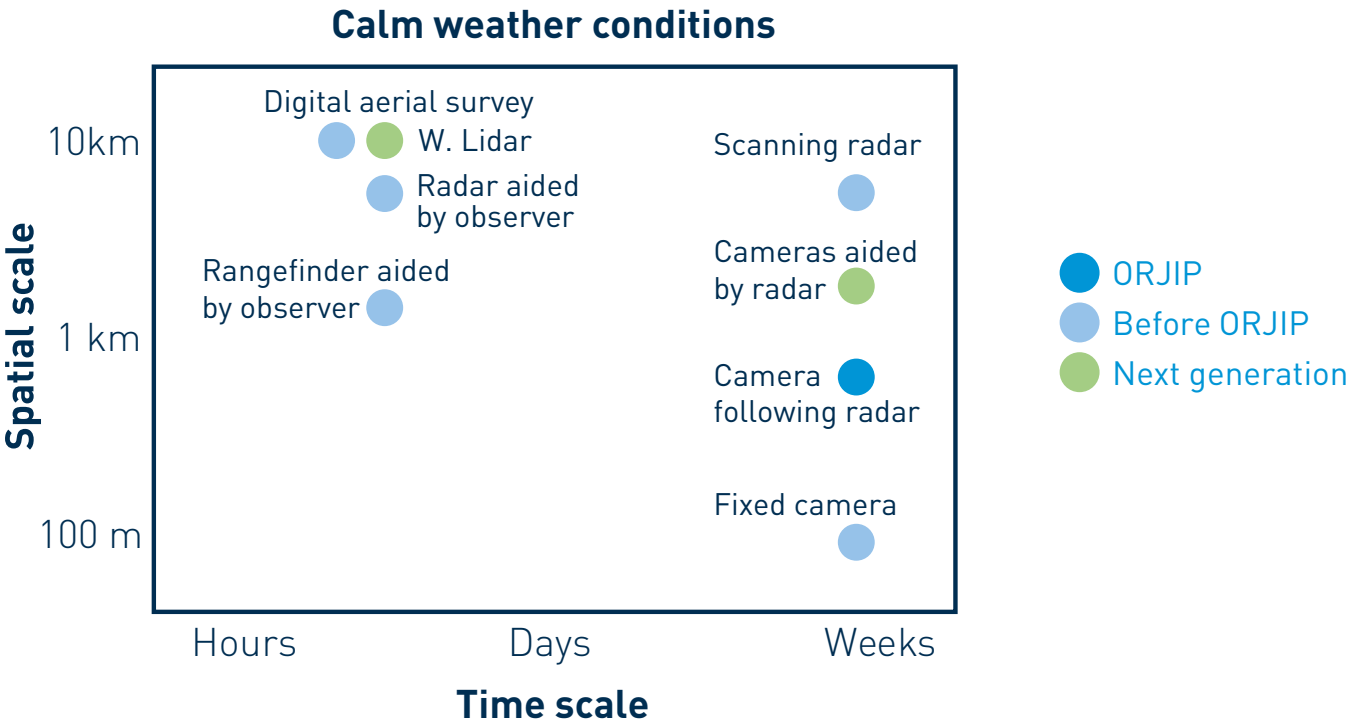
Figure 8.2. Spatio-temporal coverage of the study's equipment during *adverse weather conditions* in relation to technologies previously used and those that may be developed in the future.
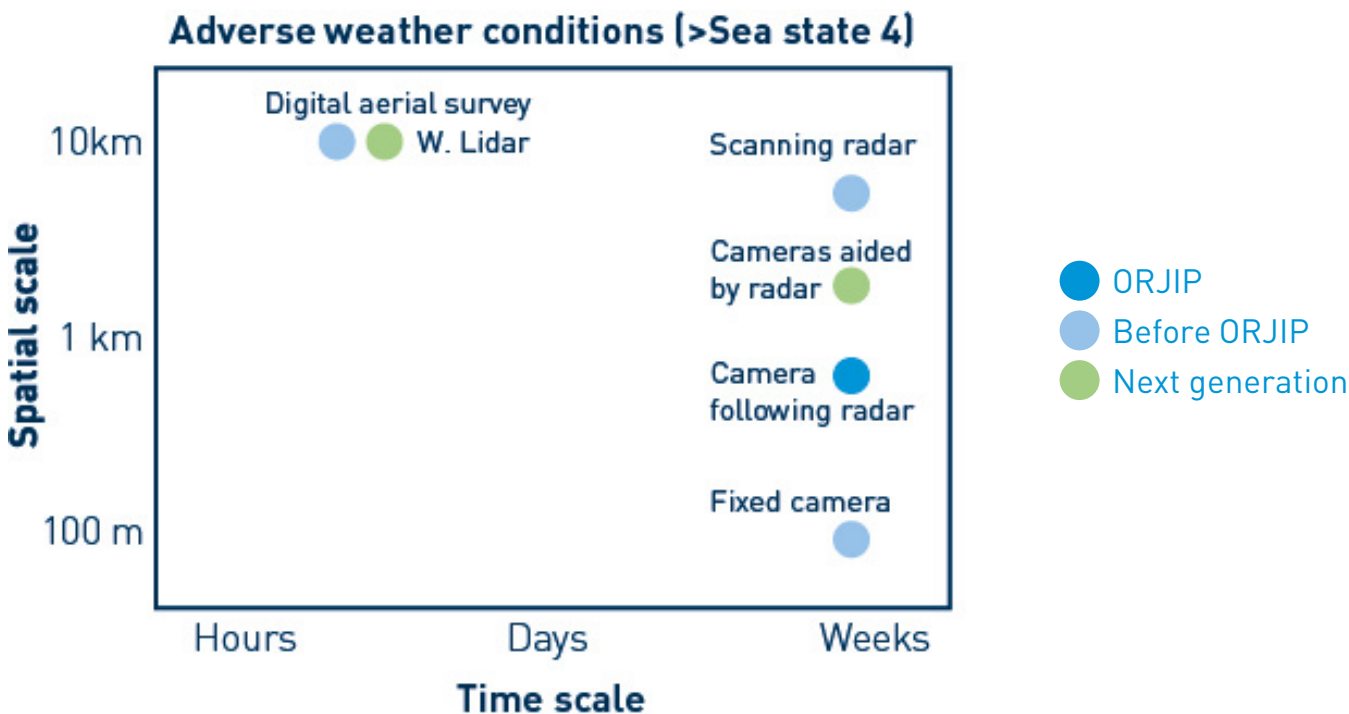
Future developments of digital aerial survey applications with LiDAR will resolve detailed flight height data for seabirds, at least during calm weather conditions. Development of video tracking with the radar-camera unit will enable the recording of videos with a duration over 20 s (as used in this study).

◇ If deployment of equipment is supported by seabird observers, it will be advantageous to improve the approach towards information recording, developing protocols that systematically record distance at which species are identified to species level (which can allow to better understand limitations and potential bias) or protocols that record fishing activity and their influence on bird behaviour observed.

8.3. INTERPRETATION AND ANALYSIS OF DATA

8.3.1. A number of methods of data analysis were considered at the inception of the study (see Appendix 8), however, the testing of all these methods was not within the scope of the study and only methods focused on the analysis of macro and meso avoidance based on track distribution were tested, which can be considered a proxy for avoidance behaviour. In line with other studies on seabird macro avoidance (Krijgsveld et al. 2011, Skov et al. 2012) methods based on assessments of behavioural responses were considered to introduce a level of subjectivity which would not suit the aim of the project.

8.4. APPLICATION OF EMPIRICAL EVIDENCE IN CRM

8.4.1. As presented in Section 7, there are a number of potential sources of error embedded in CRMs currently used, and that need to be better understood in order to ensure that collision estimates are in line with actual behaviour. The scale and direction of such errors and input parameters need to be further explored for compatibility with empirically estimated, behaviour-based, avoidance rates. One of the key issues here is the interaction between flux and avoidance behaviour based on more realistic flight speed.

8.4.2. As recommended in Section 7, avoidance behaviour should not be represented by a single value, but as a range of values that capture uncertainty around estimates. The further development and validation of CRMs that allow for the incorporation of uncertainty into CRMs is therefore recommended.

NIRAS DHI CARBON TRUST

⑨ CONCLUSIONS

9.1.1. This study has generated the most extensive dataset of observations of bird behaviour in and around an operational offshore wind farm that is currently available:

- Significant amount of identified bird tracks for the target species were collected by rangefinder (1,818 tracks) and radar (1,205 tracks – SCANTER)

- A total of 3,375 identified bird tracks were collected for the target species by rangefinder and the two radars (SCANTER and LAWR) located on the peripheral of the wind farm (turbines G01 and G05)

- Video evidence of bird behaviour inside an offshore wind farm (12,131 daylight videos + min. of 76 night videos with bird activity recorded)

- Vast number of unidentified tracks collected through radar screen dumps 24/7

- Unprecedented amount of data on flight height / flight speeds around an operational offshore wind farm recorded by use of rangefinder

9.1.2. Using an innovative combination of proven observational methods and new technologies, it has shown that target seabird species (Northern Gannet, Lesser Black-backed Gull, Herring Gull, Great Black-backed Gull and Black-legged Kittiwake), exhibit behaviours, at various spatial scales, that lead to an avoidance of the RSZ of operational offshore wind turbines.

9.1.3. These behaviours significantly reduce the risk of those seabird species colliding with rotating turbine blades than would otherwise be the case if there was no change in behaviour.

9.1.4. Data analysed at the macro scale were extracted from a range of 3 km, defined as the optimal range for the analyses given a trade-off between the optimal range of radar detection and observed bird behaviour, which has previously been observed in other studies, including Krijgsveldt et al. (2011), Petersen et al. (2006), Skov et al. (2012a) and Welcker & Nehls (2016). However, a level of uncertainty still exists regarding seabird's potential responses to wind farms beyond 3 km, which may have led to an underestimation empirical macro avoidance estimates. Similarly, there is uncertainty on whether responses recorded may be representative of adverse weather conditions and low visibility (night time conditions).

9.1.5. The level of macro avoidance in gulls reported by different post-construction projects is highly variable, and has often been estimated as negligible (Krijgsveld 2014, Deirschke et al. 2016). There seems to be particular uncertainty regarding the effect of attraction to fishing trawlers at the periphery of wind farms. Given that fishing activities at Thanet were not monitored during this study, it is therefore not known what effect fishing activities potentially might have on the distribution and macro avoidance patterns of gulls. Yet, this uncertainty could imply that macro EAR for gulls and Black-legged Kittiwake might represent a wider range of values than reported from this study, which should be taken into account when considering the level of uncertainty associated with the estimated EARs; therefore a separate uncertain component regarding this was also added.

9.1.6. To our knowledge, this is the first study to estimate empirical meso avoidance rates (including both horizontal and vertical avoidance) for the target species within a range of weather conditions and during dark hours. The vast majority of meso avoidance events recorded involve birds moving in the areas between turbine rows (99.4%) rather than showing avoidance of the RSZ by seabirds adjusting their flight height and flying below the rotor.

9.1.7. This is also one of the few studies aiming at estimating empirical micro avoidance rates within a large range of weather conditions based on actual orientation and activity of the rotor.

NIRAS DHI CARBON TRUST

9.1.8.   The sample of recorded videos of micro avoidance events (n=299) is considerably higher than the sample obtained from the fixed TADS camera at Nysted wind farm for 124 days deployment in 2004 and 2005 (9 recordings, Desholm 2005). The high false positive detection rate of the magnetron radars did not allow detailed 3-D tracking around and inside the rotor-swept zone. Future applications of high-performance radars with cameras are recommended to achieve the low false positive detection rate required for detailed tracking. Only 6 collisions were observed, representing 0.05% of recorded birds by the TADS system. Monitoring of seabird micro avoidance in other wind farms would allow documenting whether the low level of collisions is a general characteristic for the target species.

9.1.9.   The few thermal videos analysed indicate very low flight activity of target species during dark hours (<3%). In addition, unlike daytime videos an equal proportion of the thermal videos were recordings of sitting birds. The different studies documenting low nocturnal flight activity of target species strongly indicate that the level of nocturnal activity suggested by Garthe and Hüppop (2004) and commonly used for collision risk modelling may be too conservative and results in precautionary collision risk assessments. Additional analysis of night videos collected by this and other studies may provide additional information to the body of evidence currently available.

9.1.10.   The track length per unit area method, used to quantify empirical macro and meso avoidance, is considered to provide a reliable estimate of the level of redistribution of flying seabirds considered to result from the introduction of the wind farm, while taking account of the difference in the size of the areas over which track length densities are averaged and compared. Similarly, the coding protocols used to analyse empirical micro avoidance behaviour are considered to provide very good approximations to behaviour observed.

9.1.11.   These findings have important implications for Collision Risk Modelling (CRM), undertaken to predict likely collision morality rates of proposed offshore wind farms. This modelling assumes, in the first instance, that birds take no avoiding action. The predictions of these models are then corrected to account for avoidance behaviour as well as other uncertainties and inaccuracies in model assumptions. The correction factor applied is referred to as the 'Avoidance Rate'. Bird avoidance behaviour is, however, considered to be the most important source of error in uncorrected model outputs and hence the most important component of this overall 'Avoidance Rate'.

9.1.12.   The following overall EARs have been obtained, and are recommended to be used as a range in CRMs that allow to account for uncertainty. They are also considered applicable in the basic and extended version of the Band model (Band 2012). Thus, provided that empirically derived input parameters on flight speed in offshore wind farms and flight height outside offshore wind farms are applied the EARs can be readily used in the Band model. The bootstrap standards errors (describing variability) are combining with a range of assumed uncertainty components, i.e. the given standard deviation below is reflecting both variability and uncertainty.

- Northern Gannet: 0.999 ± 0.003 SD

- Black-legged Kittiwake: 0.998 ± 0.006 SD

- Herring Gull: 0.999 ± 0.005 SD

- Great Black-backed Gull: 0.996 ± 0.011 SD

- Lesser Black-backed gull: 0.998 ± 0.006 SD

- All large gulls: 0.998 ± 0.007 SD

9.1.13.   This study indicates that bird avoidance behaviour is likely to lead to a greater reduction in likely collision rates than current correction factors (avoidance rates) applied to the basic and extended Band Model assume. The EARs derived from the observations made in this study indicate avoidance behaviour that is an order of magnitude greater than that assumed in the avoidance rates currently applied to CRM. The inclusion of further information which leads to reduced uncertainty and which reduces reliance on assumptions could lead to more accurate estimates of collision risk.

NIRAS DHI CARBON TRUST

9.1.14. The key finding of this study, therefore, is that there is very strong, empirical evidence to assume very high avoidance of offshore wind turbines by the target seabird species investigated. This provides a compelling basis for using higher avoidance rates, for these species, than are currently advised for use in collision risk assessment in the UK. Those rates should be closer to those indicated by the EARs derived in this study.

9.1.15. As is the case of avoidance rates currently used, there are a number of sources of uncertainty associated with EARs, however, this study has attempted to quantify these and recommends that instead of using a mean value, a range of values are used in CRMs that allow to account for uncertainty.

9.1.16. It is recommended that Statutory Nature Conservation Bodies, and other technical advisers to planning decision-makers, consider their advice on appropriate Avoidance Rates for collision risk modelling to better reflect the EARs derived in this study.

REFERENCES

Alerstam, T., Rosén, M., Bäckman, J., Ericson, P.G.P. and Hellgren, O. (2007). Flight speeds among bird species: allometric and phylogenetic effects. PLoS Biology 5(8): e197. doi: 10.1371/journal.pbio.0050197 (open source).

Band, W. (2000). Windfarms and Birds: calculating a theoretical collision risk assuming no avoiding action. Scottish Natural Heritage Guidance Note. http://www.snh.gov.uk/planning-and-development/renewable-energy/onshore-wind/assessing-bird-collision-risks/.

Band, W., Madders, M. and Whitfield, D.P. (2007). Developing field and analytical methods to assess avian collision risk at windfarms. In De Lucas M, Janss G and Ferrer M (eds) 'Birds and Wind Power'. www.quercus.ptBand.

Band, W. (2012). Using a collision risk model to assess bird collision risks for offshore windfarms. The Crown Estate, 62pp, available at: https://www.bto.org/sites/default/.../Final_Report_SOSS02_Band1ModelGuidance.pdf.

Blew, J., Hoffmann, M., Nehls, G. and Hennig, V. (2008). Investigations of the bird collision risk and the response of harbour porpoises in the offshore wind farms Horns Rev, North Sea and Nysted, Baltic Sea, in Denmark. Part 1: Birds.

Bruderer, B. and Joss, J. (1969). Methoden und Probleme der Bestimmung von Radarquerschnitten freifliegender Vögel. Rev. Suisse Zool. 76: 1106–1118.

Camphuysen, C.J., Fox, A.D., Leopold, M.F. and Petersen, I.K. (2004). Towards standardised seabirds at sea census techniques in connection with environmental impact assessments for offshore wind farms in the U.K. A comparison of ship and aerial sampling methods for marine birds, and their applicability to offshore wind farm assessments. Koninklijk Nederlands Instituut voor Onderzoek der Zee Report to COWRIE.

Canty, A.J. (2002). Resampling Methods in R: The boot Package. Rnews 2002-3: 2-7, available at: www.r-project.org/doc/Rnews/Rnews_2002-3.pdf.

Carrillo, G. (2014). vec2dtransf: 2D Cartesian Coordinate Transformation. R package version 1.1. Available at: https://CRAN.R-project.org/package=vec2dtransf.

Chamberlain, D.E., Rehfinsch, M.M., Fox, A.D., Desholm, M. and Anthony, S.J. (2006). The effect of avoidance rates on bird mortality predictions made by wind turbine collision risk models. Ibis 148: 198-202.

Chivers, L.S., Lundy, M.G., Colhoun, K., Newton, S.F., Houghton, J.D.R. and Reid, N. (2012). Foraging trip time-activity budgets and reproductive success in the black legged kittiwake. Marine Ecology Progress Series, 456: 269-277.

Christensen, T.K., Petersen, I.K. and Fox, A.D. (2006). Effects on birds of the Horns Rev 2 offshore wind farm: Environmental Impact Assessment. NERI Report. Commissioned by Energy E2. Available at: https://ens.dk/sites/ens.dk/files/Vindenergi/baggrundsrapport_over_fugle.pdf.

Cleasby, I.R., Wakefield, D.E., Bearhop, S., Bodey, T.W., Votier, S.C. and Hamer, K.C. (2015). Three-dimensional tracking of a wide-ranging marine predator: flight heights and vulnerability to offshore wind farms. Journal of Applied Ecology, 52: 1-9.

Collier, M.P., Dirksen, S., Krijgsveld, K.L. (2011). A Review of Methods to Monitor Collisions or Micro-avoidance of Birds with Offshore Wind Turbines, Part 1: Review. Strategic Ornithological Support Services SOSS 03-A, Bureau Waaderburg bv. 38pp.

Cook, A.S.C.P., Ross-Smith, V.H., Roos, S., Burton, N.H.K., Beale, N., Coleman, C., Daniel, H., Fitzpatrick, S., Rankin, E., Norman, K. and Martin, G. (2011). Identifying a range of options to prevent or reduce avian collision with offshore wind farms, using a UK-based case study. BTO Research Report No. 580 to Defra. British Trust for Ornithology, Thetford.

NIRAS DHI CARBON TRUST

Cook, A.S.C.P., Johnstone, A., Wright, L.J. and Burton, N.H.K. (2012). A review of flight heights and avoidance rates of birds in relation to offshore wind farms. Strategic Ornithological Support Services. Project SOSS-02. BTO Report 618 for The Crown Estate.

Cook, A.S.C.P., Humphreys, E.M., Masden, E.A. and Burton, N.H.K. (2014). The avoidance rates of collision between birds and offshore turbines. BTO Research Report No. 656. British Trust for Ornithology, Thetford, 273pp.

Daunt, F., Benvenuti. S., Harris, M.P., Dall'Antonia, L., Elston, D.A. and Wanless, S. (2002). Foraging strategies of the black-legged kittiwake Rissa tridactyla at a North Sea colony: evidence for a maximum foraging range. Marine Ecology Progress Series, 245: 239-247.

Desholm, M. (2003). Thermal Animal Detection System (TADS). Development of a method for estimating collision frequency of migrating birds at offshore wind turbines. NERI Technical Report, No. 440.

Desholm, M. (2005). TADS investigations of avian collision risk at Nysted offshore wind farm, autumn 2004. National Environmental Research Institute. Ministry of Environment.

Dierschke, V., Furness, R.W. and Garthe, S. (2016). Seabirds and offshore wind farms in European waters: Avoidance and attraction. Biological Conservation 202: 59-68.

Drewitt, A.L., Langston, R.H.W. (2006). Assessing the impacts of wind farms on birds. Ibis 148 (Suppl. 1): 29–42.

Ecology Consulting (2011). Thanet Offshore Wind Farm. Ornithological Monitoring 2010-2011. Report commissioned by Thanet Offshore Wind Limited.

Elliot, K.H., Chivers, L., Bessey, L., Gaston, A.J., Hatch, S.A., Kato, A., Osborne, O., Ropert-Coudert, Y., Speakman, J.R. and Hare, J.F. (2014). Windscapes hape seabird instantaneous energy costs but adult behaviour buffers impacts on offspring. Movement Ecology, 2014, 2:1-15.

Everaert, J. (2014). Collision risk and micro avoidance rates of birds with wind turbines in Flanders. Bird Study, 61: 220-230.

Farrance, I. and Frenkel, R. (2012). Uncertainty of measurement: a review of the rules for calculating uncertainty components through functional relationships. The Clinical Biochemist Reviews, 33(2): 49–75. Available at: https://www.ncbi.nlm.nih.gov/pmc/articles/PMC3387884/ FEBI (2013) Fehmarnbelt Fixed Link EIA. Bird Investigations in Fehmarnbelt – Baseline. Volume III. Bird Migration. Report No. E3TR0011 commissioned by Femern A/S. 333 pages (available at: http://vvmdocumentation.femern.com).

Furness, R., Wade, H. and Masden, E. (2013). Assessing vulnerability of marine bird populations to offshore wind farms. Journal of Environmental Management 119: 56–66.

Furness R (2016) Qualifying impact assessments for selected seabird populations: A review of recent literature and understanding. Report commissioned by Vattenfall, Statkraft and ScottishPower Renewables, 159 pp.

Furuno (2015). Model FAR21x7. Technical Specifications. Furuno, Japan. Available at: www.furuno.com/files/Brochure/236/upload/far-21x7.pdf

Garthe, S., Grémillet, D. and Furness, R.W. (1999. At-sea activity and foraging efficiency in chick-rearing northern gannets (Sula bassana): a case study in Shetland. Marine Ecology Progress Series, 185, 93-99.

Garthe, S. and Hüppop, O. (2004). Scaling possible adverse effects of marine wind farms on seabirds: developing and applying a vulnerability index. Journal of Applied Ecology 41: 724- 734.

Garthe, S., Ludynia, K., Hüppop, O., Kubetzki, U., Meraz, J.F. and Furness, R.W. (2012). Energy budgets reveal equal benefits of varied migration strategies in northern gannets. Marine Biology, 159, 1907-1915.

Garthe, S., Montevecchi, W.A. and Davoren, G.K. (2007). Flight destinations and foraging behaviour of northern gannets (Sula bassana) preying on small forage fish in a low-Arctic ecosystem. Deep-Sea Research II 54 (2007) 311-320.

Global Wind Energy Council (GWEC) (2017). Global Wind Report. Annual market update 2016. Available at: http://www.gwec.net/global-figures/wind-energy-global-status/.

Hamer, K.C., Monaghan, P., Uttley, J.D., Walton, P. and Burns, M.D. (1993. The influence of food supply on the breeding ecology of kittiwakes Rissa tridactyla in Shetland. Ibis, 135, 255-263.

Hamer, K.C., Phillips, R.A., Wanless, S., Harris, M.P. and Wood, A.G. (2000). Foraging ranges, diets and feeding locations of gannets in the North Sea: evidence from satellite telemetry. Marine Ecology Progress Series, 200, 257-264.

Hamer, K.C., Humphreys, E.M., Garthe, S., Hene, J., Peters, G., Grémillet, D., Phillips, R.A., Harris, M.P. and Wanless, S. (2007). Annual variation in diets, feeding locations and foraging behaviour of gannets in the North Sea: flexibility, consistency and constraint. Marine Ecology Progress Series, 338, 295-305.

Hamer, K.C., Humphreys, E.M., Magalhaes, M.C., Garthe, S., Hene, J., Peters, G., Gremillet, D., Skov, H. and Wanless, S. (2009). Fine-scale foraging behaviour of a medium-ranging marine predator. Journal of Animal Ecology, 78: 880-889.

Hartman, J.C., Krijgsveld, K.L., Poot, M.J.M., Fijn, R.C., Leopold, M.F. and Dirksen, S. (2012). Effects on birds of Offshore Wind farm Egmond aan Zee (OWEZ). An overview and integration of insights obtained. Report 12-005. Bureau Waardenburg, Culemborg, Netherlands. Available at: https://www.academia.edu/2387412/Effects_on_birds_of_Offshore_Wind_farm_Egmond_aan_Zee_OWEZ_._An_overview_and_integration_of_insights_obtained

Johnston, A., Cook, A.S.C.P., Wright, L.J., Humphreys, E.M. and Burton, N.H.K. (2014a). Modelling flight heights of marine birds to more accurately assess collision risk with offshore wind turbines. Journal of Applied Ecology, 51: 31-41.

Johnston, A., Cook, A.S.C.P., Wright, L.J., Humphreys, E.M. and Burton, N.H.K. (2014b). corrigendum. Journal of Applied Ecology, 51, doi: 10.1111/1365-2664.12260.

Kahlert, J., Leito, A., Laubek, B., Luigujõe, L., Kuresoo, A., Aaen, K., Luud, A. (2012). Factors affecting the flight altitude of migrating waterbirds inWestern Estonia. Ornis Fennica 89:241–253. Available at: https://www.ornisfennica.org/pdf/latest/2Kahlert.pdf.

King, S., Maclean, I.M.D., Norman, T. and Prior, A. (2009). Developing guidance on ornithological cumulative impact assessment for offshore wind developers. COWRIE.

Klaassen, R.H.G., Ens, B.J., Shamoun-Baranes, J., Exo, K.M. and Bairlain, F. (2012). Migration strategy of a flight generalist, the Lesser Black-backed Gull Larus fuscus. Behavioural Ecology, 23: 58-68.

Korner-Nievergelt, F., Brinkmann, R., Niermann, I., Behr, O. (2013). Estimating Bat and Bird Mortality Occurring at Wind Energy Turbines from Covariates and Carcass Searches Using Mixture Models. PLoS ONE 8(7): e67997.

Kotzerka, J., Garthe, S. and Hatch, S.A. (2010). GPS tracking device reveal foraging strategies of Black-legged Kittiwakes. Journal of Ornithollogy, 151:459-467.

Krijgsveld, K.L., Lensink, R., Schekkerman, H., Wiersma, P., Poot, M.J.M., Meesters, E.H.W.G. and Dirksen, S. (2005). Baseline studies North Sea wind farms: fluxes, flight paths and altitudes of flying birds 2003 - 2004. Report Number 05-041. Bureau Waardenburg, Culemborg.

Krijgsveld, K.L., Akershoek, F., Schenk, F., Dijk, F. and Dirksen, S. (2009). Collision risk of birds with modern large wind turbines. Ardea, 97(3): 357-366.

Krijgsveld, K.L., Fijn, R., Japink, M., Van Horssen, P., Heunks, C., Collier, M., Poot, M.J.M., Beuker, D., Dirksen, S. (2011). Effect studies offshore wind farm Egmond aan Zee. Final Report on fluxes, flight altitudes and behaviour of flying birds. Bureau Waardenburg bv. Nordzee Wind. 330pp.

Krijgsveld, K.L. (2014). Avoidance behaviour of birds around offshore wind farms. Overview of knowledge including effects of configuration. Bureau Waardenburg bv.

Langston, R.H.W. and Pullan, J.D. (2003). Windfarms and birds: an analysis of the effects of wind farms on birds, and guidance on environmental assessment criteria and site selection issues. Report T-PVS/Inf (2003) 12, by BirdLife International to the Council of Europe,Bern Convention on the Conservation of European Wildlife and Natural Habitats. RSPB/BirdLife in the UK.

Maling, D.H. (1973). Coordinate Systems and Map Projections. George Philip.

Masden, E. (2015). Developing an avian collision risk model to incorporate variability and uncertainty. Scottish Marine and Freshwater Science Vol 6 No 14. Edinburgh: Scottish Government, 43pp. DOI: 10.7489/1659-1.

Masden, E.A. and Cook, A.S.C.P. (2016). Avian collision risk models for wind energy impact assessments. Environmental Impact Assessment Review, 56 (1): 43-49.

May, R.F. (2015). A unifying framework for the underlying mechanisms of avian avoidance of wind turbines. Biological Conservation 190: 179 – 187. http://dx.doi.org/10.1016/j.biocon.2015.06.004.

Mendel, B., Kotzerka, J., Sommerfeld, J., Schwemmer, H., Sonntag, N. and Garthe, S. (2014). Effects of the Alpha Ventus offshore test site on distribution patterns, behaviour and flight heights of seabirds. In: Federal Ministry for the Environment, Nature Conservation and Nuclear Safety (Eds.) Ecological Research at the Offshore Windfarm alpha ventus, pp95 – 110. DOI: 10.1007/978-3-658-02462-8_11.

Orben, R.A., Irons, D.B., Paredes, R., Roby, D.D., Phillips, R.A. and Shaffer, S.A. (2015). North or south? Niche separation of endemic red-legged kittiwakes and sympatric black-legged kittiwakes during their non-breeding migrations. Journal of Biogeography, 42, 401-412.

Pennycuick, C.J. (1997). Actual and "optimum" flight speeds: field data reassessed. Journal of Experimental Biology, 200, 2355-2361.

Pennycuick, C.J., Åkesson, S., Hedenström, A. (2013). Air speeds of migrating birds observed by ornithodolite and compared with predictions from flight theory. Journal of the Royal Society Interface. Available at: http://rsif.royalsocietypublishing.org/content/10/86/20130419.

Petersen, I.K., Christensen, T.K., Kahlert, J., Desholm, M. and Fox, A.D. (2006). Final results of bird studies at the offshore wind farms at Nysted and Horns Reef. Rønde, Denmark: Report from NERI. Available at: www.oddzialywaniawiatrakow.pl/upload/file/83.pdf.

Pettex, E., Lorentsen, S.H., Gremillet, D., Gimenez, O., Barrett, R.T., Pons, J.B., Le Bohec, C. and Bonadonna, F. (2012). Multi-scale foraging variability in Northern Gannet (Morus bassanus) fuels potential foraging plasticity. Marine Biology, 159: 2743-2756.

Plonczkier, P. and Simms, I.C. (2012). Radar monitoring of migrating pink-footed geese: behavioural responses to offshore wind farm development. Journal of Applied Ecology 49: 1187-1194.

Potts, J.M. and Elith, J. (2006). Comparing species abundance models. Ecological Modelling (199), s. 153-163.

Pouillot, R., Delignette-Muller, M.L., Denis, J.B. (2013). mc2d: tools for two-dimensional Monte-Carlo simulations. Available at: http://cran.r-project.org/web/packages/mc2d/index.html.

Rehfisch, M., Barrett, Z., Brown, L., Buisson, R., Perez-Dominguez, R. & Clough, S. 2014. Assessing Northern Gannet Avoidance of offshore windfarms. Page 211-236 in: MacArthur Green, APEM & Royal Haskoning DHV. East Anglia THREE Appendix 13.1 Offshore Ornithology Evidence Plan. Volume 3 - Document reference – 6.3.13 (1). East Anglia Three Ltd.

Ross-Smith, V.H., Thaxter, C.B., Masden, E.A., Shamoun-Baranes, J., Burton, N.H.K., Wright, L.J., Rehfisch, M.M. and Johnston, A. (2016). Modelling flight heights of Lesser Black-backed Gulls and Great Skuas from GPS: a Bayesian approach. Journal of Applied Ecology 53 (6): 1676–1685. doi: 10.1111/1365-2664.12760.

Royal Haskoning (2009). Thanet Offshore Wind Farm. Annual Ornithological Monitoring Report: 2009 survey season annual report. Final Report 9T6750.

Royal Haskoning (2011). Thanet Offshore Wind Farm. Ornithological Monitoring 2010 – 2011. Final Report 9W4696.

Safi, K., Kranstauber, B., Weinzierl, R., Griffin, L., Rees, E.C., Cabot, D., Cruz, S., Proano, C., Takekawa, J.Y., Newman, S.H., Waldenström, J., Bengtsson, D., Kays, R., Wikelski, M. and Bohrer, G. (2013). Flying with the wind: scale dependency of speed and direction measurements in modelling wind support in avian flight. Movement Ecology, 1: 1-13.

NIRAS DHI CARBON TRUST

Schmaljohann, H., Liechti, F., Bächler, E., Steuri, S. and Bruderer, B. (2008). Quantification of bird migration by radar – a detection probability problem. Ibis 150: 342-355.

Scottish Natural Heritage [SNH] (2000). Windfarms and Birds: Calculating a Theoretical Collision Risk Assuming no Avoiding Action.

Shepard, E.L.C., Williamson, C., Windsor, S.P. (2016). Fine-scale flight strategies of gulls in urban airflows indicate risk and reward in city living. Philosophical transactions of the Royal Society. Available at: http://rstb.royalsocietypublishing.org/content/371/1704/20150394#ref-19.

SNH (2010). Use of Avoidance Rates in the SNH Wind Farm Collision Risk Model. SNH Avoidance Rate information and Guidance Note. Available at: http://www.snh.gov.uk/planning-and-development/renewable-energy/onshore-wind/bird-collision-risks-guidance/.

SNH (2014). Flight speeds and biometrics for collision risk modelling. Guidance. Available at: http://www.snh.gov.uk/planning-and-development/renewable-energy/onshore-wind/bird-collision-risks-guidance/.

Skolni, M.I. (1990). Radar Handbook. 2nd Edition. McGraw-Hill.

Skov, H., Leonhard, S.B., Heinänen, S., Zydelis, R., Jensen, N.E., Durinck, J., Johansen, T.W., Jensen, B.P., Hansen, B.L., Piper, W., Grøn, P.N. (2012a). Horns Rev 2 Offshore Wind Farm Bird Monitoring Program 2010-2012. DHI/Orbicon. Orbicon/DHI Report Commissioned by DONG Energy. 134pp. Available at: https://tethys.pnnl.gov/sites/default/files/publications/Horns_Rev_2_Migrating_Birds_Monitoring_2012.pdf.

Skov, H., Heinänen, S., Jensen, N.E., Dunrinck, J., Johansen, T.W., Jensen, B.P. (2012b). Rødsand 2 Offshore Wind Farm Post Construction. Post Construction Studies on Migrating Red Kite/Landbirds. DHI Report commissioned by E.ON.

Skov, H., Desholm, M., Heinänen, S., Christensen, T.K., Durinck, J., Jensen, N.E., Johansen, T.W. and Jensen, B.P. (2012c). Anholt Offshore Wind Farm - Supplementary Baseline Surveys of Bird Migration. DHI Report Commissioned by DONG Energy.

Skov, H. and Heinänen, S. (2013). Predicting the weather-dependent collision risk for birds at wind farms. In Hull C, Bennet E, Stark E, Smales I, Lau J, Venosta (Eds): Wind and wildlife 2012. Proceedings from the Conference on Wind Energy and Wildlife Impacts. Spinger.

Skov, H., Desholm, M., Heinänen, S., Johansen, T.W. and Therkildsen, O.R. (2015). Birds and bats at Kriegers Flak - Baseline investigations and impact assessment for establishment of an offshore wind farm. DHI Report Commissioned by EnergiNet Dk.

Joint Nature Conservation Committee (JNCC), Natural England (NE), Natural Resource Wales (NRW), Northern Ireland Environment Agency (NIEA), Scottish Natural Heritage (SNH) (2014). Joint Response from the Statutory Nature Conservation Bodies to the Marine Scotland Science Avoidance Rate Review. 25th November 2014.

Terma (2012). SCANTER 5000. Surface movement radar. Technical specifications. Terma, Lystrup, Denmark.

Thaxter, C.B., Ross-Smith, V.H., Clark, N.A., Conway, G.J., Rehfisch, M.M., Bouten, W. and Burton, N.H.K. (2011). Measuring the interaction between marine features of Special Protection Areas with offshore wind farm development zones through telemetry: first breeding season report. BTO Research Report No. 590, 72pp. Available at: www.gov.uk/government/uploads/system/uploads/attachment_data/file/197411/OESEA2_BTO_Research_Report_590.pdf.

Vanermen, N., Stienen, E.W.M., Courtens, W., Onkelinx, T., Van de walle, M. and Verstraete, H. (2013). Bird monitoring at offshore wind farms in the Belgian part of the North Sea - Assessing seabird displacement effects. Rapporten van het Instituut voor Natuur- en Bosonderzoek 2013 (INBO.R.2013.755887). Instituut voor Natuur- en Bosonderzoek, Brussel.

Vanermen, N., Courtens, W., Van de walle, M., Verstraete, H. & Stienen, E.W.M. (2017). Seabird monitoring at the Thorntonbank offshore wind farm - Updated seabird displacement results & an explorative assessment of large gull behaviour inside the wind farm area. Rapporten van het Instituut voor Natuur- en Bosonderzoek 2017 (31). Instituut voor Natuur- en Bosonderzoek, Brussel. DOI: doi.org/10.21436/inbor.13185344

Vanermen, N., Onkelix, T., Courtens, W., Van de walle, M., Verstraete, H. and Stienen, E.W.M. (2014). Seabird

avoidance and attraction at an offshore wind farm in the Belgian part of the North Sea. Hidrobiologia. DOI 10.1007/s10750-014-2088-xVetronix AG (2010) Verification of technical data concerning data sheet. Verification Compliance Statement VECTOR21 Data Sheet. Art. Nr. 905 562

Votier, S.C., Bearhop, S., Witt, M.J., Inger, R., Thompson, D. and Newton, J. (2010). Individual responses of seabirds to commercial fisheries revealed using GPS tracking, stable isotopes and vessel monitoring systems. Journal of Applied Ecology, 47: 487-497

Welcker, J. and Nehls, G. (2016). Displacement of seabirds by an offshore wind farm in the North Sea. Marine Ecology Progress Series, 554: 173-182.

WindEurope (2017). Wind in power. 2016 European statistics. Available at: https://windeurope.org/wp-content/uploads/files/about-wind/statistics/WindEurope-Annual-Statistics-2016.pdf.

Winkelman, J.E. (1992). De invloed van de Sep-proefwindcentrale te Oosterbierum (Friesland) op vogels, 1: Aanvaringsslachtoffers. Arnhem, The Netherlands: RIN-rapport 92/2, IBN-DLO.

Wood, S.N. (2006). Generalized Additive Models: An Introduction with R. Chapman and Hall, London.

Zuur, A., Leno, E., Walker, N., Saveliev, A. and Smith, G. (2009). Mixed effects models and extensions in ecology. New York: Springer Science and Business Media.

Žydelis, R., Heinänen, S. and Johansen, T.W. (2015a). Sæby Offshore Wind Farm Baseline and impact assessment in relation to birds and bats. DHI Report Commissioned by EnergiNet Dk.

Žydelis, R., Heinänen, S. and Johansen, T.W. (2015b). Smålandsfarvandet Offshore Wind Farm Baseline and impact assessment in relation to birds and bats. DHI Report Commissioned by EnergiNet Dk.

APPENDICES

APPENDIX 1: SENSOR EQUIPMENT CHARACTERISTICS

1. INTRODUCTION

The monitoring system comprises the following equipment:

- **SCANTER 5000 radar** – fan beam and solid state radar with an enhanced tracking capability, able to suppress sea and ground clutter, and rain; applied with observer-aided tracking during daylight hours from turbine G01. Data collected by the SCANTER radar within 3 km from the wind farm perimeter have been used to analyse bird macro avoidance responses.

- **LAWR 25 radar** – fan beam and magnetron-based radar, applied with observer-aided tracking during daylight hours from turbine G05.

- **Vectronix 21 Aero laser rangefinders** – comparable to a handheld binocular equipped with a built-in, battery driven laser system. Rangefinders allow making recordings of distance, altitude and direction to a given object. In this study, rangefinders were operated by observers during daylight hours from turbines G01 and G05, where the selection of targets was often made through the SCANTER and LAWR radars. Data collected by rangefinders within 1.5 km have been used to analyse bird macro avoidance responses and measure flight heights.

- **Thermal Animal Detection System (TADS) and LAWR radars** – The TADS camera system consists of a pan-tilt housing with two thermal night vision cameras, programmed to connect with LAWR radar, which operated from turbines F04 and D05. Data collected by the TADS cameras and LAWR radar have been used to analyse meso avoidance and micro avoidance behaviour within the wind farm.

This Appendix provides an overview of the characteristics of the above sensors, including tests undertaken before deployment of the equipment at Thanet, and their application throughout the duration of the study. The following definitions should be considered:

- **Sensor scanning range**, defined as the scanning range set for this study in order to allow optimal detection in the main area of interest.

- **Sensor detection range**, defined as the maximum distance at which any object has been detected by the sensor. This can be determined by inspecting data collected for this study in relation to the distance to the sensor.

- **Sensor detection probability**, refers to the probability of the sensor registering a bird or a flock of birds, which is dependent on distance, orientation, shape, size, clutter, etc. Detection probability is a relative measure, and does not necessarily describe the proportion of the actual number of flying birds recorded at different distances from the radar.

- **Detection probability curve (DPC)**, defined as the probability curve for the sensor to find a bird or a flock of birds over distance.

Effective range in which individual birds are detected depend on the mathematical shape of the radar beam but also on the size of the bird (expressed as "radar cross-section" of a bird) and the specifications of the

NIRAS DHI CARBON TRUST

radar. DPCs are determined using sensor cross sections, reflecting on the size of a typical seabird. DPCs can be used to establish the sensor scanning range in order to ensure that optimal detection is reached in the area of interest.

It has been documented that detection probability may change as a function of the aspect of the flying seabird (Bruderer and Joss 1969; Schmaljohann et al. 2008), and can also vary depending on the size of the target being followed. This is because the radar cross section of a flying bird flying perpendicularly to the radar beam may be larger than a cross section of a flying bird flying at an oblique angle to the radar (in a direction towards or away from the radar beam).

2. SCANTER 5000 RADAR

The development of solid state technologies has made it possible to conduct free and flexible frequency selection over the full band (9.0-9.5 GHz) with the possibility of up to 16 sub bands, providing enhanced capacity to suppress sea and ground clutter, and rain, in comparison to a magnetron-based radar such as the LAWR 25 radar (see Section 3 of this Appendix). For this study, the SCANTER 5000 radar was used (Figure 1, Table 1).

Figure 1.   SCANTER 5000 radar installed on the laydown area of the work platform of turbine G01 at Thanet Offshore Wind Farm.

Table 1.   Specifications of the SCANTER 5000 radar.

Brand	Type	Power output	Frequency	Range cell size	Rotational speed	Antenna length
SCANTER	SCANTER 5000	0-20kW programmable	9.0-9.5 GHz programmable (16 sub bands)	3 m	60 rpm	3657 mm

Several filters were applied:

- Coherent Doppler-based processing, used to reduce or eliminate signals from slow moving and stationary objects.

- Constant false-alarm rate (CFAR) filters (Terma 2012), used to reduce sea waves, precipitation and noise, as well as to reduce time-side lobes from the pulse compression.

- Sea Clutter Discriminator, used to detect small targets normally hidden in sea clutter.

- Interference filter, used to reduce noise from other electromagnetic sources nearby.

Furthermore, the radar utilised a very short range cell size from the broad banded pulse compression, which reduced influence from precipitation and allowed recording a high resolution radar video which reduces clutter from wind turbines. The radar also utilised multiple frequencies (frequency diversity) transmitted with a time interval allowing time diversity, this was enhanced when combined with the frequency squint of

the SCANTER antennas. This technique smoothed out clutter and enhanced resolution of targets.

2.1. SCANNING / DETECTION RANGE

For this study, the scanning range of the SCANTER radar was set to 12 km in order to allow optimal detection within 6 km from the wind farm. Figure 2 shows the maximum distance at which target species were detected and followed from. Outside the wind farm, Northern Gannets and Black-legged Kittiwakes could be tracked from distances as far as 6.7 km, while large gulls were tracked from distances as far as 5.2 km. Inside the wind farm, Northern Gannet could be tracked from distances as far as 3.7 km, while tracking of Black-legged Kittiwake and large gulls was limited to distances from 3 km. Targets were subsequently identified to species level within a maximum of 2 km from the wind farm, depending on species, which means that some of the targets that were lost or did not enter the field of view for species identification by observers may have not been included in the analysis (see Appendix 2 for a comparison of tracks identified / unidentified using different equipment).

Figure 2. **Number of tracks of target species recorded by observers using the Scanter 5000 radar from turbine G01 inside and outside the wind farm. The number of tracks recorded at different distances from the radar has been corrected for the area scanned in each distance band. Data collected between 28 August 2014 and 31 December 2015.**
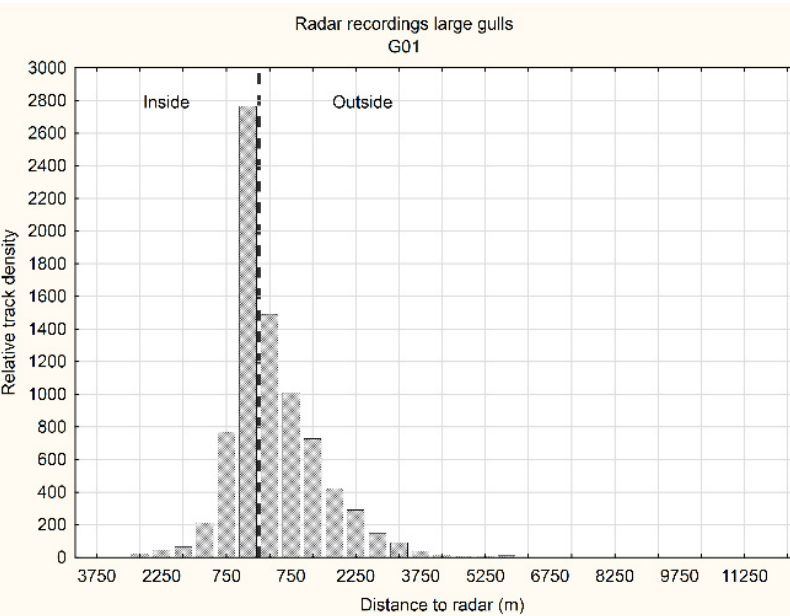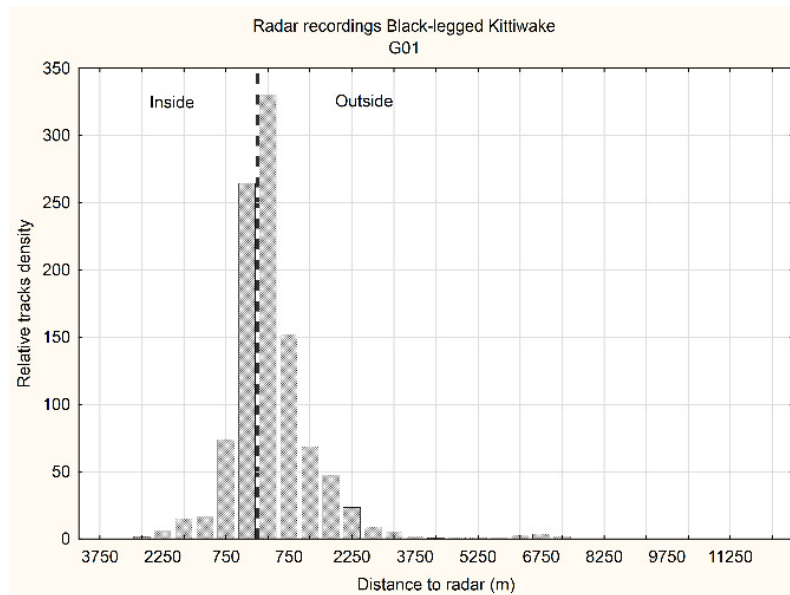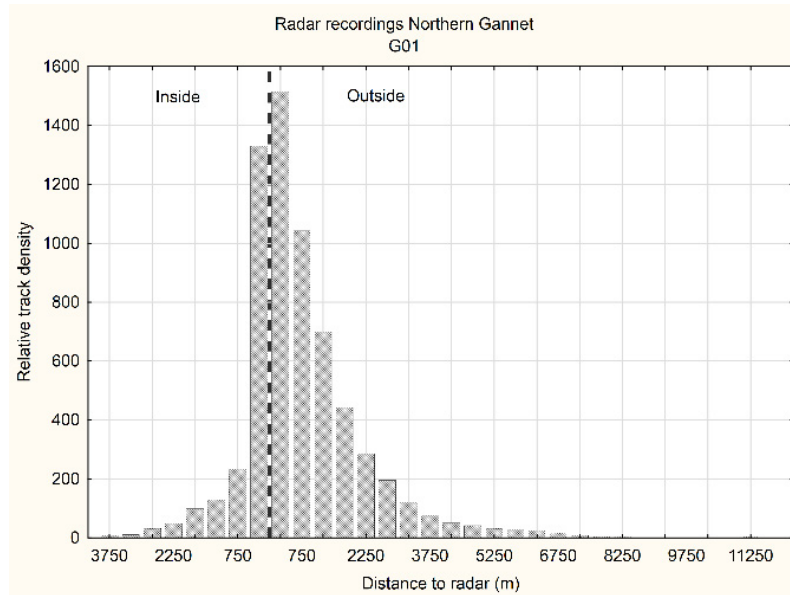
Theoretically, the SCANTER radar has a high and uniform detection probability throughout the scanned area, as indicated in Figure 3, with a detection probability close to 1.0 within the whole scanned range, and only slightly dropping after 5 km.

Figure 3. **Detection probability curve for SCANTER 5000 radar. The curve has been calculated on a radar cross section of 0.05 m² which is equivalent to that of a small seabird (Terma, pers. comm).**
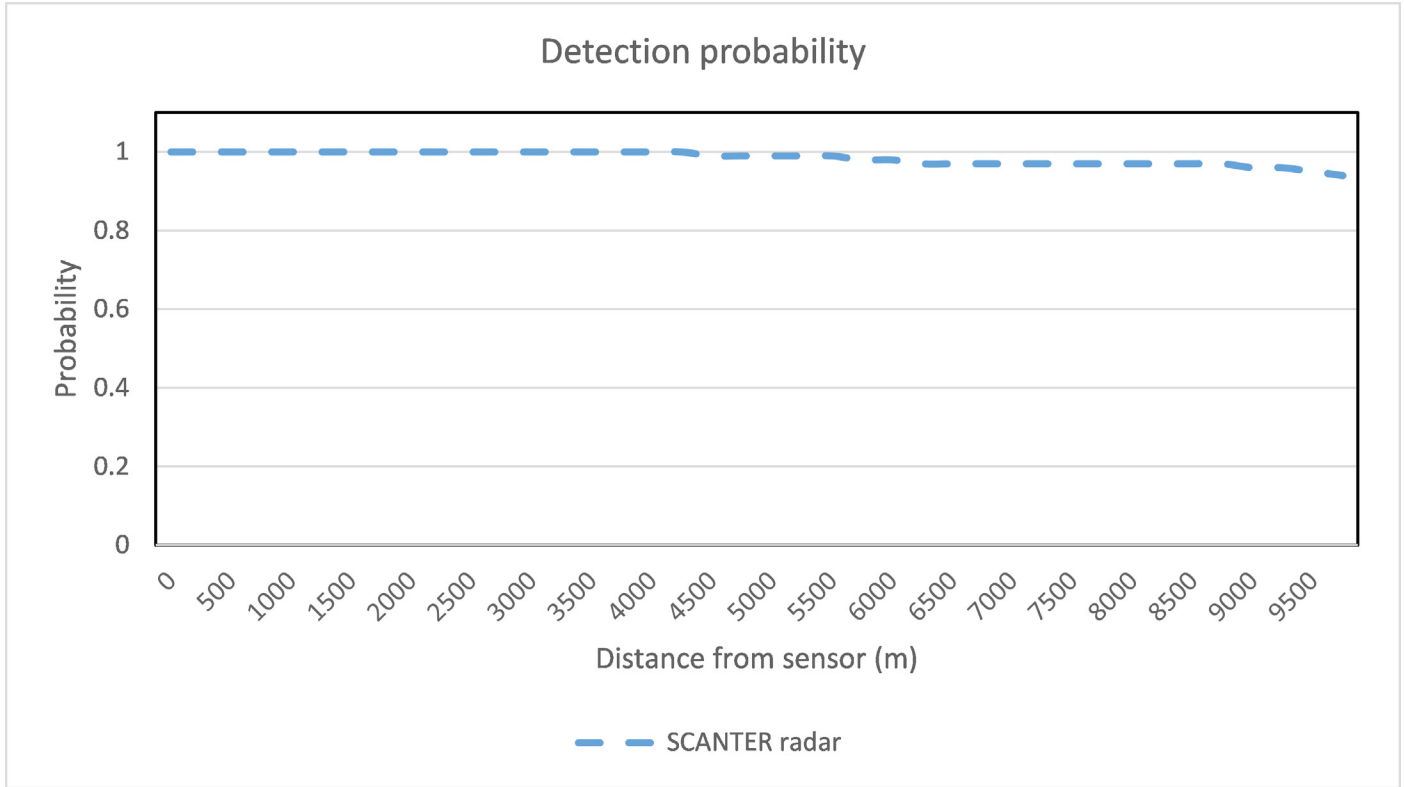
On account of the vertical angle of the radar beam, low-flying seabirds (<10 m) cannot be detected closer than 45 m from the SCANTER radar (Figure 4). For the same reason, the maximum height at which flying seabirds can be detected at 1 km distance is 385 m. However, the same limitation applies inside and outside the wind farm, making possible to compare both areas.

Figure 4. **Minimum (left) and maximum (right) detection distance versus flight altitude for the SCANTER 5000 (Terma 2012).**
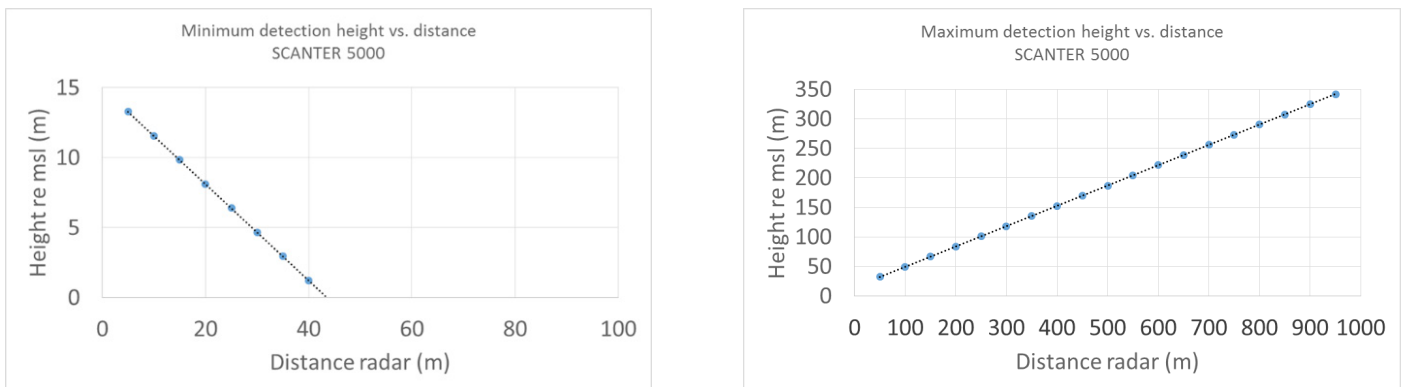
The angle of the blind sector of the SCANTER radar is visualised in Figure 5. The "side lobes" of the radar beam can reflect off bird targets along the sides of the active sector, and tracked birds moving into the blind sector may be recorded over a short distance due to the tracker software.

Figure 5. Angle of the blind sector of the SCANTER radar in turbine G01. The green line defines the blind sector for the radar. The blue and red lines define the blind sector for the rangefinder, the blue showing fully obstructed view and between red and blue partially obstructed view by the turbine metal structures.
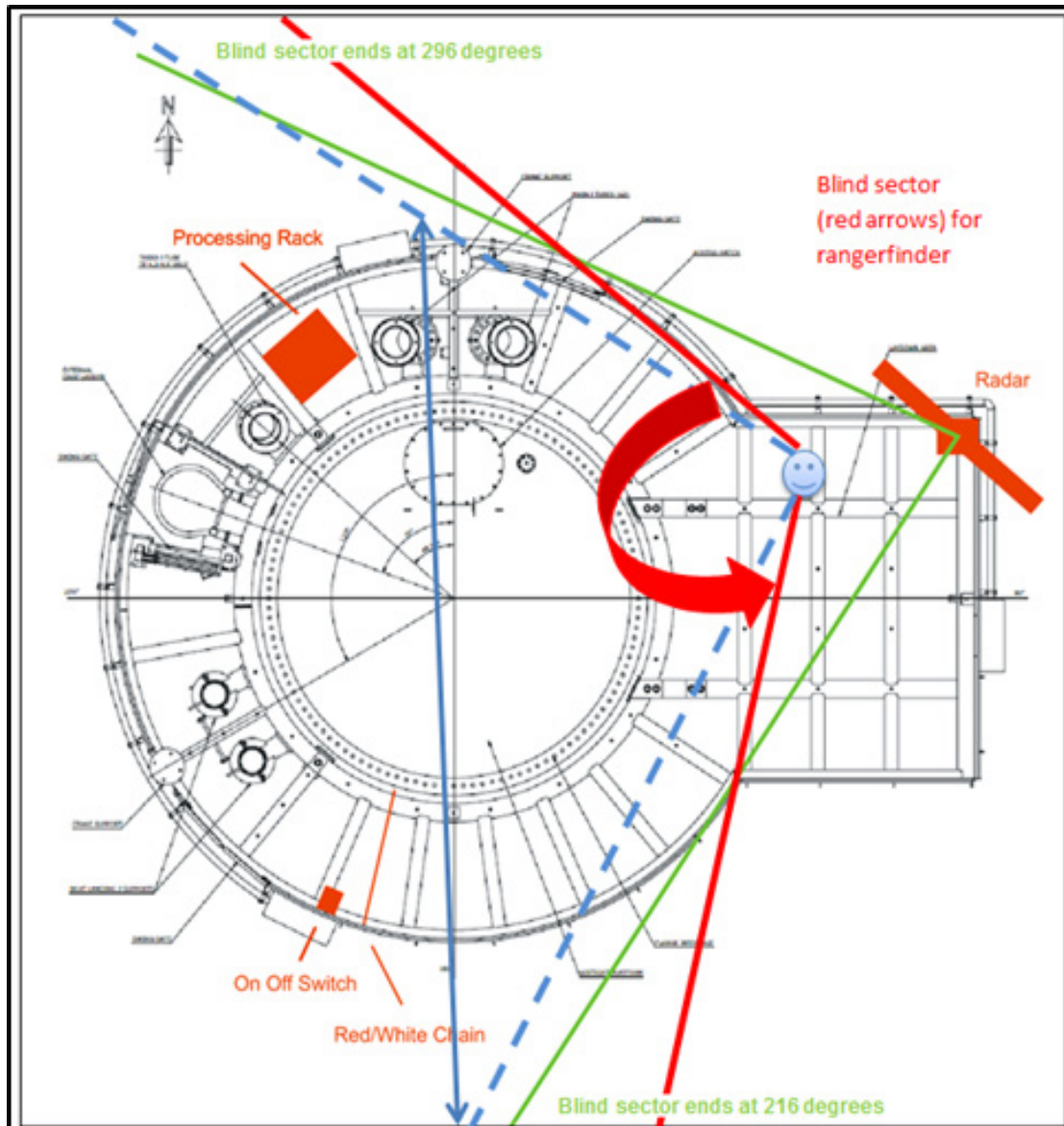
2.3. APPLICATION

The SCANTER radar was applied in order to ensure a high resolution detection of bird signals, and minimise the risk of turbines and rotors interfering with the tracking of birds.

The radar software consisted of a Tracker and Doppler Enhanced processing software, coupled with a BirdTracker GIS-based software, which enabled for real-time tracking and geo-referencing of up to ten different bird targets at a time followed on background video images (see Figure 6).

Figure 6. **Example of SCANTER 5000 radar screen dump.**
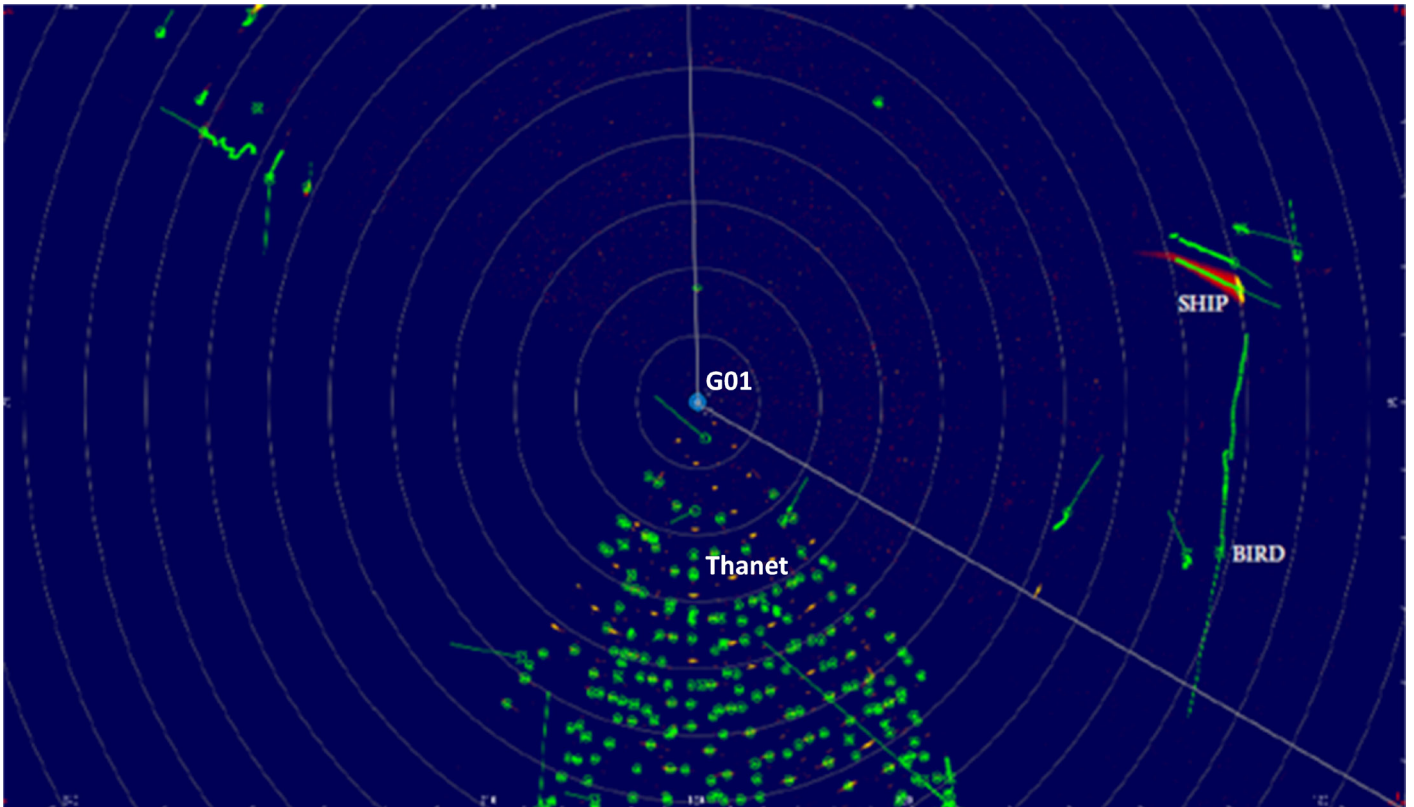
The PC screen visualising the radar images was used to select targets both inside and outside the wind farm. The observer responsible for operating the radar (technician, see Appendix 3) could follow up to 10 tracks at a time by tracing the radar track on screen. Each track had several nodes, representing the location of the target (birds) over time. In addition to the start and the end-point, directions were calculated automatically for all tracks by the radar. In a few occasions, the number of tracks detected by the radar exceeded 10 tracks, and in these cases decisions were made on which tracks to follow using a list of prioritised species (see Appendix 3).

When the target generating a potential bird track being followed came within visible range (within 1.5-2 km distance depending on species), its identity to species was sought by use of binoculars and/or telescope (see Appendix 3). When confirmed, the targets' identity together with its associated parameters (e.g. numbers of birds, age groups, behavioural activity and visually estimated flying altitude were recorded by the technician using the BirdTracker database.

It often happened that a radar target was either lost or could not be identified to species level due to distance. Irrespective of whether the target generating the potential bird track being followed could be visually identified to species (group) or not, the technician continued to follow the target using BirdTracker until lost from the radar screen.

The technician would also give instructions to the observer operating the rangefinder to track some of the targets (only able to follow one target at a time) within 1.5 km of the observer position (rangefinder reach) both inside and outside the wind farm, in which case tracking of bird would also record flight height (see Section 5 below).

In Dec 2015, the radar settings were updated in order for the radar to record images of the radar screen (referred to as "screen dumps", as shown in Figure 6) saved to disk at time intervals of two minutes, although these do not contain information which can be used to determine species. However, in case of power cuts the software required remotely re-activation, an issue which has caused periods of limited availability of screen dumps.

2.4. ASSUMPTIONS AND LIMITATIONS

- High and uniform detection probability throughout studied area both inside and outside the wind farm (up to 3 km)

- Detection probability is assumed similar inside and outside the wind farm (see Section 7.2 below)

- Blind sector between 216° and 296°

- Shading inside the wind farm due to the presence of turbine towers very limited (see Section 6.3 below)

- Data collection (at species level) only possible when observers are deployed (see Section 3.4 in main report)

- Up to 10 radar tracks can be followed at a time, requiring de selection of targets when this amount is exceeded, which was undertaken in line with the observer protocol (Appendix 3)

- Detection of seabirds typically possible within 5km, with species identification possible within 2 km, depending on species and visibility conditions (see Section 6 of this Appendix)

- Birds flying at < 10 m altitude within 45 m of the radar cannot be detected both inside and outside the wind farm

- Maximum height at which flying seabirds can be detected at 1 km distance is 285 m both inside and outside the wind farm

3. LAWR 25 RADAR

The LAWR radar is a magnetron-based radar, sensitive to sea clutter in sea states higher than Beaufort 2 (Figure 7, Table 2).

Figure 7. **LAWR radar and rangefinder.**

Table 2. **Specifications of the LAWR 25 radar.**

Type	Power output	Frequency	Horizontal angle of radar beam	Vertical angle of radar beam	Rotational speed	Antenna length
FAR 2127	25kW	9.4 GHz (X-band)	1 degree	10 degrees	24 rpm	2,400 mm

A number of settings were made in order to optimise clutter suppression and detection of birds:

- Improved antennas with an horizontal beam width of 10° degrees only, from 0° to +10°, which places all the power above the horizon, minimising the amount of sea clutter pick up, and applying more power to the area of interest

- Sea filter (suppression of noise due to waves): 30

- Rain filter (suppression of noise due to rain): 30

- Gain (increased visualisation of bird echoes): 75

- Echo stretch (enlarged bird echoes): 2

- Trail (number of seconds old radar echoes are shown on screen): 30

However, the LAWR radar was found significantly sensitive to sea clutter, affecting interpretation of data displayed on the radar screen. The LAWR radar also relies on the cross-correlation with known bird radar signatures (herring gull recorded at the test site before deployment of the equipment at Thanet (Section 4)) in order to ensure a high resolution classification of bird signals, reducing the risk of turbines and rotors interfering with the tracking of birds.

3.1. SCANNING / DETECTION RANGE

Due to the shape of the detection probability curve of the LAWR 25 radar (see Figure 9), the scanning range of the LAWR radar on G05 was set to 6 km. Figure 8 shows that outside the wind farm Northern Gannet was tracked from distances as far as 5.5 km, 5.2 km for Black-legged Kittiwake and 4 km for Large gulls. Inside the wind farm, Northern Gannets were tracked as far as 2.7 km, similarly to Black-legged Kittiwakes and large gulls. As in the case of the application of the SCANTER radar, subsequent species identification usually took place within 2 km, depending on species, so birds which may have not entered the field of view of observers for species identification and that may have been lost are not captured in the graphs below (see Appendix 2 for a comparison of tracks identified / unidentified using different equipment).

Figure 8. Number of tracks of target species recorded by observers using the LAWR 25 radar from turbine G05) inside and outside the wind farm. The number of tracks recorded at different distances from the radar has been corrected for the area scanned in each distance bin. Data collected between 28 August 2014 and 31 December 2015.

Radar recordings Northern Gannet
G05

Radar recordings large gulls
G05

Radar recordings Black-legged Kittiwake
G05
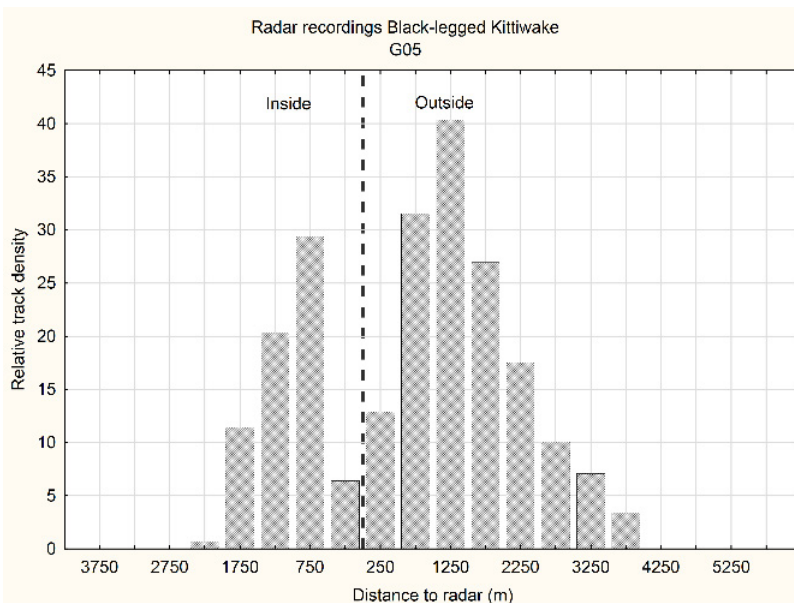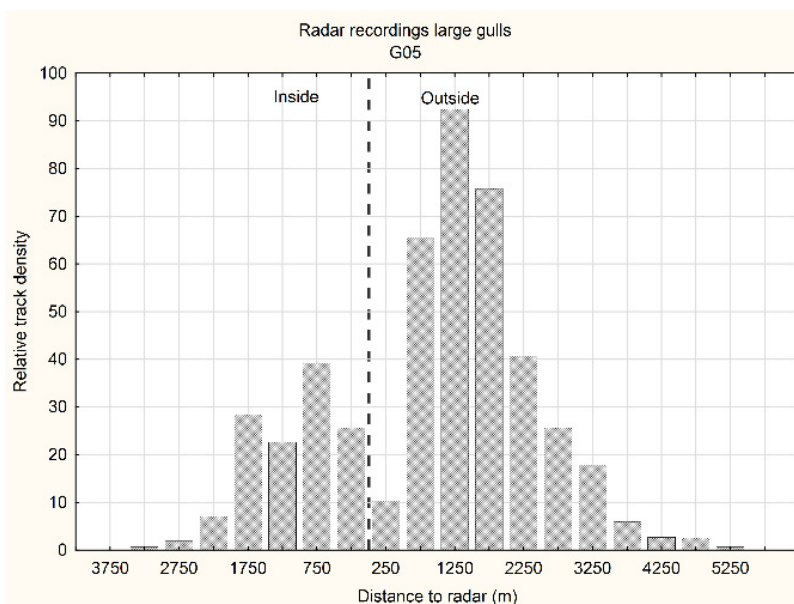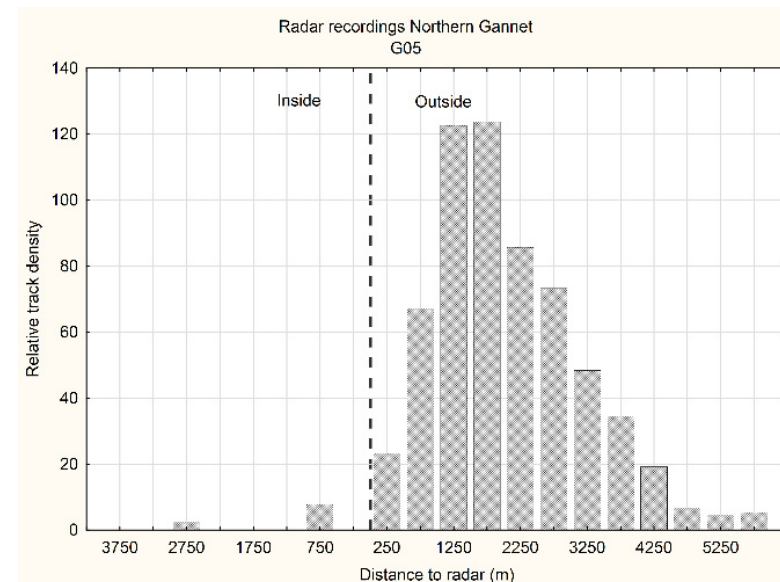
In comparison with the SCANTER radar, the LAWR radar has a variable DPC (Figure 9), with high detection (>0.67) between 1,250 and 3,000 m from the radar (FEBI 2013). This theoretical curve is affected by changes with the aspect of the flying bird and different weather conditions.

Figure 9. **Detection probability curve for the LAWR radar using a 6 km scanning range, which is based on recordings of seabirds in offshore parts of the Baltic Sea (FEBI 2013).**
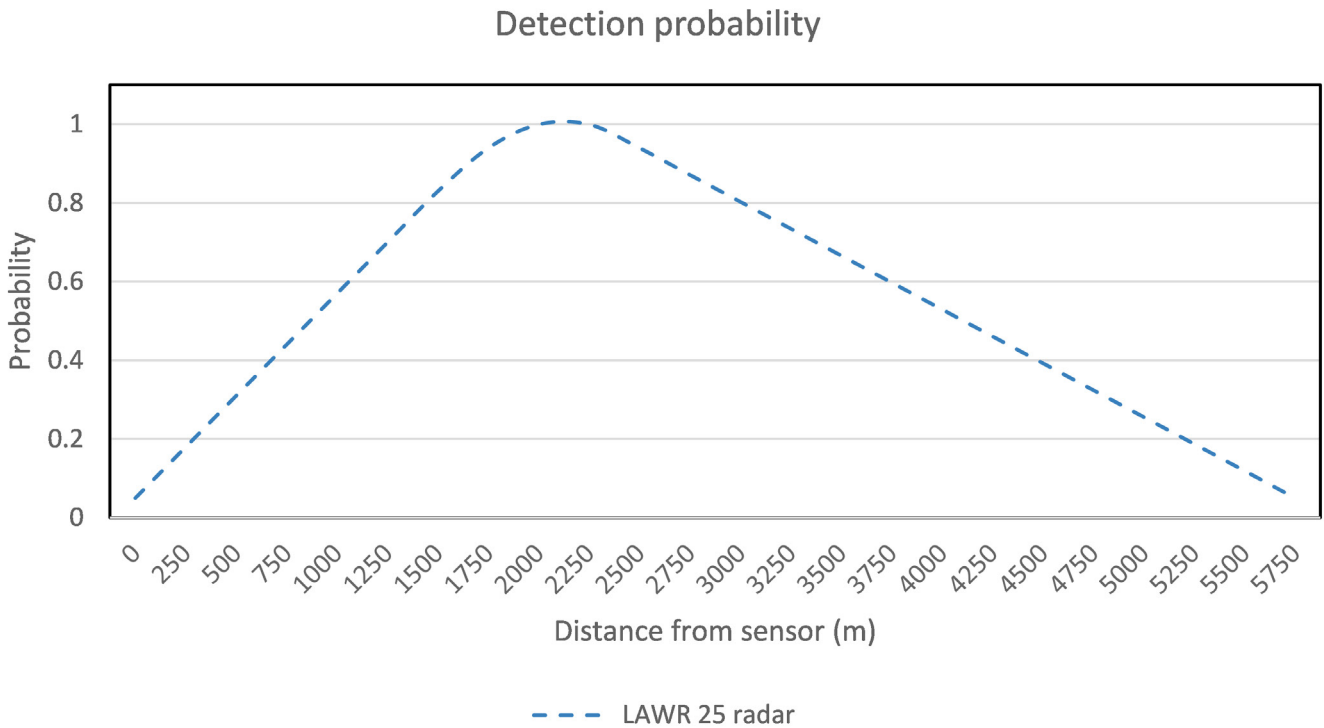
Due to the high level of energy (compared to a solid state radar) emitted close to this radar, the signal detection here is limited. This is created by the application of a so-called STC (Sensitivity Time Control) circuit, which decreases the receiver gain to zero close to the radar to prevent the receiver from saturating due to the strong signals at close range (Skolnik 1990).

On account of the vertical angle of the radar beam, low-flying (< 10 m) seabirds cannot be detected closer than 85 m from the LAWR 25 radar (Figure 10). For the same reason the maximum height at which flying seabirds can be recorded at 1 km distance is 175 m. The same applies both inside and outside the wind farm.

Figure 10. **Minimum detection distance versus flight altitude for the LAWR 25 (Furuno 2015).**
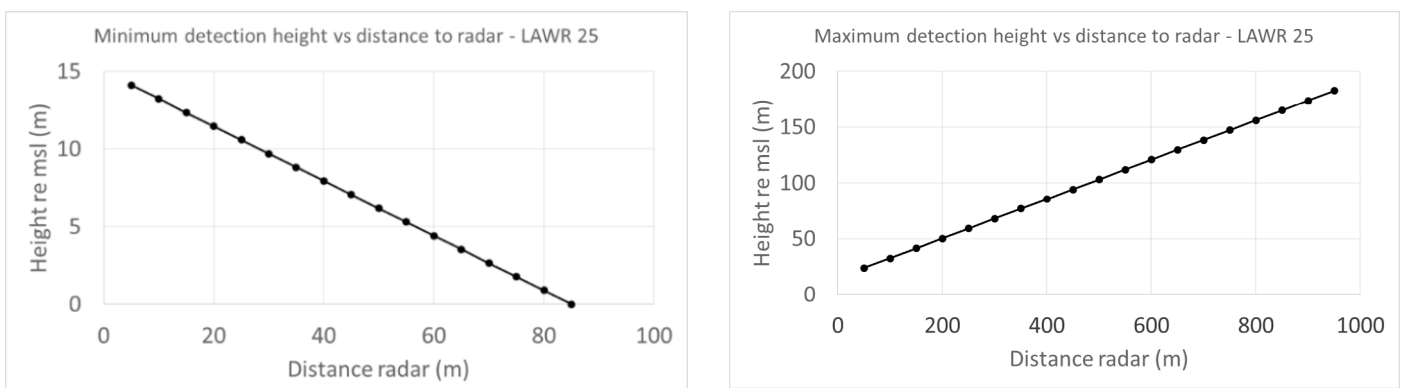
The angle of the blind zone of the LAWR radar on G05 turbine is visualised in Figure 11.

Figure 11. **Angle of the blind zone at G05 turbine transition piece for LAWR radar and rangefinder. Green line define the blind sector for the radar. Blue and red lines define the blind sector for the rangefinder, the blue showing fully obstructed view and between red and blue partially obstructed view by turbine metal structures. As in the case of the SCANTER radar, the blind sector is further considered during data processing and analysis.**
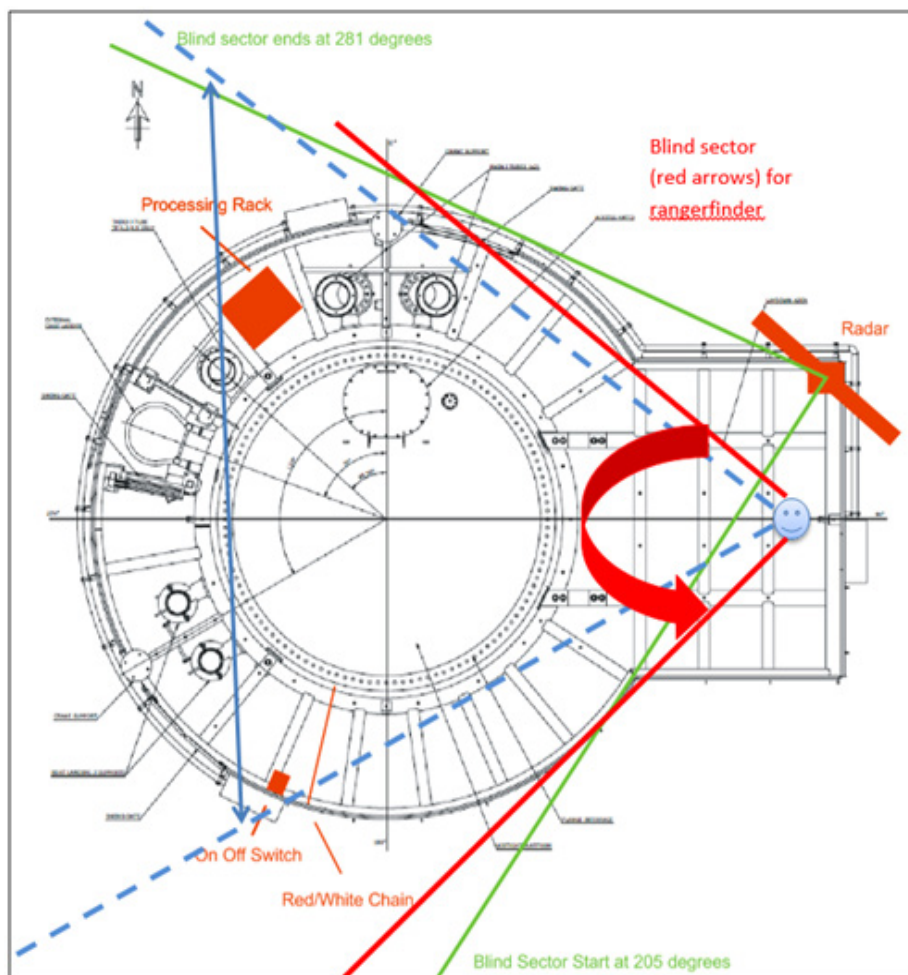
3.2. APPLICATION

As in the case of the SCANTER radar, the LAWR radar on G05 was used during day-time recording data at species level only when operated by observers. The data acquisition hardware has been developed by DHI and includes ancillary hardware linked to the systems, allowing 24 hour operation and remote control, with the automated download of screen dumps taking place once every 2 min.

The radar provided a processed image (Figure 12) and the real-time radar-tracking and geo-referencing of bird movements was undertaken during survey deployment following the same approach as in the case of the SCANTER application, with the technician selecting up to 10 targets at a time both inside and outside the wind farm from the PC screen, followed by target identification when it came within visible range (within 1.5-2 km distance depending on species) by use of binoculars and/or telescope (see Appendix 3). When confirmed, the targets' identity together with its associated parameters (e.g. numbers of birds, age groups, behavioural activity and visually estimated flying altitude were recorded by the technician using the BirdTracker database.

The technician would also give instructions to the observer operating the rangefinder to track some of the targets (only able to follow one target at a time) within 1.5 km of the observer position (rangefinder reach) both inside and outside the wind farm, in which case tracking of bird would also record flight height (see Section 5 below).

Figure 12.   LAWR 25 radar screen dumps, without (left) and with (right) sea clutter
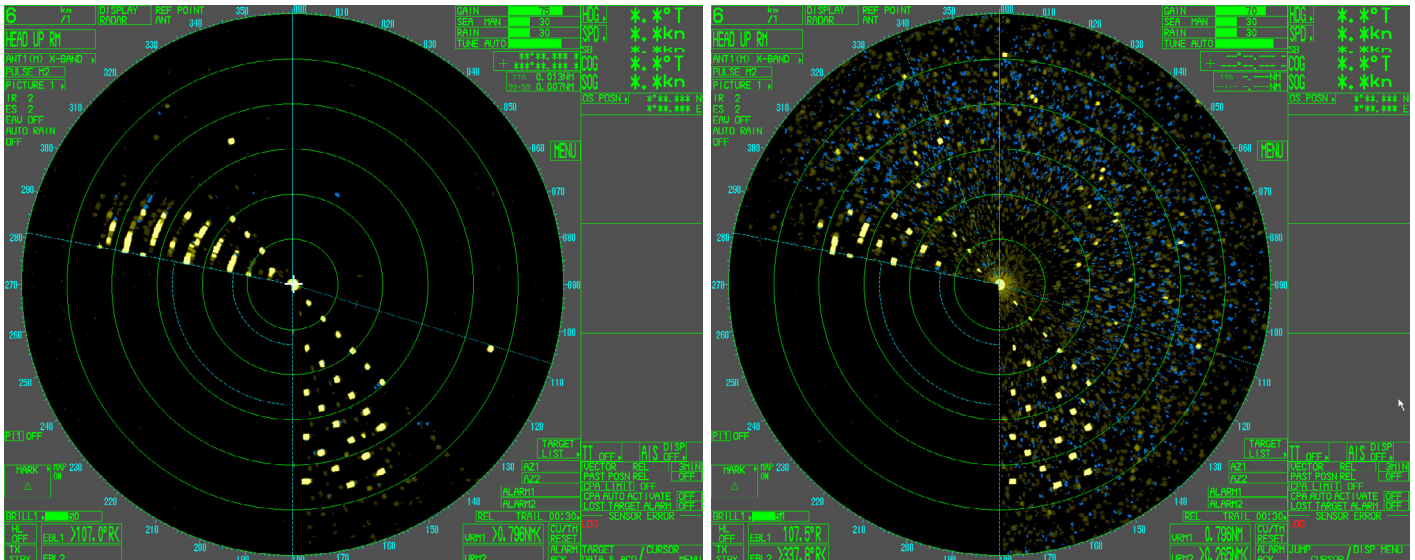
3.3. ASSUMPTIONS AND LIMITATIONS

- Detection probability varies throughout scanned area, with high detection (>0.67) between 1,250 and 3,000 m both inside and outside the wind farm (see Section 7.2 below)

- Blind sector between 180° and 280°

- Shading inside the wind farm due to the presence of turbine towers very limited (see Section 7.3 below)

- Data collection (at species level) only possible when observers are deployed (see Section 3.4 of main report)

- Up to 10 radar tracks can be followed at a time, requiring de selection of targets when this amount is exceeded, which was undertaken in line with the observer protocol (Appendix 3)

- Detection of seabirds typically possible within 5 km, with species identification possible within 1.5 km, depending on species and visibility conditions (see Section 6 of this Appendix)

- Performance sensitive to sea clutter in sea states higher than Beaufort 2, resulting in limited or no radar detection being possible by the observer team when using the LAWR 25 radar

- Birds flying at <10 m altitude within 85 m of the radar cannot be detected both inside and outside the wind farm

- Maximum height at which flying seabirds can be detected at 1 km distance is 175 m both inside and outside the wind farm

4. TESTING DETECTION PERFORMANCE BY SCANTER AND LAWR RADARS

4.1. INTRODUCTION

In 2012, before the Study was commissioned, detection performance by Terma's Scanter 5000 radar and the LAWR 25 radar was tested at the onshore location of Blåvand (Denmark) between the 13th – 17th February 2012 in order to document differences in sensitivity between the two systems in an exposed environment (different wave heights) with high densities of birds (presumably the majority were Common Scoter Melanitta nigra). The tests were undertaken by performing parallel tracking of the same bird targets by both radars. The comparison of performance was entirely based on radar screen entries.

4.2. METHODS

Bird tracking was undertaken by Marine Observers: Jan Durinck, Thomas W. Johansen, Henrik Knudsen and Per Kjær. The aim of the tests included:

a) Comparison of tracking capability in different distance bands

b) Maximum distances to which detection and tracking of birds was possible using the SCANTER radar

The studied area was divided into distance bands (or sectors) of 1 km up to 8 km from the radars positioning. The sectors selected for analysis where those less susceptible to the nearby reef influence, 204 degrees to the coast, east of the radar. Each sector was examined for 2 minutes per radar.

One observer was placed at each radar, and a third person acted as rapporteur.

Observers monitoring the radar screen would notify each other every time a bird was detected, allowing all echoes registered to be searched in both radars. Missing echoes on both radar systems were also registered.

a) *Comparison of tracking capability in different distance bands*

Given that the distribution of birds at radial distances was not known, data was not processed to correct for scanned volume in the various radar sectors. The analysis however allowed comparison of the relative sensitivity of both radars in each sector, and assessment of the detection curve to some extent.

In general, it was not possible to detect bird tracks on the LAWR radar at distances beyond 8 km.

b) *Maximum distances to which detection and tracking of birds was possible using the SCANTER radar*

The scanter radar images were divided into sections of 1x3 km between 6 – 20 km distance from the radar. Each section was examined for 2 minutes per section.

The observer monitoring the radar screen notified the number of echoes observed in each 1x3 km section, and these were attempted to be found in the field. However, due to weather and visibility constraints it was only possible to identify 3 of the tracks. It is estimated that the majority of bird tracks beyond 2 km corresponded to Common scoter (Melanitta nigra), while Common goldeneye (Bucephala clangula) presumably dominated tracks within 2 km.

4.3. ANALYSIS

Registrations obtained from both radars were tested for significant differences using T-tests. Assumptions for T-tests in the form of normal distribution were checked with histograms, while the prerequisite for

NIRAS DHI CARBON TRUST

variance between the two data series was tested with F-tests. The tests were performed for 31 combinations of distance bands and weather conditions (wave height and dry weather / rain).

4.4. RESULTS

a) General differences in resolution

The Scanter radar was found to produce bird echoes and bird tracks of significantly higher resolution and small size, allowing instant recording of track details.

The differences are visualized in Figures 13 and 14.

Figure 13. The section of survey area on LAWR25 radar screen and detection of what is supposed to be a big flock of Common Scoter flushed by a boat. Radar image was photographed at the same time as Figure 14.
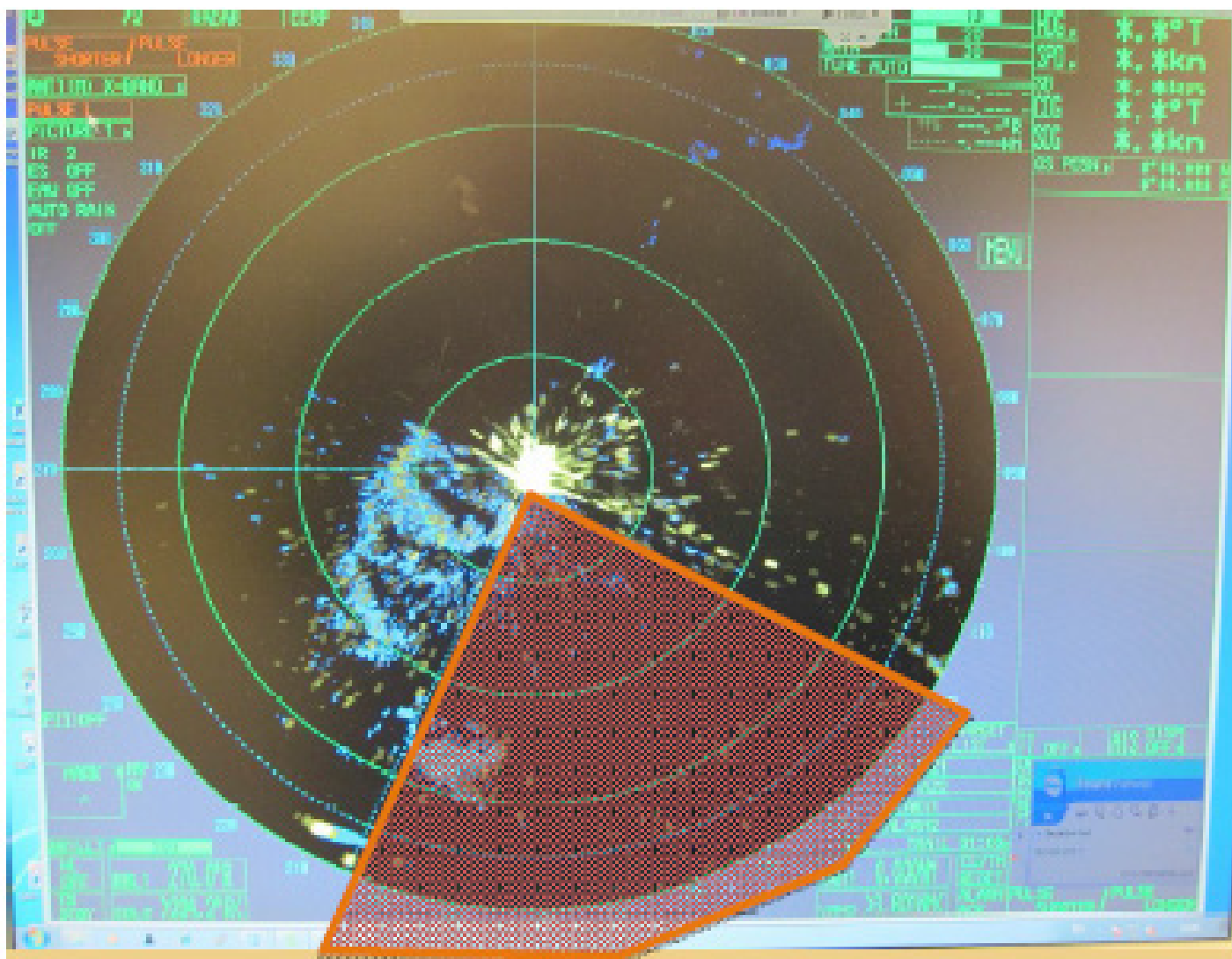
Figure 14.   Terma SCANTER radar's screen image of the same scenario as in Figure 13
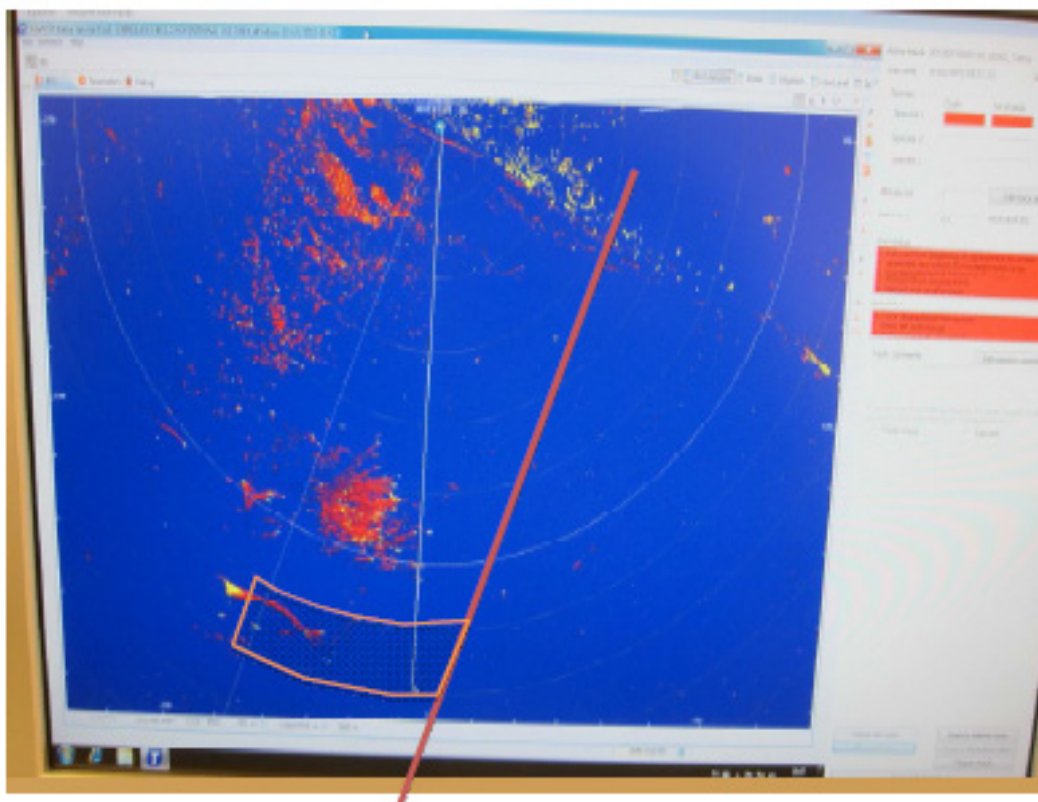
b) Comparisons of tracking performance

Observers recorded a larger number of birds with the SCANTER radar in comparison with the use of the LAWR radar (Figure 15 and 16).

Figure 15.   Distribution of bird tracks between Terma SCANTER and LAWR Radar. Terma SCANTER: 1,531 tracks and LAWR: 261 tracks.
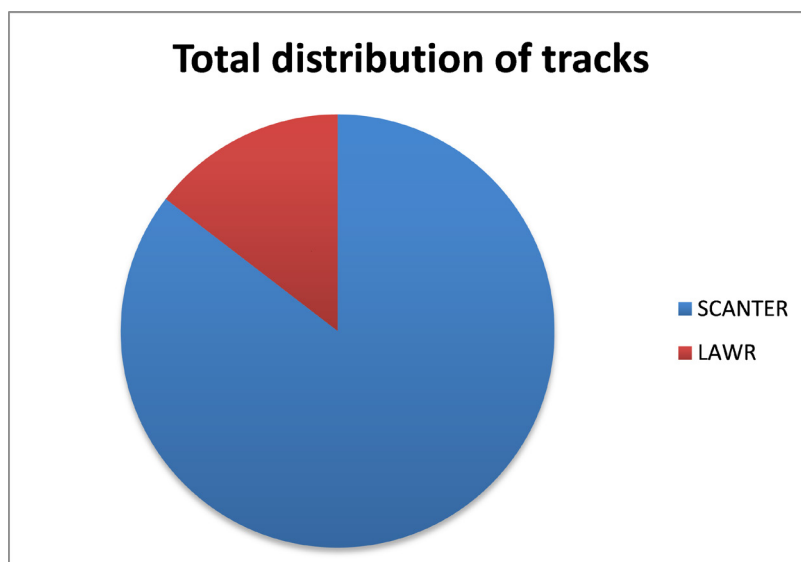
Figure 16.   Total distribution of bird trails per. day between Terma SCANTER and LAWR 25 Radar. Terma SCANTER: 1,531 bird trails and LAWR 25: 261 tracks
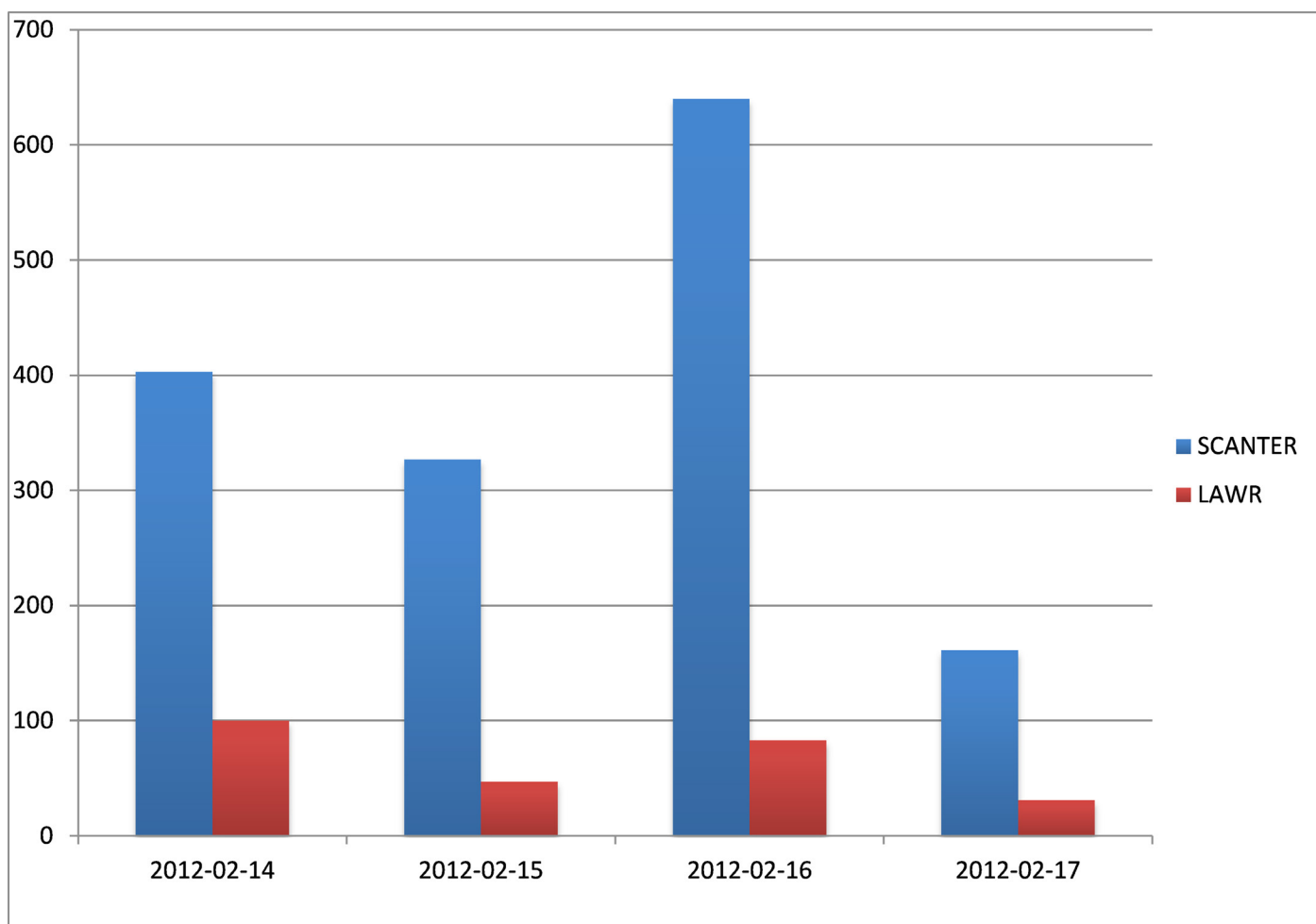
The T tests showed this difference to be significant for bird tracking over all distance bands under all weather conditions (Table 3).

Table 3.　　　Results of T tests of pairs of differences between the number of registered bird tracks between Terma SCANTER and LAWR25 radar. There have been tested for differences within 31 combinations of radial distance and weather conditions. Table shows mean and number of tracks per. 2 minutes, results of one-sided and two-sided t-tests and homogenous tests variance. The category 'Waves <3 rain 5-6 km' had too little a sample size to perform the test.

T-tests; Grouping: Radar (Blåvand radar test data_T tests.sta)

Variable	Mean SCANTER	Mean LAWR (DHI)	t-value	df	p	t separ. (var. est.)	df	p (2-sided)
Waves< 3 Dry 0-1 km	0.956522	0.391304	2.96123	44	0.004924	2.96123	37.7825	0.005272
Waves< 3 Dry 1-2 km	0.971429	0.485714	5.37587	68	0.000001	5.37587	41.4634	0.000003
Waves< 3 Dry 2-3 km	1.000000	0.590909	4.36266	86	0.000036	4.36266	67.7437	0.000045
Waves< 3 Dry 3-4 km	1.000000	0.475000	5.54684	78	0.000000	5.54684	51.6736	0.000001
Waves< 3 Dry 4-5 km	1.111111	0.400000	6.29778	88	0.000000	6.29778	87.9825	0.000000
Waves< 3 Dry 5-6 km	1.040816	0.346939	7.33974	96	0.000000	7.33974	80.6129	0.000000
Waves< 3 Dry 6-7 km	1.111111	0.111111	13.31118	70	0.000000	13.31118	70.0000	0.000000
Waves< 3 Dry 7-8 km	1.000000	0.041667	23.00000	46	0.000000	23.00000	23.0000	0.000000
Waves< 3 Rain 0-1 km	1.100000	0.000000	11.00000	18	0.000000	11.00000	9.0000	0.000002
Waves< 3 Rain 1-2 km	1.111111	0.333333	5.66025	34	0.000002	5.66025	29.6186	0.000004
Waves< 3 Rain 2-3 km	1.055556	0.166667	8.37816	34	0.000000	8.37816	28.2403	0.000000
Waves< 3 Rain 3-4 km	1.062500	0.250000	6.34335	30	0.000001	6.34335	23.5409	0.000002
Waves< 3 Rain 4-5 km	1.066667	0.200000	6.87895	28	0.000000	6.87895	23.4584	0.000000
Waves< 3 Rain 5-6 km	1.000000	0.000000		12				
Waves< 3 Rain 6-7 km	1.000000	0.250000	5.74456	22	0.000009	5.74456	11.0000	0.000129
Waves< 3 Rain 7-8 km	1.083333	0.083333	8.48528	22	0.000000	8.48528	22.0000	0.000000
Waves>= 3 Dry 0-1 km	1.142857	0.035714	3.62828	54	0.000634	3.62828	27.7499	0.001138
Waves>= 3 Dry 1-2 km	1.170213	0.170213	5.93992	92	0.000000	5.93992	60.7019	0.000000
Waves>= 3 Dry 2-3 km	1.153846	0.153846	5.44229	102	0.000000	5.44229	59.2866	0.000001
Waves>= 3 Dry 3-4 km	1.179104	0.313433	4.60497	132	0.000010	4.60497	91.7878	0.000013
Waves>= 3 Dry 4-5 km	1.283582	0.373134	4.10725	132	0.000070	4.10725	106.6476	0.000079
Waves>= 3 Dry 5-6 km	1.344444	0.355556	3.85551	178	0.000161	3.85551	118.4345	0.000188
Waves>= 3 Dry 6-7 km	1.375000	0.111111	4.21339	142	0.000044	4.21339	74.5128	0.000070
Waves>= 3 Dry 7-8 km	1.655172	0.155172	3.15200	114	0.002072	3.15200	58.1695	0.002563
Waves>= 3 Rain 0-1 km	2.350000	0.250000	3.31712	38	0.002011	3.31712	20.4887	0.003357
Waves>= 3 Rain 1-2 km	2.300000	0.266667	3.83818	58	0.000309	3.83818	30.9287	0.000573
Waves>= 3 Rain 2-3 km	2.280000	0.120000	3.47604	48	0.001090	3.47604	24.5532	0.001909
Waves>= 3 Rain 3-4 km	2.423077	0.000000	4.50138	50	0.000041	4.50138	25.0000	0.000136
Waves>= 3 Rain 4-5 km	2.772727	0.000000	3.77031	42	0.000504	3.77031	21.0000	0.001124
Waves>= 3 Rain 5-6 km	3.086957	0.043478	3.58450	44	0.000841	3.58450	22.1157	0.001642
Waves>= 3 Rain 6-7 km	2.083333	0.041667	4.16264	46	0.000136	4.16264	23.3344	0.000366
Waves>= 3 Rain 7-8 km	1.434783	0.000000	4.58028	44	0.000038	4.58028	22.0000	0.000146

NIRAS　DHI　CARBON TRUST

Variable	Valid N (Terma)	Valid N (DHI)	Std.Dev. (Terma)	Std.Dev. (DHI)	F-ratio (Variances)	p (Variances)
Waves< 3 Dry 0-1 km	23	23	0.767420	0.499011	2.3651	0.049214
Waves< 3 Dry 1-2 km	35	35	0.169031	0.507093	9.0000	0.000000
Waves< 3 Dry 2-3 km	44	44	0.304997	0.542097	3.1591	0.000258
Waves< 3 Dry 3-4 km	40	40	0.226455	0.554122	5.9875	0.000000
Waves< 3 Dry 4-5 km	45	45	0.531816	0.539360	1.0286	0.925982
Waves< 3 Dry 5-6 km	49	49	0.351140	0.560915	2.5517	0.001513
Waves< 3 Dry 6-7 km	36	36	0.318728	0.318728	1.0000	1.000000
Waves< 3 Dry 7-8 km	24	24	0.000000	0.204124	0.0000	1.000000
Waves< 3 Rain 0-1 km	10	10	0.316228	0.000000	0.0000	1.000000
Waves< 3 Rain 1-2 km	18	18	0.323381	0.485071	2.2500	0.103962
Waves< 3 Rain 2-3 km	18	18	0.235702	0.383482	2.6471	0.052257
Waves< 3 Rain 3-4 km	16	16	0.250000	0.447214	3.2000	0.030918
Waves< 3 Rain 4-5 km	15	15	0.258199	0.414039	2.5714	0.088099
Waves< 3 Rain 5-6 km	7	7	0.000000	0.000000		
Waves< 3 Rain 6-7 km	12	12	0.000000	0.452267	0.0000	1.000000
Waves< 3 Rain 7-8 km	12	12	0.288675	0.288675	1.0000	1.000000
Waves>= 3 Dry 0-1 km	28	28	1.603567	0.188982	72.0000	0.000000
Waves>= 3 Dry 1-2 km	47	47	1.069725	0.433346	6.0936	0.000000
Waves>= 3 Dry 2-3 km	52	52	1.273941	0.364321	12.2273	0.000000
Waves>= 3 Dry 3-4 km	67	67	1.402653	0.632670	4.9153	0.000000
Waves>= 3 Dry 4-5 km	67	67	1.564821	0.918428	2.9029	0.000025
Waves>= 3 Dry 5-6 km	90	90	2.249400	0.927860	5.8772	0.000000
Waves>= 3 Dry 6-7 km	72	72	2.514395	0.395594	40.3988	0.000000
Waves>= 3 Dry 7-8 km	58	58	3.605803	0.365231	97.4694	0.000000
Waves>= 3 Rain 0-1 km	20	20	2.777257	0.550120	25.4870	0.000000
Waves>= 3 Rain 1-2 km	30	30	2.854518	0.520830	30.0381	0.000000
Waves>= 3 Rain 2-3 km	25	25	3.089229	0.331662	86.7576	0.000000
ORwaves>= 3 Rain 3-4 km	26	26	2.744785	0.000000	0.0000	1.000000
Waves>= 3 Rain 4-5 km	22	22	3.449387	0.000000	0.0000	1.000000
Waves>= 3 Rain 5-6 km	23	23	4.066639	0.208514	380.3636	0.000000
Waves>= 3 Rain 6-7 km	24	24	2.394135	0.204124	137.5652	0.000000
Waves>= 3 Rain 7-8 km	23	23	1.502304	0.000000	0.0000	1.000000

Figure 17 shows mean and variation in the number of registered bird tracks for the different combinations of distances and weather conditions. The figure clearly shows that the difference between LAWR and Terma SCANTER radar is greatest at distances over 5 km and below wave heights above 2 km and / or under rainy conditions. Although the registrations cannot be used to assess the detection curve, it is observed that the sensitivity of the SCANTER radar can only be affected by poorer weather conditions at distances over 5 km.

Figure 17.   Mean and 95% confidence limits for the registered number of bird tracks on the two radar calculated for four weather scenarios.
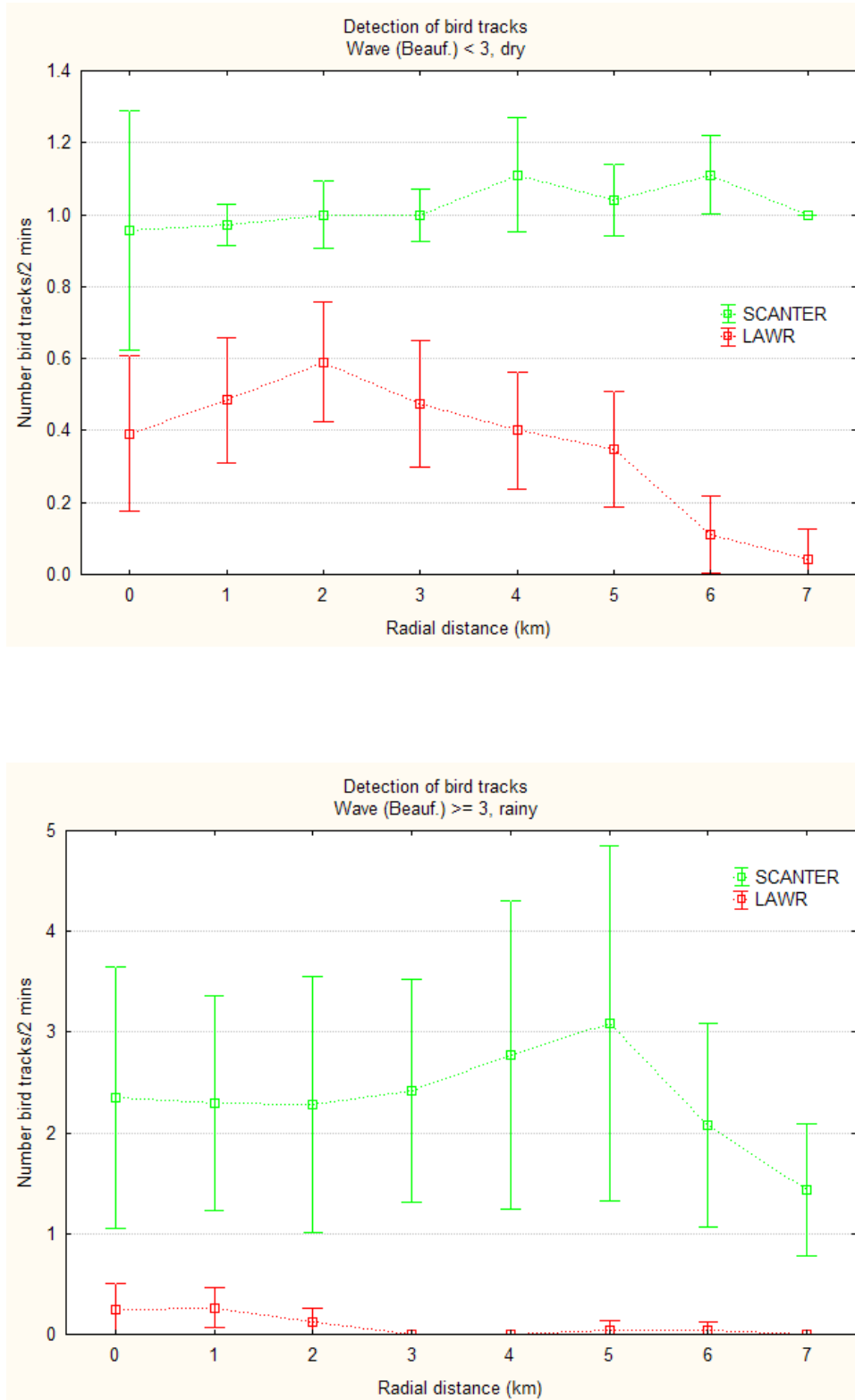
5. VECTRONIX 21 AERO LASER RANGEFINDERS

Comparable to a handheld binocular equipped with a built-in, battery driven laser system (Figure 18), rangefinders allow making recordings of distance, altitude and direction to a given object, containing three-dimensional data on bird movements.

Figure 18. Use of Vectronix Aero during tracking of bird movements.

5.1. SCANNING / DETECTION RANGE

Under optimal conditions, laser rangefinders can be used out to a distance of approximately 2 km for seabird species, depending on the angle of view and on bird species and flight behaviour (gliding, soaring or flapping).

As illustrated in Figure 19, in this study, Northern Gannet was detected and identified as far as 2.5 km from the wind farm, but large gulls and Black-legged Kittiwake were mostly detected within 1.750 km.

Figure 19. Number of tracks of target species recorded using the Vectronix 21 Aero laser rangefinders from turbines G01 and G05 inside and outside the wind farm. The number of tracks recorded at different distances from the rangefinder has been corrected for the area scanned in each distance bin. Data collected between 1 July 2014 and 31 December 2015.
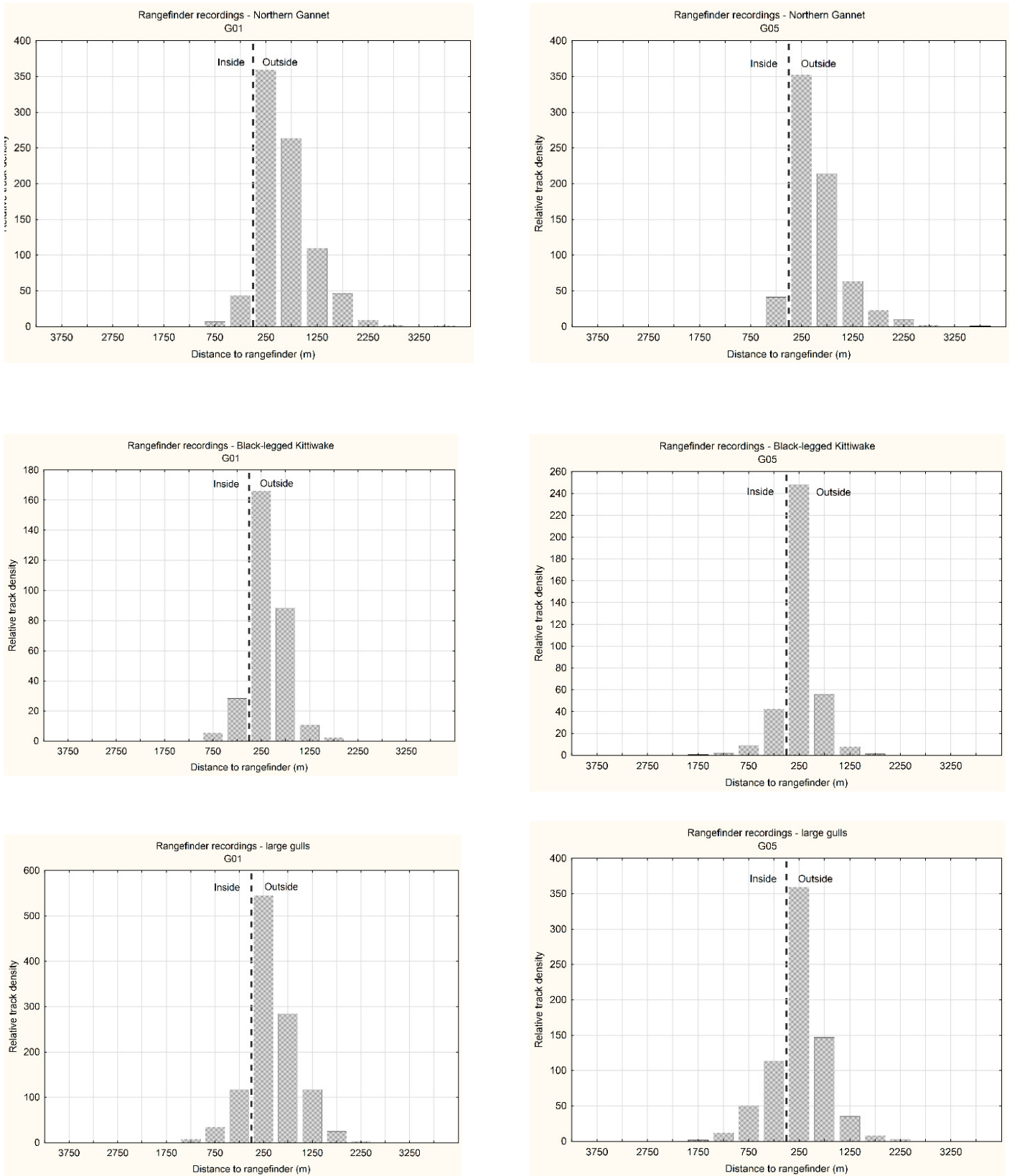
Observers using the rangefinder could not see directly behind the turbine they were standing on and also not directly behind any other turbines. The presence of the radar also obstructed the view which caused an interruption to the rangefinder operator when following tracks. Typically, but not always, a bird being followed by a rangefinder was picked up again once visible the other side of the radar.

The application software has been tested concerning functions, man-machine-interface (MMI) and applications shown in the operator manual according the standard software test procedure (Vetronix AG 2010).

5.2. APPLICATION

In most cases, the SCANTER or LAWR radar were operational to support the selection and tracking of targets by the observer operating the rangefinder, and therefore the PC screen visualising the radar images was used to select targets both inside and outside the wind farm, with some of the targets followed by the rangefinder operator (as instructed by the technician operating the radar). The rangefinder could only be used to follow one target at a time within 1.5 km of the observer position (rangefinder reach).

The rangefinder would be "fired" with approximately 3-5 seconds intervals, and positions and altitudes would be logged automatically via GPS, providing long series of recordings for an individual focal bird or bird flock. Parameters recorded by the observer included age, behavioural activity and estimated flying altitude, recorded into a logbook cross referenced against the ID codes of the track nodes assigned by the GPS device. The simultaneously tracking of the bird by rangefinder and radar were also noted.

When identifying bird species, both technician and observer estimated visually the flight height above the sea level before using the rangefinder, entered into the rangefinder log book and, if also being followed on radar, into the radar bird tracker software. The estimated flight height provided useful albeit coarse ground-truthing data in relation to the height measurements by the rangefinder.

In some cases, the SCANTER and LAWR radar were not fully operational during survey deployment, often due to technical issues with the equipment, or due to heavy sea clutter, which particularly affected the LAWR radar's performance. On these occasions, only rangefinders could be used to track birds within 1.5 km from the observer's position, at which distance species could usually be identified. In these cases, the selection of targets was made through sweeping the field of view both inside and outside the wind farm, using the binoculars and naked eye. Although not explicitly stated in the fieldwork protocol (see Appendix 3), the general approach taken by observers was to commence with the first target detected from the left side, and tracking its movement by the rangefinder until lost due to distance or visibility, subsequently noting species and associated parameters. Following the recording, the sweeping process was repeated in the opposite direction from right to left. Thus, within the range of constraints realised on the two turbine platforms on G01 and G05, the observers applied a random selection of flying seabirds.

The tracking of the bird by rangefinder but not radar was also noted.

The ability to successfully aim and hit a flying seabird with the laser of the rangefinder has been influenced by the stability of the platform (increasing rotational speed of the turbine reducing range through platform vibration by up to 50% i.e. to approximately 750 m – RW pers. obs.). In addition, platform stability, moisture content of the air column (leading to erroneous hits) and, within the wind farm, visual interference from rotating turbines when shooting at a target, reduced the frequency of nodes achievable for a track.

5.3. ASSUMPTIONS AND LIMITATIONS

- Detection range is 1.5 - 2 km, depending on species;
- Blind sector with an amplitude of 90 degrees (varying inside and outside the wind farm depending on turbine where rangefinder is used from, see above);

- Large amounts of metal, as found in offshore wind farms, can have a strong influence on the built-in digital magnetic compass of the laser rangefinders, interfering with the geo-positioning of the recorded data. To account for this, calibration data was collected regularly by measuring the individual distances to three known reference points in the wind farms using the rangefinder. These calibration points were subsequently used to spatially adjust the location of records, however, inaccuracy can be considered within the range ±10 m, which has not allowed the study's rangefinder data to be used to analyse meso avoidance behaviour inside the wind farm. Although this error cannot be quantified, it is assumed to be similar both inside and outside the wind farm;

- Only one target can be followed at any one time;

- Target selection relies on radar detection or visual screening of field view;

- The ability to successfully aim and hit a flying seabird with the laser of the rangefinder is influenced by the stability of the platform, moisture content of the air column and visual interference from rotating turbines when shooting at a target;

- The ability to successfully aim and hit a flying seabird with the laser of the rangefinder was found not to be directly proportional to the size of the bird or the surface area in view of the bird, with other unknown factors apparently influencing the success of making contact. It was however easier to successfully aim and hit a large flying seabird e.g. Northern Gannet than a small flying seabird e.g. Black-legged Kittiwake.

6. SPECIES IDENTIFICATION

At the macro scale, an observer protocol (Appendix 3) was set up to ensure consistency in the way data were collected by observers and to minimise any potential bias, instructing observers to use the radar screen to guide selection of tracks when available, or alternatively sweeping the field of view both inside and outside the wind farm. However, distance of detection and species identification by use of rangefinders, binoculars or telescope was subject to a number of factors:

- Bird behaviour - e.g. flight pattern and gregariousness. Detection of flapping birds may be possible at slightly longer distances than detection of gliding birds. Similarly birds with high rising flights may be more conspicuous than expected for their size. A flock of birds can be expected to be more conspicuous than a lone individual;

- Size of targets - greater conspicuousness occurs with larger body size;

- Flight heights - birds at low altitudes may be obscured, at times, within the troughs between waves;

- Effect of local weather and sea state on conspicuousness - e.g. visibility against calm or rough sea conditions, clear skies and cloud, and that resulting from sun glare when looking above the horizon or when reflected from the sea's surface;

- Colouration - A dark coloured bird e.g. juvenile herring gull, may be either more or less conspicuous than a light coloured bird e.g. adult herring gull, dependent upon colour contrast between bird and background;

- Direction of flight in relation to observer - a bird flying directly towards or away from the observer may be less visible to one flying across on account of the difference in visible profile.

- These factors can potentially lead to the introduction of bias in data collected. However, these biases cannot be quantified and data collected need to be considered as the best approximation to actual bird behaviour and distribution.

7. TADS CAMERA SYSTEM LINKED TO LAWR 25 RADARS

On both turbines F04 and D05 inside the wind farm, one LAWR radar was deployed in connection with an improved TADS camera to support data collection.

Each camera set-up consisted of a pan-tilt housing with two thermal night vision cameras, and a dual-function zoom daylight/lowlight colour TV camera. The zoom function allows for 26× optical zoom, and 15x (thermal)/312× (visual) digital zoom (Figure 20, Table 4).

Figure 20. **On the left FLIR Voyager III unit housing both thermal and visual cameras. On the right, configuration of the TADS.**
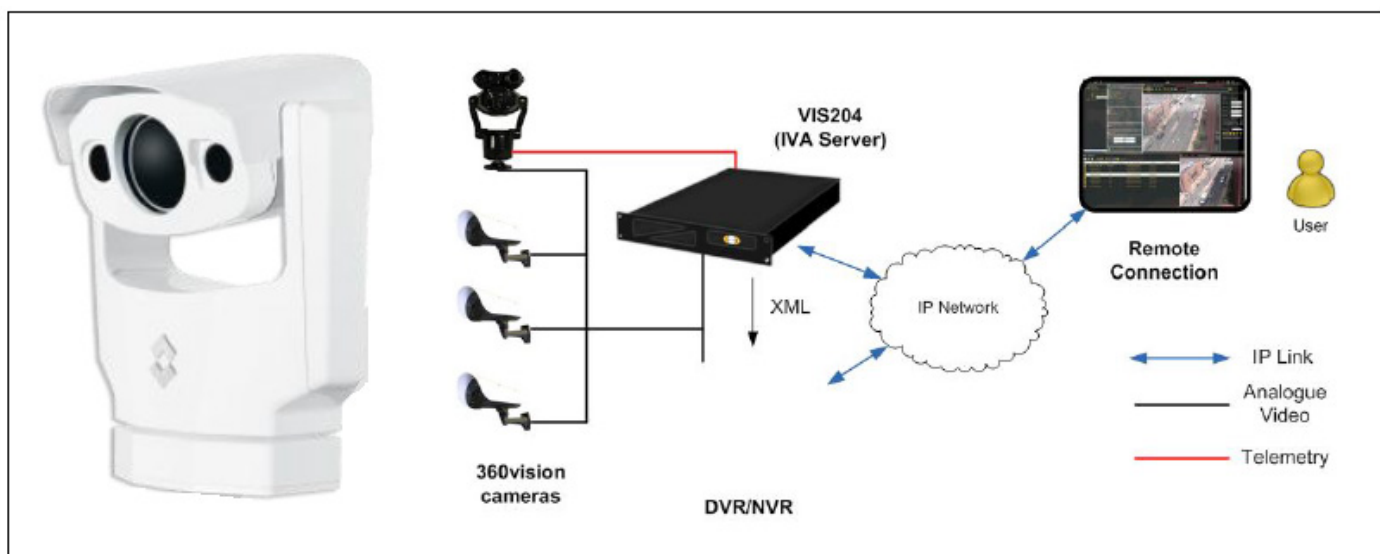
Table 4. Specifications of the LAWR 25 radar.

Thermal Imaging Specifications		Daylight Imaging Specifications	
Sensor Type	Two 320 x 240 VOx Microbolometers	Detector Type	1/4" Super HAD Daylight/Lowlight Colour CCD
FOV	20° x 15° (Wide FOV); 5° x 3.75° (Narrow FOV)	FOV	42° (h) to 1.7° (h) plus 12x E-zoom for 312x Total Magnification
Focal Length	35 mm (Wide FOV); 140 mm (Narrow FOV)	Minimum Illumination	2 lux (@f/1.6)
E-zoom	4x (15x Total Magnification)	Lines of Resolution	768 (H) x 494 (V)
Image Processing	FLIR DDE		
System specifications			
Camera Head Size		15.18" x 18.68", 15.5" x 22" Swept Volume Cylinder	
Bulkhead Box		10.42"(w) x 14.25"(l) x 6.26"(d)	
Weight		45 lb	
Pan/Tilt Coverage		360° Continuous Pan, +/-90° Tilt	
Video Output		NTSC or PAL	
Connector Types		BNC	
Power Requirements		24VDC	
Power Consumption		<50 W nominal; 130 W peak, 270 W w/heaters	
Environmental Specifications			
Operating Temperature Range		-20°C to 55°C	
Storage Temperature Range		-50°C to 80°C	
Automatic Window Defrost		Standard	

NIRAS DHI CARBON TRUST

7.1. SCANNING / DETECTION RANGE

The LAWR 25 radars were set up to have scanning range of 1,500 m, and operate 24/7 in digital communication with the TADS cameras. This had the purpose of ensuring an optimal detection range around 500 m from the radar, inter-turbine distance in Thanet.

The theoretical DPC for LAWR radars located on turbines F04 and D05 is presented below, with high detection (>0.67) between 265 and 875 m.

Figure 21.   Detection probability curve for the LAWR radars on D05/F04 using a 1500 m scanning range, which is based on recordings of seabirds in offshore parts of the Baltic Sea (FEBI 2013).
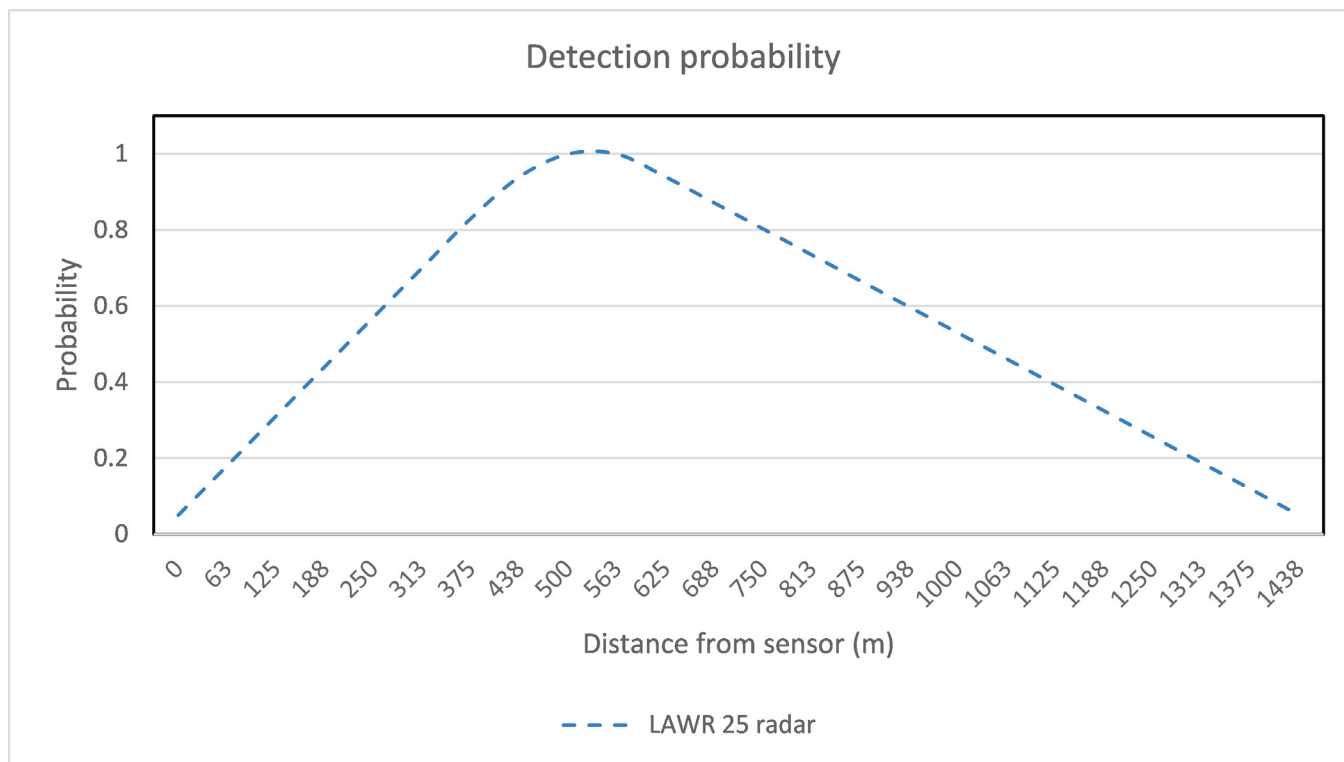
7.2. INTEGRATION OF LAWR RADAR AND TADS CAMERA

The development of software for integration of radar and camera tracking has been a major component of this study, tested in Denmark before deployment at Thanet.

The radar software package used for running the automated radar tracking could be operated remotely via internet connection, and can be subdivided into:

- FPGA based Data Acquisition

- Pre-processing System (DAPS). As part of this study, the DAPS was extended to include a Blip Detection System (BDS). The algorithms were modified to allow radial data bins corresponding to a radar pulse length to start at an arbitrary sample in the data collected from the radar, resulting in a 1.5 m radial resolution. The DAPS sampled at 100 Mhz and performed real time median filtering of data from the radar, processing 11.5 MB of data per sec.

- Software package DAPSControl, used to control the DAPS and allow for the automatic restart of the equipment in case of power failure.

In addition the Camera software, TADSTracker, was used for automated tracking and geo-referencing of species-specific track data and for storage of recorded tracks and videos.

An overview of the camera-radar tracking unit is provided in Figures 22 and 23.

Figure 22.   Overview of TADS Camera-radar tracking unit.
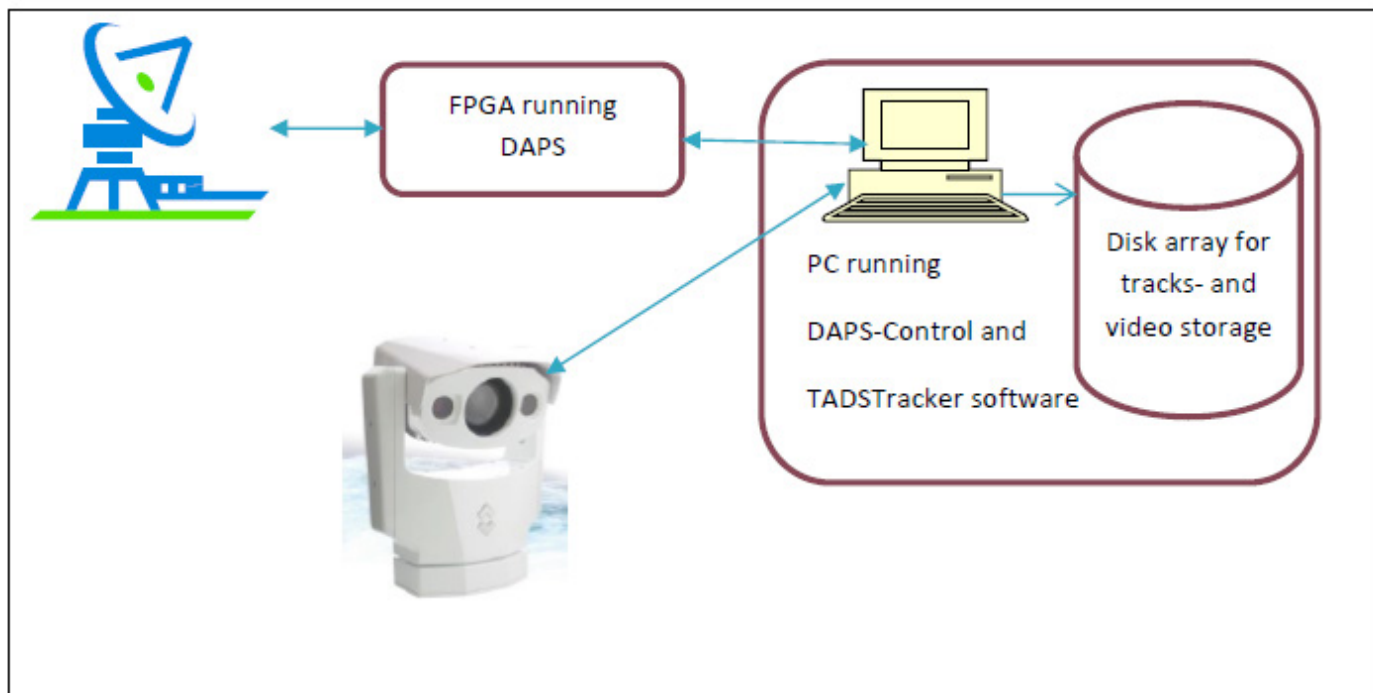
Figure 23.   TADS Camera-radar unit installed in Thanet.

Birds discovered by the radar within 1000 m (camera range) were automatically targeted by the camera (through the transmission of coordinates) and hereafter followed, tracking for around 20 s, and videoing part or the whole event of the bird passing the wind turbine. Tracking information from the radar is continuously recorded to a geo-database by the system combined with images from the camera:

- The TADSTracker receives track points (blips) from the DAPS system and matches points from the last scan. To facilitate smooth data transfer, the radar bird tracking software was updated to track points at a rate of 24 times per minute. The data connections between the systems are based on the internet language TCPIP (commonly used for interfacing). This design facilitates modular utilization of one or more computers. The computer system used in this study was capable of processing more than 500 blips per rotation.

- Using information collected for each trigger point by the radar, a selection filter selects track candidates based on cross-correlation against a reference bird signature (herring gull recorded at the test site before deployment of the equipment at Thanet), directing the TADS camera to its position.

- Whenever a camera-tracking is started the video recording is turned on. A recording of each camera monitored track are stored in the 16 TB disk-storage unit. The unique track name, issued by the TADSTracker are used as the key for playback allowing the post-processing team to click on a camera track and watch the visual seen by the camera.

- The TADSTracker software extracts low-level positioning information from the camera (orientation, elevation, zoom-factor, etc.). When the target is considered lost the TADSTracker will re-engage the camera to a new track following the coordinates received from the DAPS.

Screen dumps were also collected by the LAWR radars located on F04 and D05.

7.3. ASSUMPTIONS AND LIMITATIONS

- Radar scanning range set to 1.5 km, with detection probability varying throughout scanned area.

- Cameras recording range is 1 km, 20° field of view.

- Each TADS camera cover a total of 8 turbines within high detection zones covered by the radar.

- At the installation turbine itself the camera view is only able to cover part of the rotor, and therefore most birds recorded around the installation turbine are not used in avoidance analysis.

- Very few videos of tracks at distances beyond two rows (1 km) of turbines from the installation turbine

- Few videos of low flying birds close to the installation turbine.

- Birds flying at < 10 m altitude within 85 m of the radar cannot be detected.

- Maximum height at which flying seabirds can be detected at 1 km distance is 175 m.

- It is considered that in comparison to the LAWR radar located at the periphery of the wind farm (turbine G05), sea clutter within the wind farm was less due to drag resistance, wave reflection/diffraction from structures and the effect of a modified wind field inside and on the lee side of the wind farm. However, locally, around the foundations, breaking waves may have given rise to clutter, affecting radar performance.

NIRAS DHI CARBON TRUST

APPENDIX 2: DATA EXPLORATION (MACRO SCALE)

This appendix presents the results of a number of comparative analysis undertaken to better understand data collected at the macro scale, and any differences between data collected by different sensors, which can provide an indication on detection limitations / potential bias. Implications of any differences / similarities are further discussed to inform the interpretation of the study's results.

1. COMPARISON OF DETECTION OVER DISTANCE INSIDE AND OUTSIDE THE WIND FARM

As presented in Section 4 of Appendix 1, detection capability of the LAWR and SCANTER radar over distance was initially tested in 2012 at the coastal site Blåvand, Denmark, before the study was commissioned. These comparative tests showed that the SCANTER radar produces echoes and tracks of higher resolution, recording more birds over the same distance, and proving to be less sensitive to adverse weather conditions, with stronger performance over distances beyond 5 km.

Using data collected by the study, detection capability has also been compared using screen dumps collected automatically by both radars.

a) Screen dumps collected automatically by both radars

A quantitative comparison of bird echoes detected by both SCANTER 5000 and LAWR radar was conducted to compare detection efficiency over distance, uninfluenced by the observers' selection of tracks.

Accordingly, a total of 30 radar screen images recorded with each radar on the 24 February 2016 between 0900-0932 UTC, were selected for their good quality, recorded during calm and dry conditions. It should be noted that screen dumps do not provide information on species, and have therefore not been used to analyse / quantify empirical macro avoidance.

The extent of the overlapping detection zones outside and inside and the wind farm are shown in Figure 1.

Figure 1. **Overlapping detection zones covered by both the SCANTER 5000 radar on turbine G01 and the LAWR 25 radar on turbine G05 inside and outside the wind farm to a maximum distance of 6 km.**
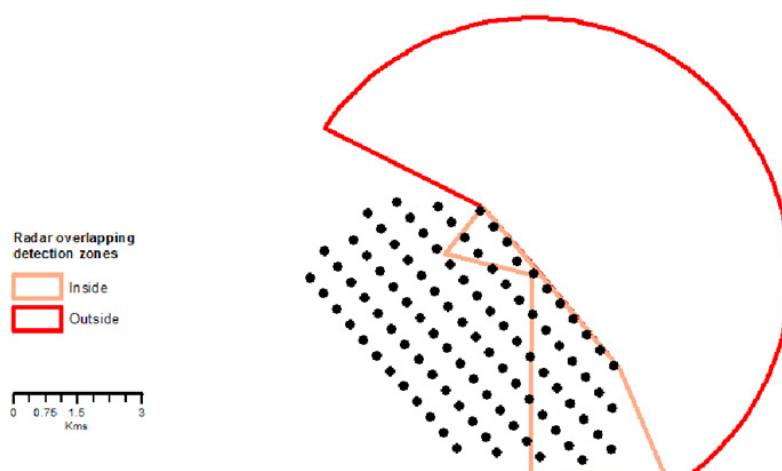
The analysis of screen dumps involved the following steps:

I. **Geo-referencing,** using spatial adjustment with the Affine algorithm in ArcGIS Spatial Analyst. The adjustment was based on three calibration points: (1) position of the radar, (2) position of easternmost point on the radar screen (6 km/12 km and 90° E from radar), and (3) position of northernmost point on the radar screen (6 km/12 km and 90° N from radar).

II. **Marking of 1 km radii** within the overlapping detection zone using GIS (Figure 2).

Figure 2.   1-km radii from turbines G01 and G05 within the overlapping detection zone.
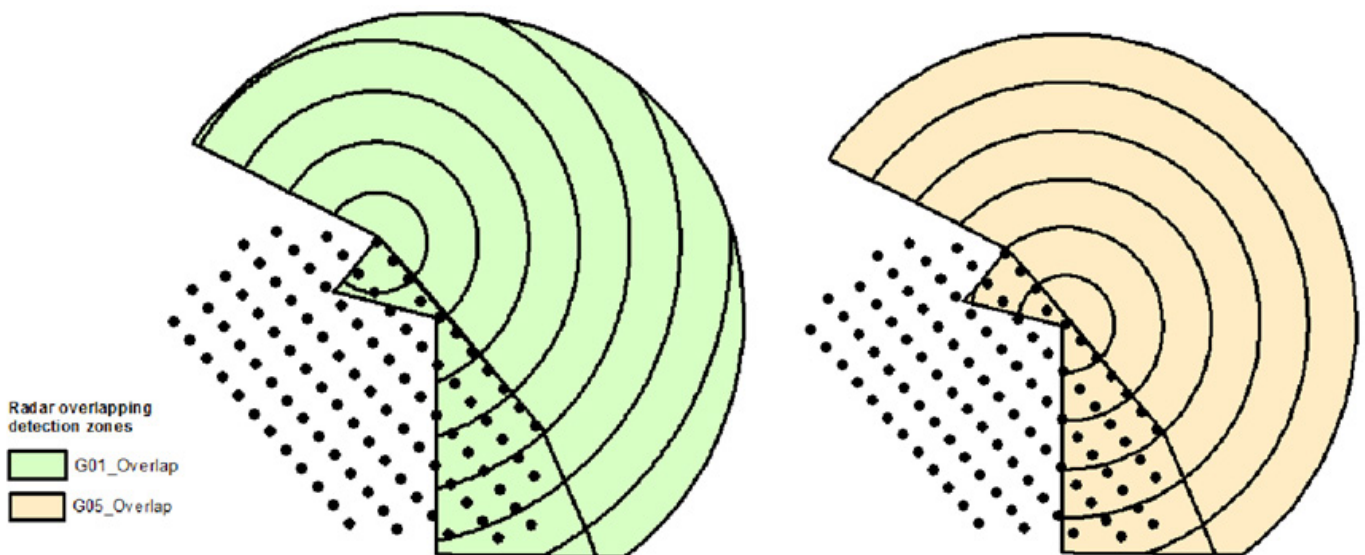
III. **Extraction of bird echoes in overlapping detection zone**, undertaken manually. This exercise already indicates the higher level of clutter suppression by the SCANTER radar in comparison with the LAWR radar. It was noted that ships could be misidentified as birds with both radars, as both generate similar signals, however, signals generated by ships tend to be stronger, often characterised by their slow speed. In contrast, birds move with a speed of 100-300 m between two adjoining screen images with 1 minute time difference.

IV. **Classification of bird echoes.** For each radar screen image, an identified bird echo was allocated to one distance interval, indicating whether it was located inside or outside the wind farm. Hence, a bird could be recorded in several distance bins during its transition over the overlapping detection zone.

As presented in Figure 3, the total number of recorded bird echoes per km^2 in each distance bin from the SCANTER radar and the LAWR 25 radar was calculated and divided by the area scanned by the radars in each bin in order to get a comparable measure of the density of echoes recorded from each radar over distance.

Figure 3. **Total numbers of recorded bird echoes per km² in each distance bin from the wind farm perimeter. The distance bins inside the wind farm are indicated as negative values, and the distance bins outside the wind farm are indicated as positive values. The middle point of each distance bin is given.**
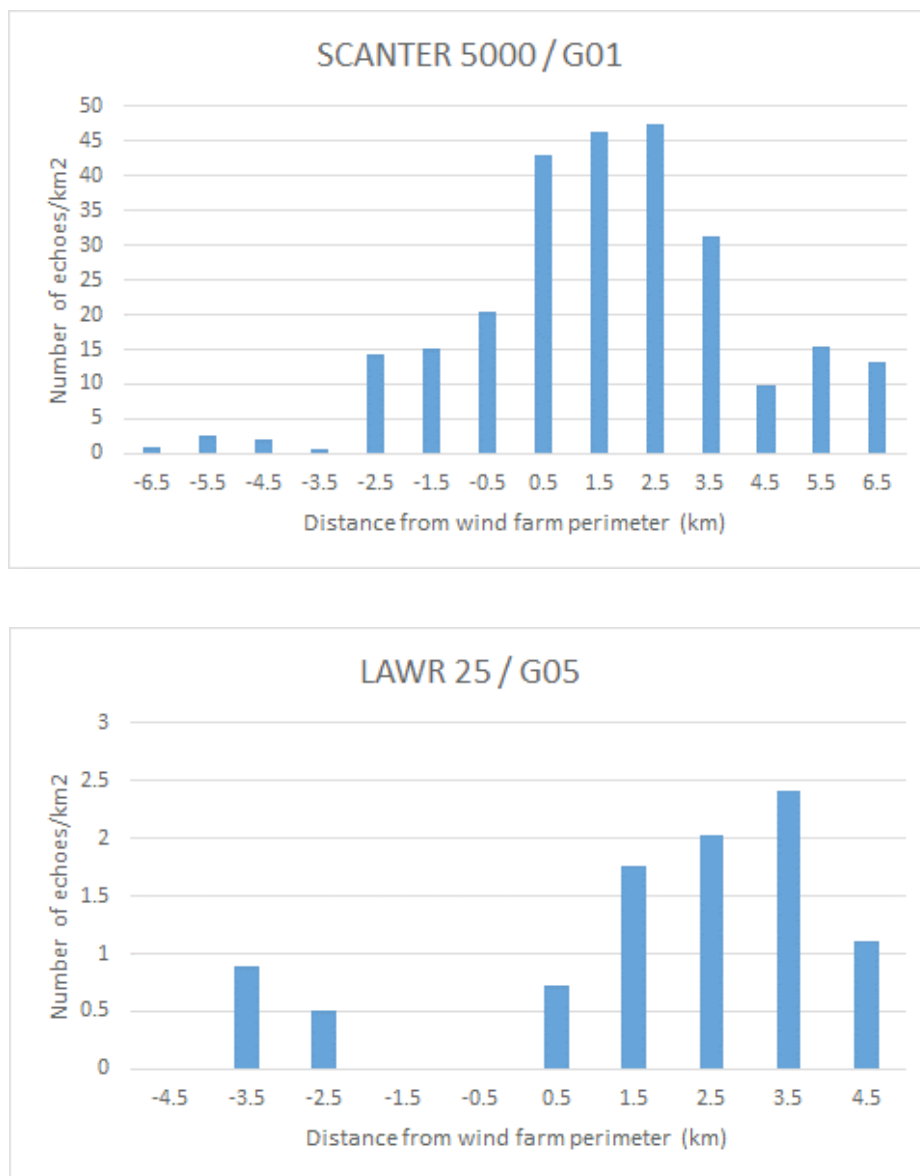
The SCANTER radar was found to record a much larger number of bird signals (at least a factor of 10) than the LAWR 25 radar, and in line with the tests undertaken in Blåvand in 2012, the SCANTER radar demonstrates a superior performance in comparison to the LAWR radar, capable of recording a higher amount of targets over distance, and throughout longer distances.

The distribution of recorded bird echoes outside the wind farm displayed a concentration of echoes from 0 to 3 km distance from the radar, followed by a sharp decline, with densities beyond 4 km being clearly lower than closer to the wind farm. Inside the wind farm, the density of detections in the 0-3 km bins was found to be approximately half of that found outside the wind farm.

The ratio of echoes detected inside / outside the wind farm was calculated, considering the total number of bird echoes corrected for area scanned by the two radars (Table 1). This shows that although the LAWR radar is less efficient in the detection of bird echoes, this limitation applies similarly inside and outside the wind farm, showing a similar proportion of detections in / out to those recorded by the SCANTER radar.

Table 1.   Total number of bird echoes per km² recorded inside and outside the wind farm by each radar.

Radar	No. echoes / km² inside the WF	No. echoes / km2 outside the WF	Ratio in / out
SCANTER 5000	4.9	26.1	5.3
LAWR 25	0.3	1.7	5.6

Comparison of bird distributions indie and outside the wind farm as collected by the equipment, can also be compared to post-construction data to assess the extent to which distribution is not a consequence of detection limitations.

b) Post-construction data collected in 2011

Post-construction data collected in 2011 (Ecology Consulting 2011), show similar trends in bird distribution inside and outside the wind farm, where a drop in number inside the wind farm can be observed. For instance, Figure 4 indicates a drop in number of counted large gulls and Northern Gannets inside the wind farm similar to the distribution recorded by the study's sensors (see Appendix 1). The data also shows a deeper penetration inside the wind farm by large gulls in comparison to Northern Gannet.

Figure 4.   Number of target species recorded during post-construction monitoring at Thanet inside and outside the wind farm within different distance bins (based on data from Ecology Consulting 2011). Note that only observations of birds recorded in transect were included and that the graph represents birds recorded over the whole area inside and around Thanet.
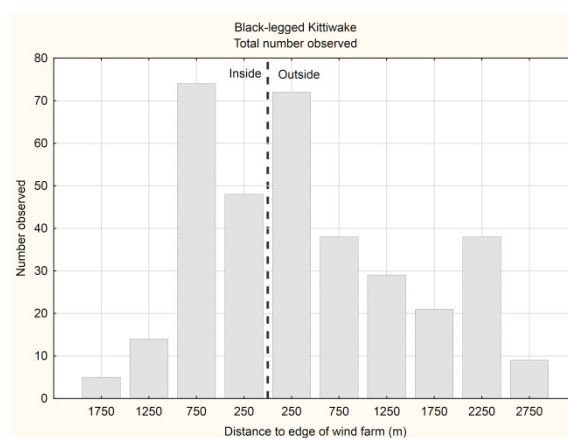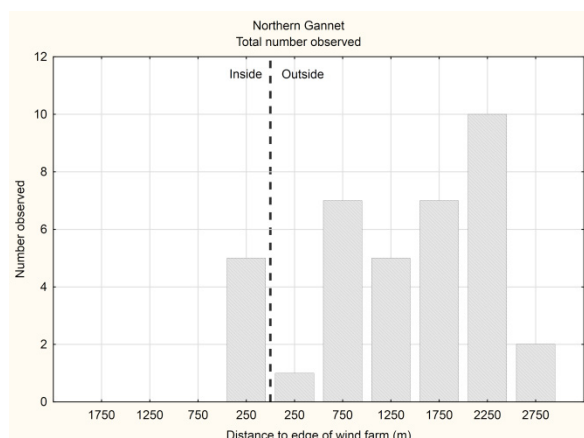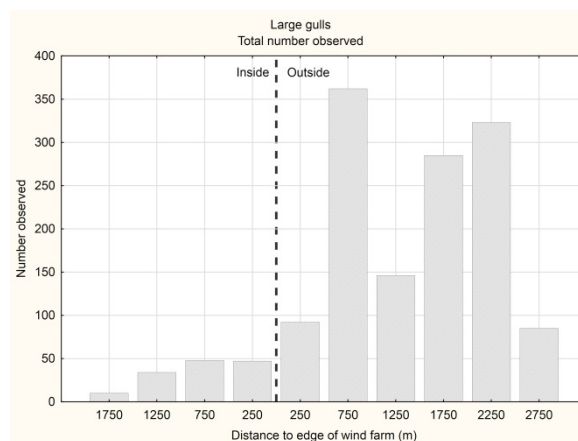
Figure 5 further illustrates distribution of birds recorded during post-construction surveys, where aggregations at the fringe (both inside and outside the wind farm) can be observed, as well as a clear drop in abundance deeper in the wind farm.

Figure 5.   Observations of Northern Gannet (upper) and herring gull (lower) recorded during post-construction monitoring at Thanet winter 2010/2011 (Ecology Consulting 2011).
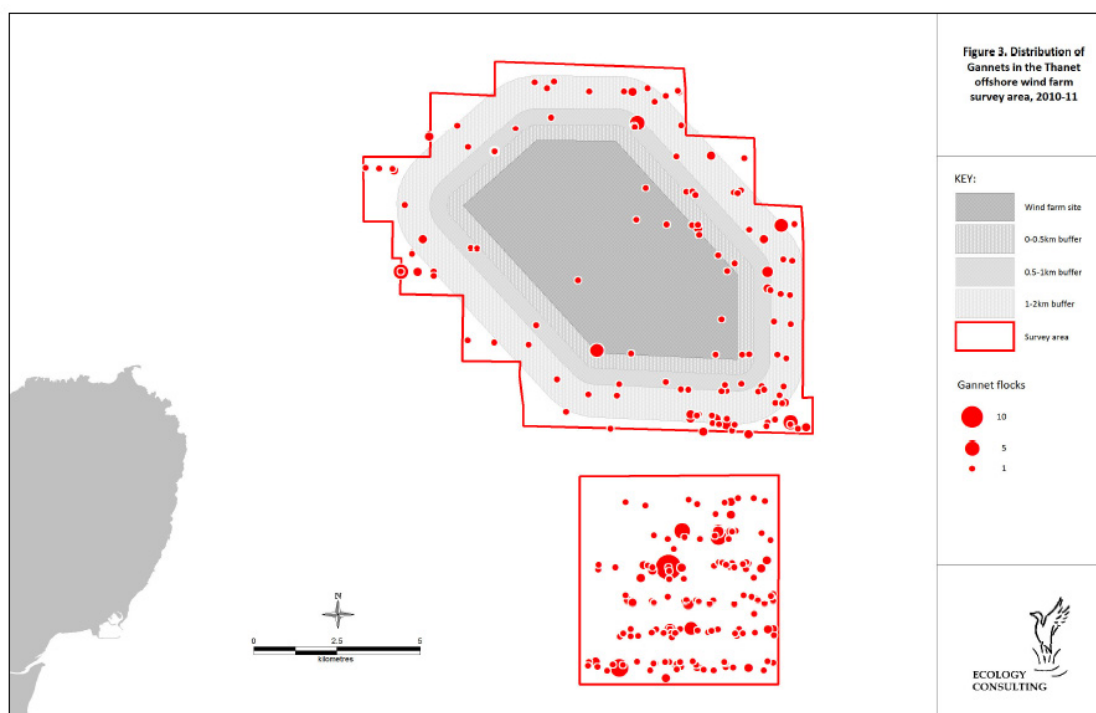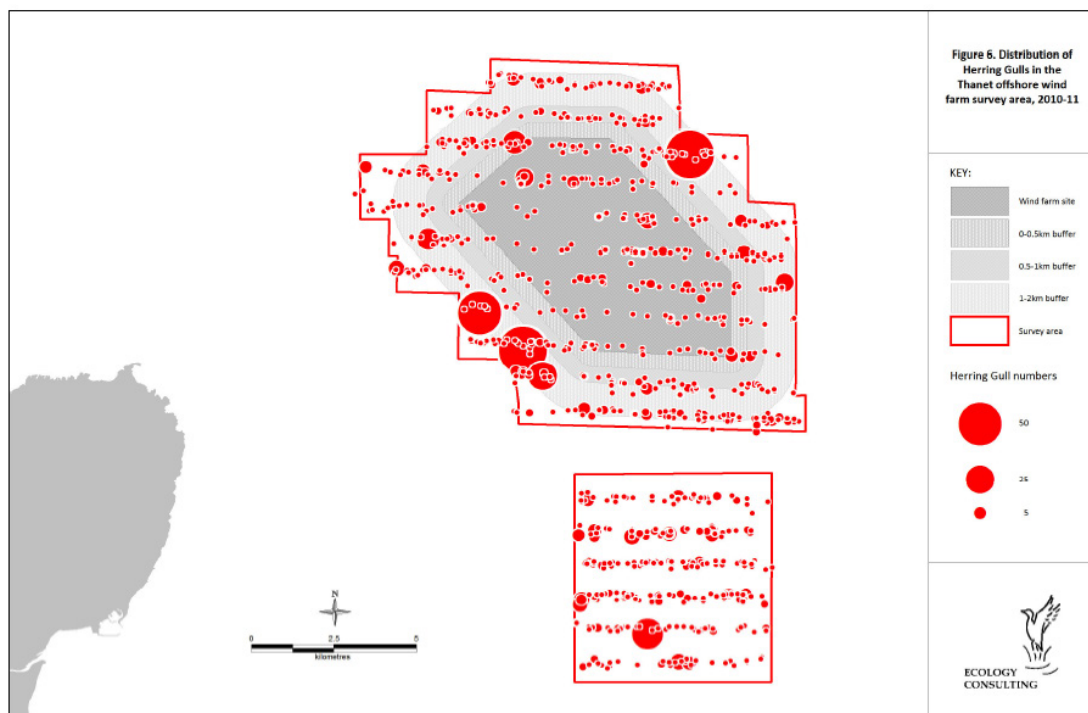
2.   COMPARISON OF MEAN FLIGHT DIRECTIONS RECORDED BY DIFFERENT SENSORS

Data collected by the radars and rangefinders can also be compared in relation to mean flight directions. Although it should be noted that there is a lack of data on bird flight activity across the blind sector. Regarding data collected from turbine G01, mean flight patterns for Northern Gannet seem consistent in radar (Figure 6) and rangefinder data (Figure 7).

Figure 6.   **Mean flight directions recorded for Northern Gannet using the SCANTER radar from turbine G01. On the right-hand figure, the mean value is noted with a black line, accompanied by associated confidence limits.**
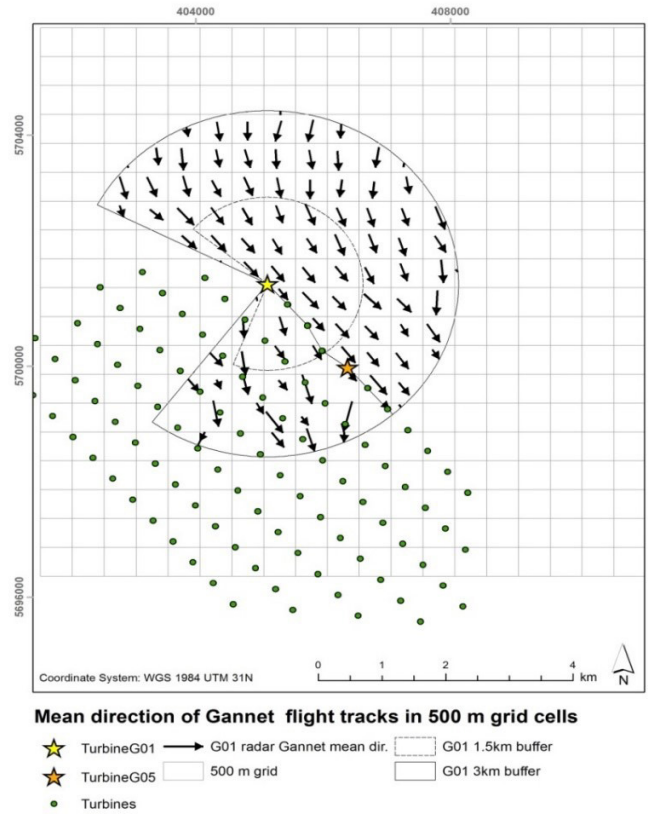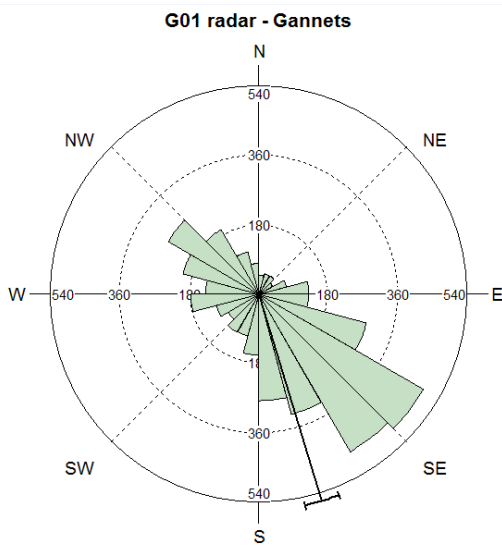
Figure 7.   **Mean flight directions recorded for Northern Gannet using the rangefinder from turbine G01. On the right-hand figure, the mean value is noted with a black line, accompanied by associated confidence limits.**
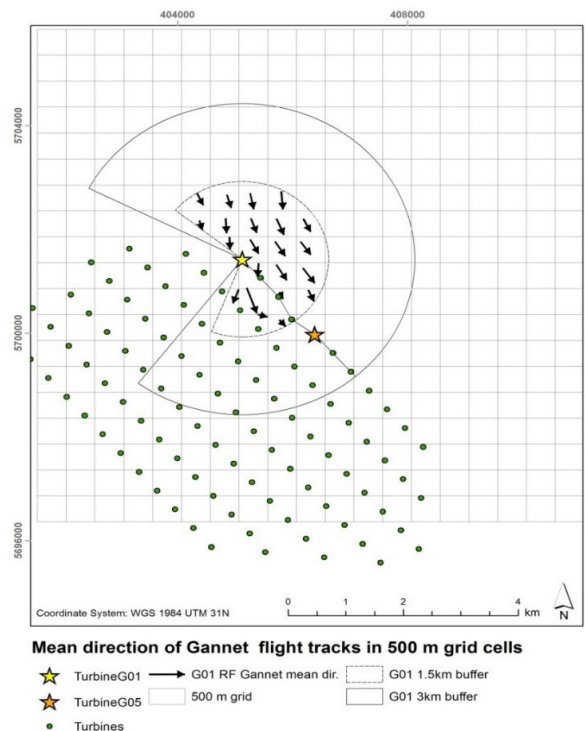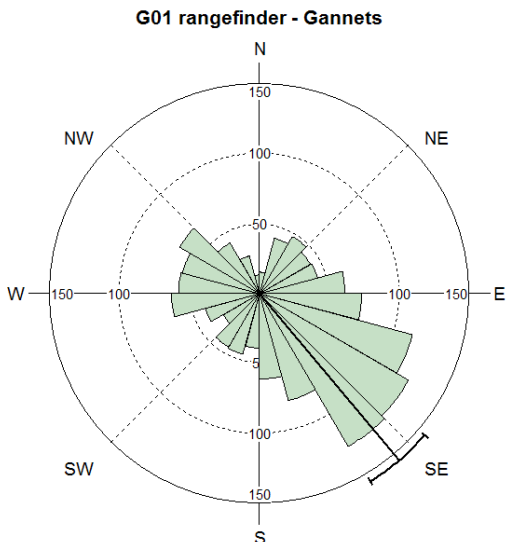
These match records obtained using the radar (Figure 8) and rangefinder (Figure 9) data from turbine G05.

Figure 8.   Mean flight directions recorded for Northern Gannet using the LAWR radar from turbine G05. On the right-hand figure, the mean value is noted with a black line, accompanied by associated confidence limits.
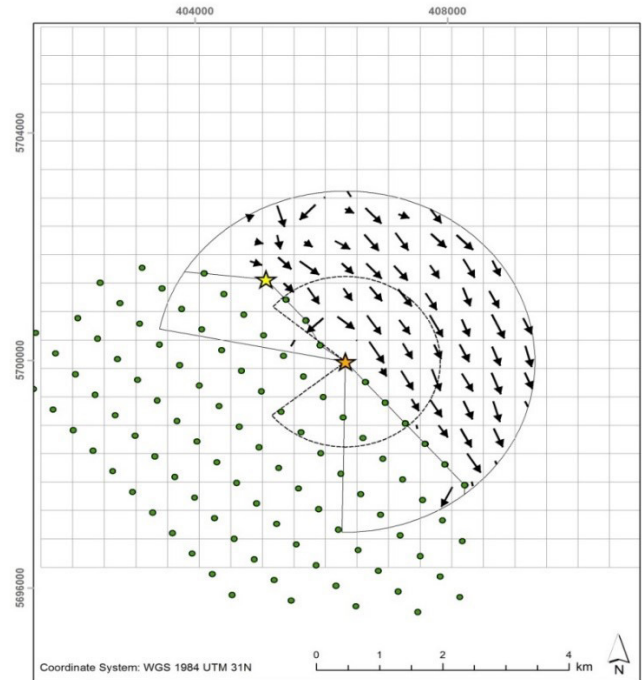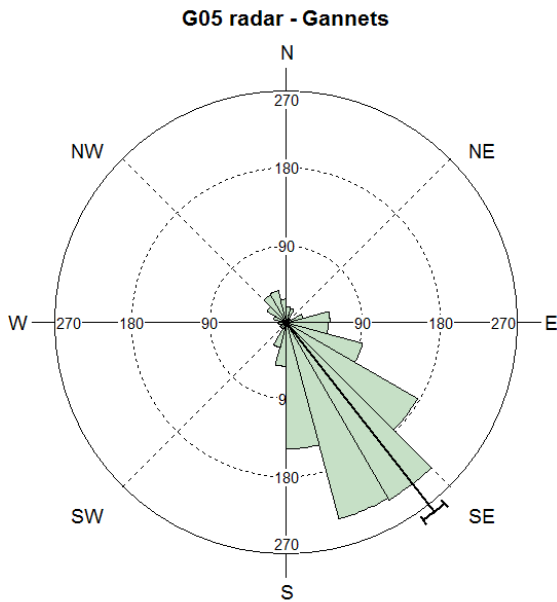
Figure 9.   Mean flight directions recorded for Northern Gannet using the rangefinder from turbine G05. On the right-hand figure, the mean value is noted with a black line, accompanied by associated confidence limits.
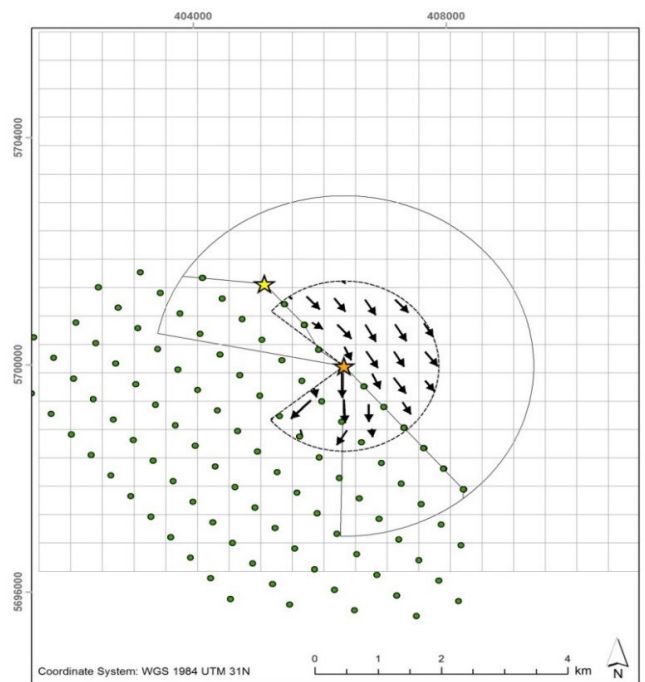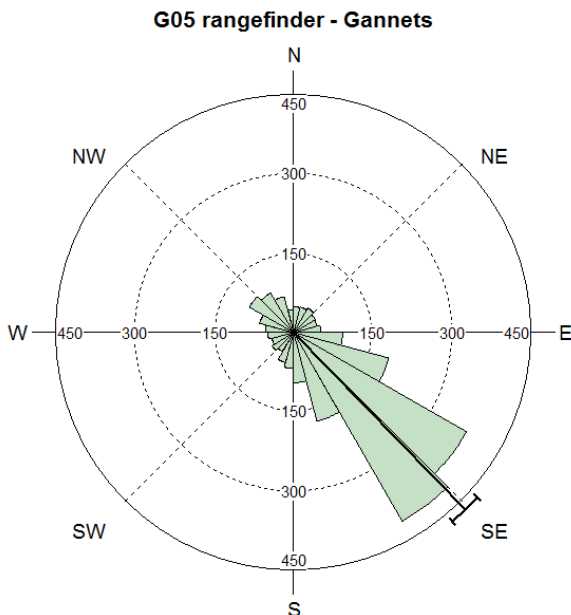
The figures show that the same mean flight direction (Southeast) was recorded by all sensors, indicating that there are no obvious signs of strong bias by a specific sensor (for example comparing rangefinders and radars). There is also no obvious strong bias with increasing distance from the turbines, in regards of mean direction of tracks.

The data collected on Northern Gannet by each sensor has also been further analysed for each season separately. Section 6.2 presents the mean flight directions for Northern Gannet recorded from turbine G01 using the scanter radar. Below, the mean flight directions recorded during each season from turbine G01 using the rangefinder (Figure 10), and from turbine G01 using the radar (Figure 11) and rangefinder (Figure 12) are presented.

Figure 10.   **Mean flight direction of Northern Gannet recorded from turbine G01 using the rangefinder.**

Figure 11. Mean flight direction of Northern Gannet recorded from turbine G05 using the LAWR radar.

Figure 12. **Mean flight direction of Northern Gannet recorded from turbine G05 using the rangefinder.**

Mean direction of Gannet flight tracks during winter
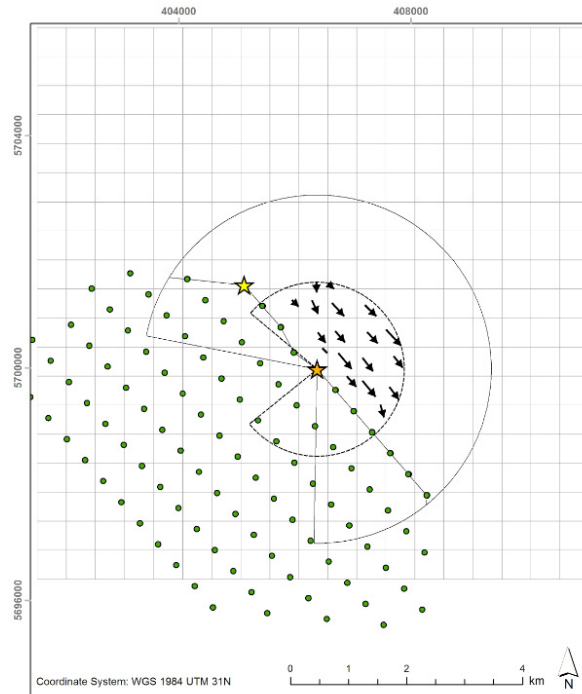
Mean direction of Gannet flight tracks during spring

Mean direction of Gannet flight tracks during summer

Mean direction of Gannet flight tracks during autumn

3. ANALYSIS OF SHADING AND CLUTTER INSIDE THE WIND FARM

To assess the potential interference of turbine presence on radar detection, a total of 120 radar screen images were selected from both SCANTER and LAWR radars (that had been positioned on turbines G01 and G05 respectively) for analysis. The selection of images were selected based on: (1) radar data availability and quality of that data (2) During hours of peak bird activity – 07:00 – 09:00 (3) A range of wind speed conditions (Low: 0 – 4 m/s; Moderate: 4 – 8 m/s; or High: > 8 m/s) in order to ensure a representative sample set based on meteorological conditions.

The shade analysis involved the development and application of models within a GIS environment to produce datasets identifying the cumulative absence of signals on the radar datasets as classified raster grid cells which defined areas of shading.

The classification process to identify areas of shade was entirely based on the DN values (colour) of the pixels in each radar geotiff. These values were extracted using multi-spectral analyses where spectral signatures were identified from the radar histograms followed by a reclassification algorithm to simplify cells into those which contain signal values and those where no signals are found.

The analysis showed that shading inside the wind farm due to the presence of turbine towers was very limited, with shaded areas of very small size. Given that the data analyses are based on bird tracks and not on raw radar echoes, data collection was considered to allow for bird tracks recorded inside the wind farm to be picked up after crossing a shaded area. Accordingly, it was not considered necessary to exclude shaded areas from macro avoidance analysis.

Figure 13.   Shading analysis results from SCANTER radar images (left) and LAWR 25 radar images (right) located on turbines G01 and G05 respectively. The pink areas denote shaded areas, while black dots represent turbine positions.
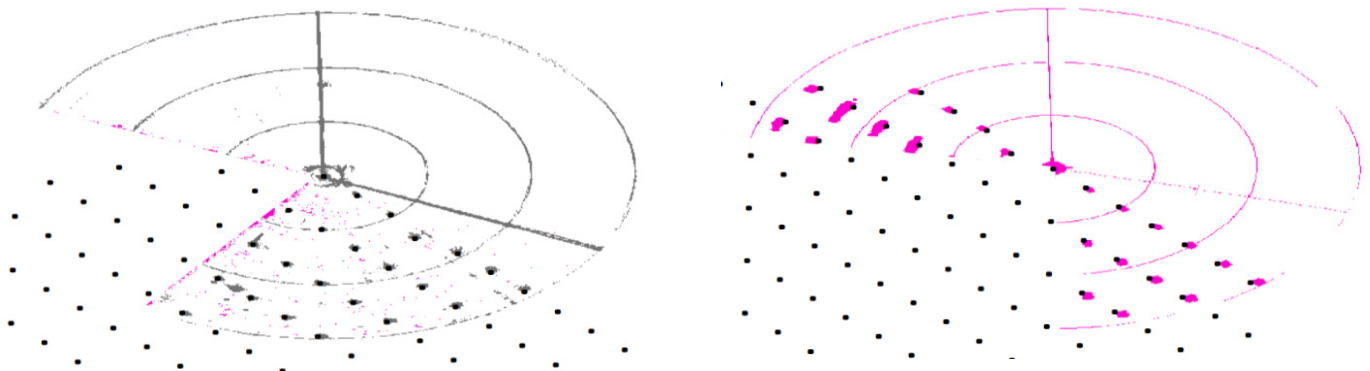
The analyses grouped by environmental conditions indicated that the clutter increased in the same manner inside and outside the wind farm, and therefore analysis were not considered sensitive to meteorological conditions.

NIRAS DHI CARBON TRUST

4. COMPARISON OF RESULTS USING DIFFERENT DATASETS AND INFORMING THE MACRO AVOIDANCE BOUNDARY

Table 2 presents the macro EAR results obtained from using different datasets at different ranges, and the difference between including the data collected using the LAWR radar (from turbine G05) or excluding it.

Table 2.   Comparison of overall macro EARs using different datasets.

	Combined Macro EAR		Combined Macro EAR (no G05 radar)		Macro EAR (G01 radar)	
	3 km	1.5 km	3 km	1.5 km	3 km	1.5 km
Northern Gannet	0.816 (0.023)	0.750 (0.027)	0.797 (0.026)	0.731 (0.028)	0.819 (0.026)	0.730 (0.035)
Black-legged Kittiwake	0.575 (0.055)	0.533 (0.052)	0.556 (0.058)	0.525 (0.055)	0.715 (0.093)	0.692 (0.087)
All large gulls	0.495 (0.037)	0.426 (0.032)	0.481 (0.038)	0.415 (0.034)	0.723 (0.031)	0.529 (0.046)
Herring Gull	0.442 (0.064)	0.424 (0.056)	0.422 (0.067)	0.408 (0.057)	0.749 (0.049)	0.633 (0.069)
Great Black-backed Gull	0.469 (0.054)	0.392 (0.044)	0.464 (0.057)	0.377 (0.047)	0.667 (0.043)	0.439 (0.061)
Lesser Black-backed Gull	0.639 (0.060)	0.504 (0.071)	0.619 (0.064)	0.505 (0.073)	0.768 (0.067)	0.543 (0.113)

	Macro EAR (G01 RF)		Macro EAR (G05 radar)		Macro EAR (G05 RF)	
	3 km	1.5 km	3 km	1.5 km	3 km	1.5 km
Northern Gannet	0.776 (0.072)	0.724 (0.077)	0.990 (0.008)	0.981 (0.019)	0.787 (0.045)	0.738 (0.052)
Black-legged Kittiwake	0.584 (0.110)	0.516 (0.112)	0.713 (0.090)	0.607 (0.132)	0.530 (0.077)	0.461 (0.077)
All large gulls	0.435 (0.083)	0.369 (0.079)	0.731 (0.054)	0.632 (0.076)	0.326 (0.069)	0.269 (0.062)
Herring Gull	0.246 (0.168)	0.198 (0.0146)	0.834 (0.096)	0.819 (0.095)	0.323 (0.101)	0.266 (0.090)
Great Black-backed Gull	0.431 (0.101)	0.365 (0.094)	0.546 (0.093)	0.569 (0.106)	0.330 (0.119)	0.272 (0.105)
Lesser Black-backed Gull	0.746 (0.103)	0.690 (0.115)	0.938 (0.042)	0.484 (-)	0.321 (0.160)	0.264 (0.142)

EARs calculated using data within 1.5 km are lower, which may be due to:

- The total inside area is kept the same (whole footprint) while the outside area decreases when the buffer range is reduced from 3 to 1.5 km

- The redistribution due to avoidance is not fully captured when the outside area is reduced to 1.5 km buffer (trade-off between detection limitations and re-distribution)

The choice of whether to use a boundary of 1.5 km as opposed to 3 km is down to interpreting whether density changes / redistribution can be considered a consequence of:

- Detection issues, i.e. there is no confidence on the data collected beyond 1.5 km, and redistribution beyond this distance is considered an artefact of detection. In this case, only data collected within 1.5 km should be used.

- Actual behaviour, i.e. there is confidence on the data, considered as an accurate representation of actual bird behaviour that shows a lower proportion of birds penetrating deeper into the wind far. This is the judgement made by the study team, and therefore considered more appropriate to use data collected within 3 km to analyse macro avoidance, which avoids overestimating density recorded inside the wind farm.

5. THE USE OF LAWR RADAR DATA IN MACRO AVOIDANCE ANALYSIS

As further described in Appendix 1, in contrast with the SCANTER radar, which has a theoretical detection curve of high probability throughout the studied area, the scanning range of the LAWR radar was set to 6 km, with detection probability known to be relative low close the radar, increasing up to a peak level between 1,500 and 2,750 m, where after dropping again (FEBI 2013). This has implications on the use of the data and how representative they can be considered to be, given that there may have been birds moving close to the radar or beyond 2.7 km not detected by the system.

In order to take these changes in detection probability into account, two different approaches to LAWR radar data treatment (in macro avoidance analysis) were considered and tested using data collected for Northern Gannet, assessing any changes to results arising from their application:

- Use of LAWR radar data that falls within the boundaries of high detection 'doughnut approach'

- Use of the LAWR radar data applying a correction factor based on the theoretical DPC for the LAWR radar.

a) Doughnut approach – methods and results

The doughnut approach is based on the use of radar data collected within the high detection range of the radar. Accordingly, a detectability threshold of 67% was used to represent the upper 1/3 of the detection curve, which results in a distance range between 1,250 and 3,000 m (Figure 14).

The application of this approach assumes that the data collected within the high detection range inside and outside the wind farm is representative of the situation inside and outside the whole wind farm.

NIRAS DHI CARBON TRUST

Figure 14. **Northern Gannet tracks collected within 1250-3000 m from the LAWR radar (turbine G05)**

Gannet tracks within 1250 - 3000 m from G05

⭐	TurbineG01	• Turbines	▦	100x100m grid
⭐	TurbineG05	— Gannet tracks	▦	Windfarm footprint
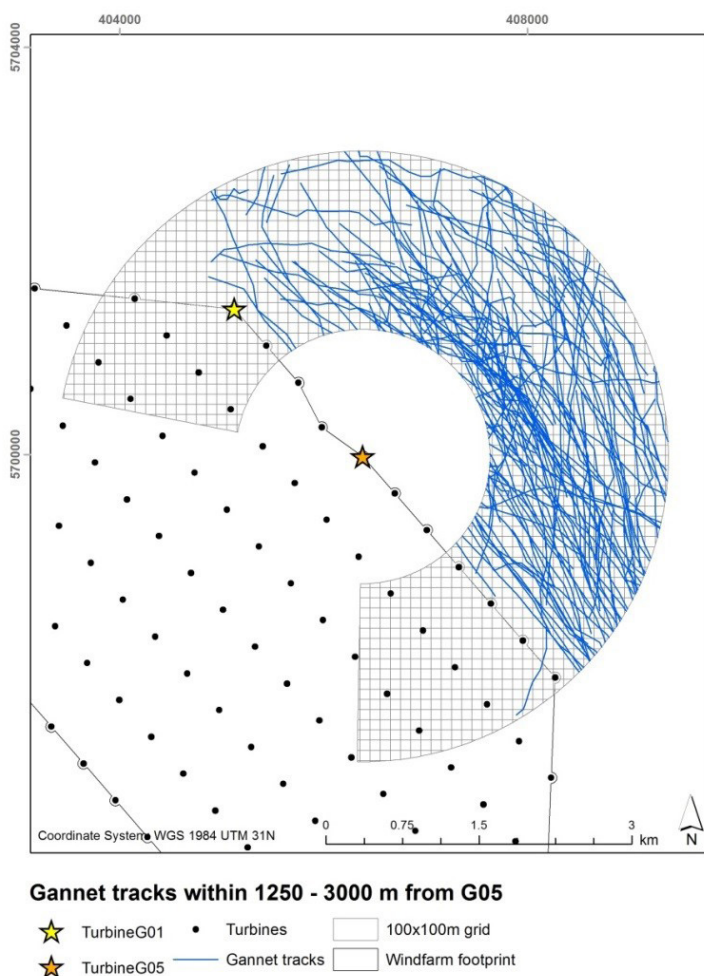
Given that the application of the doughnut approach removes any tracks detected within 1,250 km from the sensor, it identifies a single radar track detected inside the wind farm, resulting in a very high estimate of macro EAR (0.993):

Table 3. **Estimated mean track length per unit area inside and outside the wind farm applying the doughnut approach where the reference density is estimated considering a hypothetical pre-construction density of similar value but uniform inside / outside the wind farm.**

tl/unitA inside	tl/unitA outside	tl/unitA inside (pre-construction)	tl/unitA outside
0.110	21.294	16.419	16.419
Macro EAR			
0.993			

b) *Use of correction factor – methods and results*

The use of a correction factor to account for the varying detection probability with distance from the radar was suggested by the Expert Panel and applied using 500 m distance bands (Figure 15).

The mean track length per unit area was calculated for each distance band and further corrected using a band specific correction factor based on the theoretical DPC for the LAWR radar.

Figure 15.   Northern Gannet tracks collected from G05 (LAWR radar) cut in distance bands of 500 m, mean track length per unit area within each band was corrected by the indicated correction factor.
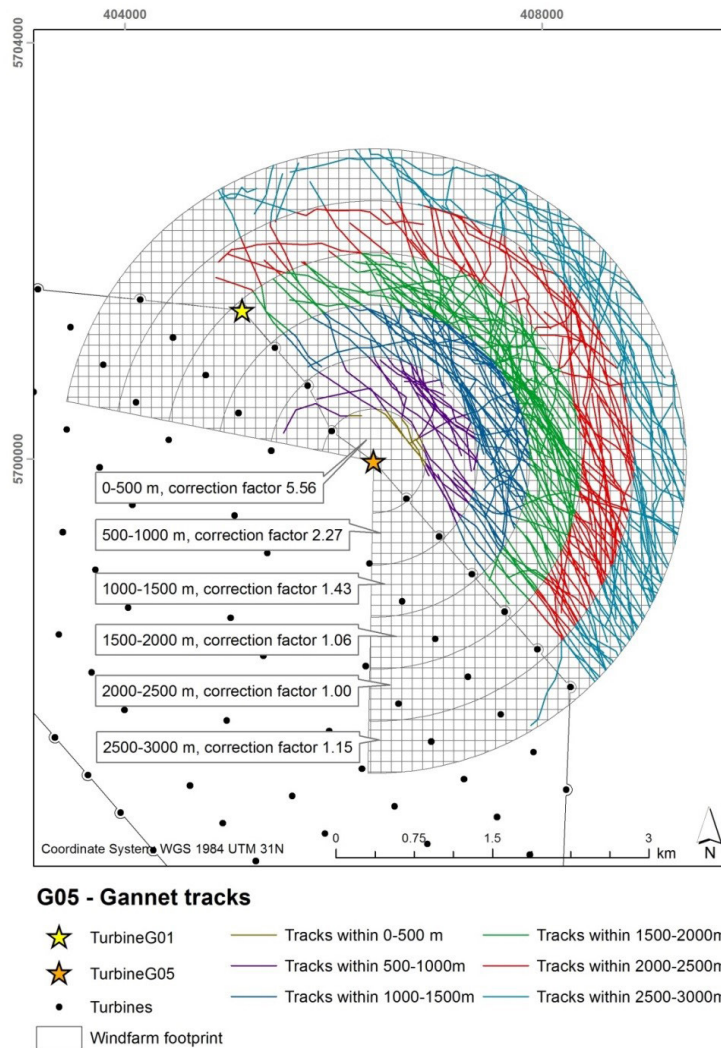
Because only two tracks were recorded inside the wind farm, the estimated avoidance rate was very high, 0.987 (Table 4).

Table 4.   Estimated mean track length per unit area inside and outside the wind farm in distance bands of 500 m and corrected values calculated with the given correction factors (CF).

Distance (m)	CF	tl/unitA inside	tl/unitA outside	corrected tl/unitA in	corrected tl/unitA out
0-500	5.56	0.000	7.988	0.000	44.415
500-1000	2.27	0.636	14.383	1.444	32.650
1000-1500	1.43	0.000	28.207	0.000	40.336
1500-2000	1.06	0.000	29.676	0.000	31.457
2000-2500	1.00	0.000	21.004	0.000	21.004
2500-3000	1.15	0.284	16.957	0.326	19.501
Mean		0.153	19.703	0.295	31.560
Macro EAR					0.987

The exercise illustrates that missing tracks particularly in a spatial context cannot readily be corrected. Only two tracks of Northern Gannet were recorded inside the wind farm, which if corrected increase potential bias, as there is no certainty on whether this is a consequence of bird behaviour or equipment limitations.

c) Conclusion

In comparison with data correction by distance, the doughnut approach is considered more appropriate, as it uses uncorrected data collected in areas where there is more confidence in detection efficiency, both inside and outside the wind farm. However, this approach assumes that these high detection areas can be considered representative of bird movements inside and outside the whole wind farm, which may not be correct, as patterns observed in post-construction data or in data collected by the SCANTER radar indicate aggregations very close to the wind farm that would not be captured if only high detection zones are used.

At the same time, the doughnut approach seems appropriate for the analysis of data collected from turbines F04 and D05 at the meso / micro scale, where representation of data is considered as inside / outside the rotor swept zone, areas covered by the high detection zone defined by the doughnut approach.

It was eventually decided not to use LAWR radar data collected from turbine G05 for the following reasons:

3. Limitations of equipment detection over distance do not provide confidence that data are representative of bird movements around the wind farm, as it is felt likely that there is an underrepresentation of bird movements within 1.2 km / beyond 2.7 km of the sensor both inside and outside the wind farm.

4. Limitations of the equipment performance during windy conditions led to challenges in the interpretation of the radar screen during fieldwork (often infested by sea clutter, see Appendix 1), limiting the amount of data that could be collected and therefore resulting in a limited sample size (465 tracks in comparison with 1,762 tracks collected by the SCANTER radar).

The use of LAWR radar data (corrected / uncorrected) was found to have a very limited influence on overall macro EARs (see Table 2, Section 4), and when used, was observed to increase its value slightly.

6. COMPARISON OF SPECIES IDENTIFICATION WITH DISTANCE INSIDE / OUTSIDE THE WIND FARM

Data collected from turbine G01 (SCANTER) was used for comparing the number of tracks that were identified to species or species group level, and the number of tracks that were not.

The distance to the radar at G01 was estimated for all measurements and for each track the closest measurement was selected for further analyses, separately for tracks identified and unidentified. Number of tracks in different distance bands inside and outside was then summed up and visualised separately inside and outside the wind farm in Figure 16 and Figure 17.

Figure 16. Comparison of tracks identified / unidentified collected from turbine G01 inside the wind farm
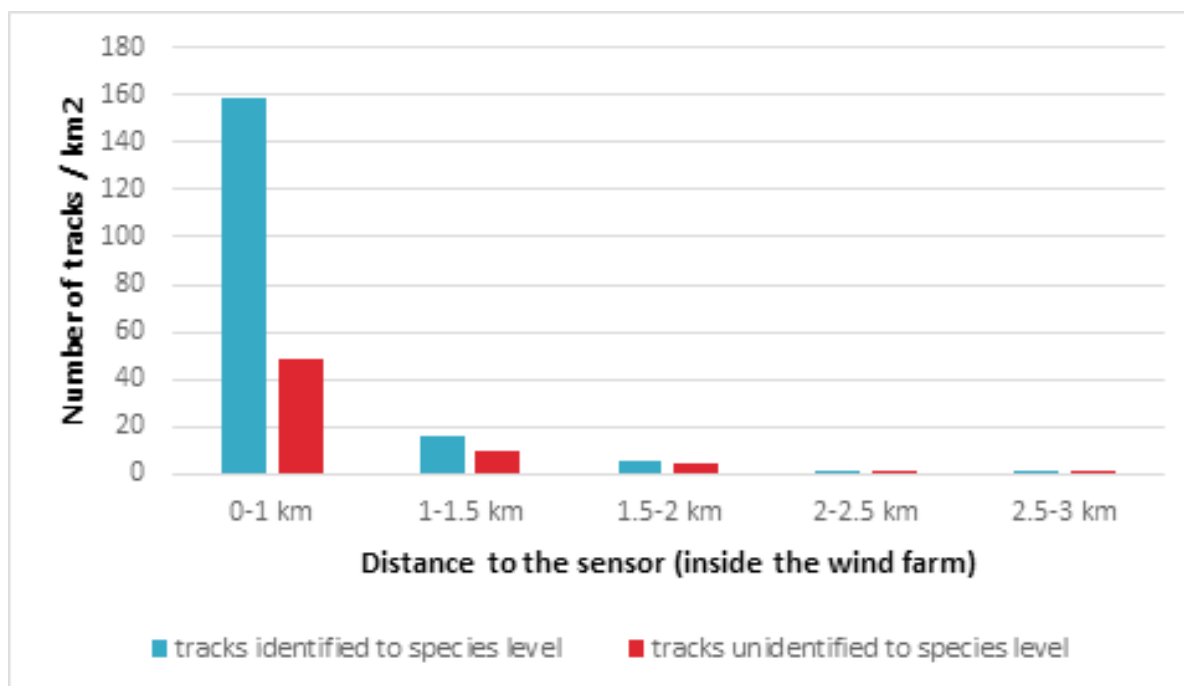
Inside the wind farm the proportion of unidentified tracks range from 24% within 1 km from the wind farm, to 45 – 50% within distance bins between 1.5 – 2.5 km, indicating that a relatively high proportion of tracks has not been identifies (flying over distances beyond which species can be identified) or due to visibility conditions, constraining species identification inside the wind farm. Unidentified tracks have not been used in the analysis / quantification of empirical macro avoidance.

Regarding the area outside the wind farm, the distribution of tracks identified / unidentified follows a similar pattern as inside (Figure 11).

Figure 17. **Comparison of tracks identified / unidentified collected from turbine G01 outside the wind farm**
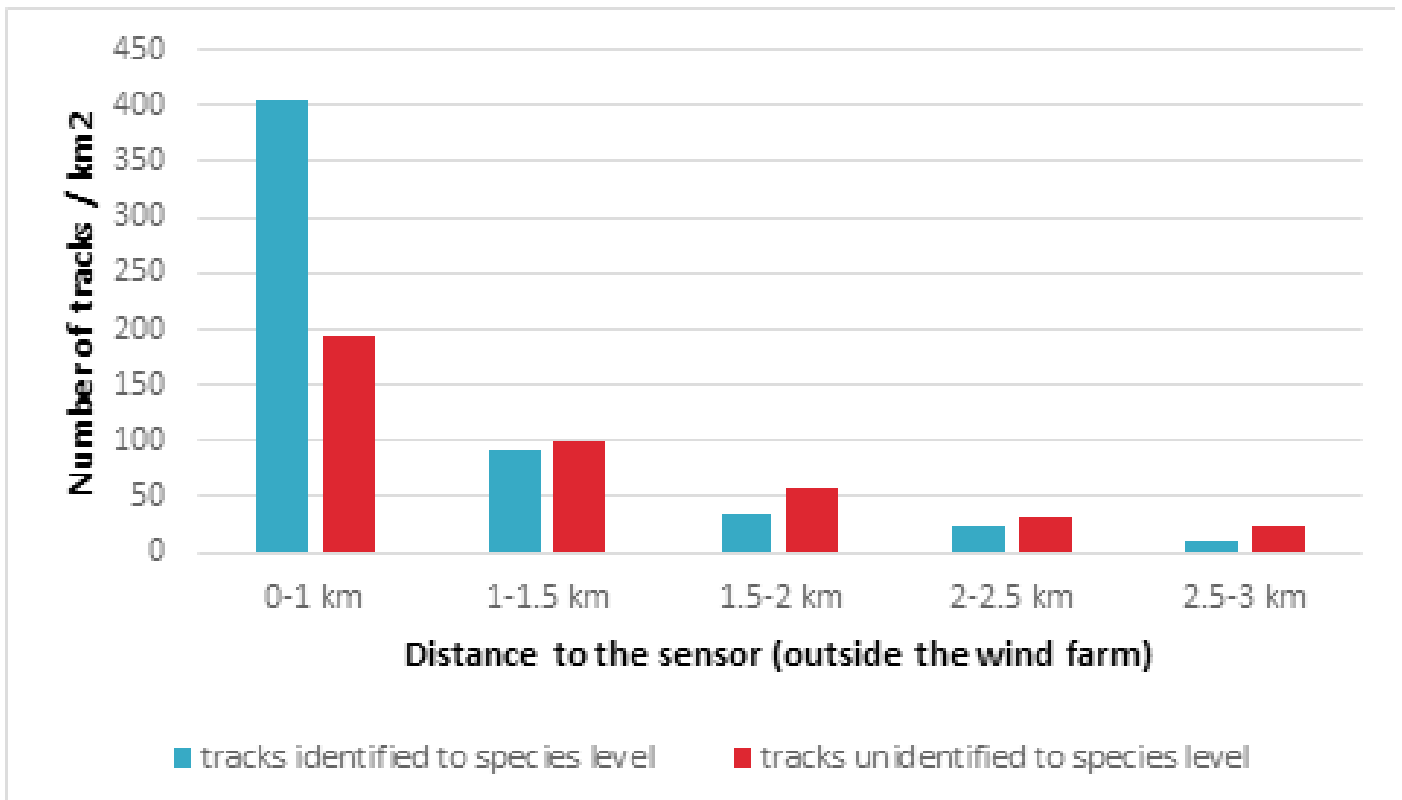
Outside the wind farm, the proportion of tracks unidentified to species level range from 32% within 1 km distance to 63% within distance bin between 1.5 – 2 km, and 69% within distance bin between 2.5 and 3 km. Again, the reasons why tracks were not identified are related to distance of targets and visibility.

The comparison of the proportion of unidentified tracks inside / outside the wind farm follow a similar pattern, with lower proportion close to the wind farm, where identification is easier, increasing as you move away from the sensor. This shows that limitations in the identification of bird tracks apply both inside and outside the wind farms, making comparisons possible, although there is a bias in identification rate in the outermost distance bands.

APPENDIX 3: OBSERVER PROTOCOL

This Appendix presents a summary of the instructions given to observer teams deployed at Thanet Offshore Wind Farm for the collection of data at the macro scale[11]. This includes instructions given during initial / follow-up training, during regular catch-ups, as well as information included in the equipment manuals, which were provided in order to ensure consistent collection of data and minimisation of any potential bias. Additional information not included in this appendix was provided in relation to equipment set-up maintenance and potential hazards associated with the operation and maintenance of the equipment.

Deployment of observer teams

Target – Achieve circa 250 days of survey deployments

Monitoring period – selected weekdays throughout July 2014 – April 2016. Transfer of observer teams to turbines subject to:

Observer availability – to comply with health and safety requirements, each deployment to a turbine requires a team of 2 or more observers with each person accredited with the Global Wind Organisation's Basic Safety Training Course certification.

◊ Operational requirements of Thanet – vessel availability subject to operational and maintenance requirements.
◊ Sea and weather conditions – cessation of transfer to/from turbines for the observer teams required when sea state reaches moderate, i.e. Beaufort force 4-5, depending on local factors such as tidal state.
◊ Equipment status – checked remotely by DHI.

Fieldwork planning

NIRAS to submit to Vattenfall's Service Team for Thanet, a fieldwork weekly plan (Mon – Fri) considering observer availability, vessel availability, weather forecast and equipment status on the week before embarkation.

Vattenfall confirms plan by Friday of the week before embarkation.

◊ Vattenfall / NIRAS checks weather forecast on the day before deployment, re-confirming or cancelling deployment.

Transfers to be made as early as 08:00, returning as late as 18:00, subject to weather conditions. Location of equipment and observers on the turbine platforms is to be maintained throughout the monitoring period.

1. Observer teams

The teams are responsible for allocating the following roles:

◊ **Technician,** responsible for operating the radar, detecting, selecting and following on the radar screen potential bird tracks (targets) using DHI BirdTracker software, and recording the information into the database. Technician guides the observer in finding targets in the field. If observer is engaged with the tracking of a target (i.e. with a rangefinder), the technician is to proceed with locating and identify to species additional targets by use of binoculars or telescope, and associate these to their respective radar tracks, maximising the collection of data.

---

[11] NIRAS (2014) Addendum: Method Statement: Monitoring Equipment Installation, Operation and Decommissioning and Observer Monitoring. Submitted to Vattenfall and Project Team, September 2014.

◊ **Observer,** responsible for visually locating targets as provided by the technician monitoring the radar screen, by means of naked eye, binoculars, telescope and/or rangefinder (to also estimate flight heights). Target to be identified where possible to species and recorded against radar and/ or rangefinder tracks together with the number and activity of the bird(s).

2. Tracking protocol

2.1. Tracking birds using rangefinder and radar

The purpose of the tracking session is to track and identify as many birds/flocks detected by the radar as possible.

When the SCANTER or LAWR radar are operational, these should be used to support the selection and tracking of targets by the Technician. The PC screen connected to the radar will display radar images that can be used to select targets both inside and outside the wind farm.

Technicians can follow up to 10 tracks at a time by tracing the radar track on screen. Each track will have several nodes, representing the location of the target (birds) over time.

When the target generating a potential bird track being followed comes within visible range (within 1.5-2 km distance depending on species), its identity to species level shall be sought by use of binoculars and/ or telescope. When confirmed, the targets' identity together with its associated parameters (e.g. numbers of birds, age groups, behavioural activity and estimated flying altitude as 'listed' by BirdTracker) shall be recorded by the technician using the BirdTracker database. Flight height above the sea level should be estimating when identifying birds to species level, as this will provide useful ground-truthing data in relation to the height measurements by the rangefinder (when used in parallel).

Irrespectively of whether the target generating the potential bird track being followed can be visually identified to species (group) or not, the technician shall continue to follow the target using BirdTracker until lost from the radar screen.

Guided by the technician, who has access to the radar screen, the observer shall also attempt to find and follow different targets in the field both inside and outside the wind farm, identifying them to species level once within species-identification range (around 1.5 – 2 km depending on species and visibility conditions), using the rangefinder, binoculars and/or telescope.

If using the rangefinder, it will only be possible to follow one target at a time within 1.5 km of the observer position, average detection range of the rangefinder.

The rangefinder shall be "fired" with approximately 3-5 seconds intervals, and positions and altitudes will be logged automatically via GPS, providing long series of recordings for an individual focal bird or bird flock. Parameters that shall be recorded by the observer from visual observation include the bird's age, behavioural activity and estimated flight altitude, using a logbook cross referenced against the ID codes of the track nodes assigned by the GPS device. The simultaneously tracking of the bird by rangefinder and radar shall also be noted.

If the number of tracks detected by the radar exceeded 10 tracks, decisions shall be made on which tracks to follow using a list of prioritised species (see Section 4 of this Appendix).

2.2. Tracking birds using rangefinder when radar "not available"

If the SCANTER or LAWR radar are not fully operational during survey deployment, only rangefinders can be used to track birds within 1.5 km from the observers position, distance from which species can usually be identified.

In this case, the selection of targets shall be made through sweeping the field of view both inside and outside

the wind farm, using the telescope or binoculars as required, commencing with the first target detected from the left side and continuing with the remaining range clockwise, repeating the process in the opposite direction once the right side of the field of view is reached.

Following loss of the target due to distance or visibility, the observer shall record for the track followed species and associated parameters. The tracking of the bird by rangefinder but not radar shall also be noted.

3. Prioritisation of target species

The prioritisation of target species shall help to concentrate efforts on the selection of target species, particularly in situations where the number of tracks detected by the radar is more than 10.

In cases when there are 10 tracks being followed and a new target of higher priority turns up, the target of lowest priority shall be dropped, and tracking of the higher priority target shall commence.

Based on the target species and anticipated sample sizes, the prioritisation of species shall follow this hierarchy (from higher to lower priority):

1. Kittiwake
2. Any large gull species
3. Northern Gannet
4. Any small gull species
5. Great Skua
6. Sandwich Tern
7. Any other seabird species
8. Any waterbird species
9. Landbird species

4. Grouping of gull species

Recordings of gulls, which cannot be identified to species level (Laridae spp.), shall be recorded in as much detail as possible, attempting to record to the level of one of the following groups:

◊ Black-backed gull sp.
◊ Large gull sp
◊ Small gull sp (excludes Kittiwake)
◊ Gull sp (excludes Kittiwake)
◊ Gull/Kittiwake sp.

5. Rangefinder calibration

The calibration of rangefinder recordings shall be made using the nacelle on nearby turbines, as opposed to the use of nacelles on the turbine of deployment. This calibration will allow to:

◊ spatially adjust horizontal positioning of records that may have been affected by metal interference
◊ spatially adjust vertical positioning of records in relation to the baseline altitude

Recordings and labels shall be double-checked in order to minimise erroneous spatial adjustments of the data.

NIRAS **DHI** CARBON TRUST

# APPENDIX 4: WIND AND VISIBILITY CONDITIONS AT THANET DURING MONITORING

An overview of the wind conditions at Thanet per month is given in the Figures below. Wind speed is in m/s. Regarding visibility conditions, the proportion of visibility measurements below 3 or 1 km per month is illustrated in the graph below, showing that visibility, below 3km is quite rare, with the exception of July and August 2014, when there was a long period with poor visibility.
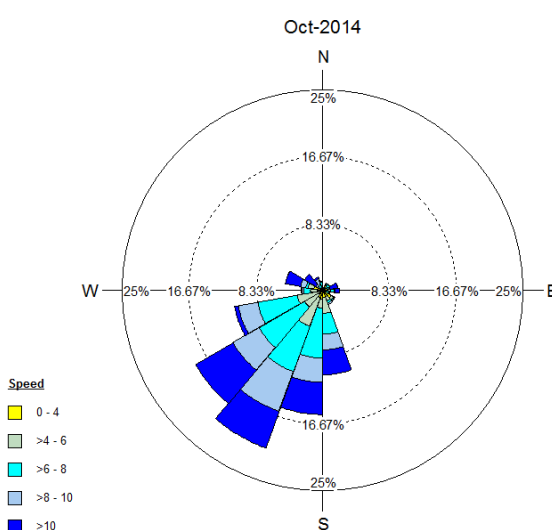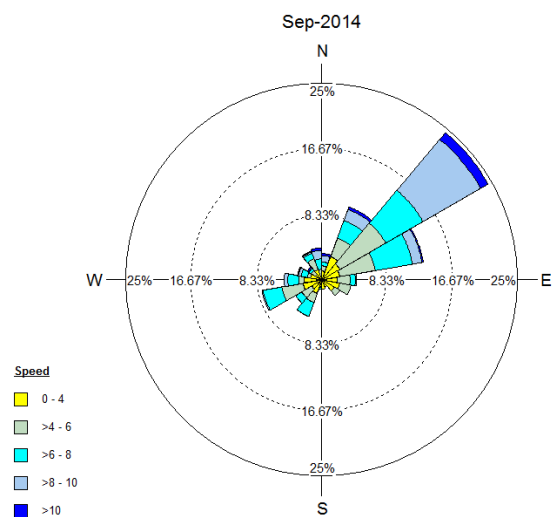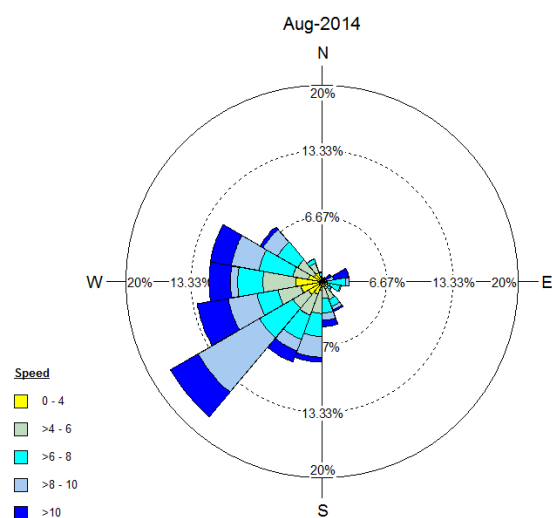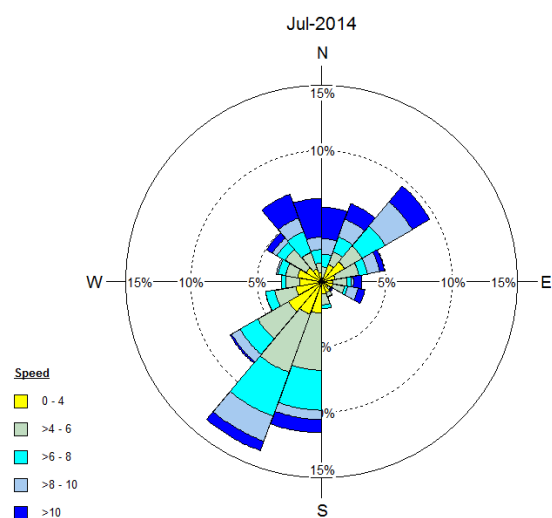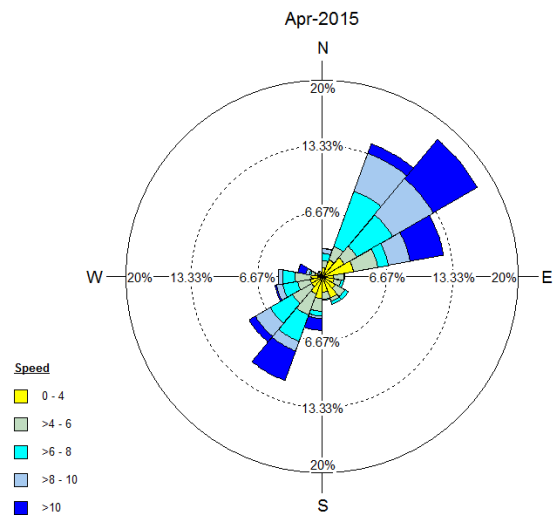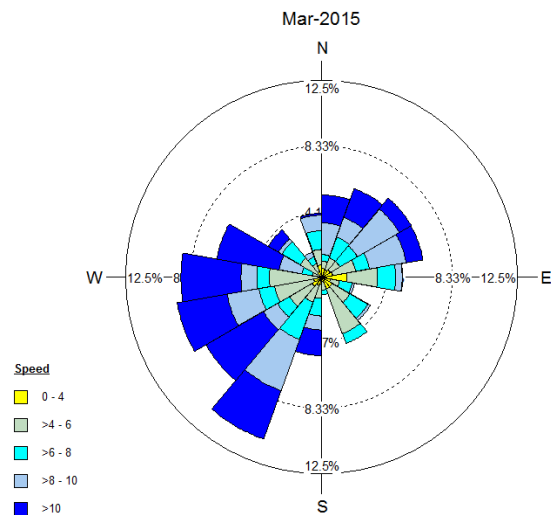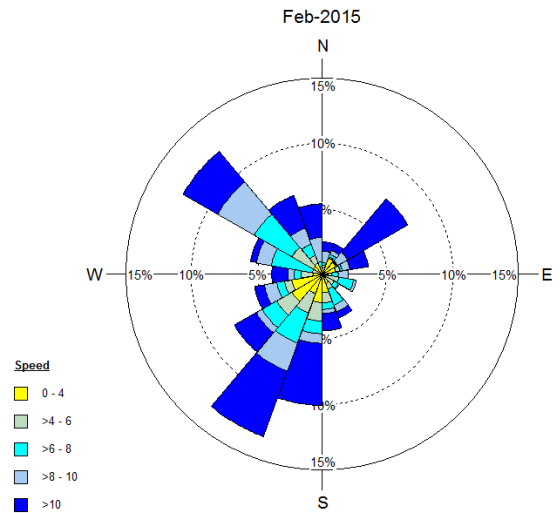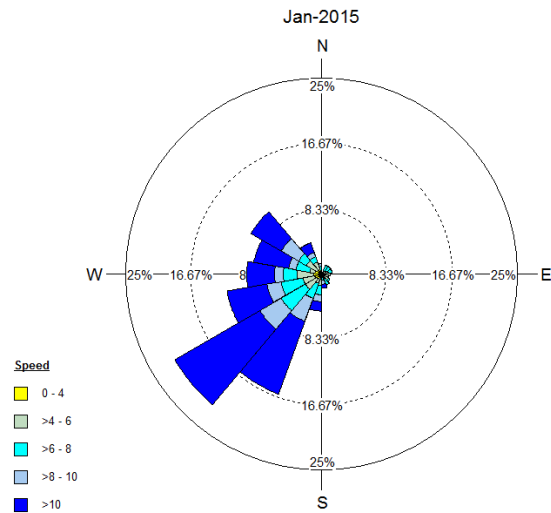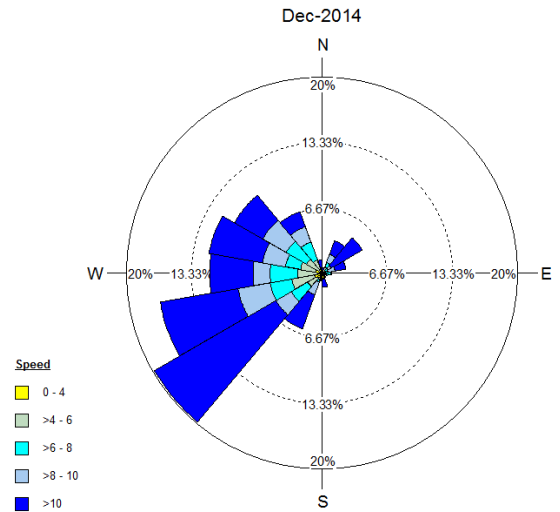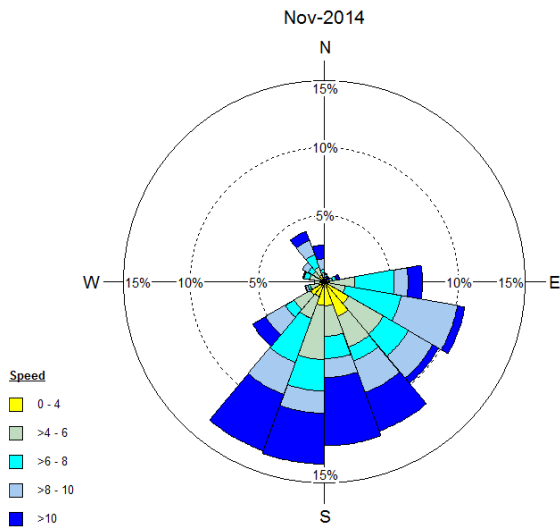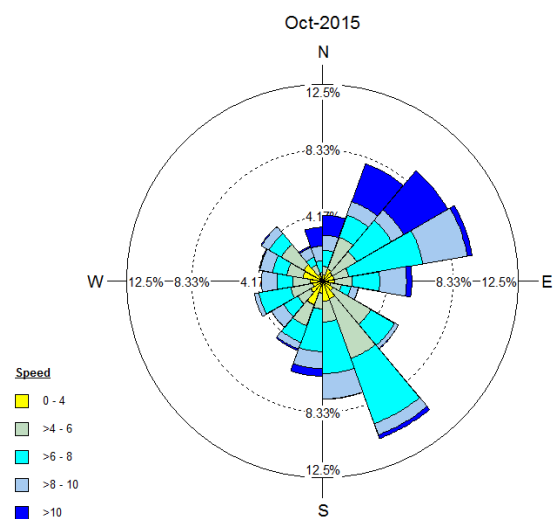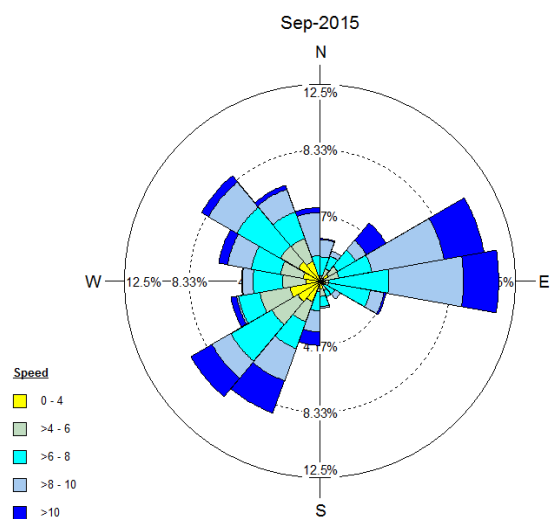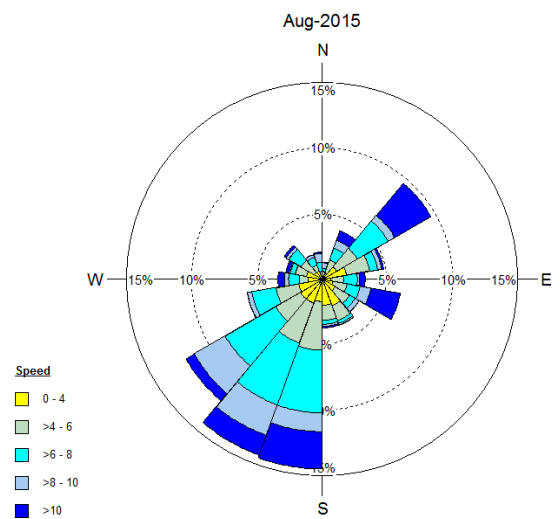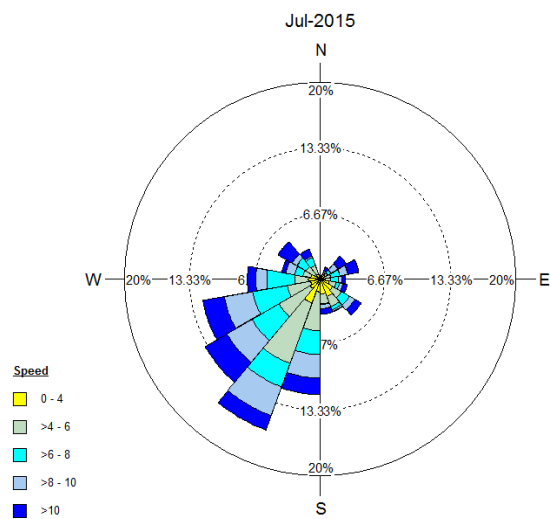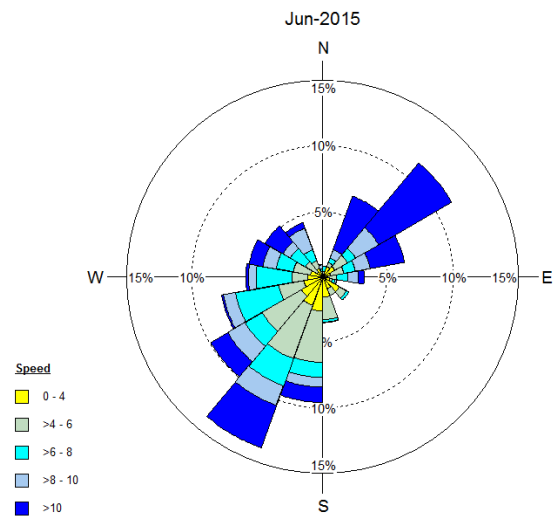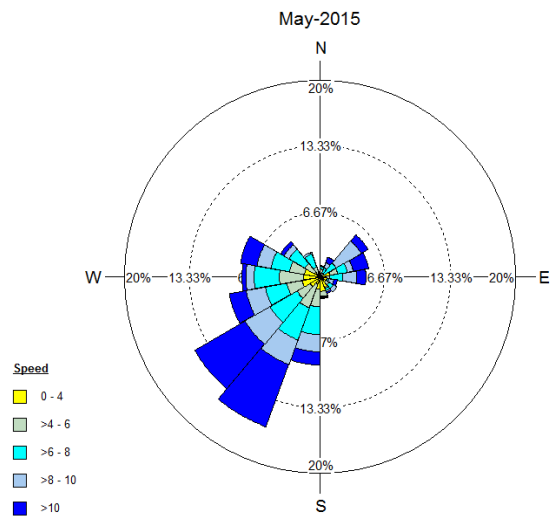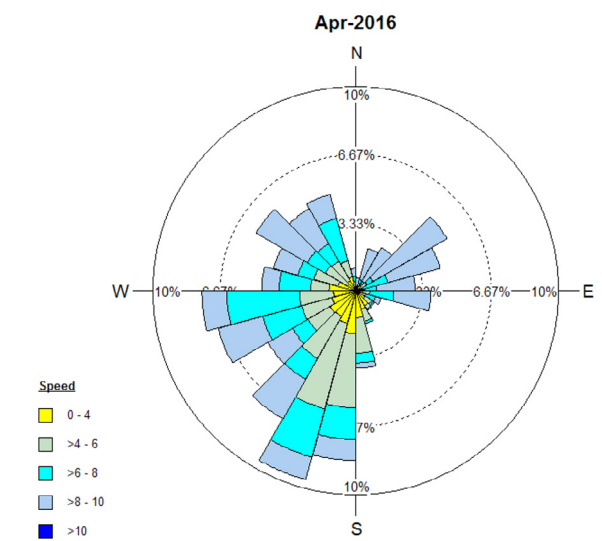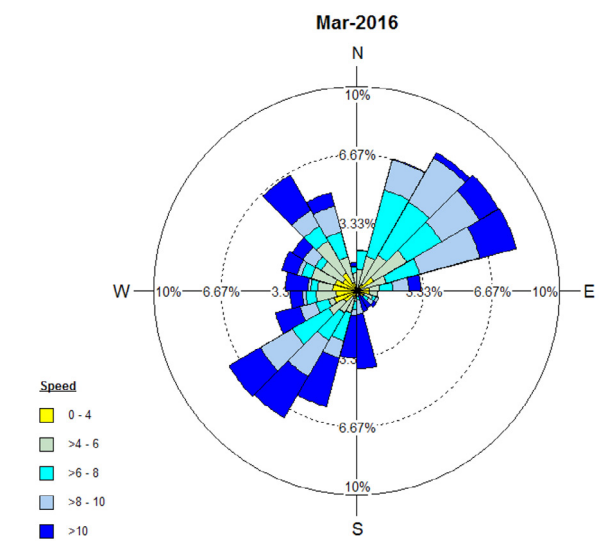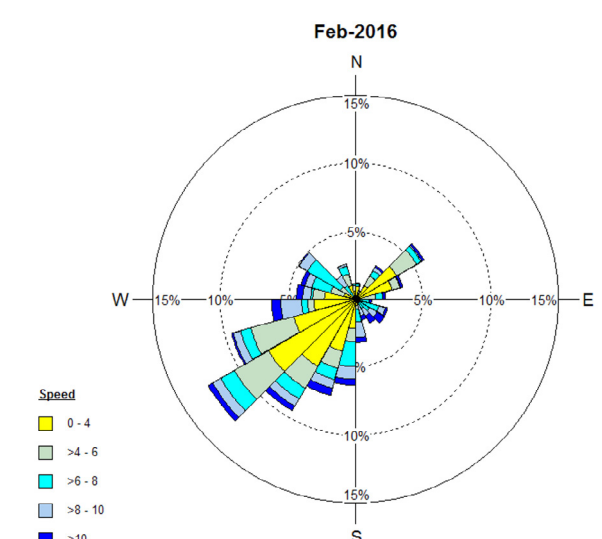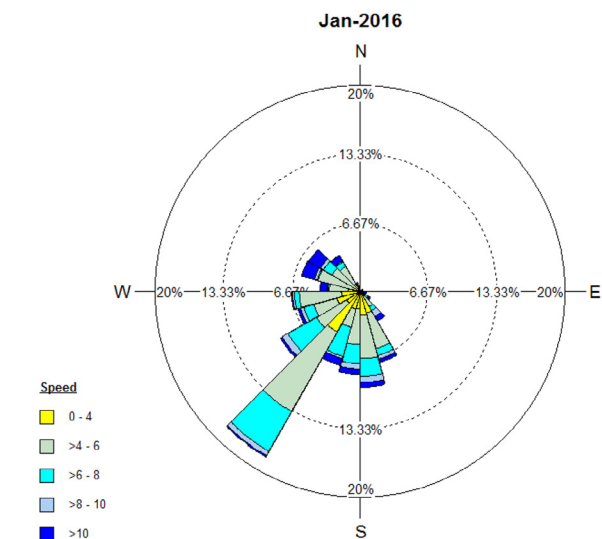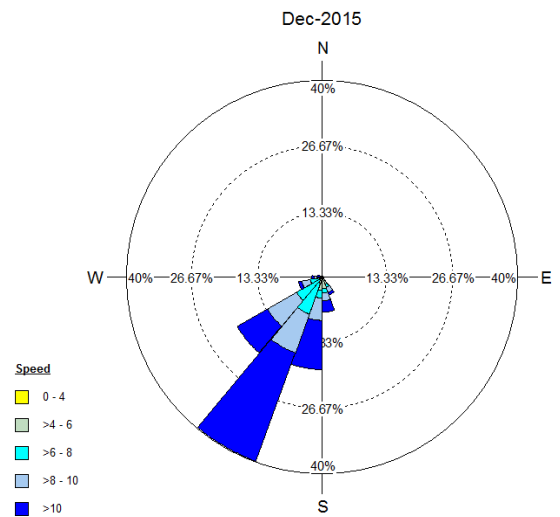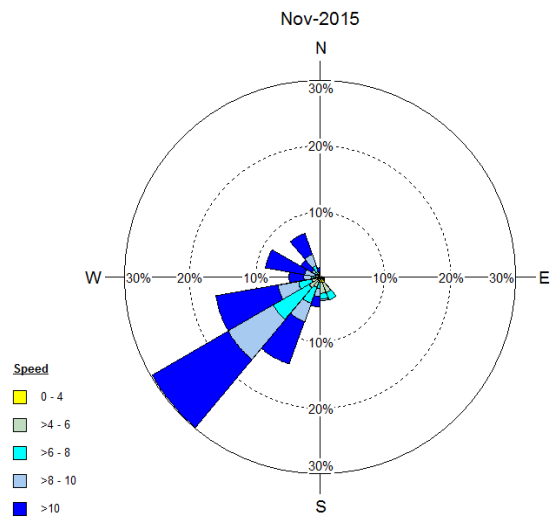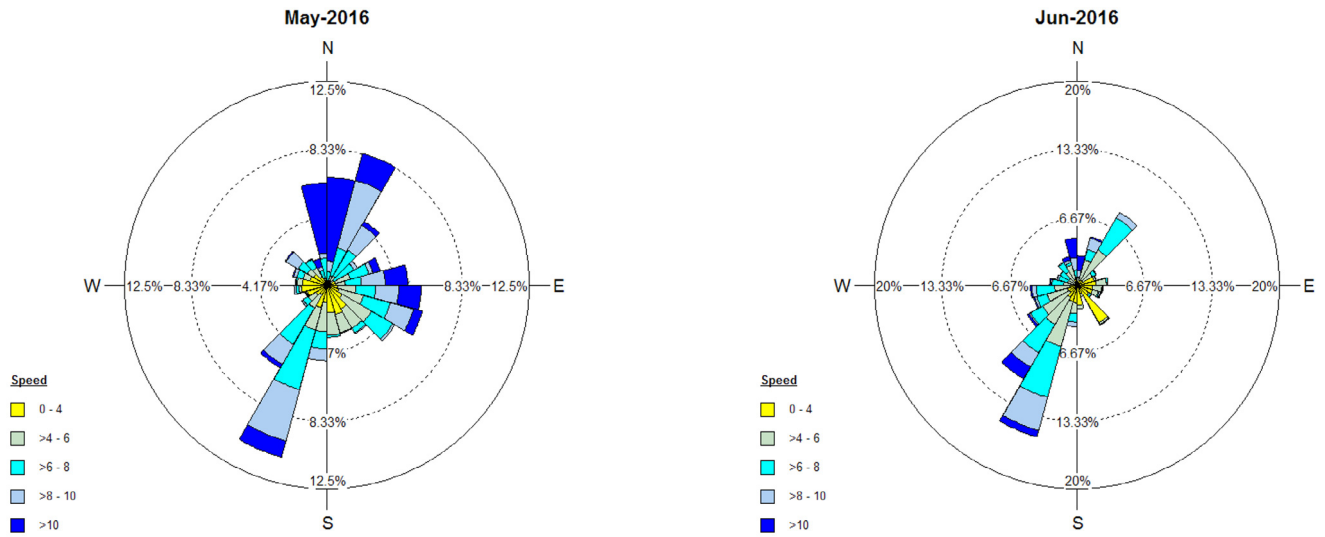
Regarding visibility conditions, the proportion of visibility measurements below 3 or 1 km per month is illustrated in the graph below, showing that visibility, below 3km is quite rare, with the exception of July and August 2014, when there was a long period with poor visibility.

APPENDIX 5: FIELDWORK EFFORT AND GUIDANCE ON THE DEPLOYMENT OF MONITORING SYSTEMS
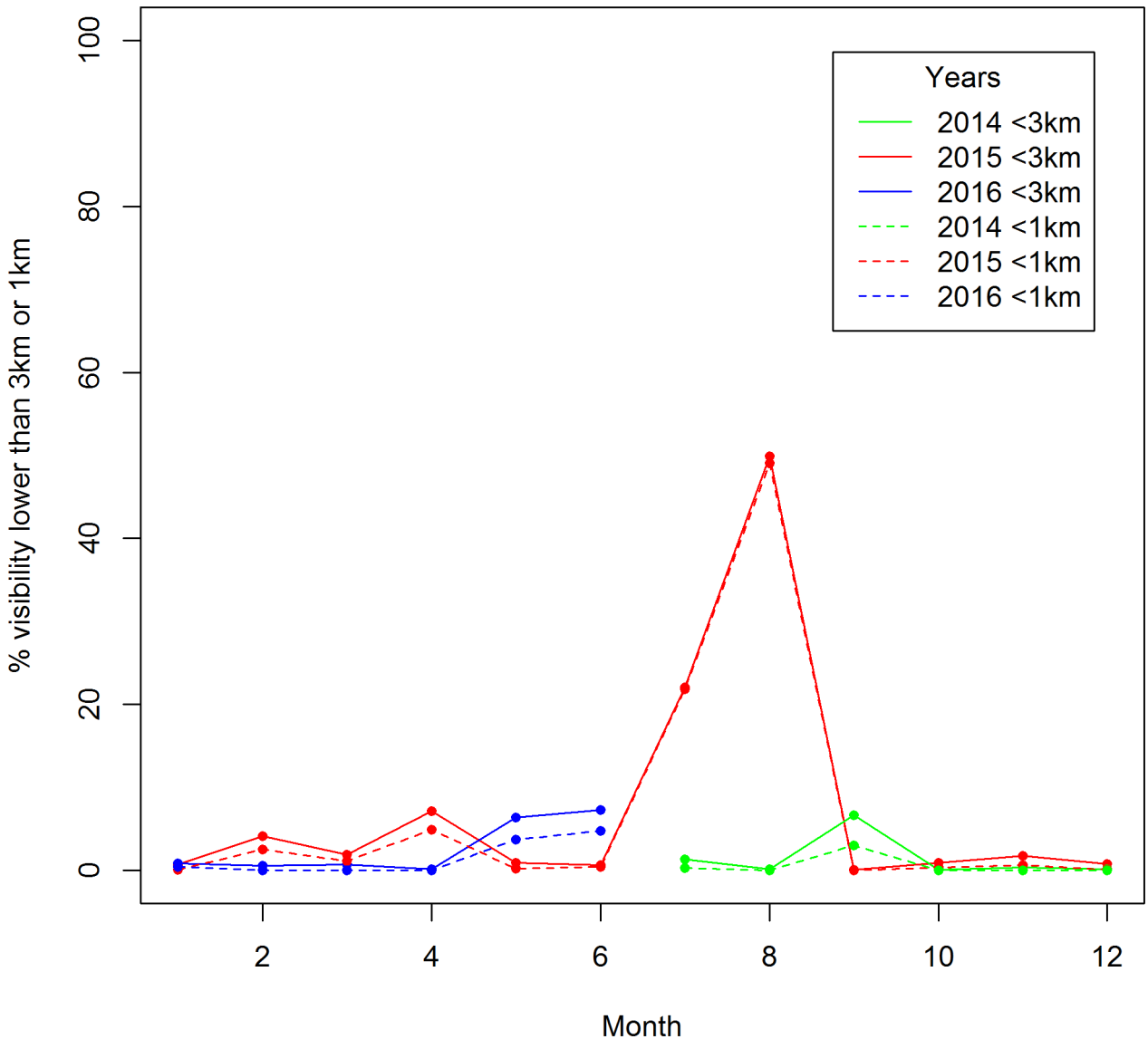
1. FIELDWORK EFFORT

The table below provides an overview of fieldwork effort from June 2014 to April 2016, where the following definitions are used:

- **Survey deployment day** – deployment days used to undertake seabird surveys at Thanet Offshore Wind Farm. These days are discounted from the 250 deployment days contracted.

- **Training deployment day** – deployment days used by DHI to train the observers in the use of the bird tracking equipment, which are separate from the 250 deployment days contracted.

- **Overall No. of downtime days** – Survey deployment days planned but cancelled after observer mobilisation, either due to last minute changes in vessel availability or last-minute decision made by Vattenfall not to proceed with transfer ("vessel downtime"); or due to an unexpected change in weather conditions ("weather downtime").

  - ◊ **Vessel downtime days** are discounted from the 250 deployment days contracted .
  - ◊ **Weather downtime days**, are discounted from the 250 deployment days contracted at lower rate than survey deployment days.

- **Technical deployment days** - deployment days used for the observers to assist DHI/Terma technicians, which are separate from the 250 deployment days contracted;

- **No. seats requested** – refer to seats requested in transfer vessel for survey deployment or training, and does not include seats requested for technicians servicing the equipment;

- **No. seats cancelled** – according to the table below a total of 769 seat requests have been cancelled, which correspond to 74% of the total number of requests. Main reasons include:

  - ◊ Weather
  - ◊ Vessel availability
  - ◊ Other, such as observer availability or strategic decision to cancel fieldwork due to associated costs on observer mobilisation.

Month	Survey deployment days (Original plan)	Survey deployment days		Training deployment days		Overall No. of downtime days	Vessel downtime days	Weather downtime days
		G01	G05	G01	G05			
Jun-14	0	0	0	3*		0	0	0
Jul-14	24	6	6	0	0	0	0	0
Aug-14	24	0	0	2	2	0	0	0
Sep-14	8	10	10	2	2	6	4	2
Oct-14	8	0	0	0	0	0	0	0
Nov-14	8	7	2	1	1	0	0	0
Dec-14	8	0	0	0	0	0	0	0
Jan-15	8	4	4	0	0	8	4	4
Feb-15	6	6	6	0	0	2	0	2
Mar-15	6	6	0	0	0	2	0	2
Apr-15	8	0	6	0	0	2	0	2
May-15	8	9	6	0	0	0	0	0
Jun-15	12	0	0	0	0	4	4	0
Jul-15	24	10	8	0	0	0	0	0
Aug-15	24	10	4	0	0	2	2	0
Sep-15	8	2	2	0	0	4	0	4
Oct-15	8	16	8	0	0	0	0	0
Nov-15	8	0	2	0	0	0	0	0
Dec-15	8	6	6	0	0	0	0	0
Jan-16	8	5	10	3	22	0	0	0
Feb-16	6	12	10	0	0	0	0	0
Mar-16	8	15	12	0	0	3	3	0
Apr-16	8	2	2	0	0	0	0	0
May-16	6	0	0	0	0	0	0	0
Jun-16	6	0	0	0	0	0	0	0
Total	250	230		18*		33	17	16

Month	Technical deployment days	No. seats requested	No. seats cancelled due to:		
			Weather	Vessel availability	Other
Jun-14	0	6	0	6	0
Jul-14	0	24	4	8	0
Aug-14	0	12	2	2	4
Sep-14	0	38	6	8	0
Oct-14	2	42	18	24	0
Nov-14	0	51	18	24	0
Dec-14	0	44	28	16	0
Jan-15	0	56	44	4	0
Feb-15	4	48	12	20	0
Mar-15	0	56	32	12	6
Apr-15	0	44	16	22	0
May-15	0	46	23	8	0
Jun-15	2	54	18	10	26
Jul-15	0	58	18	14	8
Aug-15	0	42	10	10	6
Sep-15	0	36	24	0	4
Oct-15	1	44	20	0	0
Nov-15	0	78	60	8	0
Dec-15	0	64	40	8	4
Jan-16	0	70	44	4	2
Feb-16	0	64	36	2	4
Mar-16	0	52	20	0	2
Apr-16	0	4	0	0	0
May-16	0	0			
Jun-16	0	0			
Total	9	1033	493	210	66

NIRAS DHI CARBON TRUST

2.   CONSIDERATION IN THE DESIGN AND DEPLOYMENT OF MONITORING SYSTEMS OFFSHORE

9.1.18. The deployment of monitoring equipment offshore has provided a range of lessons that may be useful in future studies, particularly when designing communication protocols and procedures to offshore transfer:

Description	Recommendations
Access to a turbine is governed by suitable weather for vessel transfer, vessel availability to the wind farm and access to the turbine itself.	• **Use several weather forecasts to identify good weather windows and plan your fieldwork.** • **Account for sufficient downtime time in your fieldwork plan to consider weather constraints.** • **Early discussion with wind farm host can provide valuable information on historical accessibility to turbines based on local weather conditions.** • **Follow the offshore wind farm operational team advice, their experience on suitability of weather conditions can be invaluable.**
Access to a turbine is also dependent on maintenance operations required at the wind farm and vessel availability	• **Early discussion with wind farm host can provide valuable information on maintenance routines and planning, access /availability of vessels.** • **Account for sufficient downtime time in your fieldwork plan to consider vessel access.**
Decision on transfer need to be made in advance, and therefore communication with offshore wind farm host is essential	• **Establish effective communication channels (key contact points) and a communication protocol that identifies decision-making while avoiding excessive administrative burden.** • **Take into account working hours of offshore wind farm teams.** • **Establish time lines for regular request / response (e.g. vessel transfer)**
Offshore activities need to have due consideration to H&S requirements	• **Agree on H&S protocol with your team and make sure it is revised and approved with the wind farm host, who may be able to guide you on specific requirements** • **Request required minimum specifications/standards for any additional equipment to be used and keep a log of certification expiry dates using an alert system that warns you in advance of any expiry dates** • **Keep a log of H&S related certifications for your team, using an alert system that warns you in advance of any expiry dates**
Equipment installed offshore is exposed to a very harsh environment	• **In order to ensure rapid response to failure, an automatic notification system that uses mobile data / of high speed data network of the wind farm can be used. This can also be set up to allow for minor issues to be solved.** • **Consider regular maintenance operations at the wind farm, which can be used to check equipment status and correct power supply**
Training of offshore teams is essential to ensure collection of data in a consistent manner	• **Provide sufficient training to your offshore in the use of the installed equipment. This should include protocols for data collection, management of technical issues and solving of minor issues, clarity on roles and responsibilities and communication protocol with wind farm host and technicians that may be accessed remotely to assist during fieldwork.**

NIRAS   DHI   CARBON TRUST

APPENDIX 6: MONTHLY BREAKDOWN OF ALL RADAR (SCANTER/LAWR) AND RANGEFINDER DATA COLLECTED FROM TURBINES G01 AND G05

* Northern Gannet **(GX)**
Black-legged Kittiwake **(KI)**
Great Black-backed Gull **(GBBG)**
Herring Gull **(HG)**
 Lesser Black-backed gull **(LBBG)**

2014							
Month	Species	Jul	Aug	Sep	Oct	Nov	Dec
SCANTER radar tracks (G01)	NG	NA	NA	5	NA	22	NA
	BLKW	NA	NA	NA	NA	9	NA
	GBBG	NA	NA	NA	NA	4	NA
	HG	NA	NA	NA	NA	1	NA
	LBBG	NA	NA	NA	NA	2	NA
RF tracks (G01)	NG	32	3	24	1	24	NA
	BLKW	1	NA	3	2	9	NA
	GBBG	1	2	41	3	6	NA
	HG	24	NA	5	NA	NA	NA
	LBBG	16	NA	13	1	6	NA
LAWR radar tracks (G05)	NG	NA	NA	3	NA	6	NA
	BLKW	NA	NA	NA	NA	NA	NA
	GBBG	NA	NA	NA	NA	NA	NA
	HG	NA	NA	1	NA	NA	NA
	LBBG	NA	NA	NA	NA	1	NA
RF tracks (G05)	NG	21	NA	27	NA	3	NA
	BLKW	NA	NA	1	NA	1	NA
	GBBG	2	NA	17	NA	NA	NA
	HG	26	NA	11	NA	NA	NA
	LBBG	16	NA	28	NA	6	NA

NIRAS DHI CARBON TRUST

2015													
Month	**Species**	**Jan**	**Feb**	**Mar**	**Apr**	**May**	**Jun**	**Jul**	**Aug**	**Sep**	**Oct**	**Nov**	**Dec**
SCANTER radar tracks (G01)	NG	NA	NA	21	NA	59	NA	69	5	1	50	NA	52
	BLKW	NA	NA	NA	NA	1	NA	1	NA	NA	1	NA	2
	GBBG	NA	NA	7	NA	13	NA	21	3	NA	49	NA	7
	HG	NA	NA	4	NA	54	NA	48	13	NA	10	NA	NA
	LBBG	NA	NA	NA	NA	70	NA	40	19	NA	5	NA	NA
RF tracks (G01)	NG	NA	8	23	NA	25	NA	27	9	4	13	NA	62
	BLKW	NA	22	NA	NA	1	NA	1	NA	NA	NA	NA	4
	GBBG	NA	5	8	NA	2	NA	11	5	NA	25	NA	18
	HG	NA	4	5	NA	15	NA	38	10	NA	5	NA	2
	LBBG	NA	3	NA	NA	20	NA	20	21	NA	6	NA	NA
LAWR radar tracks (G05)	NG	4	19	NA	NA	44	NA	32	5	NA	20	NA	4
	BLKW	NA	3	NA	NA	7	NA	NA	NA	NA	1	NA	NA
	GBBG	NA	7	NA	NA	NA	NA	1	NA	NA	9	NA	NA
	HG	NA	NA	NA	NA	17	NA	8	NA	NA	2	NA	NA
	LBBG	NA	1	NA	NA	22	NA	2	1	NA	NA	NA	NA
RF tracks (G05)	NG	14	NA	NA	NA	17	NA	19	8	NA	3	13	33
	BLKW	5	NA	NA	NA	1	NA	NA	NA	NA	NA	19	19
	GBBG	6	NA	NA	NA	1	NA	1	6	NA	2	4	9
	HG	NA	NA	NA	NA	4	NA	14	5	NA	2	1	NA
	LBBG	NA	NA	NA	NA	7	NA	5	4	NA	1	NA	1

	2016					July 2014 - April 2016
Month	Species	Jan	Feb	Mar	Apr	Total
SCANTER radar tracks (G01)	NG	16	50	233	2	585
	BLKW	23	18	21	NA	76
	GBBG	13	19	84	NA	220
	HG	9	3	45	NA	187
	LBBG	NA	1	5	2	144
RF tracks (G01)	NG	35	51	87	NA	428
	BLKW	26	50	16	NA	135
	GBBG	16	30	28	NA	201
	HG	10	10	26	NA	154
	LBBG	1	1	7	NA	115
LAWR radar tracks (G05)	NG	25	23	NA	NA	185
	BLKW	21	17	NA	NA	49
	GBBG	21	9	NA	NA	51
	HG	4	3	NA	NA	36
	LBBG	NA	2	NA	NA	29
RF tracks (G05)	NG	23	44	52	1	278
	BLKW	35	51	28	1	161
	GBBG	16	22	32	1	119
	HG	8	26	46	5	148
	LBBG	NA	1	9	1	79

APPENDIX 7: MONTHLY BREAKDOWN OF VIDEO DATA COLLECTED BY THE LAWR / TADS CAMERA SYSTEM FROM TURBINES F04 AND D05

* Northern Gannet **(GX)**
Black-legged Kittiwake **(KI)**
Great Black-backed Gull **(GBBG)**
Herring Gull **(HG)**
 Lesser Black-backed gull **(LBBG)**

2014			
Month	**Oct**	**Nov**	**Dec**
Night videos	6,173	17,519	24,370
Daylight videos	6,457	10,835	14,279
% daylight bird videos	0.6%	10.4%	5.3%
No. daylight videos analysed	36	1,132	755
Sample size by species			
GX	1	54	92
KI	-	44	2
GBBG	-	44	26
HG	3	44	6
LBBG	-	-	-
LBBG/GBBG	17	220	1
Unid. gull	1	327	48
Unid. large gull	8	271	555

2015												
Month	**Jan**	**Feb**	**Mar**	**Apr**	**May**	**Jun**	**Jul**	**Aug**	**Sep**	**Oct**	**Nov**	**Dec**
Night videos	20,620	17,358	22,677	26,209	16,918	16,619	10,058	18,561	22,086	28,585	28,442	38,434
Daylight videos	12,326	14,684	27,346	40,500	33,320	45,642	23,463	34,768	28,524	25,353	19,645	22,729
% daylight bird videos	1.8%	5.0%	2.2%	1%	0.2%	1.1%	1.2%	0.8%	0.9%	1%	2.1%	10.5%
No. daylight videos analysed	223	738	607	418	60	485	270	288	254	266	409	2,377
Sample size by species												
GX	45	83	65	4	-	10	2	1	5	5	15	619
KI	1	7	3	3	-	6	2	0	2	-	27	4
GBBG	17	-	17	5	2	10	9	3	4	4	41	61
HG	-	-	12	86	11	17	5	11	2	-	9	1
LBBG	-	-	-	21	1	0	1	4	2	-	-	1
LBBG/GBBG	-	17	-	39	10	2	9	18	15	38	66	307
Unid. gull	4	232	18	21	1					59	48	600
Unid. large gull	149	26	498	190	29	88	60	159	122	142	161	-

NIRAS DHI CARBON TRUST

	2016						Oct 2014 - Jun 2016
Month	Jan	Feb	Mar	Apr	May	Jun	Total
Night videos	28,561	25,419	26,588	26,272	24,710	12,985	459,164
Daylight videos	16,649	20,638	31,831	42,149	53,636	33,780	558,554
% daylight bird videos	4.1%	7.4%	2.4%	1.3%	1.1%	0.7%	2.3 %
No. daylight videos analysed	678	1517	773	552	561	224	12,623
Sample size by species							
GX	224	293	117	14	3	8	1660
KI	15	77	6	34	0	4	237
GBBG	25	39	22	5	1	1	336
HG	8	24	22	20	16	11	308
LBBG	0	0	6	17	11	0	64
LBBG/GBBG	7	16	26	19	6	6	839
Unid. gull			186	311	381	165	2,170
Unid. large gull	86	200	255	108	84	16	3,207

APPENDICES

APPENDIX 8: DATA ANALYSIS OPTIONS (MACRO AND MESO AVOIDANCE)

1. APPROACH FOR ESTIMATING EMPIRICAL MACRO AND MESO AVOIDANCE RATES

During the course of the study different approaches for calculating EARs has been assessed. Here the different option considered are described.

◇ At the beginning of the study **track abundance** was used for comparing the change in track abundance (outside - inside) with the track abundance outside the wind farm (or 1-abundance inside/abundance outside). However, because the size and the shape of the areas inside and outside were different it was later considered more appropriate to analyse the data as **track densities** (number of tracks/area).

I. The use of **track densities** still did not solve the issue of different sized areas and therefore track length per unit area was used.

II. A method based on the **probability of birds avoiding the wind farm** was also considered. This option was considered to allow making simulations based on the rates more robust as they could be performed using binomial theory and avoid assumptions of normally distributed data. However, bootstrapping could be used for estimation of uncertainty around the mean avoidance rates without assuming normally distributed data. Since a probability would not make it possible to describe attraction of seabirds this option is judged as not suitable for the ORJIP BCA Study.

III. A method based on **changes in track direction** was also considered, but there was consensus reached between NIRAS / DHI, BTO and Bill Band not to progress this option due to the overly subjective requirements. BTO elaborate that 'data from tracking studies show that birds flying offshore frequently change direction and do not always fly in straight lines, particularly when engaged in behaviours like area-restricted search foraging. As a consequence, it is very difficult to discern a change of direction in response to the presence of the wind farm from background variation in flight patterns'. However, it should be noted that there are members of the Expert Panel that would prefer the exploration of this option further, considered more appropriate to reflect bird avoidance behaviour.

Different formulas have also been considered these are listed and described in the table below. The option selected for analysis is highlighted in grey, and also described in Section 4 of the main body of the report.

- N_{in} is the mean track length per unit area (or track density for option 2 and 3 in the table) within the wind farm (macro) or within RSZ + buffer (meso)

- N_{ref} is the mean track length per unit area in the absence of the wind farm. It is calculated based on the assumption that pre-construction the same number of birds were present but evenly distributed in the studied area.

- N_{out} is the mean track length per unit area (or track density for option 2 and 3 in the table) outside the wind farm (macro) or outside the RSZ + buffer within the wind farm (meso)

- A_{in} is the area within the whole wind farm (macro) or within the RSZ + buffer of all wind farm turbines (meso)

- A_{out} is the whole area outside the wind farm within 3 km (macro) or the wind farm footprint area, not considering RSZ + buffer of turbines (meso)

Formula	Approach	Assumptions	Benefits	Limitations
$EAR = 1 - N_{in} / N_{ref}$ Where: $N_{ref} = (N_{in} A_{in} + N_{out} A_{out}) / (A_{in} + A_{out})$	Compares track length per unit area inside the wind farm to a situation without a wind farm i.e. the same density both inside and outside the wind farm, which is considered the reference density. The outside area is defined as the area affected by redistribution of birds due to the wind farm	• Assumes pre-construction track density would have been the same in the whole area • Assumes surveyed areas are representative of the whole wind farm	• Accounts for redistribution of bird densities due to the wind farm • accounts for different sized areas inside and outside	• It can be difficult to define the area outside the wind farm affected by redistribution.
$EAR = 1 - N_{in} / N_{out}$	Measures the degree of avoidance at the wind farm boundary, using track density outside the wind farm as a reference density	Assumes pre-construction track density throughout studied areas would have been the same of those currently observed in outside areas	• Simplicity, measures degree of avoidance at the boundary • Does not assume surveyed areas are representative of the whole wind farm	• Does not account for redistribution of birds outside the wind farm boundary • And therefore there is a risk of overestimated EARs
$EAR = (N_{out} - N_{in}) / N_{in} + N_{out})$ Or $EAR = 1 - N_{in} / (½ (N_{in} + N_{out}))$	Compares track density (inside the wind farm) with an average of densities inside and outside, using monitored areas of equal size (mirrored areas). Basically the same as the first and adopted approach, however assumes areas of the same size inside and outside	Assumes that the areas inside and outside are of equal size	Accounts for redistribution of birds outside the wind farm	• Can only be applied when comparing areas of the same size, i.e. applying a mirror approach and its consequent loss of data • The area outside the wind farm subject to increased density of birds is likely to differ from the area within the wind farm

NIRAS DHI CARBON TRUST

2. Calculation of track length per unit area in meso avoidance analysis and influence on meso EARs

Given that the data available to undertake meso avoidance analysis include a radar trigger point for all video recordings with associated tracks for some of them but not all, a special treatment of the data w required. This section provides an overview of the data treatment options considered, which were tested using an artificial track dataset to observe how they influence resulting meso EARs.

◊ Dataset used to test the different data treatment options:

- Total number of turbines covered in the analysis: 4 (in relation to F04 monitoring equipment)

- Total number of trigger points (purple points) within analysis area: 24, randomly placed along the track (blue lines) to resemble the radar trigger points available in the study data

- Total number of tracks (blue lines) within analysis area: 24, the degree of the "non-linearity" is not based on real data.

- Total number of tracks intersecting the RSZ + buffer: 5

Figure 1. **Arbitrarily created artificial tracks for methods testing, and single points representing each track.**
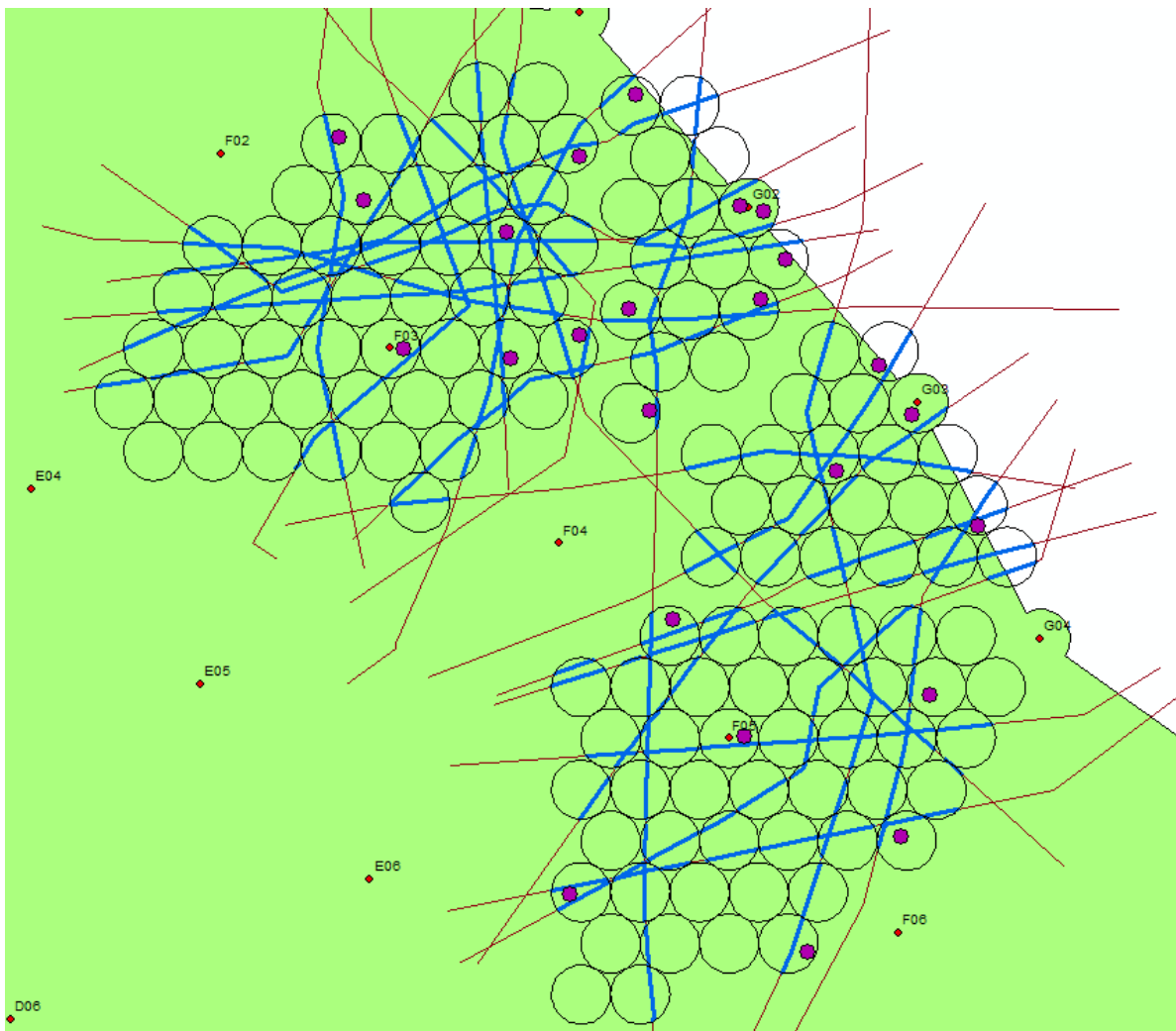
Formula used for calculating the avoidance rates is:

$$\text{Meso EAR} = 1 - N_{in} / N_{ref}$$

Where:

$$N_{ref} = (N_{in} A_{in} + N_{out} A_{out}) / (A_{in} + A_{out})$$

N_{in} is the observed mean track length per unit area within the rotor swept zone, calculated within the four turbines inside the high detections zone of each radar, i.e. in total 8 turbines,

N_{ref} is the mean track length per unit area in the absence of the wind turbines,

N_{out} is the mean track length per unit area inside the wind farm footprint (calculated inside the high detection zones of the radars at F04 and D05) but outside the rotor-swept zone (55 m circle around each turbine) of the four turbines inside the high detections zone of each radar, i.e. in total 8 turbines,

A_{in} is the area within all RSZ within the whole wind farm (not only the surveyed area) = 1.045,

A_{out} is the whole area inside the wind farm footprint = 26.662

Option 1: Application of the track length per unit area approach using complete track lengths

This would be the ideal approach to use if actual tracks were available at this scale (Figure 2), and it is therefore recommended to be used in future studies that manage to obtain track data at the meso scale. Although complete tracks are not available in this study, it is considered useful to compare the results from applying this approach with others below.

This method accounts for the flight duration within both zones (inside and outside).

- Calculated mean track length per unit area inside RSZ + buffer areas = 11.05
- Calculated mean track length per unit area outside RSZ + buffer areas =15.29
- Meso EAR = **0.270**

Figure 2. **Complete tracks assessed within a high detection zone, including four turbines (red dot) and 10m buffer zone (grey circle), 24 trigger points (purple dots) and associated radar tracks (purple lines).**
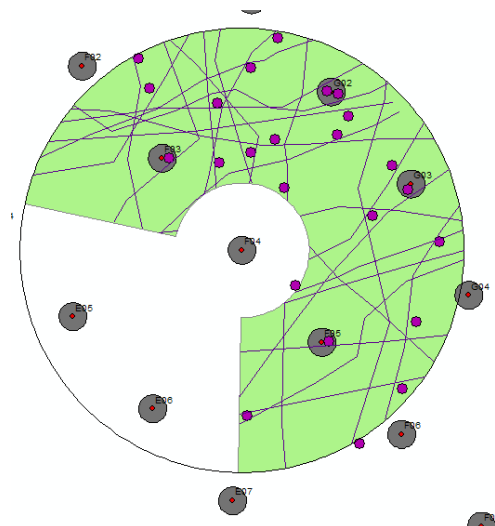
Option 2: Application of the track length per unit area approach using a circular grid, using a) track lengths and b) trigger points.

a) Using track lengths within circles. This approach would be a useful method if short tracks were available, similar to the application of a grid in macro avoidance analysis

- Calculated mean track length per unit area inside RSZ + buffer areas (only inside circle grid cells) = 11.05

- Calculated mean track length per unit area outside RSZ + buffer areas (only inside circle grid cells) = 15.92

- Meso EAR = 0.298

b) Using the initial trigger points and a mean average track length in each grid circle with a trigger point. This method does not account for the total time spent by the birds (particularly) in the outside meso zone and therefore the approach results in unrealistically low meso EAR. It is therefore apparent that the track length (or duration of bird flights within each zone) needs to be accounted for otherwise the EAR is underestimated. The mean track length used for the trigger point was calculated using the formula:

Mean random track length = πR/2

Where R is the radius of a circle and in this case the radius of the circle is 55 m.

- Calculated mean track length per unit area inside RSZ + buffer areas = 11.39

- Calculated mean track length per unit area outside RSZ + buffer areas = 1.36

- Meso EAR = -5.541

Figure 3.   Track length within circle grid or trigger points with a mean track length of a circle with radius 55 m within circle grid applied in approach 2a and 2b for calculating meso EAR.
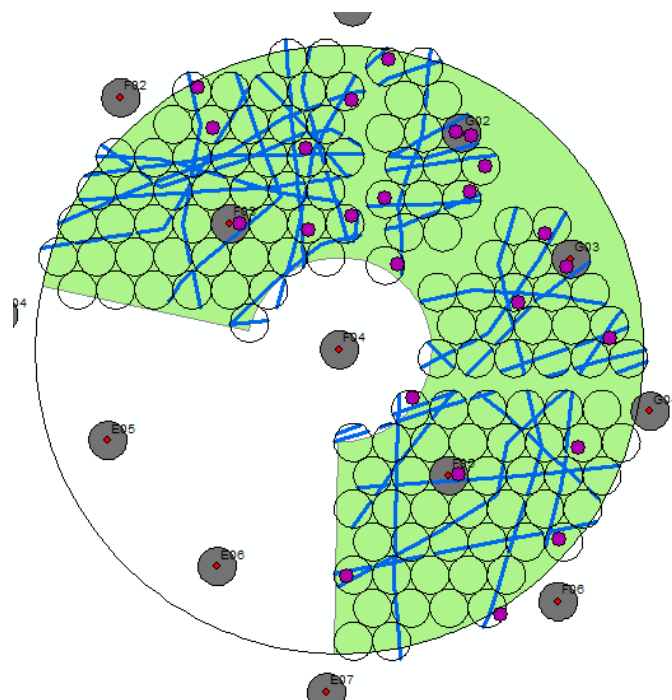
Option 3: Application of the track length per unit area using mean track lengths in the whole outside area, i.e. not using a grid: a) uncorrected and b) corrected for flight duration (based on flight speeds measured by rangefinders).

This approach uses radar trigger points and applies a mean track length (in a circle) treating the outside meso zone as a whole circle (reduced by proportion of blind sector and other removed areas). This accounts for the total flight track length both in the inside meso zone and outside meso zone. The results were compared with those given by Option 1 to assess whether mean track lengths are useful as a proxy for actual track lengths

a) Without correction: a mean track length in a circle was calculated for a circle with a radius of 875 m (the distance from the turbine to the outer boundary of the high detection zone). Because the low detection zone within 265 m from the turbine was removed together with the blind sector, the total area was ~65.35% of the full circle, the same proportion of the mean track length was used.

- Mean track length per unit area inside RSZ + buffer = 11.39 (same as approach 2b).

- Mean track length outside RSZ + buffer =13.44 (assuming that all 24 tracks flew through the outside area and subtracting the mean track length of the tracks in the inside meso zone).

- Meso EAR = **0.148.**

Figure 4. **A set of mean linear (straight) "random" tracks illustrating the basis for calculating the mean track length within a circle, the mean linear tracks were further corrected for actual mean flight duration based on flight speed information collected using rangefinder data from G01 and G05.**

APPENDICES
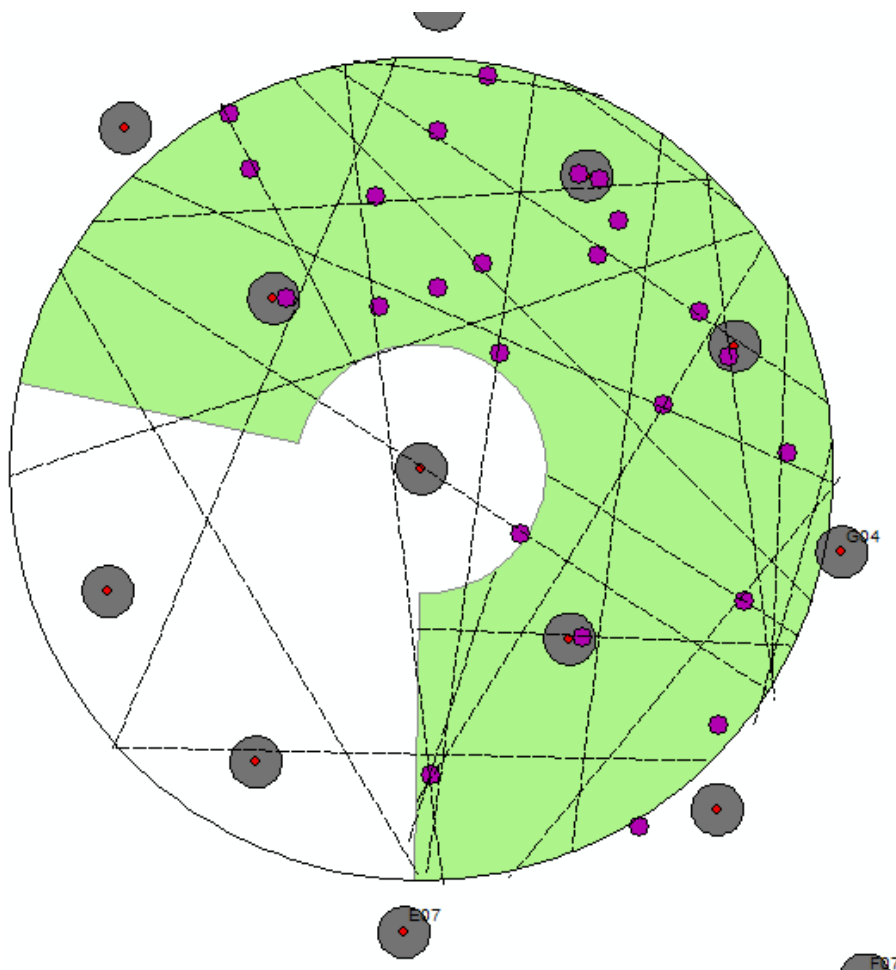
Compared with results provided by Option 1, the use of mean track lengths without correction seems to underestimate avoidance, which is considered to be related to the fact that mean track lengths assume that that birds fly in straight lines, which is not the case in reality.

b) With correction for total length of flight track: in order to account for the fact that birds do not fly in straight lines, random track lengths can be corrected using flight speed data, which allows to account for flight duration (and therefore also the length of the flight track). The rangefinder data collected by the study provided an opportunity to measure flight speed for target species (see Section 5.5 of the main body of the report) .

- Track length per unit area inside RSZ + buffer is used uncorrected and therefore the same as in approach 3a = 11.39.

- The corrected track length outside meso zone RSZ + buffer (by applying a flight speed correction factor of 1.13 for Northern Gannet) = 15.22 (for large gulls) = 16.60

- Meso EAR = 0.245 (Northern Gannet); 0.305 (Large Gulls)

Results indicate that the artificial tracks are slightly more complex (longer) than true Northern Gannet flight tracks as measured at the site using rangefinders and on the other hand shorter or less complex that true Large gull tracks (see Figure 4 below).

Results obtained by corrected mean track length provide highly similar results as those given by Option 1, and therefore comparable to a case where the dataset includes full track lengths. It is therefore considered that the use of corrected mean track lengths is a suitable method that should be applied to the study's data in order to estimate empirical meso avoidance rates.

Figure 5.   **Recorded rangefinder tracks of Northern Gannet and Herring Gull from G01.**
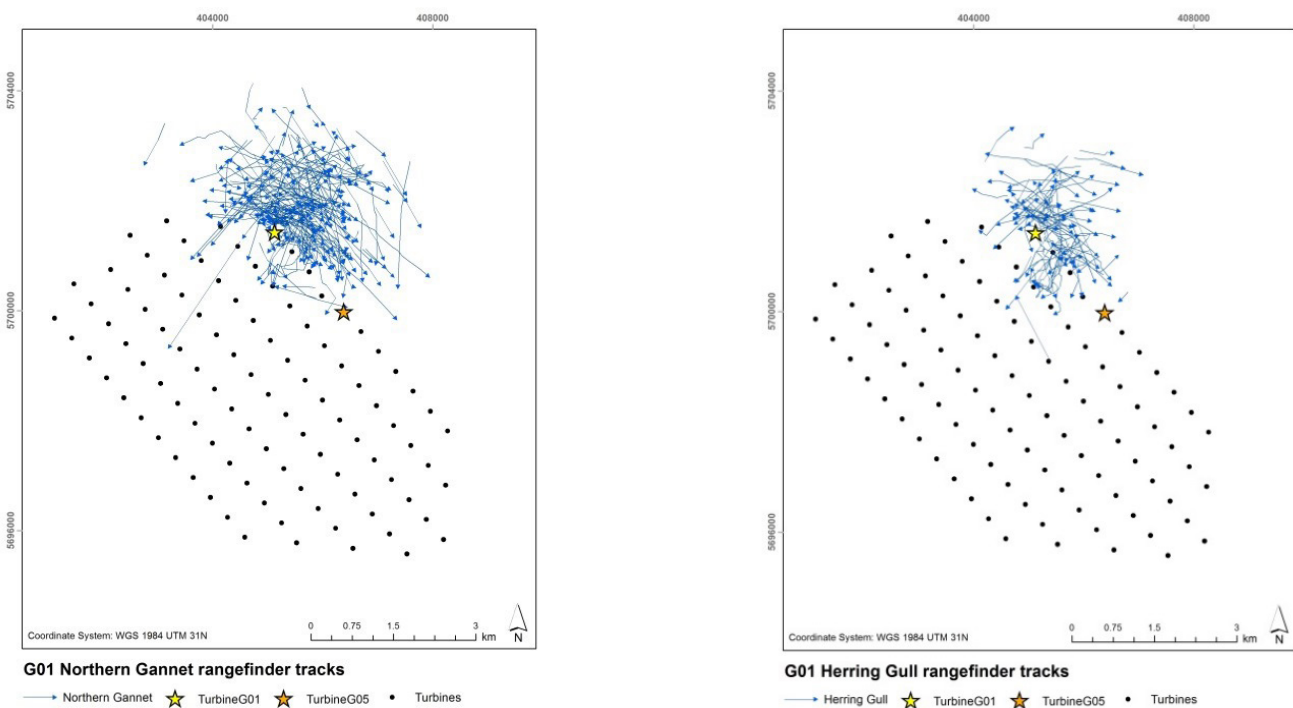
APPENDIX 9: SAMPLE SIZE AND PRECISION

A series of bootstraps on different sample sizes were ran to assess how the EAR changes when the sample size is reduced. If a very similar EAR is achieved with a range of lower sample sizes, e.g. until 75% of the data, reduced with 5% at a time, it can be regarded to indicate that a similar value would be a achieved also with a 25% larger sample size, if collected during similar conditions. In addition to the precision of the estimate, the standard deviation can be expected to decrease with increasing sample sizes. Although no defined criterion for acceptable levels of uncertainty were applied, variability in EARs for smaller sample sizes beyond the SD for the total data set was used as an indication of an unacceptable level of uncertainty.

The sample size was randomly decreased with 5% intervals from 100% to 50%, reiterated 10 times and run through the bootstrap on each data set 100 times. The results give an indication of what would happen if new surveys were to be conducted with an equal or smaller sample size.

1.   MACRO

The results for Northern Gannets indicated that a similar result would be obtained even if only 65% of the data would be collected (Figure 1). Thus, there is no reason for expecting that the estimate would change if more data would be collected. Lower sample sizes than 65% of the full data set clearly produce more variability in the results.

The results for Herring Gulls, Great Black-backed Gulls and large gulls as a group indicate that when less than 75% of the data is used the variability increases beyond the SD of the total data set (Figures 3, 4 and 5). The results for Lesser Black-backed Gull show larger variability (Figure 3.21). Based on these results it can be assumed that no major changes in the EAR estimate would be achieved with a, for example 20%, larger data set.

The results for Black-legged Kittiwake show larger variability and when less than 85% of the data is used the variability increases beyond the SD of the total data set (Figure 2).

Figure 1.   Calculation of Northern Gannet macro EAR for 10 randomly selected data sets for each 5% interval between 100%-50% of the complete data set. For each data set 100 bootstraps were run and the original EAR (red dots) and bootstrap SD (error bars was visualized. The original estimate based on the complete data set is indicated with black dashed line and the SD for the complete data set with red dashed lines.


Macro avoidance, Northern Gannet

Macro avoidance, Black-legged Kittiwake
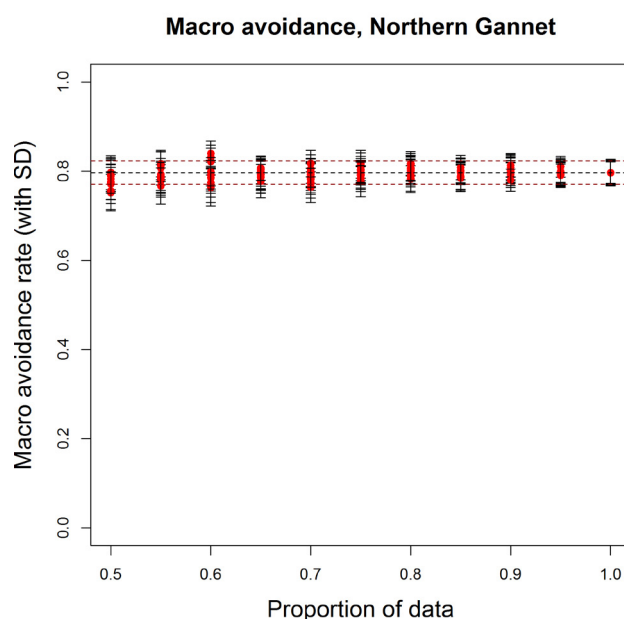
Figure 2. Calculation of Black-legged Kittiwake macro EAR for 10 randomly selected data sets for each 5% interval between 100%-50% of the complete data set. For each data set 100 bootstraps were run and the original EAR (red dots) and bootstrap SD (error bars) was visualized. The original estimate based on the complete data set is indicated with black dashed line and the SD for the complete data set with red dashed lines.
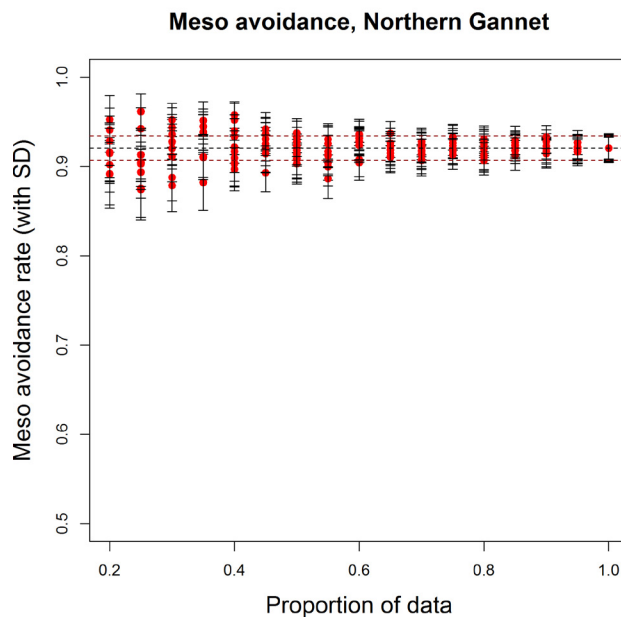
Macro avoidance, Herring Gull
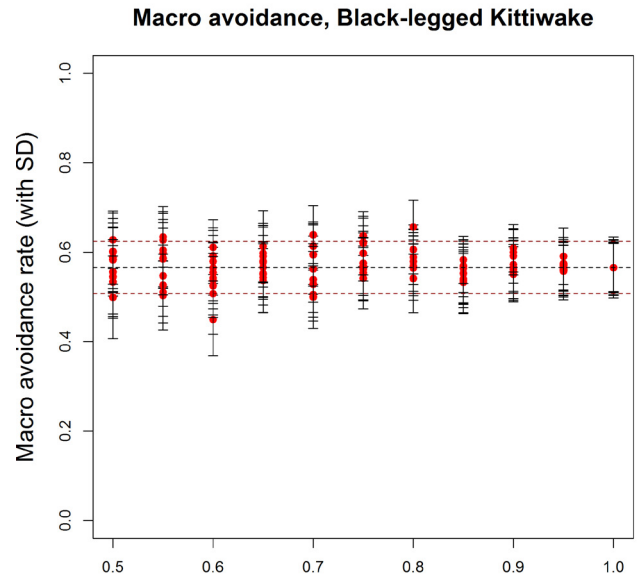
Figure 3. Calculation of Herring Gull macro EAR for 10 randomly selected data sets for each 5% interval between 100%-50% of the complete data set. For each data set 100 bootstraps were run and the original EAR (red dots) and bootstrap SD (error bars) was visualized. The original estimate based on the complete data set is indicated with black dashed line and the SD for the complete data set with red dashed lines.

Macro avoidance, Lesser Black-backed Gull
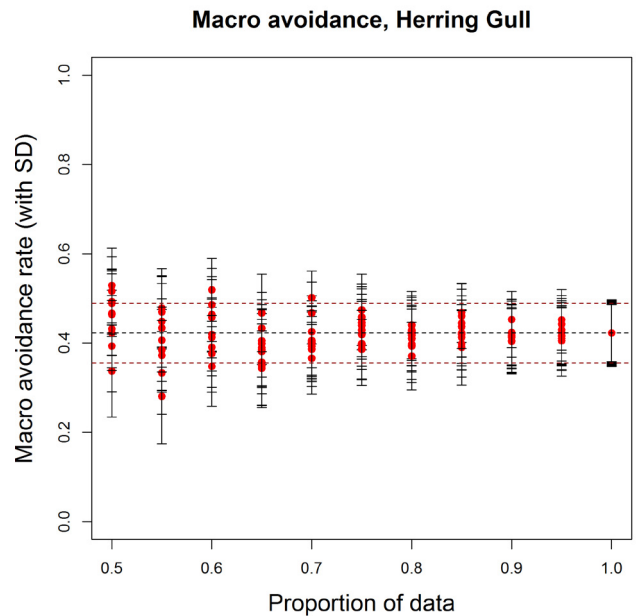
Figure 4. Calculation of Lesser Black-backed Gull macro EAR for 10 randomly selected data sets for each 5% interval between 100%-50% of the complete data set. For each data set 100 bootstraps were run and the original EAR (red dots) and bootstrap SD (error bars) was visualized. The original estimate based on the complete data set is indicated with black dashed line and the SD for the complete data set with red dashed lines.
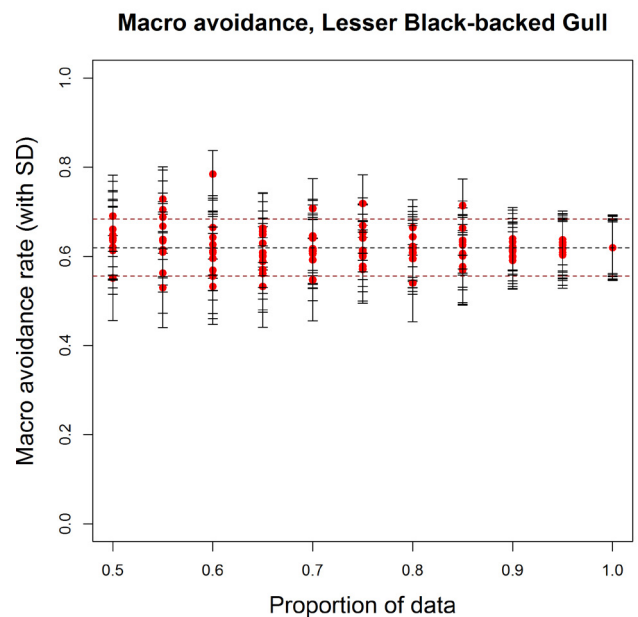
Figure 5. Calculation of Great Black-backed Gull macro EAR for 10 randomly selected data sets for each 5% interval between 100%-50% of the complete data set. For each data set 100 bootstraps were run and the original EAR (red dots) and bootstrap SD (error bars) was visualized. The original estimate based on the complete data set is indicated with black dashed line and the SD for the complete data set with red dashed lines.

Macro avoidance, Great Black-backed Gull
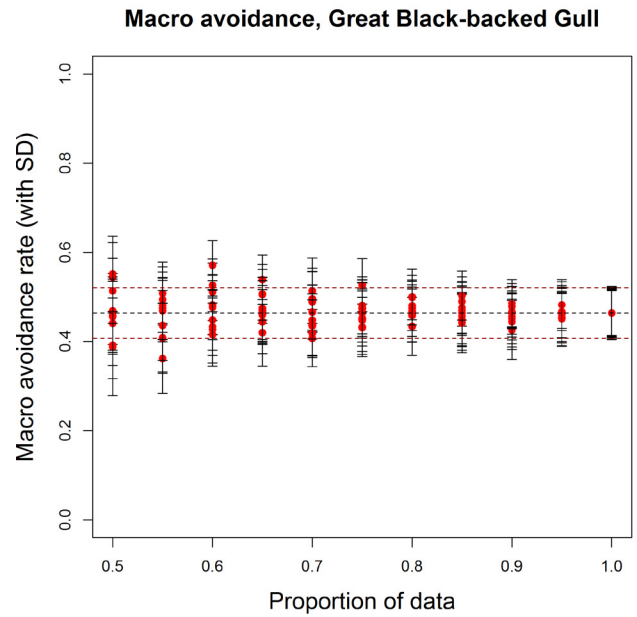
Figure 6. Calculation of large gull (combined) macro EAR for 10 randomly selected data sets for each 5% interval between 100%-50% of the complete data set. For each data set 100 bootstraps were run and the original EAR (red dots) and bootstrap SD (error bars) was visualized. The original estimate based on the complete data set is indicated with black dashed line and the SD for the complete data set with red dashed lines.

Macro avoidance, large gulls
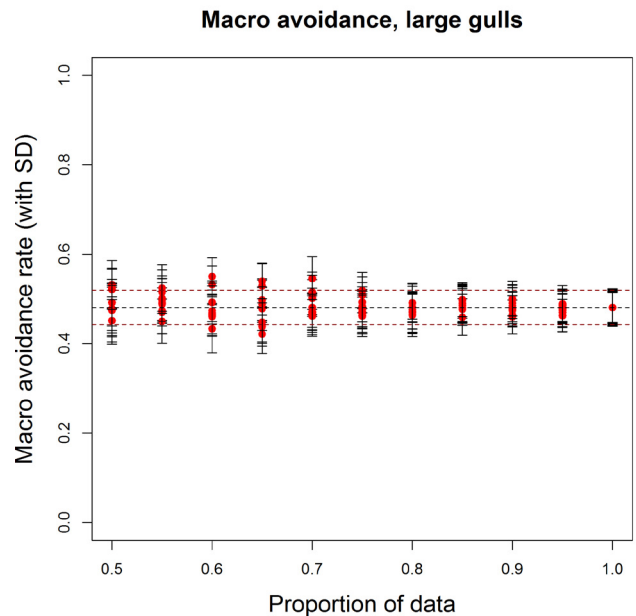
2. MESO

In order to further assess how the meso EAR would change with a different sample size a series of bootstrap analyses were ran by iterating the meso EAR function randomly for reduced sample sizes. The bootstrap was conducted on 20% of the data, increasing the data set by 5% at a time up to 100% (complete data set). This procedure was done 10 times and for each sample size the bootstrap was conducted with 100 iterations. This analysis indicates whether a different result would be expected if more data would be collected during similar conditions.

For Northern Gannet, the estimated meso EAR based on 70% of the data is still within the SD (±0.014) of the complete data set, (Figure 7). In other words, produces similar results. Sample sizes lower than 50% of the full data set clearly produce more variability in the results.

Figure 7. Calculation of Northern Gannet meso EAR for 10 randomly selected data sets for each 5% interval between 100%-20% of the complete data set, i.e. in total 170 data sets. For each data set 100 bootstraps were run meaning 17 000 estimations of EAR. For each the original estimate (red dots) and bootstrap SD (error bars) is visualized for all data sets. The original estimate based on the complete data set is indicated with black dashed line and the SD for the complete data set with red dashed lines.

For Black-legged Kittiwake the sample sizes below 75% results in an EAR estimate outside the SD of the full data set (Figure 8). The standard deviation around the Kittiwake estimates are however larger (± 0.033) due to the relatively low sample size. Therefore an increase in sample size would reduce the variability, however no major changes in the estimate would be expected.

Figure 8. Calculation of Black-legged Kittiwake meso EAR for 10 randomly selected data sets for each 5% interval between 100%-20% of the complete data set, i.e. in total 170 data sets. For each data set 100 bootstraps were run meaning 17 000 estimations of EAR. For each the original estimate (red dots) and bootstrap SD (error bars) is visualized for all data sets. The original estimate based on the complete data set is indicated with black dashed line and the SD for the complete data set with red dashed lines.
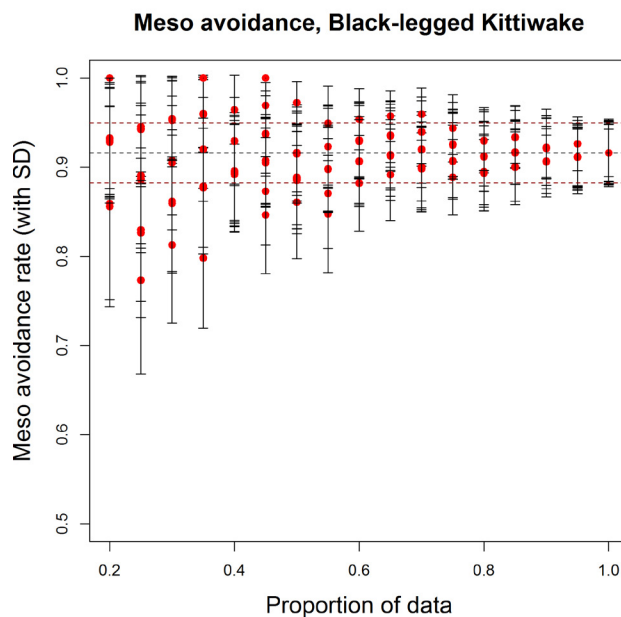
For large gulls and unidentified black-backed gulls larger variability of estimated meso EARs was achieved for sample sizes below 65% (Figure 9 and 12). Similar to the Black-legged Kittiwake, the results for Herring Gulls (Figure 10) and Great Black-backed Gulls (Figure 12) show larger variability due to low sample sizes, and when less than 70% and 65% respectively for herring gull and Great Black-backed Gull of the data is used the variability increases beyond the SD of the total data set. A large sample size (of e.g. 20%) would therefore potentially yield a lower variability for these species, however most likely not a very different meso EAR estimate.
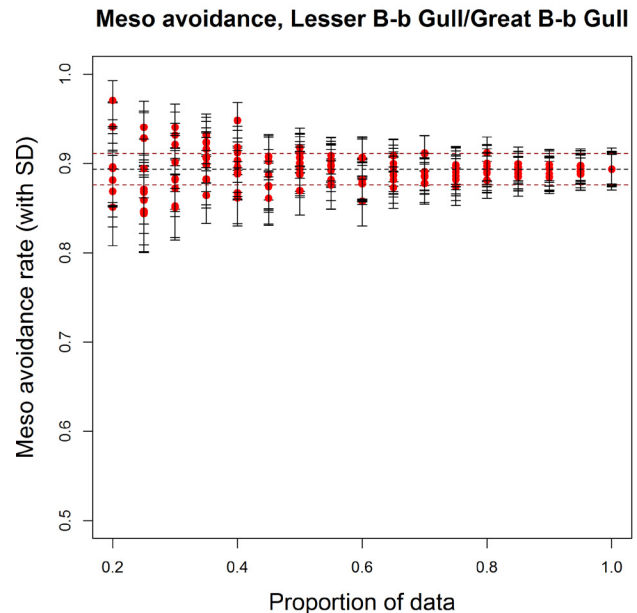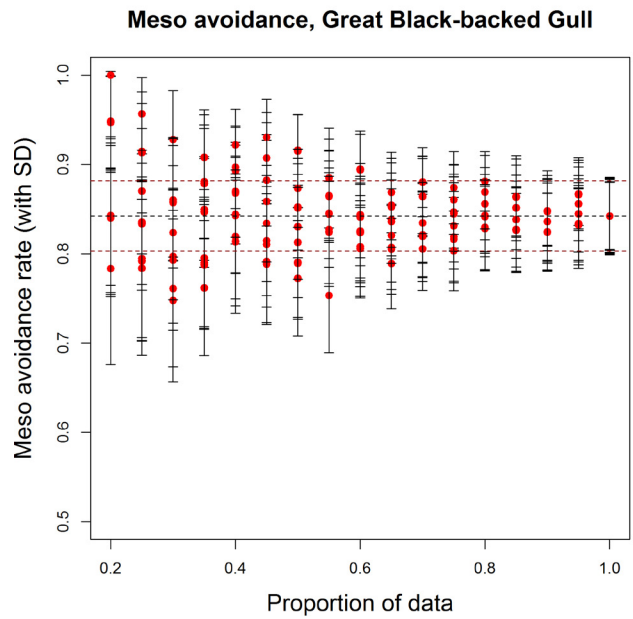
Figure 9.   Calculation of large gull meso EAR for 10 randomly selected data sets for each 5% interval between 100%-20% of the total data set, i.e. in total 170 data sets. For each data set 100 bootstraps were run meaning 17 000 estimations of EAR. For each the original estimate (red dots) and bootstrap SD (error bars) is visualized for all data sets. The original estimate based on the complete data set is indicated with black dashed line and the SD for the complete data set with red dashed lines.

Meso avoidance, large gulls
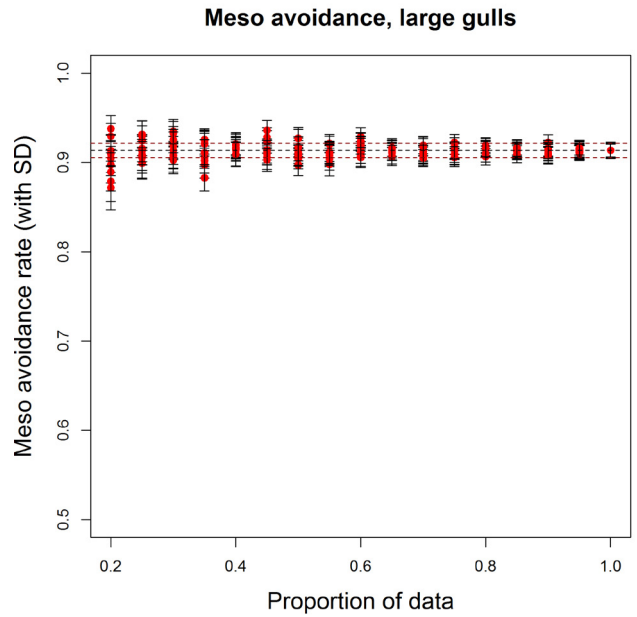
Figure 10.   Calculation of Herring Gull meso EAR for 10 randomly selected data sets for each 5% interval between 100%-20% of the complete data set, i.e. in total 170 data sets. For each data set 100 bootstraps were run meaning 17 000 estimations of EAR. For each the original estimate (red dots) and bootstrap SD (error bars) is visualized for all data sets. The original estimate based on the complete data set is indicated with black dashed line and the SD for the complete data set with red dashed lines.

Meso avoidance, Herring Gull
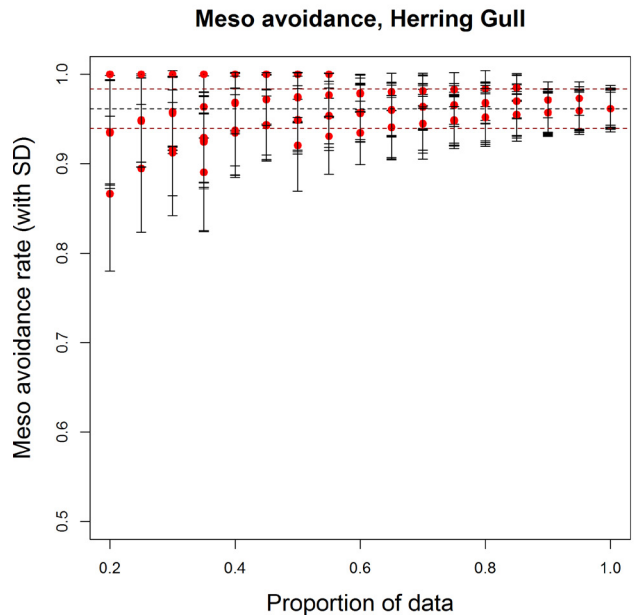
Figure 11.   Calculation of Lesser Black-backed Gull/Great Black-backed Gull meso EAR for 10 randomly selected data sets for each 5% interval between 100%-20% of the total data set, i.e. in total 170 data sets. For each data set 100 bootstraps were run meaning 17 000 estimations of EAR. For each the original estimate (red dots) and bootstrap SD (error bars) is visualized for all data sets. The original estimate based on the complete data set is indicated with black dashed line and the SD for the complete data set with red dashed lines.

Meso avoidance, Lesser B-b Gull/Great B-b Gull

Figure 12. **Calculation of Great Black-backed Gull meso EAR for 10 randomly selected data sets for each 5% interval between 100%-20% of the complete data set, i.e. in total 170 data sets. For each data set 100 bootstraps were run meaning 17 000 estimations of EAR. For each the original estimate (red dots) and bootstrap SD (error bars) is visualized for all data sets. The original estimate based on the complete data set is indicated with black dashed line and the SD for the complete data set with red dashed lines.**

Meso avoidance, Great Black-backed Gull

3. MICRO

Similar bootstrap assessments of the sample sizes as made for macro and meso EARs indicate that even a relative large increase in sample size would most likely not change the results notably (Figure 13 and 14). Estimated EARs for those two groups were within the SD of the complete set when using at least 75% of the available data. However, a larger micro data set would potentially allow for a species-specific assessment.

Figure 13. **Calculation of large gull micro EAR for 10 randomly selected data sets for each 5% interval between 100%-20% of the complete data set, i.e. in total 170 data sets. For each data set 100 bootstraps were run meaning 17 000 estimation of EAR. For each the original estimate (red dots) and bootstrap SD (error bars) is visualized for all data sets. The original estimate based on the complete data set is indicated with black dashed line and the SD for the complete data set with red dashed lines.**
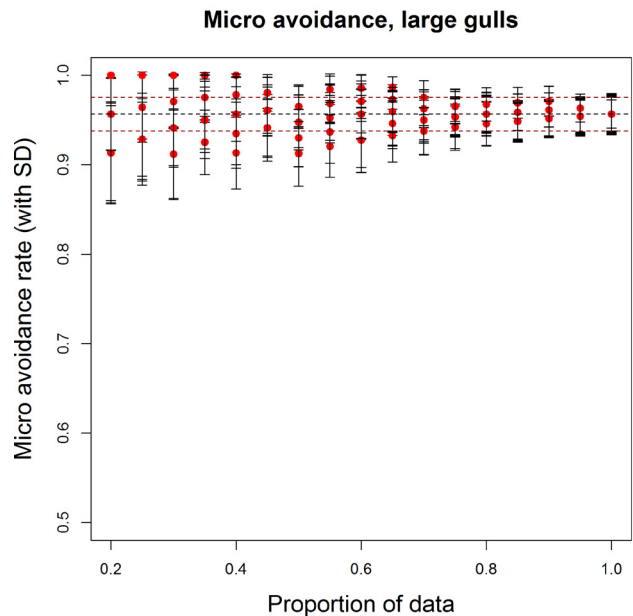

Micro avoidance, large gulls

Figure 14. Calculation of all seabird micro EAR for 10 randomly selected data sets for each 5% interval between 100%-20% of the total data set, i.e. in total 170 data sets. For each data set 100 bootstraps were run meaning 17 000 estimations of EAR. For each the original estimate (red dots) and bootstrap SD (error bars) is visualized for all data sets. The original estimate based on the complete data set is indicated with black dashed line and the SD for the complete data set with red dashed lines.

Micro avoidance, all seabirds
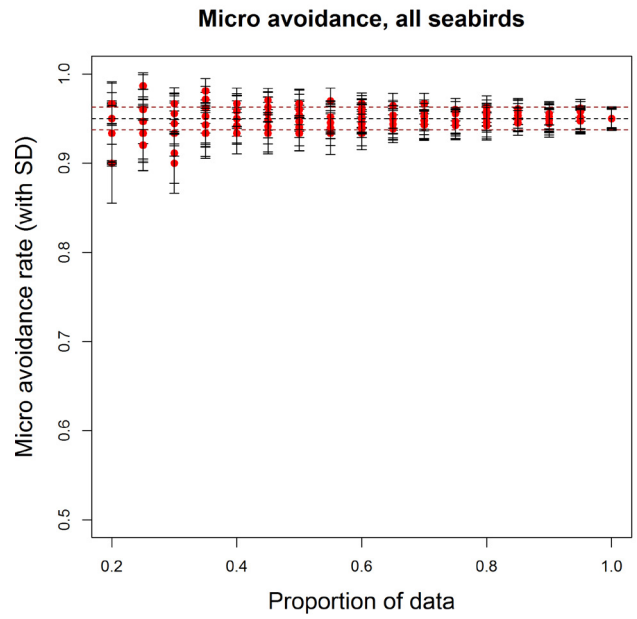
APPENDIX 10: INFLUENCE OF FLIGHT SPEED AND PRE-CONSTRUCTION BIRD DENSITIES ON FLUX FACTOR

In order to test how the flux factor in the Band model changes when the flight speed and pre-construction density are altered, a simple sensitivity test was undertaken using the Band model calculation sheets.

Bird flight speeds are highly variable (see example from e.g. Thaxter *et al.* 2011, below) depending on environmental factors, notably wind direction. The duration of a long "wiggly" track is also different than the duration of a straight track. The duration of a straight track can be calculated based on the actual flight speed recorded based on a fine temporal resolution (Safi *et al.* 2013).

Figure 1.   **Recorded flight speeds of two Lesser-black backed gulls (20 km/h = 5.6 m/s and 60 km/h = 16.7 m/s), illustrating high variability. Source: Thaxter *et al.* 2011.**
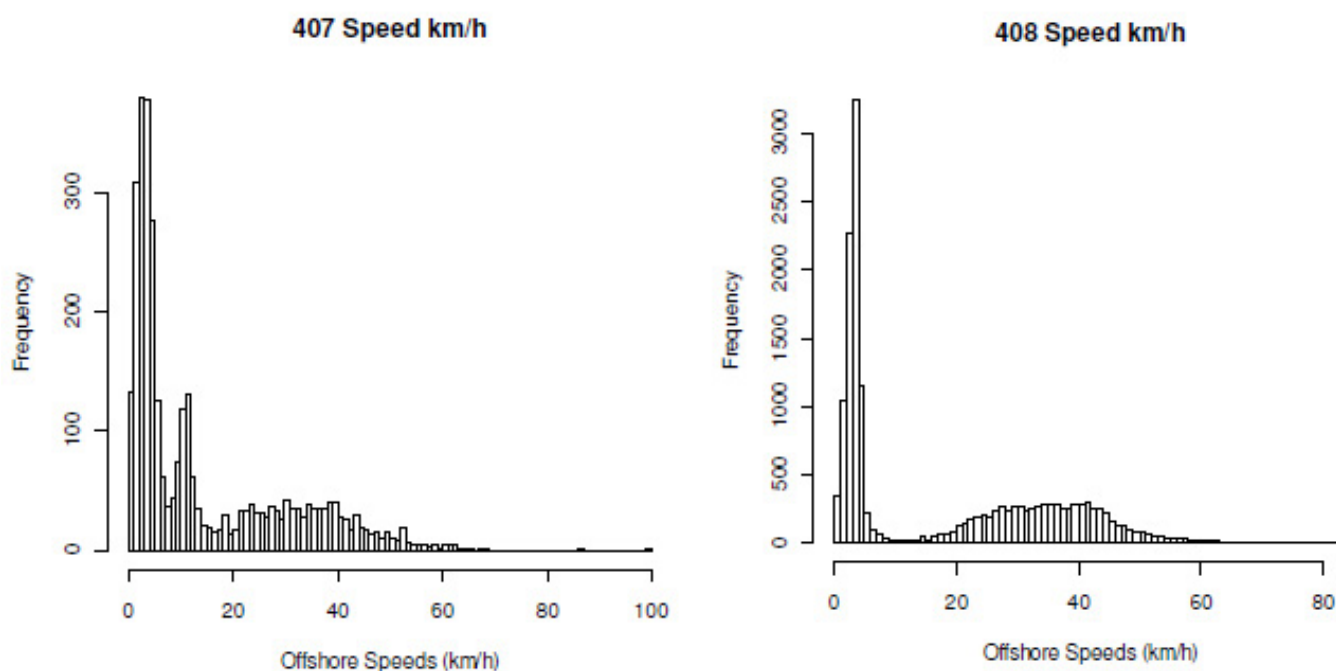
The following sensitivity test was undertaken (on hypothetical data) to test how the flux factor in a Northern Gannet model changes with flight speed and pre-construction density variations.

Parameter variations:

Defined flight speed of 14.9 m/s was altered by reducing the speed by 0.2 m/s at a time (ranging from 14.9 to 10.1 m/s), keeping all other parameters in the model constant. Flight speed at the rotor-swept zone fixed at 14.9 m/s (for calculating probability of colliding when crossing the rotor).

Use of pre-construction densities of 0.1 and 0.09.

Resulting flux factor (based on varying flight speed ranging from 10.1 to 14.9) multiplied with the collision risk estimate of a model with the flight speed set to 14.9 m/s, and the use of different avoidance rates were used to illustrate the change.

Results - The flux factor linearly decreases with decreasing flight speed and a small drop of pre-construction density further reduced the flux markedly (see Figure 2 upper graph).

Implications on actual number of predicted collisions – Comparison of initial scenario with a flight speed of 14.9 m/s and pre-construction density of 0.1 birds/km2 against a flight speed of 10.1 m/s and density of 0.09 birds/km^2. The difference between the two scenarios was close to 50% for the same avoidance rate used (Figure 2 lower graph). These results are consistent with the findings of Masden (2015), who showed that collision models are sensitive to changes in flight speed.

Figure 2. **The below graph illustrates changes in flux factor against a range of flight speeds, for two pre-construction densities. The lower graph illustrates the difference between a "high collision risk" scenario (14.9 m/s and 0.1 birds/km^2) and a "low collision risk scenario" (10.1 m/s and 0.09 birds/km^2), from the upper graph, against four different avoidance rates.**
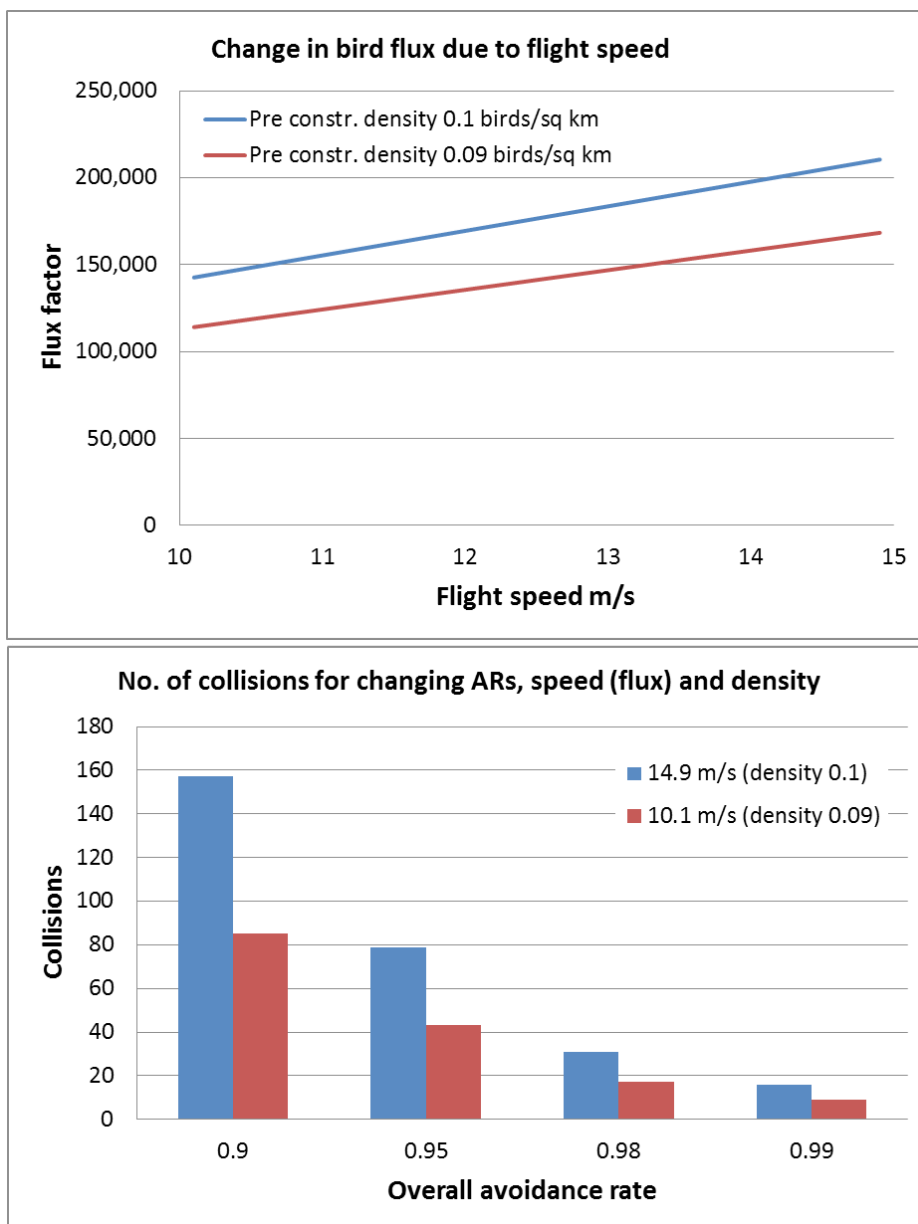
About the Carbon Trust

The Carbon Trust is an independent company with a mission to accelerate the move to a sustainable, low carbon economy. The Carbon Trust:

> advises businesses, governments and the public sector on opportunities in a sustainable, low carbon world;

> measures and certifies the environmental footprint of organisations, products and services;

> helps develop and deploy low carbon technologies and solutions, from energy efficiency to renewable power.

The company has approximately 180 staff with over 30 nationalities, based in the UK, China, Brazil, Mexico, South Africa and the USA. The Carbon Trust's experts come from a diverse range of professional backgrounds, including engineering, policy, academia, and business management.

www.carbontrust.com

+44 20 7170 7000